Quantifying and Understanding the Tropical Peatlands of the Central Congo Basin

Greta Christina Dargie

Submitted in accordance with the requirements for the degree of Doctor of Philosophy.

The University of Leeds

School of Geography

December 2015

The candidate confirms that the work submitted is her own and that appropriate credit has been given where reference has been made to the work of others.

Acknowledgements

Firstly I would like to thank my main supervisor Professor Simon Lewis for giving me the opportunity to spend so much time in the truly wild and remote swamps of the Cuvette Centrale; an experience which I will remember for the rest of my life. I would also like to express my gratitude to Simon and to my supervisor Dr Ian Lawson, originally at the University of Leeds and now at the University of St. Andrews, for the time and effort they put into my project, for accompanying me in the field and, finally, for getting me to the end. I also thank my supervisor Dr Ed Mitchard at the University of Edinburgh for his never ending patience and time that he gave when I was carrying out the remote sensing work. Finally I thank my supervisor Professor Sue Page at the University of Leicester for her support and advice throughout the PhD.

This project involved a lot of fieldwork in the Republic of Congo, none of which would have been possible without my CASE partner, Wildlife Conservation Society-Congo. Their logistic support provided by the WCS staff, in particular Tim Rayden, Felin Twagirashyaka, Moussavou Fridrich Terrance, Paul Telfer and Amy Apokempner made the project possible.

I would like to thank the following at the Université Marien Ngouabi: Professor Loumeto Jean Joel for his logistical support and advice and Moutsambote Jean-Marie for help with plant identification. Very special thanks go to Ifo Suspense who not only played a fundamental role in the success of the fieldwork, but went out his way to make me feel at home in the Republic of Congo.

For their excellent hospitality during fieldwork I thank the following villages: Bokatola, Bolembe, Bondoki, Bondzale, Ekolongouma, Ekondzo, Itanga, Mbala and Moungouma. Tropical swamps can be inhospitable environments and fieldwork was not always easy. Therefore I was impressed by the strength and determination shown by the following when assisting me in my fieldwork and touched by their kindness towards me: the late Abia Platini, Angoni Tresor, Bitene Cesar, Bobetolo Jean Bosco, Bonguento Crepin, Dibeka Justin, Elongo Bienvenu, Carlos, Ismael Mokondo, Iwango Michel, Makweka Gerard, Mandomba Landry, Miyeba Cesar, Mobembe Amalphi, Moniobo Belen Ekous, Mosibikondo Freddy, Mouapeta Fulgence, Ngongo Guy, Nsengue Gothier, Nzambi Lionel, Saboa Jean, Chancel, Gerry and Emanuel. I also give a big thanks to Abdoul Rahïm, a man who seems capable of solving any problem that comes his way and is therefore a very valuable man to know when working in the Likouala Department.

With regards to fieldwork, the biggest thanks are reserved for Bocko Yannick and Mbongo Roger. I thank them both, not only for the many months they spent helping me with fieldwork, but for their help with the logistical planning, teaching me how to survive in the swamp forest, the excellent meals and most importantly for making my fieldwork an enjoyable experience.

I would also like to thank the following: Dr Serge Kouob, for accompanying me on my first field trip and his help with plant identification; David Ashley, Rachel Gasior and, in particular, Martin Gilpin for their assistance and advice with laboratory analysis; Andy Baird for helpful discussions; Duncan Quincy for providing support with remote sensing and GIS; David Harris for help with plant identification; Pauline Gulliver for support with the radiocarbon analyses; my fellow PhD students, for making my time in the School of Geography a really good one. Special mentions go to Dr Freddie Draper, who has been a good friend throughout, Dr Thomas Kelly, who gave helpful advice from beginning to end and Dylan Young, for solving many of my R troubles.

For the funding for my research I'd like to thank the Natural Environment Research Council (NERC) and WCS-Congo for the core PhD funding for my stipend, and my supervisor Simon Lewis for providing funds via a Philip Leverhulme Prize, the EU GEOCARBON project and a Royal Society University Research Fellow grant to fund travel costs, my many months of fieldwork, and the equipment needed.

Finally I would like to thank my family and close friends for their support and encouragement throughout. In particular, I would like to thank my parents, who have always encouraged me to keep going and take the opportunities that come my way. Although Mum is not here to see the finished thesis, she always said I would get there. Spending weeks at a time wading through a Congolese swamp was not so daunting when I knew I had a mum at home, who, no matter how far away, would always find a way to help out if she could.

Abstract

The world's second largest tropical wetland is found in the central Congo Basin. Ambiguous grey-literature reports of peat, coupled with the large area of wetland suggest this region may be a globally significant carbon store. In this thesis I aim to establish whether this region, known as the Cuvette Centrale, harbours significant peatlands, to characterise them, compute the first estimate of peatland extent and C stocks based on ground data, to determine the factors which led to peat initiation and their maintenance today.

Fieldwork within the Likouala Department, Republic of Congo, confirmed widespread peat presence. Peat-vegetation associations were recorded in the field, which combined with remotely sensed radar, optical and elevation data was used to estimate the area of peatland; at 145,529 km^2 (95% CI, 134,720-154,732 km^2), the Cuvette Centrale is the single most extensive tropical peatland complex in the world. The peat is shallow (maximum depth: 5.90 m) and characterised as non-domed, nutrient poor systems, occupying large interfluvial basins. Area measurements combined with those of peat depth, bulk density and C concentration, collected in the field, suggest a total peat C stock of 30.2 Pg C (90% CI, 27.8-32.7 Pg C). This increases the current global tropical peatland C stock estimate from 88.6 Pg C to 115.8 Pg C.

Radiocarbon dates show peat initiated early Holocene (dated from 10555 cal yrs BP onwards), with a possible Mid- to Late-Holocene hiatus in peat accumulation, with both likely linked to changes in regional precipitation. Pressure transducers measuring the peatland water tables, rainfall estimates and water source geochemistry imply that the peatlands today are predominantly rain-fed systems.

My discovery that the Congo Basin, not tropical Asia, is home to the world's largest single peatland complex elevates the current global peatland C stock estimate from 88.6 Pg C to 115.8 Pg C and will require new regional management plans if the destructive fate of tropical Asian peatlands are to be avoided in central Africa.

Contents

Acknowledgements i
Abstract iii
Contents iv
List of Figures viii
List of Tables xi
List of Abbreviations xiii
Chapter 1: Thesis Rationale and Background 1
1.1. Thesis Rationale 1
1.2. Thesis Outline 1
1.3. Literature Review 2
1.3.1. Central African Rain Forest 2
1.3.2. The Congo Basin 4
1.3.3. Swamp Forest Vegetation in the Congo Basin 6
1.3.4. Peat Definition 12
1.3.5. Hydrological and Geochemical Classification of Peatlands 12
1.3.6. Peat Initiation 14
1.3.7. Peat Accumulation 16
1.3.8. Peatlands and Carbon Storage 19
1.3.9. The Distribution of Tropical Peatlands and Their Carbon Stocks 20
1.3.10. African peatlands 21
1.3.11. Highland Tropical Peatlands of Africa 22
1.3.12. Lowland Tropical Peatlands of Africa. 29
1.3.13. Lowland Peatlands of the Cuvette Centrale 33
1.3.14. Summary of African Peatlands. 37
1.4. Site Description 37
Chapter 2: Discovery of Extensive Lowland Peatlands within the Central Congo Basin 41
2.1. Abstract 41
2.2. Introduction 41
2.3. Chapter Aims 43
2.4. Methods 43
2.4.1. Site Identification 43
2.4.2. Sampling Methods 49
2.4.3. Peatland Surface Topography 52
2.4.4 Laboratory Methods 55
2.4.5. Peat Depth Corrections 55

2.5. Results 56
2.5.1. Remote Sensing as a Methodology to Locate Peatlands within the Congo Basin 56
2.5.2. Peatland Topography 61
2.5.3. Peat Depth 64
2.6. Discussion 65
2.6.1. Use of Remote Sensing to Identify Peatlands 65
2.6.2. Peatland Vegetation 66
2.6.3. Peat Depth and Topography 70
2.7. Conclusion 73
Chapter 3: Peatland Properties of the Central Congo Basin. 74
3.1. Abstract 74
3.2. Introduction 74
3.3. Aims 76
3.4. Methods 76
3.4.1. Site Description 76
3.4.2. Sub-sampling of Peat Cores in the Field 76
3.4.3. Surface pH and Electrical Conductivity 76
3.4.4. Bulk Density 77
3.4.5. Carbon and Nitrogen 77
3.5. Results 78
3.5.1. Surface pH and Electrical Conductivity 78
3.5.2. Bulk Density 80
3.5.3. Organic Matter Content 84
3.5.4. Carbon and Nitrogen 85
3.5.5. Peat Properties Under Different Vegetation Types 91
3.6. Discussion 92
3.6.1. Peatland Surface pH and Conductivity 92
3.6.2. Peat Bulk Density 94
3.6.3. Peat C and N Concentrations 98
3.6.4. Relationship Between Vegetation and Peat Properties 99
3.6. Conclusions 100
Chapter 4: Peatland Extent and Carbon Stocks in the Central Congo Basin. 102
4.1. Abstract 102
4.2. Introduction 102
4.3. Aims 104
4.4. Methods 105

4.4.1. Site Description 105
4.4.2. Peatland Area 105
4.4.3. Peatland Carbon Estimates 109
4.4.4. Aboveground Carbon Stock Estimates. 112
4.5. Results 114
4.5.1. Maximum Likelihood Classifications and Peatland Extent. 114
4.5.2. Spectral Signature of Land Cover Classes 117
4.5.3. Belowground Peatland Carbon Stock Estimates 120
4.5.4. Aboveground Peatland Carbon Stock Estimates 121
4.6. Discussion 122
4.6.1. Peatland Area 122
4.6.2. Estimating Peatland C stocks 129
4.6.3. Aboveground Peatland C Stocks 134
4.7. Conclusions 135
Chapter 5: Peatland Initiation and Development in the Central Congo Basin 136
5.1. Abstract 136
5.2. Introduction 136
5.3. Aims 138
5.4. Methods 139
5.4.1. Site Description 139
5.4.2. Radiocarbon Dating and Age Models 139
5.4.3. Peat Humification Analysis 140
5.5. Results 141
5.5.1. Radiocarbon Dates 141
5.5.2. Humification Analysis 146
5.6. Discussion 148
5.6.1. Peatland Initiation 148
5.6.2. Peat Accumulation Through Time 149
5.6.3. Radiocarbon Date Inversions 150
5.6.4. Peat Initiation and Accumulation at Ekondzo 151
5.6.5. Distinctions in Lowland Peatland Formation Across the Tropics 152
5.7. Conclusions 153
Chapter 6: Central Congo Basin Peatland Hydrology 154
6.1. Abstract 154
6.2. Introduction 154
6.3. Aims 156

6.4. Methods....156
6.4.1. Site Description....156
6.4.2. Continuous Water Table Measurements....157
6.4.3. Peatland Metal Cation Concentrations....162
6.4.4. River and Rainwater Chemistry....163
6.4.5. Loss on Ignition Residues....164
6.5. Results....164
6.5.1. Water Table Data....164
6.5.2. River and Rainwater Characteristics....177
6.5.3. Surface Peat and OM Metal Cation Concentrations....180
6.5.4. Peat Metal Cation Concentrations Down Core....182
6.5.5. LOI Residues....192
6.6. Discussion....194
6.6.1. Relationships Between Hydrology and Peat Depth and Vegetation....194
6.6.2. Determining the Role of Rain and Rivers in Peatland Inundation....195
6.6.3. Semi-Diurnal and Diurnal Water Table Fluctuations....198
6.6.4. Peatland Groundwater Recharge....199
6.6.5. Peatland Drainage....200
6.5.6. Phenomena Affecting Magnitude of Below Surface Peatland Water Table Fluctuations....201
6.6.7. Oscillations in Peat Surface Elevation....203
6.6.8. Water Table Time Series of the Seasonally Flooded Forest....204
6.6.9. River and Rainwater Characteristics....205
6.6.10. Determining Sources of Peatland Nutrient Inputs from Water and Peat Chemistry....208
6.6.11. Down Core Cation Concentrations....211
6.6.12. Origin of Surface Inorganic Matter....212
6.7. Conclusions....212
Chapter 7: Conclusions....214
7.1. Key Findings....214
7.3. Future Work....216
7.2. Implications....218
References....221
Appendix....242

List of Figures

Title		Page
Figure 1.1	Location map of Africa.	7
Figure 1.2	Origins of peatland extent estimates presented in the literature for the Republic of Congo	35
Figure 1.3	Origins of peatland extent estimates presented in the literature for the Democratic Republic of Congo.	35
Figure 1.4	Overview site map showing the study region within the Likouala Department, Republic of Congo.	38
Figure 1.5	Mean monthly rainfall and temperature for Impfondo, Likouala Department, Republic of Congo.	40
Figure 2.1.	PALSAR HH imagery of the study sites within the Cuvette Centrale.	48
Figure 2.2.	Relationship between ASTER GDEM elevation and mean tree height.	53
Figure 2.3.	Relationship between mean tree height and the difference between the estimated ground surface and SRTM DEM.	54
Figure 2.4.	Relationship between peat depths estimated by the metal pole method and by loss on ignition	56
Figure 2.5.	Photo showing hardwood swamp. Centre, March 2014.	58
Figure 2.6.	Photo showing *Raphia laurentii* palm dominated swamp. Ekolongouma, February 2012.	59
Figure 2.7.	Photo showing *Raphia hookeri* palm dominated swamp occupying a channel which drains the swamps. Itanga, March 2013.	59
Figure 2.8.	Along transect mean tree height, estimated ground surface and peat depth.	61
Figure 2.9.	Photo showing curled black trunk fibres of *Raphia hookeri*.	69
Figure 3.1.	Boxplot of peat bulk densities for each site.	80
Figure 3.2.	Peat bulk density variation down core and along transect.	81
Figure 3.3.	Peat bulk density plotted against organic matter content.	83
Figure 3.4.	Mean core peat bulk density plotted against total core peat depth.	84
Figure 3.5.	Boxplot of peat organic matter contents for each site.	85
Figure 3.6.	Boxplot of peat C concentrations, peat N concentrations and peat C/N ratios for each site.	86
Figure 3.7.	Peat C and N concentrations and C/N ratios down core.	88
Figure 3.8.	Peat C concentration plotted against loss on ignition.	90
Figure 3.9.	Peat C concentration plotted against peat bulk density.	90
Figure 3.10.	Peat C/N ratios plotted against peat bulk density.	91
Figure 4.1.	Regression slope values from an ANCOVA where square root bulk density is the dependent variable, core is the independent variable and depth down core is the covariate, plotted against total core depth.	112
Figure 4.2.	Peatland probability map derived from 1000 maximum likelihood classifications.	116
Figure 4.3.	Boxplot of land cover class ground truth point values for Landsat ETM+, PALSAR and SRTM datasets.	118

Figure 4.4.	Boxplot of sensitivity analysis fort each component of the peatland belowground C estimates.	121
Figure 4.5.	Boxplot of AGC for palm dominated swamp and hardwood swamp.	122
Figure 5.1.	Linear age-depth model for the Ekolongouma cores.	144
Figure 5.2.	Basal peat median age estimates plotted against basal peat sample depth.	146
Figure 5.3.	Peat accumulation rates plotted against basal peat sample depth.	146
Figure 5.4.	Down core absorbance recorded by spectrophotometer for the Ekolongouma cores.	147
Figure 5.5.	A section of the Ekolongouma 9 km core.	151
Figure 6.1.	OSFAC Landsat ETM+ ROC mosaic showing the study region within the Likouala Department and the location of the 14 pressure transducers and water sample locations.	159
Figure 6.2.	Photo and schematic of pressure transducer installed in the field.	160
Figure 6.3.	Schematic showing why the specific yield of peat would result in increases in water table height that are greater than the rainwater input.	161
Figure 6.4.	Full time-series of peatland water table levels along each transect.	167
Figure 6.5.	Low amplitude, high frequency noise visible in a subsection of the water table time series.	170
Figure 6.6.	Power spectral diagrams from the spectral analysis of the water table time series subsections shown in Fig. 6.5.	171
Figure 6.7.	Barologger atmospheric pressure measurements at Bondzale 5 km and detrended water table fluctuations measured by pressure transducer at Bondzale 6 km.	172
Figure 6.8.	Relationship between monthly CIWT (for months when the water table is consistently above the peat surface) and TRMM monthly rainfall.	173
Figure 6.9.	March 2014 water table time series for the 4 km Bondzale location and TRMM daily rainfall estimates for the Bondzale region.	173
Figure 6.10.	Relationship between TRMM monthly rainfall and rain gauge monthly rainfall for Epena village for the time period of February 2013 to April 2014.	174
Figure 6.11.	TRMM monthly rainfall estimates over the period of Jan. 2012 to Dec. 2014	175
Figure 6.12.	Bar plot of CDWT for all location where water tables were consistently above the peatland surface for October 2013 and December 2013.	177
Figure 6.13.	Mean Ca/Mg ratios for the rain, Likouala aux Herbes River and Ubangui River water samples.	180
Figure 6.14.	Surface peat and surface organic matter mean cation concentrations under swamp vegetation across the nine sites.	181
Figure 6.15.	Surface sample Ca/Mg ratios for the nine transects.	182
Figure 6.16.	Down core cation concentrations and loss on ignition values for the 6 km Bondoki core.	184
Figure 6.17.	Down core cation concentrations and loss on ignition values for the 6 km Bondzale core.	185
Figure 6.18.	Down core cation concentrations and loss on ignition values for 20 km Centre core.	186

Figure 6.19. Down core cation concentrations and loss on ignition values for the 9 km Ekolongouma core. 187
Figure 6.20. Down core cation concentrations and loss on ignition values for 5 km Ekondzo core. 188
Figure 6.21. Down core cation concentrations and loss on ignition values for the 6 km Itanga core. 189
Figure 6.22. Down core cation concentrations and loss on ignition values for the deepest Makodi core. 190
Figure 6.23. Down core cation concentrations and loss on ignition values for 6 km Mbala core. 191
Figure 6.24. Schematic showing water table depth across a flat surfaced peatland occupying a basin. 194
Figure 6.25. Peatland water table time series from Quistococha, a Peruvian lowland peatland, taken from (Lawson et al., 2014). 196
Figure 6.26. Atmospheric tides recorded in an atmospheric pressure time series presented in Zurbenko and Potrzeba (2013) 199
Figure 6.27. Schematic showing the Reverse Wieringermeer Effect. 202
Figure 6.28. Schematic showing the Lisse Effect. 202

List of Tables

Title		Page
Table 1.1	Lebrun and Gilbert (1954) classification of Congolese swamp forest.	8
Table 1.2	Evrard (1968) classification of Congolese swamp forest.	9
Table 1.3	Betbeder at al. (2014) wetland map EVI class description.	11
Table 1.4	Remote sensing derived values of wetland areas from the literature for the Congo Basin.	12
Table 1.5	Factors influencing peatland initiation.	15
Table 2.1.	Remote sensing products used to locate field sites.	45
Table 2.2.	Summary of sampling strategy for each site.	50
Table 2.3.	Information recorded for vegetation descriptions of vegetation plots.	52
Table 2.4.	Descriptions of vegetation classes encountered in the field and their association with peat.	57
Table 2.5.	Description of variations in land cover characteristics along the Bondoki transect.	60
Table 2.6.	Peat depth measurements under swamp forest vegetation.	65
Table 2.7.	Wetland classes (excluding open water classes) featured in vegetation maps of the Congo Basin/ Cuvette Centrale derived from classifications of remote sensing data.	67
Table 2.8.	Peat depths reported in the literature for lowland tropical peatlands.	72
Table 3.1.	Ground/flood water pH and conductivity along each transect.	79
Table 3.2.	Output from a One-way ANCOVA of where bulk density is the dependent variable, depth down-core is the covariate and core is the factor.	84
Table 3.3.	Comparison of mean peat bulk densities for hardwood swamp and palm dominated swamp for corresponding peat core depths using Wilcoxon–Mann–Whitney test.	92
Table 3.4.	Mean peat C and N concentrations and C/N ratios under hardwood swamp and palm dominated swamp for all samples and surface samples only.	92
Table 3.5.	Tropical peatland surface pH and electrical conductivity measurements.	94
Table 3.6.	Peat properties taken from the literature for lowland tropical peatlands in South East Asia and Amazonia.	97
Table 4.1.	Classification land cover classes.	106
Table 4.2.	Remote sensing products used in the maximum likelihood classifications in chapter 4.	107
Table 4.3.	Output from a One-way ANCOVA of where bulk density is the dependent variable, core is the factor and depth down-core is the covariate.	111
Table 4.4.	Land cover class area estimates from the 1000 maximum likelihood classifications.	115
Table 4.5.	Overall accuracy and accuracy per class for the peatland probability map derived from the 1000 maximum likelihood classifications.	115
Table 4.6.	Peatland belowground C estimates for the three different methods used to estimate peat C stocks.	120

Table 4.7.	Mean, standard deviation and standard deviation expressed as a percentage of the mean for the four variables used in estimating peatland belwoground C stocks.	120
Table 4.8.	Study region peatland belowground C estimates for the three different methods used to estimate peat C stocks.	121
Table 4.9.	Peatland total aboveground C for palm dominated swamp and hardwood swamp.	122
Table 5.1.	AMS Radiocarbon results for the 9 peat samples sent for analysis.	142
Table 5.2.	AMS Radiocarbon results for the mid-core peat samples from the three Ekolongouma cores.	143
Table 5.3.	Average peat accumulation rates and LORCA for each core with a radiocarbon dated basal sample.	145
Table 6.1.	Distribution of belowground pressure transducers across sites and along transects.	160
Table 6.2.	Water table data and peatland characteristics along each transects for the time period of 6th April 2013 to 30th March 2014.	166
Table 6.3.	Maximum positive rate of change in water table levels as recorded by the pressure transducers, across all location at the four sites.	169
Table 6.4.	Monthly evapotranspiration estimates for the Congo Basin derived from three studies: Matsuyama et al. (1994), Rodell et al. (2011) and Lee et al. (2011)	176
Table 6.5.	River and rain water pH and cation concentrations from the Likouala Department.	179
Table 6.6.	Origin of mineral material in surface and basal peat samples.	193
Table 6.7.	Maximum rainfall intensities recorded in tropical regions taken from the literature.	196
Table 6.8.	Congo Basin water chemistry data from this study and others.	207
Table 6.9.	Congo Basin water metal ratios from this study and others.	208
Table 6.10.	Cation concentrations of tropical surface peats taken from this study and the literature.	210

List of Abbreviations

aboveground biomass	AGB
aboveground carbon	AGC
accelerator mass spectrometry	AMS
Advanced Land Observation Satellite	ALOS
Advanced Spaceborne Thermal Emission and Reflection Radiometer	ASTER
African Humid Period	AHP
Bog Growth Model	BGM
calibrated year Before Present	cal yrs BP
Centrale Africa Mosaic Project	CAMP
cumulative decrease in water table	CDWT
cumulative increase in the water table	CIWT
Democratic Republic of Congo	DRC
diameter at breast height	DBH
digital elevation model	DEM
dissolved organic carbon	DOC
Earth Resource Satellite	ERS
electrical conductivity	EC
Enhanced Thematic Mapper	ETM+
enhanced vegetation index	EVI
European Space Agency	ESA
evapotranspiration	ET
Geoscience Laser Altimeter System	GLAS
Global Digital Elevation Map	GDEM
Global Rain Forest Mapping	GRFM
greenhouse gas	GHG
Holocene Peat Model	HPM
Ice, Cloud and Land Elevation Satellite	ICESat
inductively coupled plasma optical emission spectrometry	ICP-OES
Intertropical Convergence Zone	ITCZ
Japanese Earth Resources Satellite	JERS
Last Glacial Maximum	LGM
leaf area index	LAI
long-term rates of carbon accumulation	LORCA
loss on ignition	LOI
moderate resolution imaging spectroradiometer	MODIS

near infrared	NIR
organic matter	OM
particulate organic carbon	POC
Peat Decomposition Model	PDM
phased array L-band Synthetic aperture radar	PALSAR
Radar Forest Degradation Index	RFDI
rate of change	RC
Republic of Congo	ROC
Satellite Pour l'Observation de la Terre	SPOT
shortwave infrared water stress index	SIWSI
Shuttle Radar Topography Mission	SRTM
Synthetic Aperture Radar	SAR
The International Mire Conservation Group	IMCG
Thematic Mapper	TM
Tropical Rainfall Measuring Mission	TRMM
United Nation's Reduced Emissions from Deforestation and Forest Degradation in Developing Countries	UN REDD+

Chapter 1: Thesis Rationale and Background

1.1. Thesis Rationale

Tropical peatlands are now widely recognised for their important role in carbon storage, sequestration and, if disturbed, C emissions (Page et al., 2011, Page et al., 2002). However, a lack of data from peatland environments across the tropics means there are substantial scientific gaps in our knowledge of tropical peatlands. For Africa the knowledge of peatland occurrence, C storage and formation is particularly poor. However, within the wetlands of the central Congo Basin, referred to as the Cuvette Centrale, there is some evidence to suggest that there are peat deposits underlying the swamp forests, which reportedly could be up to 30 m thick (Markov et al., 1988). The Cuvette Centrale is located between both the Republic of Congo (ROC) and the Democratic Republic of Congo (DRC) and despite being the second largest tropical wetland in the world (Keddy et al., 2009), is one of the most poorly studied terrestrial regions on Earth. It is estimated that 3 Pg C could be stored within the peatlands of the ROC and DRC (Page et al., 2011). However, the lack of empirical data from these two countries means that current estimates of peatland extent and C stocks are unsubstantiated. Furthermore, to this day there appears to be no published empirical data confirming the presence of peatlands in the Cuvette Centrale.

In this thesis I address the uncertainty surrounding the peatlands of the Cuvette Centrale, by using field and laboratory measurements to firstly confirm the presence of peat within the region, then secondly, to characterise the peatlands in terms of their vegetation and peat properties and, in combination with remote sensing data, their surface topography. Through the classification of remote sensing data, I map and quantify peatland extent, which I then combine with *in situ* data to provide the first empirically based estimates of peatland C stocks for the Cuvette Centrale. I then consider the factors which may have led to and affected peat initiation and development through time. Finally I identify the hydrological mechanisms which maintain the peatlands in the present day. After summarising the main findings of this project, I consider the implications of this work in terms of policy, identifying potential threats to these peatlands and the priorities for future research.

1.2. Thesis Outline

Chapter 1. In this chapter I provide a review of the key background literature to the thesis. More specifically I summarise the state of knowledge of the Congo Basin and its wetlands. I review peat literature in terms of its definition, formation and role in the C cycle, alongside a brief overview of the distribution of tropical peatlands before a more

detailed investigation of what is known of African peatlands, in particular peatlands of the Cuvette Centrale.

Finally I provide a detailed site description of the Cuvette Centrale and more specifically the Likouala Department, Republic of Congo (ROC), where fieldwork was undertaken.

Chapter 2. In this first data chapter a remote sensing methodology used to identify potential peatland sites within the Cuvette Centrale is described and evaluated. Data on peatland vegetation, peat depth and topography are presented and discussed.

Chapter 3. This data chapter presents and discusses data on Cuvette Centrale peat properties, specifically; C concentration, N concentration, bulk density, organic matter content and surface pH and electrical conductivity.

Chapter 4. This data chapter uses ground truth field data to classify remote sensing data in order to map peatland extent, which is then combined with data from Chapter 2 and 3 to estimate peatland C stocks for the entire Cuvette Centrale.

Chapter 5. This data chapter uses peat radiocarbon dating to determine the timing and process of peat initiation and development in the Cuvette Centrale.

Chapter 6. This data chapter uses hydrological data measured *in situ* and remotely, alongside geochemical data to determine the hydrological mechanisms which maintain the Cuvette Centrale peatlands today.

Chapter 7. This chapter summarises the main conclusion of the thesis and discusses the implications of these findings in terms of policy and potential threats faced by these peatlands. Finally recommendations are made for areas of research that should be prioritised in future work.

1.3. Literature Review

1.3.1. Central African Rain Forest

Central Africa is dominated by the second largest block of tropical rainforest (Hansen et al., 2013), covering approximately 2,490,000 km^2 (Parmentier et al., 2007). The majority of this rainforest is located in the Congo Basin, with the Democratic Republic of Congo (DRC) containing around half of this forest and the rest being largely distributed across the Republic of Congo (ROC), Cameroon and Gabon (Primack and Corlett, 2005, Mayaux et al., 2004). The most noticeable difference between African rainforests and those of South America and South East Asia is a lower plant species diversity (Parmentier et al., 2007, Primack and Corlett, 2005) and a lower stem density (Lewis et al., 2013) in African rainforest. Aboveground biomass (AGB) of African rainforest is, however, similar to South

East Asian rainforest and generally higher than Amazonian rainforest (Lewis et al., 2013). A unique feature of African rainforest is the occurrence of large-scale patches of monodominant forest. Although patches of monodominant forest can be found in rainforests elsewhere in the world, in Central Africa monodominant patches can stretch over areas that are hundreds of square kilometres (Primack and Corlett, 2005).

Climate, on average, also differs between African rainforests and those of South East Asia and Amazonia. Overall African rainforests have a drier, more seasonal climate, with annual rainfall ranging from 1500-2500 mm yr^{-1}(Primack and Corlett, 2005). This compares to an annual rainfall of 2000-3000 mm yr^{-1} for Amazonia and ca. 3000 mm yr^{-1} or more for South East Asia (Primack and Corlett, 2005). The lower diversity of African rainforests is linked to the palaeoclimatic history of the continent. A change to cooler drier climates in the Early and Middle Miocene saw a contraction in forest extent, but coinciding with continental uplift, meant there were few suitable refuges for lowland forests to persist. The result was high extinction rates. The mid and late Pliocene was another period of large scale extinction, again linked to a change to a cooler, drier climate (Morley, 2000). Whilst forests re-expanded during periods of higher precipitation, biodiversity levels did not recover to their original levels (Parmentier et al., 2007, Morley, 2000). This is thought to be the cause of a general absence of tree species adapted to higher moisture regimes (Parmentier et al., 2007).

In contrast to the tree species diversity, African rainforest is known to have much higher species diversity of large mammals and primates than South America or Asia, which include species such as the African elephant (*Loxodonta cyclotis*), hippopotamus (*Hippopotamus amphibious*) and the western lowland gorilla *(Gorilla gorilla gorilla*) (Primack and Corlett, 2005, Hughes and Hughes, 1992). These large mammals play an important role in determining the structure and composition of the rainforest, through for example creating and maintaining openings (Omeja et al., 2014, Primack and Corlett, 2005) and through seed dispersal, particularly large seeded species (Effiom et al., 2013, Vanthomme et al., 2010, Beaune et al., 2013, Blake et al., 2009). It has also been suggested that animal seed dispersal not only affects species composition, but also the carbon (C) storage of the forest, as species dependent on animal-dispersal tend to be slow growing, longer lived and have a higher wood density; their replacement with lower density tree species (Brodie and Gibbs, 2009) or a higher liana abundance (Jansen et al., 2010) may reduce the overall forest C stocks. Therefore the increased hunting pressure over recent decades not only threatens animal biodiversity but also could have significant impacts on forest structure, biodiversity and C storage (Abernethy et al., 2013).

Although humans have been present in Central Africa far longer than any other tropical region, the impact of human activity in this region has been much less severe (Primack and Corlett, 2005). Deforestation rates remain some of the lowest for tropical regions (Kim et al., 2015) and have been in decline in recent years (Mayaux et al., 2013), although some countries have seen an increase (Kim et al., 2015). The low deforestation rates are mainly attributed to mineral and oil dependent national economies in Central Africa, rather than industrial-scale agriculture as major export revenue generators (Rudel, 2013). The development of these sectors has caused rural to urban migration and stronger economies have permitted the cheap importation of food, reducing the demand for and viability of an industrialised agriculture sector (Rudel, 2013). All of this has resulted in rural regions which lack infrastructure, preventing large scale exploitation of the forests (Justice et al., 2001), and with low density and poverty stricken populations, where small scale agriculture is one of the main drivers of deforestation (Rudel, 2013). This compares to South East Asia and Amazonia, where large scale, industrialised agriculture and forest plantations are one of the biggest causes of deforestation (Rudel, 2013).

1.3.2. The Congo Basin

The Congo Basin, located between 9°N and 14°S and longitudinally between 11°E and 31°E (Laraque et al., 2009), is the second largest drainage basin in the world, draining in total 3.7 million km^2 (12% of the African continent; Keddy et al., 2009). It is an intracratonic basin i.e. it is located within the continental interior, away from the influence of the plate margins and is subsiding slowly (Crosby et al., 2010, Buiter et al., 2012). Despite its size, the Congo Basin is grossly understudied. There is general consensus that Congo Basin subsidence was initially the result of a Neoproterozoic rift (Crosby et al., 2010, Daly et al., 1992, Kadima Kabongo et al., 2011). However, why the Congo Basin continues to subside is unknown, although a number of competing theories have been put forward. These include the presence of dense material at the base of the lithosphere causing subsidence (Hartley and Allen, 1994), convective down-welling possibly caused by the detachment of cooler dense material at the base of the lithosphere (Simmons et al., 2007, Downey and Gurnis, 2009) or by small mantle plumes rising below the basin edges (Crosby et al., 2010, Forte et al., 2010), subsidence driven by tectonic uplift of swells surrounding the basin (Sahagian, 1993), or finally, subsidence as a result of increased sediment load (Buiter et al., 2012). The geology of the sediments that fill the basin is not well determined; only four deep wells have been drilled for the entire basin (Buiter et al., 2012, Kadima et al., 2011). Of what is known it can be said that the geology of the Congo Basin varies from cretaceous rock outcrops in the south, Triassic to Jurassic rock in the south-west and east, to a much younger geological surface of Holocene alluvium in the north-west of the Congo Basin (Master, 2010).

Within the centre of the Congo Basin is the low lying bowl shaped hydrological drainage basin of the Congo River and its tributaries referred to as the Cuvette Centrale. Almost entirely wetland, the Cuvette Centrale is the second largest tropical wetland in the world (Keddy et al., 2009). The terms "Congo Basin" and "Cuvette Centrale" are used interchangeably for both the intracratonic basin as well as the smaller bowl shaped hydrological basin (Kadima et al., 2011). For clarity in this work the term "Congo Basin" refers to the entire intracratonic basin, whilst the term "Cuvette Centrale" refers specifically to the bowl shaped hydrological basin. The Cuvette Centrale lies between both the ROC and the DRC. In the ROC the Cuvette Centrale is the largest drainage basin, draining 232,320 km^2 of the country, which covers most of the eastern side (Hughes and Hughes, 1992), whilst in the DRC it covers a much larger area of 774 562 km^2 (Hughes and Hughes, 1992). The bowl-shaped topography of the Cuvette Centrale is very gentle with altitudes only varying between 324-330 m a.s.l. within the ROC and between 310-500 m a.s.l. within the DRC (Hughes and Hughes, 1992). The Cuvette Centrale is located in the area of the Congo Basin underlain by Holocene alluvium (Master, 2010), which as a result of the low gradients experiences very little erosion (Laraque et al., 2009).

Although thought to be part of a cratonic mass, evidence suggests that the Cuvette Centrale is not seismically inert; aeromagnetic surveys have identified a series of north-east, south-west trending faults and horsts within the Cuvette Centrale (Master, 2010). These faults and horsts have been put forward as explanations for a number of distinctive features of the Cuvette Centrale. Firstly, despite the low gradient of the landscape, which might be expected to encourage river meandering, many of the rivers of the Cuvette Centrale are noted to follow very straight paths. It is thought that these fault lines confine the rivers, at least along part of their course (Master, 2010, Kadima et al., 2011). Secondly, there are a number of isolated, extremely shallow lakes, which include the well-known and distinctive Lac Télé in the ROC and Lac Tumba in the DRC. Lac Télé is particularly distinctive being almost circular in shape and there was once speculation that it was of impact origin (Laraque et al., 1998). Master (2010) however, has disregarded this theory, as some aspects of the lake geometry are inconsistent with an impact event and there is a lack of impact features such as an overturn rim, ejecta blanket and a central uplift. Furthermore, an impact origin ignores the presence of the other isolated, shallow lakes in the region. Like the rivers, it has been hypothesised that the lakes are a result of fault lines. In a low gradient landscape, even a subtle fault line could be enough to inhibit drainage and cause pooling of water (Master, 2010). The shallow nature, circular shape and presence of pioneer wetland species surrounding Lac Télé and other lakes in the region suggest that these lakes are slowly terrestrialising (Master, 2010). An alternative theory put forward is that the lakes in the region are the remnants of a much larger lake that once

filled the Cuvette Centrale (Goudie, 2005). The idea of a Palaeo-lake Congo comes from an article by Peters and O'Brien (2001) and has been cited by others e.g. Inogwabini et al. (2013) and Reynolds et al. (2011). However care should be taken when citing the article by Peters and O'Brien (2001); the authors do not present any actual evidence for the existence of a lake other than a hypothetical map based on work by de Henizelin (1963) and Cahen (1954). Cahen (1954) states that there was a lake in the Cuvette Centrale in the Pliocene, but it is not clear where he/she derived this idea. Likewise, de Heinzelin (1963) presents a map of Neogene Africa, which he/she describes only as "tentative" and "inexact" and states that the idea of lakes occupying the major African basins may "not necessarily be true". Even Peters and O'Brien (2001) themselves describe their map as "highly conjectural", but say that this hypothetical lake could have been present as recently as the Early Pleistocene, before being drained by a coastal river breach. Yet this idea seems unlikely given that a depocentre of sediments thought to be of Albian-Turonian age have been identified beneath the Cenozoic Congo deep-sea fan, suggesting that the Congo River has been draining the interior of the Congo Basin possibly as far back as the Late Cretaceous and has been suggested to follow a course similar to the one today (Anka et al., 2010). Whether the result of fault lines inhibiting drainage or the remnants of a palaeo-lake, a large proportion of the Cuvette Centrale is now covered by swamp forest.

1.3.3. Swamp Forest Vegetation in the Congo Basin

The literature available on the ecology of the Congo Basin wetlands is very limited, with the majority of publications dating back some years. In particular there is a distinct lack of information on swamp forest vegetation (Keddy et al., 2009). The literature available can largely be categorised into two groups. The first group consists mainly of publications dating back to the 1950s up until the 1990s and provides quite general descriptions of the area and the vegetation classes found within this wetland. The second group is the more recent literature that has been published in the last 15 years or so and has largely been concerned with delineating and mapping varying vegetation classes in the Congo Basin through the use of remote sensing. Overall there is a lack of consistency in the way in which the swamp forest vegetation, the general distribution of which is shown in Figure 1.1, is described and classified. This probably results from the fact that the literature is so scarce and spans a considerable period that there has been no requirement to standardise the vegetation classes.

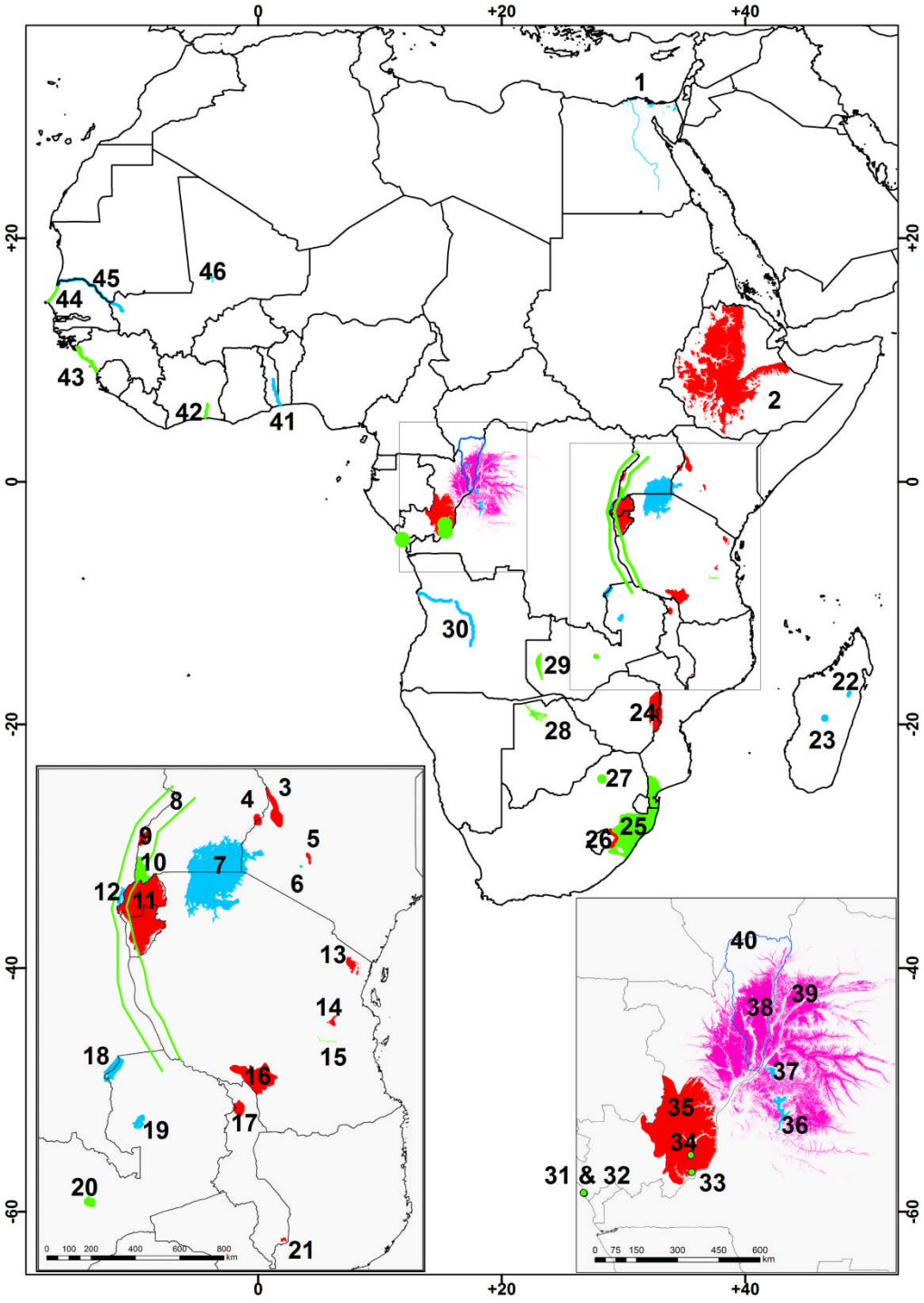

Figure 1.1. Location map of Africa showing many of the places referenced in the text of this literature review. Colours correspond to: Blue) water bodies and rivers; Red) highland regions; Green) other; Pink) Cuvette Centrale swamp forests. The bottom right inset shows an enlargement of the Republic of Congo and the Cuvette Centrale. The bottom left inset shows an enlargement of the East African region. Each feature is number and refers to: 1) River Nile and Nile Delta; 2) Ethiopian Plateaux (highlands); 3) Cherangani Hills; 4) Mt. Elgon; 5) Aberdare Range; 6) Lake Naivasha; 7) Lake Victoria; 8) Western Rift Valley; 9) Rwenzori Range; 10) Kigezi Region; 11) highlands of Rwanda and Burundi; 12) Lake Kivu; 13) Usambara Mountains; 14) Lukwangule Plateau; 15) Ruaha; 16) Kipengere Range; 17) Nyika Plateau; 18) Lake Mweru; 19) Lake Bangweulu; 20) Lukanga Swamp; 21) Mulanje Massif; 22) Lake Aloatra; 23) Tritrivakely Lake; 24) Inyanga Mountains; 25) Maputaland coastal plain; 26) Drakensberg Range; 27) Waterberg Range; 28) Okavango Delta; 29) Upper Zambezi Valley; 30) River Cuanza; 31) Songolo; 32) Coraf; 33) Ngamakala Pond; 34) Bois de Bilanko; 35) Plateau Batéké; 36) Lac Mai-Ndombe; 37) Lac Tumba; 38) Lac Télé; 39) Cuvette Centrale; 40) Likouala Department; 41) River Mono; 42) Agneby Marsh; 43) Guinean Coast; 44) Niayes region; 45) Senegal River; 46) lakes surrounding Timbuktu, Mali.

However, there seems to be a general consensus that the swamp forest in the Cuvette Centrale can be divided into forest which is permanently inundated and forest which is, to varying degrees, periodically inundated. Lebrun (1936b) (cited in Richards (1952)) describes periodically inundated forest as being relatively species poor and lacking a herb layer. Tree density is described as being less than typical *terra firme* forest. Species present include those from the genera *Chrysophyllum*, *Cynometra*, *Maba*, *Oubanguia* and *Uapaca*. Permanently inundated forest is reported as having a higher tree species diversity and higher tree density than periodically inundated forest, with a species rich undergrowth. Dominant species include *Chrysophyllum laurentii*, *Uvariastrum pynaertii* and species of *Parinari, Mitragyna, Copaifera* and *Uapaca*, with these last three genera tending to form relatively homogeneous stands. However, at a later date Lebrun and Gilbert (1954) (cited in Richards (1996)) and Evrard (1968) categorise swamp forest of the Congo Basin into several forest associations. Lebrun and Gilbert (1954) group Congolese swamp forest into five forest associations determined by varying periods of inundation (Table 1.1).

Table 1.1. Lebrun and Gilbert (1954)'s classification of Congolese swamp forest based on period of inundation (cited in Richards (1996)).

Class	Description
Forets ripicoles colonisatrices	Pioneer communities of shrubs and small trees continually or almost continually flooded and actively promoting soil accretion.
Forets riveraines	Riverine forests with long periods of submergence and short periods of emergence and moderate accretion.
Forets periodiquement inondees	Periodically flooded forests with long periods of emergence and little accretion.
Forets marecageuses	Swamp forest which never dries out, whether periodically flooded or not.
Alluvial valley forests	Liable to flooding but normally well drained.

Evrard (1968), on the other hand, categorises the forest on the basis of vegetation succession, with several categories of seral community and what he describes as the two main types of mature swamp forest, providing some species names associated with these forest communities (Table 1.2). Hughes and Hughes (1992) provide an extensive list of swamp forest species present in the Congo Basin. However, they do not give any indication as to which species are dominant, which associations occur or whether particular species are associated with permanently or periodically inundated forest. As the presence of peat is at least partially determined by the degree to which the organic matter (OM) is exposed to oxic conditions (see Section 1.3.6), being able to easily distinguish between vegetation

communities which are associated with permanently or periodically inundated conditions could be a key way to quickly identify likely areas of peat deposits.

Table 1.2. Evrard (1968)'s classification of Congolese swamp forest based on forest succession.

<table>
<tr><th colspan="5">Seral Forest</th></tr>
<tr><td>Alchornea cordifolia thickets.</td><td>A Macaranga lancifolia- Harungana robynsii association.</td><td>An association of the palm Raphia laurentii.</td><td>A Raphia sese association.</td><td>A Uapaca heudelotii- Parinari congensis association.</td></tr>
<tr><th colspan="5">Mature Forest</th></tr>
<tr><td rowspan="2">Seasonally flooded Oubanguia africana- Guibourtia demeusii association- an A storey at 35-40m and a B storey at 20-25m, canopy cover of about 60-90%. Below is a close packed layer of trees 8-15m high and scanty undergrowth. Oubanguia africana and Scytopetalum pierreanum most abundant species where there is rapid flow of flood water. Guibourtia demeusii dominates where current is less strong. Have flanged tree trunks rather than buttressed trunks.</td><td colspan="4">Entandrophragma palustre-Coelocaryon botryoides alliance divided into two associations, both of which are found on permanently waterlogged organic soils.</td></tr>
<tr><td colspan="2">a) Rothmannia megalostigma- typical of wide depressions where flood water is impounded by natural levees, having had most of its sediments removed so that only organic matter is really left. Under these conditions peaty soils form and there is an even ground surface.</td><td colspan="2">b) Lasiodiscus mannii- prefers sites where the stream drains into wide low lying valleys, carrying sand in suspension during floods. Soil is a mixture of sand and OM. Develops a hummocky surface which is stabilised by tree roots. The taller trees in this association only reach 25-35m. Shallow root systems and expanded bases with conspicuous flutings or indistinct buttresses. Pneumorhizae (aerial roots) are common.</td></tr>
</table>

Owing to its size and inaccessibility, the development of remote sensing techniques has brought new opportunities to map the vegetation communities of the Congo Basin, which would not have been possible from the ground. Synthetic aperture radar (SAR) data has been particularly valuable, offering continuous coverage of the Congo Basin and, with microwaves able to penetrate through clouds, it overcomes the problem of persistent cloud cover (Mayaux et al., 2004), which can seriously hinder the usefulness of optical data for mapping in this region (Lindquist et al., 2008). For the detection of wetlands SAR has proved especially useful. Firstly, it has been noted that whilst lowland rain forest has quite a diverse canopy cover in terms of species composition and age distribution, swamp forest, by comparison, tends to be more homogenous in terms of species composition and stand height (De Grandi et al., 2000a, Mayaux et al., 2002). In terms of the textural properties of the radiation backscatter this results in a smooth texture associated with swamp forest and a rougher texture associated with lowland rain forest (De Grandi et al., 2000a, Mayaux et al., 2002). De Grandi et al. (2000b) took advantage of these properties to produce one of the first classifications of swamp forest vegetation in the Congo Basin; using the Centrale Africa Mosaic Project (CAMP) datasets, which are derived from the European Space Agency (ESA) Earth Resource Satellite (ERS) C-band SAR, they produced a 200 m resolution map of the entire Congo Basin delineating areas swamp forest and lowland rain forest. In the same year a second map of swamp forest vegetation in the

Congo Basin was published by De Grandi et al. (2000a), again at a 200 m resolution but this time using the Global Rain Forest Mapping (GRFM) project Japanese Earth Resources Satellite (JERS)-1 L-band SAR mosaic. The longer wavelength of L-band means that, unlike C-band, the signal can penetrate the forest canopy and reach the forest floor. In swamp forests where standing water is present, the proportion of the L-band radar signal returned to the sensor is higher owing to what is known as the double bounce mechanism, whereby the radar signal first interacts with the tree trunks and then is reflected off the standing water back towards the antenna (Richards et al., 1987, Hess et al., 1990). This means that areas of inundated forest should appear brighter in radar imagery relative to non-inundated forest. The map by De Grandi et al. (2000a), produced using L-band, included a swamp forest class and an inundated forest class in addition to two classes of lowland rain forest and a savannah/grassland class. Although not specifically stated by the authors, it is assumed here that the inundated forest class of De Grandi et al. (2000a) is meant to represent areas of permanent inundation, whilst the swamp forest class is only periodically inundated. Following on from these two classifications Mayaux et al. (2002) went on to use the CAMP and GRFM SAR datasets in combination to produce another 200 m resolution classification of the Cuvette Centrale. Similarly to de Grandi et al. (2000a), they included a periodically and permanently inundated forest class and also included a swamp grassland class. This classification was later incorporated in the 1 km resolution 2000 land-cover map of Africa (Mayaux et al., 2004).

Despite the challenges of creating a cloud free mosaic, optical data have been used to map the vegetation communities of the Congo Basin. With a daily temporal resolution, Vancutsem et al. (2009) were able to use the large Satellite Pour l'Observation de la Terre (SPOT)-VEGETATION imagery dataset to create cloud free mosaics for the entire DRC for two time periods; December to January and May to June. With the Congo Basin straddling the equator, having mosaics from two different seasons is an advantage, as the inverse seasonality means that the same vegetation communities north and south of the equator can be at different phenological stages and appear as different vegetation classes in the imagery. The classification run using SPOT-VEGETATION imagery produced 18 vegetation classes for the DRC, of which three were wetland classes: edaphic forest, aquatic grassland and swamp grassland. The authors state that the edaphic forest, however, is an amalgamation of multiple types of wetland forest, such as temporarily flooded forest, swamp forest and riparian forest. They also acknowledge that in their vegetation map, the edaphic class is possibly under-represented, owing to the relatively course spatial resolution (1km) of SPOT-VEGETATION and the tendency for this class to form narrow, linear strips along river courses. Gond et al. (2013) also use optical data to map forest of the Congo Basin. Specifically, they used two moderate resolution imaging

spectroradiometer (MODIS) products, the enhanced vegetation index (EVI) data and the Surface Reflectance data, with the latter product being used to calculate a shortwave infrared water stress index (SIWSI), to run an unsupervised classification. Parameters of the classification were adjusted until the classification output was visually similar to the 1 km resolution 2000 land-cover map of Africa by Mayaux et al. (2004). Their final map included two swamp classes: swamp forest and swamp. For map validation forest inventory data and a vegetation map of Cameroon was used, however it appears that no forest plots from within the swamp region were used in the validation process.

The three of the most recent attempts to map the wetlands of the Congo Basin have also made use of optical data but in combination with SAR and elevation data. These studies take quite different approaches to each other and the preceding studies discussed above. Rather than mapping different vegetation classes, Bwangoy et al. (2010) used a combination of Landsat Thematic Mapper (TM) and Enhanced Thematic Mapper (ETM+), JERS-1 L-band SAR data and Shuttle Radar Topography Mission (SRTM) elevation data to produce a wetland probability map for the Congo Basin, where each pixel has a percentage probability of containing wetland. Bwangoy et al. (2013) went on to produce an updated version of this map, using higher resolution SAR and SRTM elevation data for the DRC only, which they used to assess the vulnerability of wetlands within the DRC to deforestation. The most recent map by Betbeder et al. (2014) is perhaps the most interesting. A combination of MODIS EVI imagery was used to first classify the Cuvette Centrale into vegetation classes. This was then compared with the results of a non-supervised classification of phased array L-band SAR (PALSAR) data from two acquisition dates and with elevation data from the Ice, Cloud and Land Elevation Satellite (ICESat) Geoscience Laser Altimeter System (GLAS) instrument. Each EVI vegetation class was then assigned inundation, elevation and canopy height characteristics. From this Betbeder et al. (2014) tried to label their classes using a combination of the classification scheme developed by Evrard (1968) (shown in Table 1.2) and an Amazonian wetland classification by Junk et al. (2011). Table 1.3 shows their four EVI classes and descriptions.

Table 1.3. Betbeder et al. (2014)'s wetland map EVI class description for the Cuvette Centrale.

EVI Class	Description
EVI 1	Forests subjected to seasonal flood pulse, located alongside rivers.
EVI 2	Forests subjected to stable water levels, average elevation of 304 m and a maximum canopy height of 20 m.
EVI 3	Forests subjected to seasonal short lasting flood pulses, with low amplitude, an average elevation of 306 m and a maximum canopy height of 30 m.
EVI 4	Non-flooded forests, average elevation of 311 m and a maximum canopy height of 40 m.

Although each study differs in their categorisation of swamp vegetation, the general distribution of the various swamp vegetation classes are similar between the different wetland maps. Not all studies provide a value for swamp area; however, of the studies which give do values, there are some differences (Table 1.4). One important point to note is that all the classifications were either unsupervised or used training data derived from the visual inspection of Landsat imagery or national or regional vegetation maps. Even more importantly, all maps, with the exception of Bwangoy et al. (2010) who make use of some forest plot data, were validated using vegetation maps and high resolution imagery rather than ground truth points. Whilst cost and logistics make obtaining data difficult, without field data, one can never be sure that, in an area as understudied as the Congo Basin, the labels given to each class are a fair representation of what is actually occurring on the ground.

Table 1.4. Values of wetland area for the Congo Basin derived from classifications of remote sensing data.

Study	Area (km^2)	Notes
Mayaux et al. (2004)	9360	Wetland area for the DRC and ROC. Unclear as to whether this also includes mangrove forest and swamp grasslands.
Vancutsem et al. (2009)	102,452	Area of edaphic forest for the **DRC only**.
Bwangoy et al. (2010)	359,556	Area of pixels with a ≥50 % probability of being wetland.
Betbeder et al. (2014)	230,000	Combined area of seasonally flooded and permanently flooded forests (i.e. EVI classes 1 to 3 shown in Table 1.3).

1.3.4. Peat Definition

The term "peat" is used widely with little consensus on the actual definition of what constitutes peat. In general terms peat is a surface layer of soil comprised of semi-decomposed vegetation, with a very high organic matter (OM) content which has usually arisen, at least in part, through waterlogging-induced anoxia. Variations in the definition of peat are usually related to the depth and OM content of the peat, with required minimum depths ranging from 30-50 cm and OM contents from 30-75% (Beek et al., 1980, Charman, 2002, Page et al., 2011, Limpens et al., 2008, Joosten, 2009, Lähteenoja et al., 2009b). This lack of consistency when defining peat means it is difficult to make direct comparisons between published datasets. This situation is made worse by the fact that many studies do not state their definition of peat e.g. Anshari et al. (2010), Beilman et al. (2008), Buffam et al. (2010).

1.3.5. Hydrological and Geochemical Classification of Peatlands

In the simplest terms classifications of peatland systems are largely related to the hydrological functioning and trophic status of the peatland. The most universal and clearly

defined terms are “ombrotrophic” and “minerotrophic” peatlands. An ombrotrophic peatland is one where the water table is maintained by precipitation alone and the only nutrient inputs to the system are from atmospheric deposition (Rydin and Jeglum, 2006, Charman, 2002). A minerotrophic peatland is one which, in addition to precipitation, receives water inputs from other sources e.g. ground water flow, runoff or a water body and as a result has additional sources of mineral input to that of atmospheric deposition (Charman, 2002, Rydin and Jeglum, 2006). Beyond these two categories is a vast array of subdivisions based on further hydrological and trophic specifications as well as vegetation, peatland morphology, developmental history and geographical location. However, because different countries or research groups apply different terminologies or apply different definitions to the same terminology (for examples see Taylor, 1983, Ruuhijärvi, 1983, Botch and Masing, 1983, Hofstetter, 1983, Zoltai and Pollett, 1983, Thompson and Hamilton, 1983) and because there is an overlap in colloquial and scientific terminology, there is a great deal of confusion in the literature when peatland classes are referred to (Charman, 2002, Rydin and Jeglum, 2006, Moore and Bellamy, 1973, Moore, 1987). As an example the word “mire” is considered by some to specifically refer to all peatland types (Ruuhijärvi, 1983), whilst it can also be used as a general word for wetland (Charman, 2002). Likewise, the term “swamp forest” is often considered to imply a minerotrophic forested wetland (Moore, 1987, Rydin and Jeglum, 2006), however in tropical settings where a large proportion of peatlands are forested, the vegetation is frequently described as “swamp forest” whether the peatland is minerotrophic or ombrotrophic (e.g. Lähteenoja et al., 2009a, Page et al., 1999). If these classification systems cause more confusion than insight, then they do not serve much purpose and should probably not be implemented. However, even the terms ombrotrophic and minerotrophic are not as clear cut or informative as they initially appear. Firstly a peatland can be both minerotrophic and ombrotrophic in parts. For example, if climatic conditions are wet enough, peat accumulation in a minerotrophic peatland may continue above the influence of water table, leading to the development of a peat dome. In this instance the top of the peat profile is ombrotrophic whilst the bottom of the profile and areas surrounding the dome are minerotrophic (Rydin and Jeglum, 2006). Another example is a peatland with a hummock-hollow system. Here the hollows can be in receipt of ground water flow, whilst the hummocks can be permanently above its influence (Moore, 1989). Secondly, the trophic status of an ombrotrophic and a minerotrophic peatland may not necessarily be very different, if for instance mineral input from atmospheric deposition is high, which can be the case in coastal, volcanic or industrialised regions (Moore and Bellamy, 1973, Charman, 2002). Likewise, depending on the geological setting, degree of erosion and rate of flow, water inputs from groundwater, runoff or

flooding may not necessarily have a high mineral concentration (Moore and Bellamy, 1973, Charman, 2002).

1.3.6. Peat Initiation

In order for peat formation to occur, organic productivity must exceed decay (Charman, 2002, Moore, 1989, Moore, 1987). Being a wetland soil, for all peatlands this is at least partially the result of anoxic conditions driven by waterlogging, resulting in reduced microbial activity. However, high levels of acidity, low nutrient concentrations, low temperatures, low litter quality and physical inaccessibility of the OM can also play a role in limiting microbial activity and therefore retarding decomposition (Moore, 1989, Moore, 1987, Clymo, 1983). Additionally, in some ecosystems the positive balance between accumulation and decomposition can partly arise from high levels of OM production (Moore, 1987, Moore, 1989, Clymo, 1983).

With waterlogging being the one fundamental precondition to peat formation, conventionally it has been thought that peat initiation results from two mechanisms: terrestrialisation and paludification. Terrestrialisation is the process by which a water body gradually becomes infilled with OM (Charman, 2002, Sjörs, 1983, Rydin and Jeglum, 2006). This process can be aided by a drop in lake levels through, for example, a change to a drier climate, allowing vegetation to encroach further into the lake (Ruppel et al., 2013). Peatlands formed through terrestrialisation will tend to have a fairly consistent increase in peat depth towards the interior of the peatland which is a result of the basin shape. Another indication of the process of terrestrialisation is the presence of gyttja or lake muds underlying the peat deposit and overlying the mineral substrate (Ruppel et al., 2013).

Paludification is the process by which relatively dry terrestrial environments become waterlogged through a change in local hydrological conditions. This in turn slows the decomposition of OM allowing the initiation of peat formation (Charman, 2002, Sjörs, 1983, Rydin and Jeglum, 2006). This change in hydrological conditions can be brought about by a number of factors briefly summarised in Table 1.5. Whilst it may be a single influential factor which leads to peat initiation, it may also be a combination of factors. For example Pajunen (1996) describes how lava flows were necessary for the formation of hydrological basins in the highlands of Rwanda and Burundi, but peat initiation did not happen until there was also a shift to a more humid climate.

Table 1.5. Factors influencing hydrological conditions and therefore peatland initiation (adapted from Charman (2002) with additional examples taken from Pajunen (1996) and Ruppel et al. (2013)).

Factor	Examples
Climate	Changes in precipitation and evapotranspiration affecting the water balance. Changes in sea level leading to changes in the base level and on shore drainage.
Pedogenic processes	Change in soil properties leading to reduced vertical drainage, for example podzolisation and formation of an iron pan.
Vegetation	Change in vegetation community which leads to a change in soil moisture conditions, for example loss of tree coverage can lead to reduced evapotranspiration allowing waterlogged conditions to develop.
Geomorphology	Subsidence or uplift changing drainage patterns and changing base levels. Damming of depressions through for example lava flows or landslides.
Anthropogenic activities	Deforestation leading to waterlogged soils. Burning of vegetation leading to reduced porosity of soil through high charcoal presence.

Once peat formation has begun, peatland autogenic processes can influence water tables adjacent to the peatland and allow the peatland to spread laterally. Therefore an indication of paludification is much younger basal ages at the peatland margin than the peatland interior (Charman, 2002).

Although not always seen as being distinct from paludification (Charman, 2002), there is a third mechanism of peat initiation, termed "primary mire formation" (Ruppel et al., 2013, Kuhry and Turunen, 2006, Rydin and Jeglum, 2006, Sjörs, 1983). Primary mire formation is when peat forms directly on to a wet mineral soil, which has recently been exposed through, for example, deglaciation, a drop in sea levels or crustal uplift exposing continental margins or a recently deposited mineral soil (for example volcanic deposits or alluvial plains) (Ruppel et al., 2013, Kuhry and Turunen, 2006, Sjörs, 1983, Rydin and Jeglum, 2006). The key difference between this and paludification is that, under primary mire formation, the mineral soil did not first go through a dry terrestrial phase prior to peat formation. Ruppel et al. (2013), who argue for a distinction to be made between the two, say that primary mire formation can be identified in the field by peat directly overlying inorganic sediments such as sand, gravel or clay, whilst peat formed through paludification will have an organic soil layer separating the peat and underlying mineral horizon, which is remnant of the vegetation communities preceding peat initiation. However, as the authors acknowledge, there are instances where a mineral soil or bare rocks may be exposed for a long time before peat initiation occurs, but without

experiencing any intermediate soil development. The example Ruppel et al. (2013) give is peat development on glacial moraines, which may have been exposed for several millennia before peat initiation occurs. Ruppel et al. (2013) also argue that there is a distinction to be made between paludification and lateral expansion of peatlands, arguing that the latter can occur at any peatland site following on from any of the three processes of peat initiation. The important point here is not what terminology should be applied, but that peatland initiation and development can be complex, with regions or individual sites sometimes having developed through multiple processes. However, as Ruppel et al. (2013) acknowledge, it may not always be possible to distinguish between these processes. Furthermore, there may also be uncertainty in what are the causes of initiation and what is merely correlated with peat initiation. For instance, Charman (2002) gives the example of reduced tree cover and peat initiation: whilst reduced tree cover could be the cause of peat initiation through reduced evapotranspiration (ET) leading to waterlogging, it could also be that both reduced tree cover and peat initiation are the result of climatic factors and are merely coincident with one another. In this instance, determining cause or correlation from palaeorecords could be impossible.

1.3.7. Peat Accumulation

Understanding the process of peat accumulation and development is complicated by the fact that peatland properties and processes which affect OM accumulation and decomposition vary spatially (both vertically and laterally) and also temporally. External controls can cause variability, but even in their absence, variability of these properties would still occur as a result of internal processes and feedbacks (Belyea and Baird, 2006). Models are often used to aid understanding of peatland development. One of the original and very widely cited conceptual models of peatland development Clymo's (1984) peat Bog Growth Model (BGM). In the BGM a peat profile is comprised of two distinct zones, the acrotelm and the catotelm. These terms were first coined by Ingram (1978). The acrotelm refers to the surface layer of the peatland which sits above the water table for at least part of the year, and therefore conditions are periodically anaerobic. The catotelm is the lower layer of peat which is permanently below the water table and therefore conditions are permanently anoxic. The acrotelm and catotelm are also said to differ in their hydraulic conductivity and microbial populations, with both being higher in the acrotelm (Ingram, 1978). In the BGM (Clymo, 1984), OM enters the peat profile at the surface. Owing to the partially aerobic conditions of the acrotelm, the OM undergoes some level of decomposition. As the decomposition process continues the OM loses its structural integrity and eventually compacts under the overlying mass of OM which is continually being deposited at the peatland surface. This compaction results in reduced pore space and therefore reduced hydraulic conductivity driving the water table above this layer of

reduced permeability. In other words the OM has been incorporated into the catotelm. Here decomposition of the OM occurs at a much lower rate owing to anoxia. The peatland continues to grow until mass loss from the ever thickening catotelm equals the OM inputs. Whilst this model is widely referred to when discussing peatland accumulation and development, it is also acknowledged that it has its limitations. Firstly, the only spatial dimension considered in the BGM is the vertical dimension; lateral processes are not considered. Secondly it assumes that rates of OM input and peat decomposition, and peat properties such as bulk density, water table height and vegetation coverage, remain constant through time. There are now a number of models which encompass spatial and temporal variability in these processes and properties (for a brief review of current peat development models see Baird et al. (2011)). The vast majority of conceptual and empirical models of peatland development have been developed for temperate and boreal peatlands. To date there have been few attempts to conceptualise and model peat accumulation and development in the tropics (Kurnianto et al., 2015). This is important because there are some crucial differences between the circumstances in which peat accumulation occurs in the tropics.

One of the most obvious differences between tropical peatlands and those of higher latitudes is the higher temperatures under which tropical peatlands form. Typically higher temperatures should result in higher rates of OM decay (Gholz et al., 2000). However, permanently waterlogged conditions, in combination with low mineral status and high levels of acidity, mean that peat can accumulate under relatively high temperatures (Thompson and Hamilton, 1983) and sometimes at rates much higher than typically found in boreal or temperate peatlands. For example accumulation rates of up to 4.76 mm yr^{-1} have been reported for South East Asian peatlands (Anderson, 1983), with the average rate estimated at ca. 2 mm yr^{-1} (Sorensen, 1993) and accumulation rates ranging from 0.94-4.88 mm yr^{-1} have been reported for Peruvian Amazonian peats (Lähteenoja and Roucoux, 2010). This compares with typical rates of 0.2-0.8 mm yr^{-1} for boreal and temperate regions (Gorham, 1991). It has generally been assumed that the higher accumulation rates of tropical peatlands are the result of higher plant productivity (Moore, 1989). Recently, however, it has been suggested that these higher accumulation rates could in fact be linked to OM quality limiting decomposition (Ono et al., 2015, Yule and Gomez, 2009, Chimner and Ewel, 2005). In a litterbag experiment in a Micronesian forested peatland Yule and Gomez (2009) found endemic species leaf litter to decompose considerably more slowly than leaf litter from non-peatland species. They suggest that leaf physical and chemical adaptations of endemic species are the cause, possibly driven by pressures to avoid herbivory in a nutrient poor environment. Two more studies of OM decomposition in Micronesian peatlands suggest that it is the slow decomposition of tree

fine root systems which permits peat accumulation (Chimner and Ewel, 2005, Ono et al., 2015). The much higher decomposition rates of leaf litter meant that this source of OM contributed very little to peat accumulation (Chimner and Ewel, 2005, Ono et al., 2015) even when on an annual basis the mass of leaf litter supplied to the peatland exceeded that of root inputs (Chimner and Ewel, 2005).

The findings of Chimner and Ewel (2005) and Ono et al. (2015) are important because a large proportion of tropical peatlands are forested, but many of the empirical and conceptual models of peat accumulation and development are set up for bryophyte, sedge, grass or shrub vegetation (e.g. Baird et al. (2011), Clymo (1984), Lapen et al. (2005), Borren and Bleuten (2006), Yu et al. (2001)) and not forested peatlands. Generally in these models OM inputs are treated as being homogenous i.e. a single decomposition rate is applied to the OM. However, as discussed above, this is not necessarily the case in forested peatlands. Furthermore, current peatland development models tend to only consider OM inputs from the surface and do not consider OM contributions from roots. The exception to this is the Peat Decomposition Model (PDM) by Frolking et al. (2001), which was later incorporated into the Holocene Peat Model (HPM; Frolking et al., 2010).

The PDM incorporates a rooting zone where fresh OM mass can be added annually to the peat that is within the rooting zone. This newly added OM increases the net decomposition of the peat layer, on the assumption that fresh litter has a higher decomposition rate. Although the inclusion of a rooting zone was designed to reflect accumulation in grass and sedge peatlands this view of peatland accumulation is a much better reflection of how tropical peatlands operate than models which view OM inputs as only coming from the peatland surface. Additionally the PDM allows for root inputs below the water table. This is probably a key process that most other peatland models neglect: not all OM inputs need necessarily pass through the aerated acrotelm and may directly enter the peat body below the point of permanent saturation. This scenario seems likely in a forested peatland where trees must have roots deeper than the water table. One limitation of the PDM is that the same decomposition rate is applied to OM which enters at the peatland surface and OM which enters below the water table. Frolking et al. (2001) justify this by arguing that although below the water table, conditions in the catotelm must be at least partially aerated in order for roots to grow.

The PDM and HPM were subsequently modified to include trees as a new plant functional type and applied to a tropical setting (Kurnianto et al., 2015). As well as modifications to climate and seasonality, rooting depth was increased to 0.5 m (although this is probably overly conservative; Ono et al., 2015) and litter inputs were partitioned into leaves, wood and roots to better reflect tropical peatland conditions. Whilst the Kurnianto et al. (2015)

say that the modified PDM/HPM produced results consistent with observations for South East Asian peatlands, they state that a lack of empirical data particularly hydrological data, decomposition data and vegetation data limits the ability of the model to represent tropical peatland processes. Therefore our conceptual understanding of tropical peatlands is relatively limited compared to that of temperate or boreal peatlands.

1.3.8. Peatlands and Carbon Storage

Peatlands are mostly comprised of semi-decomposed OM and very little mineral content and therefore have high carbon (C) contents. They cover a relatively small proportion of the Earth's surface (ca. 3%; Rydin and Jeglum, 2006) but are estimated to store around a third of the soil C stock (480 Pg C; Page et al., 2011). However, there is a large degree of uncertainty in peatland C stock estimates, owing to a lack of data on peatland extent, volume or depth, C concentration and bulk density, which are the variables required when estimating peatland C stocks. This is true of all regions (Yu, 2012), but is particularly true of tropical regions (Lawson et al., 2015).

For a peatland to be acting as a C sink, the uptake of CO_2, via photosynthesis, followed by incorporation of the dead plant tissue into the peatland, must exceed C losses in the form of CO_2 and CH_4, via plant respiration and peat decomposition, and dissolved organic C (DOC) and particulate organic C (POC) in drainage water from the peatlands (Limpens et al., 2008). Overall, it is estimated that northern hemisphere peatlands have acted as a net C sink over the Holocene, resulting in a net atmospheric cooling effect from these peatlands of -0.2 to -0.5 W m^{-2}, which continues to this day (Frolking and Roulet, 2007).

Worldwide the ability of a peatland to act as a net C sink is often threatened by land use conversion of peatlands for agricultural purposes or forestry plantations. This tends to coincide with drainage, exposing the peatlands to oxidation, erosion and an increased fire risk (Hooijer et al., 2010, Hooijer et al., 2012, Page et al., 2002, Hirano et al., 2014, Jauhiainen et al., 2012). A further threat is that of global climate change (Wu and Roulet, 2014). Being dependent solely on precipitation means that ombrotrophic peatland systems are at particular risk from future changes in regional precipitation. This is not simply just a case of the amount of rainfall, but also the seasonality of rainfall and the intensity of dry periods. Under prolonged periods of oxic conditions in the acrotelm, decomposition of the OM can occur rapidly (Thompson and Hamilton, 1983). It has been suggested that even after rewetting, the by-products of aerobic decomposition can enhance anaerobic decomposition leading to further emissions even after the drought has ended (Fenner et al., 2011, Fenner and Freeman, 2011).

The large quantity of C stored in peatlands and their potential to act as a C sink or, if perturbed, act as C source has led to the inclusion of peatland restoration or conservation projects in the United Nation's Reduced Emissions from Deforestation and Forest Degradation in Developing Countries (UN-REDD+) programme (UNFCCC, 2012) and voluntary C offsetting schemes (VCS, 2015). However, for many regions in the tropics the inclusion of peatlands in C offsetting schemes is prohibited by the lack of quantitative data.

1.3.9. The Distribution of Tropical Peatlands and Their Carbon Stocks

The vast majority of the world's peatlands are located within the temperate or boreal regions, with an estimated extent of 346 $x10^6$ km^2 to 359$x10^6$ km^2 (Gorham, 1991, Immirzi et al., 1992). Despite the much warmer climate which should result in much higher rates of decay, peat formation can also occur in the tropics, as long as OM decay is in some way impeded by waterlogged, anoxic conditions. Tropical peatlands are usually defined by their latitudinal position. Page et al. (2011) define tropical peatlands as those located between 23.5°N and 23.5°S, whilst Andriesse (1989) uses the range 35°N and 35°S which encompasses more subtropical regions. The spatial extent of tropical peatlands is estimated to be between 33-50$x10^6$ km^2 (Page et al., 2011, Immirzi et al., 1992) i.e. between 9-14% of the global peatland extent. However, the tropical peatland C stock is estimated to be between 15-19% of the global peatland C stock, with a best estimate of 89 Pg C (Page et al., 2011). This is because some tropical peatlands can be of considerable depth (occasionally up to ca. 30 m), resulting in a greater volume per area (Page et al., 2011).

Within the tropics it is estimated that South East Asian peatlands comprise 56% of the total tropical peatland area, which equates to 247,800 km^2 and store an estimated 69 Pg C (Page et al., 2011). South America follows with 26% of the total tropical peatland area (107,486 km^2) and an estimated C stock of 10 Pg C, then Africa with 12% of the total tropical peatland area (55,800 km^2) and an estimated C stock of 7 Pg C (Page et al., 2011). The remaining known tropical peatland area and C stocks are distributed between the Caribbean and the rest of Asia (Page et al., 2011).

South East Asian peatlands are relatively well documented and studied, mainly as a result of the increasing pressures they face from agriculture, timber production, oil palm plantations and forest fires leading to their rapid degradation (Page et al., 2011, Grace et al., 2014, Page et al., 2002, Hooijer et al., 2012, Hooijer et al., 2010, Yule, 2010). Whilst undoubtedly less extensive, research into South American peatlands has been much more limited and detailed studies have been relatively recent, with the first major publications being less than ten years old (e.g. Lähteenoja et al., 2009a, Lähteenoja et al., 2009b). Having said this, considerable progress has already been made with first estimates of

peatland extent and C stocks having already been made for one drainage basin in western Amazonia (Draper et al., 2014) soon after confirmation of peatlands within the region (Lähteenoja et al., 2009a). However, with more recent discoveries of peatlands in other regions of the Amazon (Lähteenoja et al., 2013), it is likely that any current estimates of South American peatland extent and C storage could face considerably revision in the future.

The true extent and C stocks of African peatlands is even more uncertain. African peatlands remain largely unstudied and estimates of peatland extent and volume are based on a handful of largely anecdotal references (e.g. Bord na Mona, 1985, IMCG, 2011, Joosten and Clarke, 2002). Furthermore C stock estimates for African peatlands have relied on C and bulk density estimates based on South East Asian data. In a search of the published literature, only three studies were found to report C concentrations for peatland sites in Africa (McCarthy et al. (1989): Okavango Delta, Botswana; Aucour et al. (1996): Kashiru peatbog, Burundi; Bourdon et al. (2000): Tritrivakely, Madagascar). No studies were found that report bulk density data.

1.3.10. African peatlands

Collating information on African peatlands from the literature is challenging, firstly because the literature is very sparse, and secondly because much of it is brief, vague and frequently missing fundamental information such as the specific location, extent or peat depth. There is also often ambiguity as to whether the authors are actually describing true peat deposits or just organic soils. Consequently, for most areas, verification of peat presence, extent or depth is still required.

To date the most comprehensive collation of information on African peatlands is probably the 1985 report by the Irish fuel company Bord na Mona, entitled "Fuel Peat in Developing Countries". Bord na Mona (1985) retrieved a large proportion of their information from unpublished reports or seminars, a lot of which were focused on the use of peatlands as a source of fuel, but also some published literature. If I have been able to obtain the original source of Bord na Mona's information then I refer directly to that source (e.g. Duese, 1966, Beadle and Lind, 1960, Jacot-Guillarmod, 1962), otherwise I cite Bord na Mona (1985). The International Mire Conservation Group's (IMCG) "*Global Peatland Database- Africa"* also provides a synthesis of much of the available information on African peat on a country by country basis. However, this database is of limited use since the citations in text are not accompanied by the full reference. Therefore tracking down the original reference is not always possible. For the most part, any figures for peat extent presented by the IMCG are taken from the Bord na Mona (1985) report.

Bord na Mona (1985) restate the assumption of Thompson and Hamilton (1983), that whilst swamps are very abundant across Africa, true peatlands are rare and are restricted to highland areas and occasionally along coastal regions under mangrove swamp. This assumption is based on the idea that the higher temperatures and lower rainfall limit peat development in lowland inland areas (Thompson and Hamilton, 1983), but as discussed later on, this assumption does not seem valid, as peat deposits can be found in lowland, inland areas across Africa. In total, Bord na Mona (1985) report on the possibility of peat being present in 19 African countries, but state that few have been surveyed and therefore many peat deposits remain unconfirmed. Of all the regions mentioned by Bord na Mona (1985), they consider the following highland regions to be the main areas of peat formation in Africa:

1. The highlands of Rwanda and Burundi
2. Kigezi Region of southwest Uganda and the adjacent highland areas of the DRC
3. Aberdare Range and Cherangani Hills in western Kenya
4. The Ethiopian Plateaux
5. Drakensberg Range of South Africa/ Lesotho
6. Ruwenzori Range of Uganda/ DRC
7. Kipengere Range in southern Tanzania
8. Nyika Plateaux and Mulanje in Malawi
9. Mt. Elgon in Kenya

What is known of the distribution of tropical African peatlands is discussed more fully in the three following sections, which are divided into highland tropical peatlands, lowland tropical peatlands and then specifically peatlands of the Cuvette Centrale.

1.3.11. Highland Tropical Peatlands of Africa

Of the main peatland regions listed by Bord na Mona (1985) all would be classified as tropical peatlands under the definitions provided by Page et al. (2011) and Andriesse (1989), with the exception of the peatlands of the Drakensberg Range, South Africa and Lesotho, which being located approximately between 28.5°S to 30°S, would be considered sub-tropical under the definition of Page et al. (2011). Although the nine main peatland regions can all be defined as tropical, all are high altitude regions and therefore the peatlands are not forming under typical tropical climates, but instead forming under cooler montane climates. From the few studies which report average annual temperatures, most of these peats seem to be formed under average temperatures of 15-17°C (Bonnefille and Chalie, 2000, Aucour et al., 1999, Bourdon et al., 2000, Gasse and Van Campo, 2001),

although slightly higher temperatures (19-21°C) are reported for other sites (Pajunen, 1996).

Of the main peatland regions listed by Bord na Mona (1985), the most extensively covered and well documented peatlands are those of the Rwandan and Burundian highlands. Both Duese (1966) and Pajunen (1996) provide detailed accounts of multiple Rwandan and Burundian peatlands. Neither provide coordinates for their sites, but they do provide names, two of which are the same sites. Duese (1966) reports peatland pH, OM content, C content, depth, area and volume estimates, as well as vegetation communities associated with the peatlands. Pajunen (1996), having sampled some of the sites on a grid covering the entire peatland, reports results from an extremely large data set for nine peatland sites, presenting peatland cation concentrations, C, N, S and P concentrations, OM content, depth, area and vegetation communities, as well as radiocarbon dates and peat and C accumulation rates. These peatlands are situated at altitudes ranging from 1350-2300 m a.sl. (Duese, 1966, Pajunen, 1996) and are mainly found either at the headwaters of streams or along river courses and are largely maintained by stream flow or are spring fed (Pajunen, 1996, Duese, 1966). However, there are reports of true ombrotrophic, domed peat bogs or minerotrophic peatlands which are ombrotrophic in parts (Pajunen, 1996). This mix of minerotrophic and ombrotrophic peatlands is reflected in the peatland surface pH values, which range from 4.0 to 7.1. Volcanic and tectonic activity in the area has been a large factor in peat development in this area through the blockage or partial blockage of valleys or through the change in topographic gradient, impeding drainage and allowing peat initiation (Duese, 1966, Pajunen, 1996). Although climate has also played a role in peat initiation, the important role of non-climatic factors, mean that the timing of peat initiation across the sites has not been simultaneous, with peat basal dates spanning the time period 20200 to 1940 calibrated years Before Present (cal yrs BP; Pajunen, 1996, Aucour et al., 1999). Pajunen (1996) report peatland extents ranging from 0.002 to 1400 ha (Pajunen, 1996) and Duese (1966) report estimated peatland volumes of 0001 to 1.5 km^3. However, it is not always clear whether these areas refer to peat extent or swamp extent and it is not clear how Duese (1966) estimated peatland volume. Peat depths reported for this region are highly variably, ranging from less than 1m (Duese, 1966) to, at one particular site (Ndurumu Swamp, in Burundi), over 30m (Pajunen, 1996). The vegetation communities associated with these peat deposits are not always described. However, from what has been reported, it seems that these peat deposits are largely sedge dominated. In particular *Cyperus papyrus, C. latifolius, C. denudatus* and *Miscanthidium* spp. are species commonly reported (Pajunen, 1996, Duese, 1966). *Syzygium* spp. are the most commonly reported tree species associated with these peat deposits (Pajunen, 1996, Duese, 1966, Thompson and Hamilton, 1983). Similarly, peat composition is largely

described as being composed of sedge, in particular *Cyperus papyrus*, and often of woody deposits, derived mainly from *Syzygium* spp. forest (Pajunen, 1996). Occasionally even peat which currently has no tree coverage has been found to contain woody deposits, implying some degree of tree coverage at one point in the peatland's development (Pajunen, 1996).

In addition to Bord na Mona (1985), the Ugandan peatlands of the Kigezi region and the Ruwenzori Range, now known as the Rwenzori Range, are also commented on by Thompson and Hamilton (1983), Pfadenhauer (1993), Beadle and Lind (1960), who Bord na Mona (1985) obtain most of their information from, and Shier (1985). However, for every African country, Shier (1985) presents near identical information to the Bord na Mona (1985) report and although is not always cited it can be assumed this information comes directly from their report. Peatlands in Uganda are reported at altitudes up to 3900 m a.s.l (Thompson and Hamilton, 1983). Although some of the Ugandan peatlands are described as bogs (Thompson and Hamilton, 1983), it is not clear whether they are truly ombrotrophic, as Beadle and Lind (1960) describe *Sphagnum* sp. dominated "bogs", which are non-domed and in receipt of low nutrient ground water. In terms of vegetation Beadle and Lind (1960) state that the majority of Ugandan swamps are covered in *Cyperus papyrus*, but at altitudes above 2000 m a.s.l. *C. papyrus* becomes less common and is replaced by other sedge and grass species. It seems that species such as *Carex runssoroensis* are abundant in the Rwenzori Range peatlands (Thompson and Hamilton, 1983, Beadle and Lind, 1960, Pfadenhauer et al., 1993), as well as *C. monostachya*, *Lobelia* spp. herbs and *Alchemilla* spp. (flowering plant) (Pfadenhauer et al., 1993). The sedge *Pycreus nigricans* or *Pycreus* sp. is reportedly common for the Kigezi Region peatlands (Thompson and Hamilton, 1983, Shier, 1985). *Syzygium* sp. fens are also said to occur in the Kigezi Region (Shier, 1985). Peatland extent in Uganda is reported to be 14200 km^2 (Shier, 1985, Bord na Mona, 1985). In terms of depth, Beadle and Lind (1960) report depths up to 10 m for the Ugandan Rwenzori peatlands. Pfadenhauer et al. (1993) cite more modest depths up to 6 m for the Rwenzori peatlands of Uganda and the DRC. For the Kigezi region depths greater than 11 m have been reported for two specific swamps, Muchoya Swamp and Echuya Swamp (Thompson and Hamilton, 1983) and Beadle and Lind (1960) report depths of 10-16 m for the Western Highlands which encompasses the Kigezi region. In addition to the Kigezi region and Ruwenzori Range, peatlands also occur around Lake Victoria and other lakes within the region, as well as in the Western Rift Valley, with *Cyperus papyrus* mentioned as the vegetation type for both these regions (Shier, 1985, Pfadenhauer et al., 1993, Beadle and Lind, 1960). No peat depths are given for the Western Rift Valley peatlands and the lake edge peat deposits in the Lake Victoria region are largely shallow peats, less than 1 m in depth (Beadle and Lind, 1960).

Given that the high altitude peatlands of the DRC are found in same mountain ranges as the peatlands of Uganda, the characteristics described above for the Kigezi region and Rwenzori Range will very likely apply to the peatlands of these regions found within the borders of the DRC. In addition to the information above, Bord na Mona (1985) report peat depths of 1-15 m or more for some of the peats found in volcanic craters just south of Lake Kivu, located in the mountainous region that is an extension of the Kigezi Region, at around 1600-2000 m a.s.l. Bord na Mona (1985) report that individual peatland areas range from 0.5-10 km^2.

Although Bord na Mona (1985) do not discuss the Drakensberg Range peatlands of South Africa, beyond listing them as one of the main regions of peat formation, they do report that the highlands of Lesotho, which include the Drakensberg Range, contain many small peatlands forming around springs and valley heads. Jacot-Guillarmod (1962), who Bord na Mona (1985) cite, provides a more detailed account of the Lesotho highland peatlands. Jacot-Guillarmod (1962) describes the montane peatlands as consistently coinciding with springs, but also frequently form raised bogs, suggesting that many have developed an ombrotrophic surface. These bogs are either dominated by *Danthonia drakensbergensis* or *D. macowani* grasses, the reed *Juncus glaucus* var. *acutissimus* or *Kniphofia caulescens*. Peatlands can also be found in the Lesotho lowlands. Although described as lowlands, these peatlands actually lie between 1700 and 2000 m a.s.l. (Bord na Mona, 1985, Jacot-Guillarmod, 1962). However, Jacot-Guillarmod (1962) describes these lowland peatlands as "immature" and different from the "true peat bogs" of the mountain regions, suggesting that they may not be particularly deep peat deposits. Overall, a Bord na Mona ground survey found the peatlands of Lesotho to be small (0.002-0.02 km^2) and shallow (<2 m) and contain high levels of mineral matter eroded from the adjacent slopes (Bord na Mona, 1985). Although no reference to Drakensberg peatlands in South Africa could be found elsewhere in the literature, there is reference to a high altitude peatland in the Waterberg Range, in the north east of South Africa. This peatland, known as Wonderkraten spring mound, is a domed peatland formed by one of many springs found along a fault line (McCarthy et al., 2010). It reaches 8 m thick and the site appears to have started accumulating peat in the Pleistocene, with basal dates of >35 k a (McCarthy et al., 2010). The dominant vegetation of the peatland is *Carex acutiformis* (McCarthy et al., 2010).

Despite considering them to be the main regions of peat formation in Africa, Bord na Mona (1985) do not provide any information on the remaining five of nine locations listed in Section 1.3.10. However, although not extensive, there is some information available in the literature for these regions which is discussed below.

In addition to the Bord na Mona (1985) report, the only further mention of the Aberdare Range peatlands, Kenya, that I could find, comes from Thompson and Hamilton (1983) and Hedberg (1964). However, no specific information is given other than these peats are found at altitudes above 3000 m a.s.l. and are associated with *Carex monostachya* and *C. monostachya* mires or peat bogs, which are said to be widespread in the area, but only occasionally form peat. Only one other source, aside from Bord na Mona (1985), could be found which makes reference to the Cherangani peatlands, Kenya; Hamilton (1982) describes a peatland, Kaisungor Swamp, located in a valley at 2900 m a.s.l. from which two peat cores have been sampled. Peat thickness was 3.7 m and 4.17 m for the two cores, with the thickest peat deposit having a basal age of 27750 cal yrs BP. The following species were listed as being present in the swamp: *Alchemilla ellenbeckii*, *Anagallis serpens*, *Carex* sp., *Cyperus denudatus*, *Eriocaulon schimperi*, *Kniphofia thomsonii*, *Lobelia aberdarica* and *Dendrosenecio johnstonii*. On Mount Elgon, Kenya, Hamilton (1982) describes three sites containing peat deposits which have been cored. Their elevations range from 2880 to 3940 m a.s.l. The three sites appear to be rather small in extent with Hamilton (1982) giving the dimensions of one site as being 750 x 50 m and describes another as being only 20 m wide. At one site only the top 50 cm of peat was cored, at another the profile is a series of buried peat deposits, less than 50 cm thick, interspersed with thicker clay deposits. However at the third site Hamilton (1982) describes a 2.04 m peat core with a basal date of 6505 yrs BP and suggests that peat may be deeper in other sections of the peatland. The dominant vegetation for the sites includes *Carex runssoroensis, Pycreus nigricans, Scirpus fluitans, Swertia* cf. *crassiuscula, Alchemilla johnstonii, A. ellenbeckii, Lobelia aberdarica, Eriocaulon volkensii, Hydrocotyle* sp. and *Panicum* sp. Hedberg (1964) also mention peatland ecosystems on Mount Elgon up to elevations of 4100 m a.s.l. similar to those of the Aberdare Range, although the specific peat bogs he refers to are in fact on the Ugandan side of the mountain. He also mentions Mount Kenya as another location where these peatlands can be found. Although they do not describe it as peat, Jones and Muthuri (1997) describe a “detritus” layer 1-2 m thick, formed from aerial, root and rhizome biomass, which has undergone little decomposition, below *Cyperus papyrus* swamp at the edges of Lake Naivasha (1890 m a.s.l.), Eastern Rift Valley, Kenya.

For Ethiopia, Bord na Mona (1985), describe the location of peatlands simply as the Ethiopian Plateaux, which here is assumed to refer to the entire highland regions of Ethiopia, covering most of the country. In the limited literature available, the Bale Mountains are referred to more than once as containing peatlands. Dullo et al. (2013) describe two small peatlands in the Sanetti Plateaux, Bale Mountains, at an altitude of ~4000 m a.s.l. The two peatlands are largely covered by *Carex* species and *Eriocaulon schimperi*, and the high concentrations of Ca and Mg, along with a surface pH of ca. 6,

indicate that the peatlands are minerotrophic. The maximum peat thickness recorded by Dullo et al. (2013) was 2.4 m. Mohammed and Bonnefille (1998) describe a 1.65 m peat core taken from a site called Tamsaa Swamp, Bale Mountains located at 3000 m a.s.l. The swamp is dominated by Cyperaceae sp. , *Juncus* sp. and *Alchemilla* sp. Radiocarbon dating of the peat indicates that peat initiation took place before 13000 yrs BP. Hamilton (1982) describes a 2.5 m thick peat deposited at an elevation of 3830 m a.s.l. in Danka Valley, Bale mountains. Radiocarbon dating of the basal peat indicates that peat initiation took place much later than at Tamsaa Swamp, at 7920 cal yrs BP. Hamilton (1982) also describes a thicker (3 m) and older peat core, with a basal date of 11500 cal yrs BP, taken from 4040 m a.s.l. on Mount Badda in the Aurussi Mountains, north of the Bale Mountains. Hamilton (1982) does not describe the vegetation associated with these peatlands. Lamb et al. (2007) also describe a ~40 cm thick buried peat deposit in lake sediments of Lake Tana, located at the head of the Blue Nile River. The radiocarbon dating shows the peat to have accumulated between 15,700 to 15,100 yrs BP.

No mention of peatlands on the Mulanje monadnock could be found in the published literature and only one study could be found for the peatlands of the Nyika Plateaux, Malawi. Meadows (1984) describes peat cores sampled for palynological work, from two sites on the plateaux. The elevation of these two sites is not given, but the Nyika Plateaux itself lies between ca. 2100 to a maximum 2607 m a.s.l. The area of the sites is also not given but from a map included in the article, it appears that one site is ca. 10 km long and less than 1 km wide, whilst the other is ca. 2.5 km long and less than 1 km wide. The thickness of the peat cored at the larger site is 1.5 m whilst at the smaller site it is 5.3 m. However, it is not clear whether the cores were taken in the deepest section of the peatlands. Radiocarbon dating suggests that peat initiation was around 3800 cal yrs BP at the deepest site. Meadows (1984) describes the vegetation cover of the two sites simply as being comprised of grass and sedges.

In the literature there are further examples given of high altitude African peatlands or possible peatlands some of which are not mentioned in the Bord na Mona (1985) report. For instance the Tanzanian side of Lake Victoria is also said to have *Cyperus papyrus* meadows (Pfadenhauer et al., 1993); presumably if these are associated with peat in Uganda it is likely that in Tanzania they will also be associated with peat. Additionally there are said to be terrestrialised lakes dominated by Cyperaceae sp. and *Dryopteris* sp. at altitudes of 1000-2000 m a.s.l. in the Ruaha area of Tanzania (Pfadenhauer et al., 1993) and *Carex monostachya* and *Deschampsia* sp. dominated fens found on Kilimanjaro, which could also be peat forming (Pfadenhauer et al., 1993, Hedberg, 1964). Although perhaps not truly high altitude peatlands, with elevations ranging from 935 to 950 m a.s.l., in the

Usambara Mountains (part of the Eastern Arc Mountains) Mumbi et al. (2014) describe three peatland site used for palynological work. The extent of these sites are not reported, but the maximum peat depth cored was 1.5 m. The dominant vegetation associated with these peatlands is *Cyperus alopecuroides*, *Typha latifolia* and *Paepalanthus* sp., although one site is under sugar cane, rice and amaranth plantations. Radiocarbon dates are presented but contamination issues mean it is hard to say when peat initiated, but certainly no early than late Holocene. Peatlands are also mentioned for the Lukwangule Plateau, another region of the Eastern Arc Mountains, Tanzania (Frontier-Tanzania, 2005).

In Zambia, terrestrialised areas surrounding Lake Bangweulu in the north, Lukanga Swamp in the Provincia Centrale and Lake Mweru on the Zambia-DRC border, all located above 1000 m a.s.l., are said to have Cyperaceae mires (*Scleria* sp., *Rhynchospora* sp., *Kyllingia* sp.) with *Dryopteris* species, which are often associated with floating mats and may be peat forming (Pfadenhauer et al., 1993, Shier, 1985). In the Upper Zambezi Valley, Zambia, Burrough and Willis (2015) describe three peatland sites which they cored for palynological work. The elevation of the peatlands range from 1011 to 1499 m a.s.l. Two of the peatlands are dominated by grass species, with *Loudetia simplex*, *Cyperus* sp. and *Typha* sp. the most common. The third site is a grassland-scrub woodland mosaic, with dominant grass species such as *Tristachya nodiglumis, Digitaria gazensis* and *Eragrostis trichophora* and dominant tree species such as *Burkea Africana, Guibourtia coleosperma, Acacia erioloba, Terminalia sericea* and *Pterocarpus angolensis.* Cored peat thickness ranged from 0.37 to 0.99 m and basal ages of the peat ranged from 1692 to 6004 cal yrs BP. No areas for the three peatlands were reported.

In the eastern side of Zimbabwe, in the Inyanga Mountains, Tomlinson (1974) describes peat deposits at two locations; one a *Sphagnum* sp. filled hollow and a pond. From the map provided it appears that the two sites are situated somewhere between 2000 and 2100 m a.s.l. The peat deposits reach ca. 1 m and 1.75 m, with the base of the shallower peat deposit being <700 yrs BP. The age of the deeper deposit is not clear.

Finally, high altitude peatlands are also present in Madagascar, with several studies describing a high altitude (1778 m a.s.l.) 3 m thick peat deposit on top of ca. 40 m of lacustrine sediments in a crater lake, named Tritrivakely Lake, located in the central part of the Ankaratra Plateau (Bourdon et al., 2000, Disnar et al., 2005, Gasse and Van Campo, 2001). The lake is rain fed and therefore its form is dependent on seasonal and interannual climatic fluctuations. On an interannual basis the lake levels can be highly variable (e.g. Bourdon et al. (2000) report the lake to be completely dry in 1992 and then

in 1994 lake levels reached 2 m) and so the site varies between a circumneutral water body to an acidic hummocky bog dominated by *Cyperus madagariensis, C. papyrus, Heliocharis equisetina, Leersia hexandra*. Lake Alaotra, in the north east of the highlands, is another lake thought to contain peat deposits (IMCG, 2011, Bord na Mona, 1985). It is possible that there may be a number of crater lakes and areas of higher elevation associated with peat formation in Madagascar, with peat possibly reaching up to 7 m thick (IMCG, 2011).

1.3.12. Lowland Tropical Peatlands of Africa.

As previously mentioned, lowland tropical peatlands are not thought to be extensive in Africa and largely confined to coastal regions (Thompson and Hamilton, 1983). The countries cited as having coastal peatlands are Egypt, Guinea, Ivory Coast, Mauritania, Mozambique, Senegal, South Africa, Togo and the ROC. Guinean coastal peatlands are reported to occur in lagoonal areas, deltas and river valleys along the coast (Shier, 1985). An extent of 5250 km^2 is given for Guinean peatlands (Pfadenhauer et al., 1993, Shier, 1985) or histosols more broadly (Bord na Mona, 1985), the latter term being one which incorporates peat, but is not restricted to peat. With regards to depth, the only information available in the literature is that all deposits are "shallow" (Bord na Mona, 1985). The mangrove saline peat deposits are said to be dominated by *Rhizophora* sp. (Shier, 1985) and the freshwater coastal swamps dominated by *Raphia* sp. (Shier, 1985, Bord na Mona, 1985). Like Guinea the Ivory Coast is also said to have peatlands in its deltas and river valleys along the coast (Bord na Mona, 1985, Shier, 1985, Lappalainen and Zurek, 1996). In particular an area known as Agneby Marsh is known to contain peat. It is said to cover an area of 320 km^2 (Lappalainen and Zurek, 1996, Bord na Mona, 1985, Shier, 1985), although part of this is now under banana plantation (Lappalainen and Zurek, 1996). The peat is said to be woody and overlain by *Raphia* sp. and *Mytragyna ciliata* (Lappalainen and Zurek, 1996). Further up the coast from Guinea, Senegal is also said to have peatlands forming in the Niayes region in inter-dune depressions (Bord na Mona, 1985, Shier, 1985). These peat deposits are said to be on average 3-4 m deep (Bord na Mona, 1985), but range from 1-10 m (Bord na Mona, 1985, Shier, 1985) and individually are small in extent (0.01-0.1 km^2) (Shier, 1985, Bord na Mona, 1985). Further north in Mauritania, Weaver et al. (1990) mentions peat deposits along the Atlantic coast south of Nouakchott and along the Senegal River Valley. They describe them as being similar to the Senegalese peat deposits. A very brief, and old reference is made to a peat deposit near the Togo coast, in the valley of the river Mono (Dubois and Dubois, 1939). The article is available from the journal's archive as a scanned copy of the original and is of low resolution, therefore it is hard to decipher the units of measurement but it is possible that there is 1.55 m of peat.

Along the Central West African coast, in the ROC, two sites are confirmed to contain peat (Elenga et al., 2001). One of the sites, named Songolo, is located in the coastal plain at only 5 m a.s.l., covered by a forest-grassland mosaic dominated by *Cyperus papyrus*, with *Raphia* sp. and *Alstonia* sp. present. The peat core taken at this site is ca. 1.8 m thick and dates back to ca. 5000 cal yrs BP (Elenga et al., 2001). The other site, named Coraf, is located directly on the shoreline at only 1 m a.s.l. It is not clear what the overlying vegetation is, but the deposit reaches 0.6 m thick and is older than 3000 cal yrs BP (Elenga et al., 2001).

On the other side of the continent, along the south east coast, peat deposits are found in the Maputaland coastal plain, KwaZulu-Natal, South Africa. At elevations <50 m a.s.l. peatlands are found forming mostly in coastal lake systems as well, as interdune depressions (Ellery et al., 2012, Thamm et al., 1996, Grundling et al., 2013). The mire system of this region, named the Natal Mire Complex, is extensive and is said to stretch northwards into Mozambique (Thamm et al., 1996). This is consistent with the Bord na Mona (1985) report, which describes peat deposits accumulating in depressions between old coastal dunes in Mozambique, which are locally referred to as machangos. Reported areas for individual peatlands in the Maputaland coastal plain vary from 0.08-15 km^2 (Thamm et al., 1996, Grundling et al., 2013) and depths up to ca. 10 m have been reported (Grundling et al., 2013). However, these values should be used with a degree of caution, as it seems that the definition of peat used in this region would not comply with definitions of peat use by most studies (i.e. an OM content >30%) and some of the area and depth values presented refer to what would normally be considered a histosol rather than specifically peat (e.g. Grenfell et al., 2010). Peat initiation in the region seems largely to have been the result of aggradation of floodplains, as a result of sea level changes, leading to the blockage of valleys, which subsequently became flooded (Grundling et al., 2013, Ellery et al., 2012). Radiocarbon dating of basal samples suggests there is a geographical divide of those of Holocene age in the north of the region and those dating back to the Late Pleistocene in the south of the region (Grundling, 2004). The majority of the peatlands are dependent on groundwater flow (Grundling et al., 2013, Thamm et al., 1996, Ellery et al., 2012), although Thamm et al. (1996) describe one of the peatlands as being domed in the centre, suggesting it is possibly ombrotrophic in parts. Peatland vegetation is a mix of sedge communities and in places swamp forest with species such as *Ficus trichopoda, Hibiscus tiliaceus, Syzygium cordatum* and *Rauvolfia caffra* present (Grundling et al., 2013, Thamm et al., 1996, Clulow et al., 2013).

Finally, along the north coast of the continent in Egypt extensive studies of the Nile Delta sediments have found buried Holocene peat deposits (Dominik and Stanley, 1993, Howa and Stanley, 1991). These coastal marsh peatlands formed through a combination of

submergence, which resulted from land subsistence and rising sea levels, and the damming of water bodies and the formation of lagoons and back-barrier marshes as a result of sediment distribution and migration by coastal and fluvial processes which allowed damming of water bodies and formation of lagoons and back-barrier marshes where peat could accumulate (Howa and Stanley, 1991). However, it is not clear whether, in addition to these buried peat deposits, peat can still be found to be accumulating in the Nile Delta.

References are also made in the literature to non-coastal lowland peatlands in Angola, Botswana, Liberia, and the ROC. The information available for Angola is extremely limited but peatlands are said to occur in the valley of the River Cuanza (Bord na Mona, 1985, Shier, 1985). They are described as extensive (Shier, 1985), but no actual estimate of extent is given. Bord na Mona (1985) report that some of the peatlands are covered by alluvium, suggesting that these peatlands are subject to dynamic fluvial processes and may not be stable.

Within the ROC, palaeoecological studies carried out in the ROC confirm the presence of peat deposits, inland, on the Plateaux Batéké. The Plateaux Batéké, covering an area of 12,000 km^2 and ranging in altitude from 600 to 886 m a.s.l., is largely covered with wooded savannah, with hydromorphic forests found in depressions on the plateaux (Elenga et al., 1991, Elenga et al., 1994). It is within these depressions that peat deposits have been found. One site, an 8 km wide depression, named Bois de Bilanko (see Fig. 1.1), is vegetated with *Syzygium* spp. forest and rafts of Gramineae spp. and Cyperaceae spp. (Elenga et al., 1991). Despite the well-drained sandy soils which surround the depression, peat has been able to accumulate through the formation of an iron pan in the depression (Elenga et al., 1991). Only the top 60 cm of peat was recovered, but Elenga et al. (1991) speculate that peat depths in the centre of the depression, which was unreachable, could be as much as 4 m. Despite the peat being shallow, a fossilised piece of wood taken from near the base of the core returned an age of 10850±200 yrs BP (Elenga et al., 1991). A second site, Ngamakala Pond (see Fig. 1.1), is a smaller depression of 750 m by 200 m largely covered with *Sphagnum* spp. and patches of *Alstonia boonei* (Elenga et al., 1994). Two peat cores taken at this site, reaching depths of ca. 3 m and ca. 1.5 m, have basal dates of 24200±480 yrs BP and 3300±140 yrs BP respectively (Elenga et al., 1994). As these cores were collected for palaeoecological purposes rather than a specific interest in peat accumulation in the Plateaux Batéké region no indication is given as to whether peat can be found in other forested depressions on the plateaux.

In Botswana the Okavango Delta (which is actually a subaerial fan, not a delta; Stanistreet and McCarthy, 1993) is an unusual example of a tropical peatland formed under very arid

conditions (where rainfall is 500 mm yr^{-1}; Stanistreet and McCarthy, 1993). The Okavango Delta is not mentioned in the Bord na Mona (1985) report, but there have been many studies on the Okavango Delta, which have come out over a period of decades, that either focus directly or indirectly on the peatlands within the fan. Despite the arid conditions, the continuous ground water flow from the channels to the adjacent swamps, along with seasonal overtopping of the channels (McCarthy et al., 1991), has allowed substantial peats deposits to accumulated. Although it is unclear what is the maximum depth recorded, channel cross section diagrams frequently show peat banks of 3-4 m or more (Cairncross et al., 1988, Ellery et al., 1989, McCarthy and Ellery, 1997, Tooth and McCarthy, 2004, Stanistreet et al., 1993). Despite seasonal flooding, the low gradients of the fan mean that very little sediment is held in suspension and therefore the peats receive low levels of mineral matter (McCarthy et al., 1989). They are predominantly covered in *Cyperus papyrus* (Ellery et al., 1990, McCarthy et al., 1989, McCarthy and Ellery, 1997), which, owing to its dense cover and strong root network, substantially slows the erosion of the peat banks (Stanistreet et al., 1993, Stanistreet and McCarthy, 1993, Tooth and McCarthy, 2004). In the lower reaches of the fan *Cyperus papyrus* abundance declines and *Miscanthus junceus* becomes dominant (McCarthy and Ellery, 1997, Ellery et al., 1990, McCarthy et al., 1989). The low gradients of the fan mean that channel abandonment, possibly linked to tectonically-driven channel aggradation (Ellery et al., 1995), is a common phenomenon. Channel abandonment leaves peat deposits vulnerable to desiccation, fire (both at the surface and sub-surface) and subsidence (Ellery et al., 1989, Gumbricht et al., 2002).

Subsurface fires of buried peat deposits have also been identified in Mali. Unusually high ground surface temperatures (up to 750°C), vegetation die back and holes and fractures in the ground emitting smoke, have previously been attributed to the onset of volcanic activity in the region surrounding Timbuktu (Svensen et al., 2003). However, it has now been shown that subsurface combustion of lacustrine peat deposits during the dry season is the cause of these phenomena (Svensen et al., 2003). The thickness of these peat deposits is not clear, however a trench dug in one of the combustion sites in the region revealed a ca. 70 cm thick peat deposit (Svensen et al., 2003). Svensen et al. (2003) estimate that lacustrine deposits cover approximately 1000 km^2 in the region. No reports have been found relating to the presence of peat deposits at the surface in Mali.

In Liberia, valley bottom swamps are described as containing peatlands covered in *Raphia* sp. and *Loeserna* sp. (Bord na Mona, 1985). No specific location is given for these peatlands, but the total peatland extent is said to be 400 km^2 and peat depth are described as rarely being more than 0.5 m (Bord na Mona, 1985).

In addition to the areas listed above Weaver et al. (1990) also mention that peatlands are present in Sudan of unknown extent. The IMCG (2011) also list several other African countries said to possibly contain peatlands: Algeria, Benin, Burkino Faso, Cameroon, Equatorial Guinea, Gabon, Ghana, Guinea Bissau, the island of Mauritius, Namibia and Sierra Leone. These have mostly been included in the estimates of Page et al. (2011) for African peatland extent and C stocks. They have not been included in the discussion here, however, because the IMCG (2011) fail to provide the full reference for their information and therefore it has not been possible to follow up their sources. What this suggests though is that peatland ecosystems are possibly wide spread across the continent but poorly documented in the literature.

1.3.13. Lowland Peatlands of the Cuvette Centrale

The Cuvette Centrale, despite being Africa's largest wetland, receives relatively little attention from Bord na Mona (1985). However, Bord na Mona (1985) do report that peat deposits can be found in the north of the ROC, in river valleys of the Motaba and Ibengo rivers, which are tributaries of the Ubangui river. However, it is unclear where Bord na Mona obtained this information from. The only reference they provide for the ROC is the FAO/UNESCO (1971-1978) 1:5,000,000 Soil Map of the World. Given the scale of the map and that Bord na Mona have named specific river valleys, it seems unlikely that this information came from this source. Nevertheless, the information could still be correct. Evrard (1968) described the swamp forests of the region to be underlain by very organic soils with an OM content of 40-70%, which he says in places can be considered to be peat. Furthermore, a study of dwarf crocodiles in the Likouala swamp forests (in the north-east of the ROC, see Fig. 1.1) describe the crocodiles using peat to make nests (Riley and Huchzermeyer, 1999).

If peat is commonly associated with swamp forest vegetation in the Cuvette Centrale then given the size of the region, peatland extent could be quite considerable within the ROC and DRC. Figures of 400 km^2 and 2900 km^2 are commonly quoted figures for the DRC and ROC respectively for the extent of peatlands, histosols, mire extent or organic soils. All these references can be traced back, if indirectly, to the FAO/UNESCO (1971-1978) 1:5,000,000 Soil Map of the World (Figure 1.2 and 1.3). However, whilst the text which accompanies this map does provides an area estimate of 400 km^2 for eutric histosols in the DRC, for the ROC, the area estimate is actually 2970 km^2 for dystric histosols. For both the DRC and ROC, the Soil Map of the World shows the majority of the countries' histosols to be located in the Cuvette Centrale. However, in the accompanying text there is no mention of peat other than the following, ambiguous, statement under the description for the tropical swamp forest vegetation class; "*The occurrence of grasslands of Echinochloa*

stagnina and E. pyramidalis, Leersia hexandra, Phragmites mauritianus and Cyperus papyrus is determined by the thickness of the peat and the depth of the water". The sources of information for the FAO/UNESCO (1971-1978) 1:5,000,000 Soil Map of the World for the ROC and DRC are the 1:2,000,000 soil map entitled "*Le sols du Congo*" by De Boissezon et al. (1963) for the ROC and the 1:5,000,000 soil map entitled "*Carte (1:5000000) des sols et de la végétation du Congo belge et du Ruanda-Urundi*" by Sys (1960) for the DRC. The ROC soil map by De Boissezon et al. (1963) includes a soil class described as including peaty soils or semi-peaty soils. This class covers the area of the Cuvette Centrale within the ROC. According to the FAO/UNESCO (1971-1978), the ROC soil map by De Boissezon et al. (1963) was produced by extrapolating associations between soils and other environmental variables, such as vegetation, climate, geomorphology etc., rather than actual ground surveys. The DRC soil map by Sys (1960) has not been obtained, therefore it is not possibly to check whether it describes peat or peaty soils. The DRC soil map is based on some soil survey data, but largely it is based on extrapolation of soil associations with other environmental variables (FAO/UNESCO, 1971-1978). For the ROC an additional figure of 16177 km^2 is used by Page et al. (2011) for the maximum peatland extent. This was derived from the IMCG (2011) Global Peatland Database, which in turn cite van Engelen and Huting's (2002) unpublished interpretation of the "World Soil Map". It is unclear whether this is the same as the FAO/UNESCO (1971-1978) 1:5000000 Soil Map of the World. For the DRC Page et al. (2011) used 10000 km^2 for the maximum peatland extent. This was taken from Andriesse (1989), who use this figure for the extent of organic soils in the DRC. Where this figure originally comes from is unclear as Andriesse (1989) does not provide a reference. Finally Joosten et al. (2012) conjecture an area estimate of 180,000 km^2 for the entire Cuvette Centrale. This is based on the assumption that around half of the estimated wetland area by Bwangoy et al. (2010) for the Cuvette Centrale is underlain by peat. Therefore it is clear that there is a lot of uncertainty and speculation surrounding any current peatland extent estimates for the Cuvette Centrale and it appears that these estimates are not based on ground data.

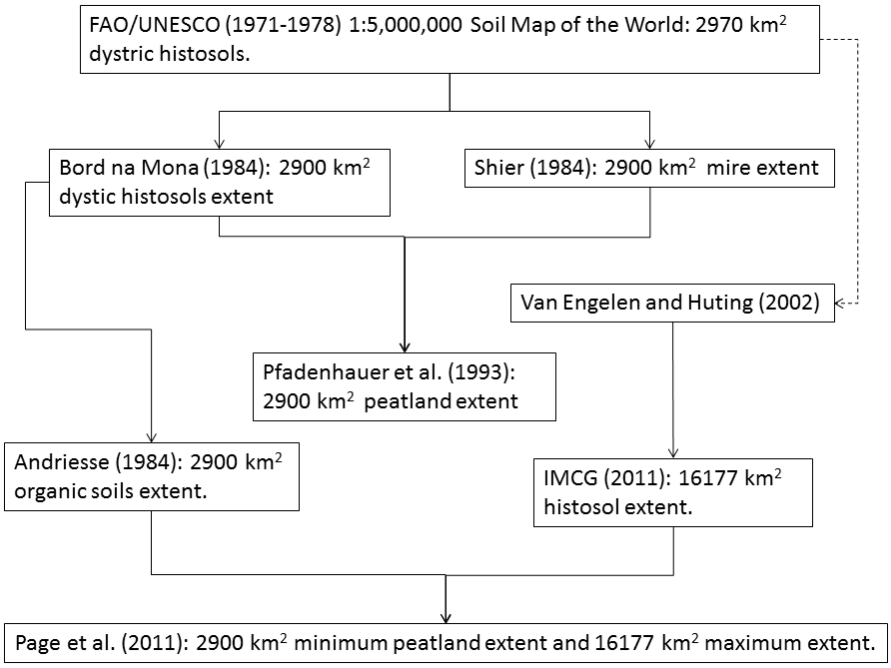

Figure 1.2. Diagram showing the origins of peatland extent estimates presented in the literature for the Republic of Congo. The dashed line between van Engelen and Huting (2002) and the FAO/UNESCO (1971-1978) 1:5000000 Soil Map of the World indicates that it is unclear as to whether this is really the source of this estimate.

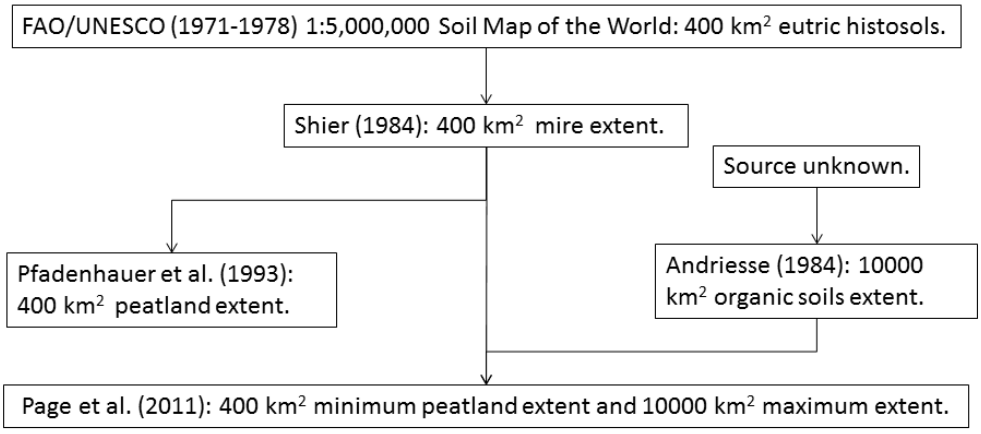

Figure 1.3. Diagram showing the origins of peatland extent estimates presented in the literature for the Democratic Republic of Congo.

Depth estimates for the Cuvette Centrale are even more ambiguous than area estimates. Exceptional peat depths have been cited for both the DRC and the ROC. Bord na Mona (1985) report peat depths of 1 to 15 m for the DRC. This figure is cited as coming from an unpublished Bord na Mona (1980) report "Musisi Bog- Zaire Survey and Pilot Scheme". These peatlands, however, are not located in the Cuvette Centrale, but rather in the Bukavu region near Lake Kivu, which is part of the Virunga volcanic range; therefore these are high altitude peatlands. Shier (1985) also reports depths of 1 to 15 m for the Bukavu

region in the DRC. He/she does not provide a reference but the information provided is identical to that of the Bord na Mona (1985) report, so presumably this is where the information was sourced. Page et al. (2011) cite two sets of depth ranges for the DRC; 1 to 15 m and 30 to 60 m. They cite Shier (1985) and Bord na Mona (1985) as the sources. However, neither Shier (1985) nor Bord na Mona (1985) report depths of 30 to 60 m for the DRC. Markov et al. (1988) report peat depths of 0.6 m for the DRC in mangroves along the Congo River. Pfadenhauer et al. (1993) indirectly cite Bouillenne et al. (1955) as also reporting depths of 0.5 to 0.6 m for a "peat-like substance" under mangroves along the Congo River. It is possible that along the chain of citations the "60 cm" has been misquoted or mistranslated as 60 m. However the IMCG (2011) cite Schneider (1958) as reporting peat depths of up to 30 m in the DRC near Lake Kivu. It has not, so far, been possible to obtain this reference to verify whether Schneider (1958) does actually report 30 m peat deposits for the DRC. Either way it is possible the depths presented by Page et al. (2011) are an amalgamation of the 30 m reported by Schneider (1958) and a misquotation of the 0.60 m reported by Bouillenne et al. (1955) and re-reported by Markov et al. (1988).

With regards to the ROC very large peat depths have also been reported. Markov et al. (1988) report peat depths of up to 30 m. Page et al. (2011) use this figure as their maximum peat depth estimate for the ROC. However, it is not clear exactly where this figure comes from. Markov et al. (1988) mention the place names "Mosaki" and "Likvaly", but these places could not be located on any maps. The IMCG (2011) speculate that these places are in fact in the DRC, suggesting that the 30 m of peat reported by Schneider (1958) near Lake Kivu is the same peat deposit reported by Markov et al. (1988) for the ROC. However, according to Evrard (1968), whilst the organic or peat soils under the swamp forest vegetation are normally ca. 1 m, they can in very exceptionally instances, reach depths of 17 m, but yet again, no location is given. Therefore the location of these very thick deposits remains unknown and unconfirmed.

In terms of C stocks, Page et al. (2011) estimate that the ROC has the largest peatland C stocks in Africa, with an estimated 2.4 Pg C, largely owing to the assumed peat depths. With an estimated 0.6 Pg C for the DRC, the estimates of Page et al. (2011) suggest that the peatlands of the Cuvette Centrale contain ca. 3 Pg C. This is considerably less than the estimated 9 Pg C by Joosten et al. (2012) for the entire Cuvette Centrale (both the ROC and DRC). This was obtained from their previously mentioned area estimate and a more conservative speculation that peat depth in the Cuvette Centrale is only ca. 1 m. The unsubstantiated assumptions on which these two estimates are based, and the disparity between them, highlights the uncertainty in current peatland C stock estimates for the Cuvette Centrale.

1.3.14. Summary of African Peatlands.

Many of the sources included in the review of African peatlands are ambiguous, vague and in need of verification. However, the picture which emerges from all these sources is that African peatlands are seemingly widespread, with a total of 26 countries, spanning the entire continent, cited as harbouring peatlands. Furthermore, it appears that peatlands are found forming under a wide range of environmental conditions, from very arid lowlands (e.g. the Okavango Delta), to cooler, wetter highland regions (e.g. peatlands of the Rwandan and Burundian highlands) and along a number of coastal fronts (e.g. North, West, Central and Southern Africa). Therefore, there is a high range of diversity among the African peatland ecosystems, with examples of both ombrotrophic and minerotrophic peatlands (including peatlands dependent on spring, ground, marine, fluvial and lacustrine waters), acidic to circumneutral peatlands and a wide range of peatland vegetation communities, from sedge and grass dominated systems to swamp forest communities. Although efforts were made to obtain as much of the published literature as possible, it is more than likely that more information is available on African peatlands either in unpublished or not widely publicised literature, especially in older literature held in institutes of old-colonial powers. Having said this, it is clear from the literature reviewed here, that with the exception of a few studies (e.g. Pajunen, 1996, Duese, 1966, McCarthy et al., 2010, McCarthy et al., 1989 (and subsequent works)), the quality of information provided seldom permits a good understanding of the peatland ecosystems described and almost none allow an estimation of peatland C stocks. Therefore there are still significant unknowns regarding African peatland ecosystems, with this being particularly true of certain regions such as the Cuvette Centrale.

1.4. Site Description

The Cuvette Centrale is the low lying hydrological basin within the central Congo Basin, through which the Congo River flows, a river second only to the Amazon River in terms of discharge (Keddy et al., 2009). The Cuvette Centrale is reported to cover an area of ca. 1,000,000 km^2 and is shared between the ROC and DRC (Hughes and Hughes, 1992) and is the second largest tropical wetland in the world (Keddy et al., 2009). Its elevation ranges from 324 to 500 m a.s.l. and the topography varies little (Hughes and Hughes, 1992). It is generally considered to be seismically inert although fault lines and horsts have been identified and are considered to have an influence on the direction of the hydrological flow through the basin (Master, 2010, Kadima et al., 2011). The topographical homogeneity of the region means that a large proportion of the Cuvette Centrale experiences regular inundation and as a result a considerable proportion of the region is covered by swamp forests, with *terra firme* forest confined to higher ground (Hughes and Hughes, 1992).

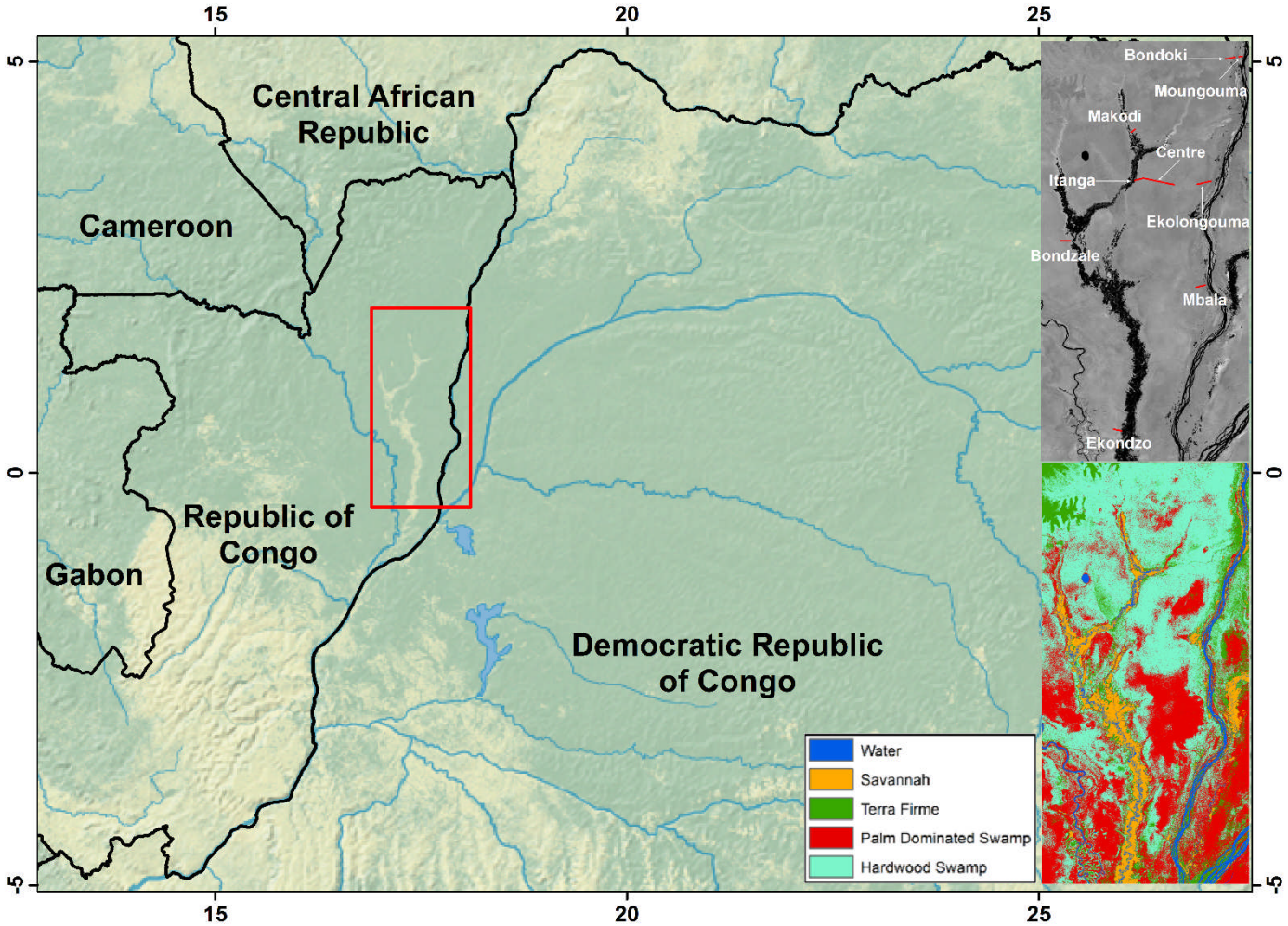

Figure 1.4. Main: Overview site map of the Cuvette Centrale showing the the ca. 36,000 km² study region (red rectangle) within the Likouala Department, ROC. Top right inset: ALOS PALSAR HH imagery of the study region (corresponding to the area of the red rectangle), with the nine transects, used for sampling in this study, shown in red (see Chapter 2). Bottom right inset and adjacent legend: the spatial distribution of vegetation types for the region (corresponding to the area of the red rectangle), derived from a maximum likelihood classification of multiple remote sensing products (see Chapter 4).

Fieldwork for this thesis was undertaken in the Likouala Department, north-east ROC (Fig. 1.1). The majority of the Department lies within the Cuvette Centrale. The Department has an area ca. 66,000 km^2 and has a population of ca. 154,000 people (Centre Nationale de la Statistique et des Etudes Economiques du Congo, 2016). The majority of the population reside along the rivers of the region or along the single main road, which connects the three main settlements, Impfondo (the capital), Doungou and Epena. Impfondo is located next to the Ubangui River, a major white water tributary of the Congo River. The Ubangui River forms the political border between the ROC and DRC. The other main river in the Department is the Likouala aux Herbes, a black water river which eventually joins the Congo River just below the political boundary between the Likouala and Cuvette departments. The mean annual temperature recorded at Impfondo is 25.6°C (Samba et al., 2008) and the mean annual rainfall is ca. 1,700 mm yr^{-1} (Samba and Nganga, 2012). Owing to the migration of the Inter Tropical Convergence Zone (ITCZ) rainfall in the region has a bimodal distribution, with a peak in rainfall occurring in April/May as the ITCZ migrates north and a larger peak in rainfall in September/October as the ITCZ migrates south (Fig. 1.4.). Elevation in the Likouala Department ranges from 229 to 752 m a.s.l. (USGS, 2006). The underlying geology of the region consists of patches of siliceous and kaolinite clay and silicified sandstone or sand in the north-north west at higher elevations, whilst Quaternary alluvium underlies the rest of the region (ORSTOM, 1969). The higher ground in the north-north west of the region is occupied by *terra firm*e forest. In the rest of the region *terra firme* forest is largely confined to the levees of the Ubangui and along a ridge that runs from the Likouala aux Herbes River to Lac Télé. The rest of the region is largely swamp forest or forest which is periodically inundated. Areas of savannah can be found along the Likouala aux Herbes river and its tributaries and surrounding human settlements (ORSTOM, 1968).

The human impact in the Likouala Department is largely confined to the north-north west of the region where large logging concessions cover the entire upland *terra firme* forest areas (Brandt et al., 2014). Artisanal diamond mining also occurs within the region (Mobbs, 2014). However at lower elevations within the Likouala Department in the Cuvette Centrale, the swamp forests are little disturbed and the largest human impact in this area is probably the use of fire to maintain savannah regions, at the expense of forest regeneration (Posner et al., 2009).

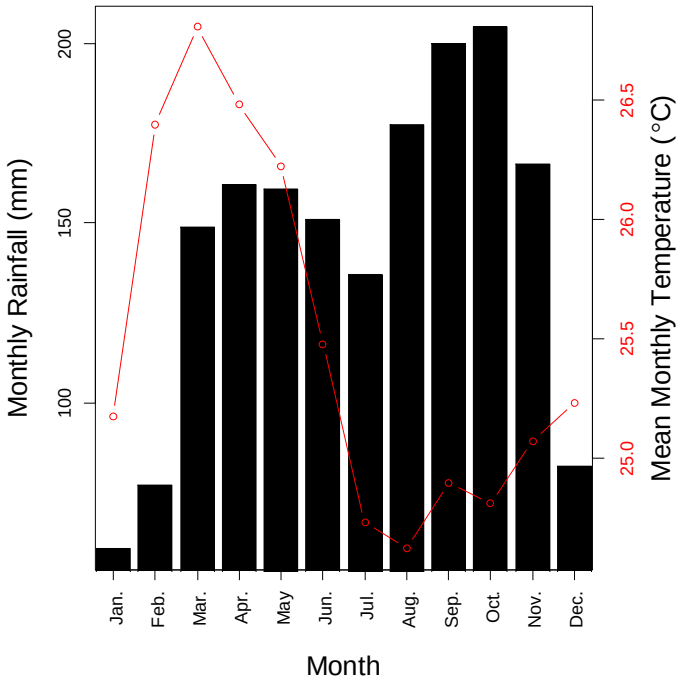

Figure 1.5. Mean monthly rainfall (measured over 1932-2007) and temperature (measured over 1981-2010) for Impfondo, Likouala Department, ROC. Rainfall data from Samba and Nganga (2012). Temperature data from KNMI Climate Explorer (2015).

Chapter 2: Discovery of Extensive Lowland Peatlands within the Central Congo Basin

2.1. Abstract

Reports that peat can be found underneath the swamp forests of the Cuvette Centrale have been around for many decades, but to this date there are no published quantitative data confirming the presence of these peatlands. Here multiple remote sensing products were used to locate fieldwork sites thought to have environmental conditions suitable for peat accumulation within the Likouala Department, ROC, Cuvette Centrale. Peat was found at all sites predicted to be accumulating peat, proving the remote sensing method to be effective at identifying undocumented peatlands. *In situ* depth measurements under swamp forest vegetation gave a mean peat depth (± st. dev.) across all sites of 2.24±1.61 m. The maximum peat depth recorded was 5.9 m. This shows the Cuvette Centrale peatlands to be of similar depth to those of lowland Amazonia, but shallower than South East Asian peatlands. An SRTM digital elevation model (DEM) corrected for canopy height was used to determine peatland topography and showed the peatlands to be non-domed systems. The flat peatland surfaces combined with an observed trend of increasing peat depth with distance from peatland margin suggests that these peatlands occupy large shallow interfluvial basins.

2.2. Introduction

Peat soils are formed by the build-up of slowly decomposing organic matter (OM) under waterlogged anoxic conditions. As they form they sequester carbon (C), and if left intact can be considerable C stores. They cover a relatively small percentage area of the Earth (~3%; Rydin and Jeglum, 2006) but their large C stocks per unit area mean they store an estimated 480 Gt C, which is around a third of the global soil C pool (Page et al., 2011). The majority of the world's peatlands are found in the boreal and temperate zones, but an estimated 89 Gt C is thought to be stored in tropical peatlands, with the majority in South East Asia (Page et al., 2011). However estimates for the tropics should be treated with caution, because for regions outside of South East Asia, very little information is available on the locations or true extent of tropical peatlands. This is particularly true for Africa, where estimates are largely based on one particular grey literature report, *"Fuel Peat in Developing Countries"* by Bord na Mona (1985), and the recycling of old claims with little evidence basis. The Republic of Congo (ROC) is estimated to contain the largest peatland resources across the African continent, based on an area best estimate of 16177 km^2 and a depth best estimate of 7.5 m (Page et al., 2011). However these best estimates are derived from ambiguous sources. For example it is unclear whether widely cited area estimates for the ROC, on which Page et al. (2011) base their best estimate, refer to peatlands or

histosols, with the latter term encompassing, but not being limited to, peatlands (see Fig.1.2, Chapter 1). Likewise, the 7.5 m depth assumed by Page et al. (2011) is a more cautious interpretation of reports that peat depths in the ROC can each up to 30 m (Markov et al., 1988). No specific location is given for these 30 m deep peats and it is unclear whether the reports are actually referring to peatlands within the ROC. Therefore current estimates of peatland extent in the ROC are not based on empirical data.

The ROC, along with the Democratic Republic of Congo (DRC), houses one of the largest wetlands in the tropics, the Cuvette Centrale ('Central Basin'). Despite its size, very little is known about the Cuvette Centrale in terms of its origin, vegetation species composition and hydrology (Campbell, 2005). Under the swamp vegetation, extensive organic deposits with a high OM content (40-70%) are reported to occur and are occasionally true peat deposits (Evrard, 1968). Evrard (1968) state that these organic soils are usually 1 m in depth, but very rarely can reach 17 m in depth. Again however, no data or specific locations are provided. Therefore it appears that no study has yet published empirical data on the underlying substrates of the Cuvette Centrale swamps and the extent of these peat deposits remains unverified. This may be due, in part, to the size, remoteness and inaccessibility of the Cuvette Centrale. However, with more and more satellite data becoming freely available, there is now the opportunity for previously undocumented peatlands to be identified via remote sensing, mainly through the identification of vegetation types associated with peat occurrence (e.g. Lähteenoja et al., 2009b, Draper et al., 2014).

Whilst area estimates have the potential to be detected remotely, measurements of peat properties such as peat depth, bulk density and C concentrations requires fieldwork. Currently there is a real lack of *in situ* measurements of these peat properties and this is a source of large uncertainty in tropical peatland C stock estimates. The need for more *in situ* measurements applies to the whole of the tropics and unless efforts are made to collect this fundamental data, advancements in this area of research can only ever be of limited extent (Lawson et al., 2015).

Filling in the knowledge gaps surrounding tropical peatlands is not only important for improving terrestrial C stock estimates, but also for identifying and protecting valuable ecosystems. In South East Asia land use change, drainage and fire have led to the degradation and destruction of many of the peatlands with serious implications for biodiversity, ecosystem services and greenhouse gas (GHG) emissions (Page et al., 2002, Hooijer et al., 2012, Posa et al., 2011, Posa, 2011, Jauhiainen et al., 2012). Whilst the situation in South East Asia is critical, if there is the political will, action can be taken to prevent further damage to peatland ecosystems. However, protecting peatland ecosystems

in other regions of the tropics and identifying any possible threats to their existence is not possible if they remain undocumented.

In this chapter I describe how remote sensing data was used to identify sites thought to have environmental conditions suitable for peat accumulation within the Likouala Department, ROC, Cuvette Centrale. I present the results from extensive fieldwork in the Likouala Department, which confirm the presence of peat at all sites predicted to accumulate peat. Associations between peat occurrence and vegetation communities are identified and described with the aim of using this information to map the peatlands of the Cuvette Centrale (Chapter 4). Finally peat depth and peatland topography data are presented and used to infer the geometry of these peatlands, which is later used to inform ideas of peatland development (Chapter 5).

2.3. Chapter Aims

The aims of this chapter are firstly to identify sites which are potentially accumulating peat within the Likouala Department, ROC, Cuvette Centrale, using multiple remote sensing datasets to predict locations with environmental conditions suitable for peat accumulation. Secondly, having identified these sites, the aim is to provide empirical data confirming the presence or absence of peat at these sites, through fieldwork. The third aim is to characterise these peatlands in terms of their vegetation cover, depth and geometry. The objectives here are to use *in situ* vegetation data to establish whether specific vegetation types are associated with peat, which could later be used to map peatland extent, to use *in situ* depth measurements to obtain an estimate of peat depth for the Cuvette Centrale based on empirical data and to combine *in situ* measurements with remote sensing elevation data to determine peatland geometry.

2.4. Methods

2.4.1. Site Identification

I used four remote sensing products (Table 2.1) to identify the most likely locations of peat accumulation within the 36,000 km^2 area selected in the Likouala Department (Fig. 2.1). Peat accumulation was considered most likely in areas experiencing waterlogging and with a supply of OM from overlying vegetation. Therefore a digital elevation model (DEM) derived from the Shuttle Radar Topography Mission (SRTM) was used to identify depressions in the landscape where water might pool and radar data (Advanced Land Observation Satellite (ALOS) Phased Array type L-band Synthetic Aperture Radar (PALSAR)) was used to identify areas of high reflectance indicative of standing water or soil with a high moisture content. Optical data (Landsat Enhanced Thematic Mapper (ETM+) and Google Earth) were used to identify forested areas which would provide OM

inputs into possible peatlands. More explicitly, the SRTM DEM obtained from C-band radar typically measures ground elevation but in forested areas, the inability of C-band to penetrate forest canopies, means that depressions in a forested landscape could be owing to a decrease in elevation, a decrease in canopy height or a more open canopy, which permits increased penetration of the C-band signal. The last two scenarios are not suggestive of the direction of water flow, however, a decrease in canopy height or an increase in canopy openness could still be indicative of peat, as spatial patterns in hydrology and nutrient status across a peatland are often reflected in vegetation successions (Page et al., 1999). L-band, with its longer wavelength than C-band, is able to penetrate forest canopies and therefore has long been recognised as useful for detecting conditions on forest floors. Typically, flooded forests have higher HH backscatter (i.e. a higher proportion of the signal which was transmitted in a horizontal polarisation is received in a horizontal polarisation) than non-flooded forests, due to the double bounce mechanism, whereby the radar signal first interacts with the tree trunks and is then reflected off the standing water back towards the antenna (Richards et al., 1987, Hess et al., 1990). Therefore areas with potential standing water were identified from a red, green, blue display of PALSAR HH-HV-HH imagery, with areas of high HH backscatter appearing as pink. Like other forested areas swamp forests may also have a high HV backscatter signal (i.e. a higher proportion of the signal which was transmitted in a horizontal polarisation is received in a vertical polarisation), due to volume scattering of the radar signal as it passes through the canopy. Therefore a Radar Forest Degradation Index (RFDI) created from a PALSAR polarization ratio of (HH - HV) / (HH + HV), was used to exaggerate slight differences between the two polarizations for each pixel, helping to differentiate between forest and inundated forest. Imagery of Landsat ETM+ bands 4, 5 and 7 displayed as red, green and blue were used to identify vegetation potentially associated with peatlands. This was used because Landsat Thematic Mapper (TM) imagery has been used successfully to identify tropical peatlands in Amazonian Peru, with forested peatlands appearing as red and non-forested peatlands appearing as blue when bands 4, 5 and 7 are displayed as red, green and blue (Lähteenoja et al., 2009b). In this study Landsat ETM+ was used instead of Landsat TM because the band wavelengths of the two satellites are near identical, but Landsat ETM+ imagery is more recent. Finally one of the sites described below (named Ekolongouma) was initially identified from Google Earth, because it stood out as a large distinctive area within the landscape.

Table 2.1. Remote sensing products used to locate field sites in the Likouala Department, ROC, Cuvette Centrale.

Product	Spatial Resolution	Acquisition Date	Product Description	Data Provider and Repository	Detection Capability
Landsat ETM+	30 m	18th Feb. 2001	Bands 4, 5 and 7 displayed as red, green and blue respectively.	NASA/USGS (http://earthexplorer.usgs.gov/)	Different vegetation classes.
ALOS PALSAR 50 m Orthorectified Mosaic Product	50 m	10th Sep. 2007 to 17th Jun. 2009	Both polarised (HH) and cross polarised (HV) imagery used in a HH-HV-HH red, green, blue display.	JAXA EORC (1997) (http://www.eorc.jaxa.jp/ALOS/en/kc_mosaic/kc_map_50.htm)	Differentiates areas of inundated forest from non-flooded forest.
RFDI	50 m	10th Sep. 2007 to 17th Jun. 2009	Created from a PALSAR polarization ratio of (HH - HV) / (HH + HV), used to exaggerate slight differences between the two polarizations for each pixel.	Original data from JAXA EORC (1997) (http://www.eorc.jaxa.jp/ALOS/en/kc_mosaic/kc_map_50.htm)	Differentiates areas of inundated forest from non-flooded forest.
SRTM DEM	~90 m	Feb. 2000	Void filled 3-arc second version.	USGS (2006) (http://earthexplorer.usgs.gov/)	Depressions in landscape where water could accumulate. Shorter or more open canopy, indicative of wetland vegetation succession.
Google Earth	15-30 m	-	Optical satellite imagery from a variety of sources.	Google Earth (https://www.google.co.uk/intl/en_uk/earth/explore/products/)	Different vegetation classes.

Nine field sites were identified using these remote sensing products. Eight of these were hypothesised to contain peat and one was not. None of the sites visited had a formal name and so were named informally by me after the nearest village or fishing camp. The eight sites that were hypothesised to contain peat are as follows: Bondoki, Bondzale, Centre, Ekolongouma, Ekondzo, Itanga, Makodi and Mbala. Moungouma is the site which was not hypothesised to contain peat. These field sites were visited over three expeditions which took place from January to February 2012, January to July 2013 and March to May 2015.

As one of the first sites to be visited Makodi Swamp was selected because the Landsat ETM+ imagery indicated that, relative to the overall area being considered, vegetation cover varied greatly over a small spatial area. This meant data points could easily be obtained for a wide variety of vegetation covers, which would later be of use for classifications of remote sensing imagery (see Chapter 4). Also the SRTM DEM suggested there was a shallow depression in the form of what was possibly an old meander, suggesting the presence of a backswamp, which have been found to accumulate peat in other regions of the tropics (e.g. Householder et al. (2012)). Finally the PALSAR HH-HV-HH and RFDI images suggested that the area could be inundated.

Ekolongouma Swamp was also visited on the first fieldtrip and was chosen as a site because it stood out as a large distinctive area within the landscape. The optical imagery (Google Earth and Landsat ETM+) indicated that the vegetation was distinct from other parts of the landscape, with variations in reflectance properties organised in ring-like patterns suggestive of a mire system. The PALSAR HH-HV-HH and RFDI images suggested that the area was inundated and the SRTM DEM suggested either that the area was a shallow topographic depression, or that the forest canopy dropped systematically towards the centre of the site, either of which could be consistent with the presence of a wetland.

Bondoki Swamp, Bondzale Swamp, Itanga Swamp, Ekondzo Swamp, Mbala Swamp and Moungouma Swamp were visited on the second trip. The remote sensing products used in the site selection remained the same, but an additional aid was the results of a supervised maximum likelihood classification of Landsat ETM+ imagery, carried out in ENVI 4.6.1. This classification was carried out after the first field trip and the regions of interest used to run the classification were based on observations made in the field. The objective when selecting these new sites was still to predict and locate peat, but an additional objective was to have sites to sample which were representative of the region and provide data which could be used for scaling up peatland carbon stock estimates (see Chapter 4) and determining mechanisms of peat formation (see Chapter 5) and maintenance (see Chapter

6). More specifically sites were selected to cover a wide geographical area, different vegetation types (including vegetation types thought not to be associated with peat), to incorporate old fluvial features as well as interfluvial regions, and to ensure that sites adjacent to white water and black water river systems were equally represented. The Moungouma site was hypothesised not to contain peat because remote sensing imagery suggested it consisted of old meanders belonging to the Ubangui River. It was hypothesised that whilst peat probably does form within old river channels, peat would not form within old river channels of the Ubangui, based on the assumption that, as a white water river, the nutrient content and pH level of the Ubangui waters would be too high to allow peat formation (Thompson and Hamilton, 1983).

The final field campaign (March to May 2015) assessed whether peatlands extend fully across the large interfluvial area between the Likouala aux Herbes and the Ubangui rivers. The transect (termed "Centre") began at the end of the Itanga transect, but on a trajectory towards the Ekolongouma transect, reaching the mid-point between the two rivers. The results help determine whether peat depths continually increase with increasing distance from the swamp edge.

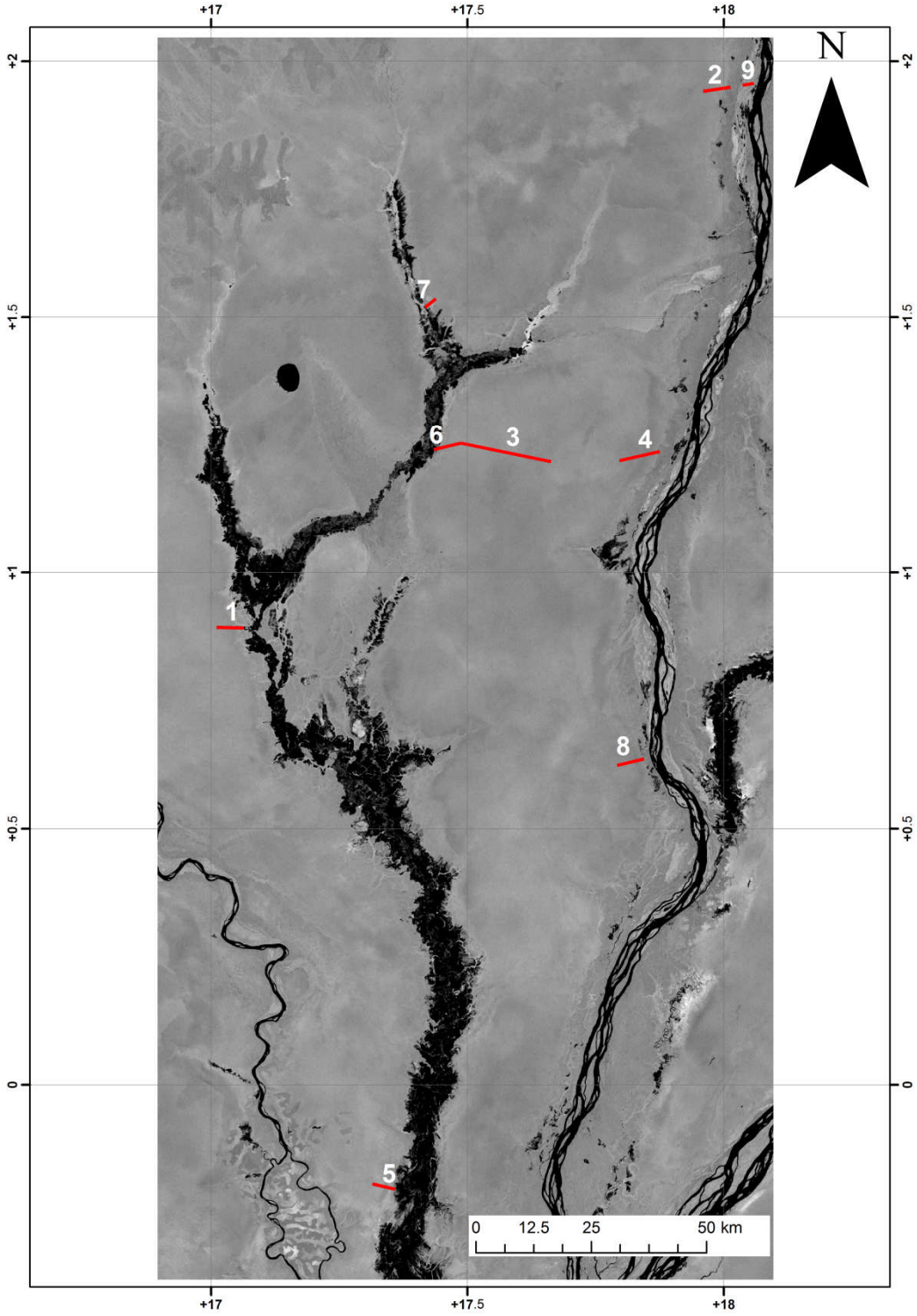

Figure 2.1. PALSAR HH imagery of the study sites within the Cuvette Centrale. The numbered red lines show the location of the nine transects of this study, which are as follows: 1. Bondoki 2. Bondzale 3. Centre 4. Ekolongouma 5. Ekondzo 6. Itanga 7. Makodi 8. Mbala 9. Moungouma.

2.4.2. Sampling Methods

2.4.2.1. Transect Sampling

The nine sites were visited and sampled for peat, water and vegetation characteristics along a transect. Transect length and orientation were predetermined using remote sensing imagery and ArcGIS 9.0. A GPS (manufacturer: Garmin, Hampshire, U.K.; model: GPSmap 60CSx) and compass were used in the field to ensure transect coordinates and orientation were followed correctly. Transect lengths varied from 2.5 km up to 20 km (Table 2.2). Occasionally slight modifications to transect length and orientation were made in the field for logistical reasons, which were usually time constraints or having to camp near to a water source.

2.4.2.2. Peat Cores

Peat cores were taken for the purposes of determining peat depth (see section 2.4.5) and for recovering samples for analysis of peat properties (Chapter 3). At six sites peat cores were taken every kilometre along the transect, unless no peat was present. The Centre transect, being 20 km long, was sampled every 4 km. Along the Makodi transect, the high variability in vegetation cover over the short distance meant sampling was every 200 m. The Moungouma transect crossed multiple old channels, therefore, rather than core at regular intervals, cores were taken at each channel and interchannel feature along the transect. At all sites additional cores were also taken at points along the transects that were thought to be old or seasonal channels. These channels were identified prior to arrival in the field from ALOS PALSAR and Landsat ETM+ imagery. In total 61 cores were extracted and brought to the UK for analysis (Table 2.2).

Peat cores were taken with a 0.5 m long Russian type corer (manufacturer: Eijkelkamp, Giesbeek, The Netherlands). Peat cores were subsampled in the field by cutting up the peat core with a knife whilst still inside the corer and then placing each subsample inside sealed plastic bags for transportation out the field. At all sites sampling of the peat profile continued until the underlying mineral layer was reached.

Table 2.2. Summary of sampling strategy for each field site within the Likouala Department, ROC, Cuvette Centrale.

Site	Transect Length (km)	No. of Cores	No. of Vegetation Plots	No. of Peat Depth Measurements (inc. measurements made by coring)	Additional Sampling
Bondoki	6	5	8	16	N/A
Bondzale	6	5	7	19	N/A
Centre	20	5	5	80	N/A
Ekolongouma	9	8	10	32	1 core and vegetation plot north of the transect.
Ekondzo	5	5	6	17	4 vegetation plots south west of the transect on the same trajectory, but on the other side of the river. No cores taken at these points because there were no peaty soils to sample.
Itanga	6	7	8	18	N/A
Makodi	3	13	16	18	3 cores south east of the transect taken within vegetation plots which were already established. 2 cores and vegetation plots north west of the transect.
Mbala	6	6	8	20	N/A
Moungouma	2.5	3	8	5	N/A
Total	**63.5**	**63**	**80**	**225**	**-**

NB. The number of cores taken along each transect does not equate to the number of vegetation plots along each transect because cores were only taken at points where there was peaty soil. The number of cores taken includes cores which were later found not to be truly peat (i.e. an OM content ≥65% to a depth of at least 30 cm; see section 2.4.5).

2.4.2.3. Peat Depth Measurements

In addition to obtaining peat depth estimates directly from peat cores, depth measurements were made by probing the peat with metal poles. Metal poles were inserted into the ground until the poles were prevented going any further by the underlying mineral layer. It was clear that the underlying mineral layer had been reached when the poles were removed from the ground, due to clay adhering to the surface of the poles. Measurements would be made from the peat surface to the point on the pole where there were the first visible signs of mineral soil. These additional peat depth measurements were made every 250 m between coring sites along each transect, with the exception of Makodi Swamp and Moungouma Swamp, where no additional peat depth measurements were made.

At 24 coring points, distributed across the Bondoki, Bondzale, Centre and Ekolongouma transects, peat depth was measured both by taking a core and by the metal pole method, to calibrate the metal pole measurements with those of the peat cores.

2.4.2.4. Aboveground Vegetation

Every kilometre along each transect a 20 by 40 m vegetation plot was established, regardless of whether or not peat was present. If additional peat cores were taken, for example in old channels, a vegetation plot would also be established, so that each peat core had a corresponding vegetation plot. Along the Makodi Swamp and Moungouma Swamp transects, vegetation plots were more frequent in order to coincide with the belowground sampling and were therefore located every 200 m along the Makodi transect and at every channel and interchannel feature along the Moungouma transect. Along the Centre transect, vegetation plots also coincided with peat coring points and so were located every 4 km.

The vegetation plots allow aboveground biomass (AGB) estimations (see Chapter 4) and a classification of the vegetation types associated with lowland peatland ecosystems. For each plot a description of the vegetation was made (Table 2.3), then all trees with a diameter at breast height (DBH) ≥10 cm were measured for diameter at a height of 1.3 m from the ground unless stilt roots, buttresses or a deformity were present, in which case the measurement was taken 30 cm above the respective trunk deformation. Trees were identified to species level, where possible, or failing that genus or family level. Within each plot five tree height measurements were taken with a laser hypsometer (manufacturer: Nikon, Kingston upon Thames, UK, model: Laser 550A S). Tree height measurements were taken for estimations of canopy height and for use in AGB allometric equations (see Chapter 4).

Additional vegetation descriptions were also made every 250 m along each transect, with the exception of the Makodi Swamp and Moungouma Swamp transects, following the same procedure as for the description of the vegetation plots (Table 2.3). Five tree height measurements were also made at these points. The purpose of these tree height measurements were solely for detecting changes in canopy height along the transect and not for use in AGB allometric equations.

Table 2.3. Information recorded for vegetation descriptions of vegetation plots and at least every 250 m along each transect.

Item	What was recorded
1. Vegetation class	One of the following was selected: -savannah -*terra firme* -seasonally flooded forest -hardwood swamp -*Raphia laurentii* palm dominated swamp -*Raphia hookeri* palm dominated swamp -other
2. Species Composition	Which species dominates and common species in canopy and understory.
3. Topography	Whether the terrain was flat or undulating. If undulating, an estimate was made by eye of size and frequency of undulations.
4. Flood regime	One of the following was selected*: -seasonally flooded -seasonally flooded, but only in major wet season (Sept. to Nov.) -never flooded
5. Disturbance activity I. Treefall	One of the following was selected: -None -Minor (tree <40 cm dbh) -Major (tree >40 cm dbh)
II. Fire	One of the following was selected: -None -Surface -Surface and trees
6. Anthropogenic Activity	A record was made of whether there were signs of: -Hunting -Non-timber forest product harvesting -Trails (footpaths) -Trees <10cm DBH cut -Trees >10 cm DBH cut

*The flood regime was not always apparent and the local knowledge of the field assistants had to be relied upon.

2.4.3. Peatland Surface Topography

To assess if the sampled Congo peatlands are domed systems I estimated the height of the peatland surface along each transect using a corrected DEM method. A deployed differential GPS (manufacturer: Trimble Navigation Limited Integrated Technologies, Sunnyvale, California, U.S.A., model: Ashtech ProMark 100 GNSS Survey Receiver) failed to provide meaningful data, likely due to the canopy cover and poor satellite coverage and levelling techniques were not possible over the distances covered, with tree coverage reducing visibility. The details of the corrected DEM method are given below.

Advanced Spaceborne Thermal Emission and Reflection Radiometer (ASTER) Global Digital Elevation Map (GDEM) 30 m resolution and SRTM 1 arc second (equivalent to 30 m resolution) scenes (available from http://earthexplorer.usgs.gov/) covering the area of the nine transects were mosaicked together in ENVI 4.6.1. Using the GIS software QGIS

2.4.0, ASTER GDEM and SRTM DEM values were extracted for each sampling point along each transect. The ASTER GDEM is derived from stereoscopic techniques applied to the visible and near-infrared (VNIR) imagery and unlike the SRTM DEM, should measure the top of forest canopies. Therefore it was predicted that an estimation of the ground surface (G; m a.s.l) could be obtained through the following equation:

$$G = E_{ASTER} - H \quad [2.1]$$

Where E_{ASTER} is the ASTER elevation (m a.s.l.) and H is the mean of the five tree heights (m) measured at each sample point. However, it was clear that at some sites the ASTER data was too noisy and was not a good measurement of canopy height. Therefore this was done only for sites where the ASTER GDEM seemed reasonable i.e. where variations in canopy height along the transect seemed to correspond to variations in ASTER GDEM elevation, and where the ASTER GDEM was not consistently lower than the SRTM data. These sites were Itanga and Ekolongouma (Fig. 2.2).

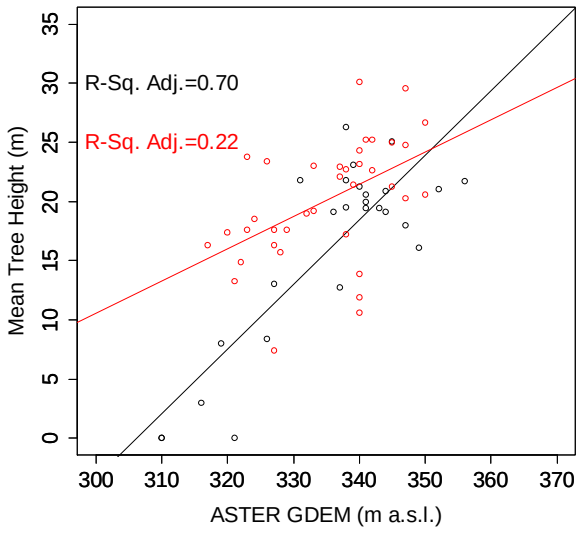

Figure 2.2. Relationship between ASTER GDEM elevation (m a.s.l.) and mean tree height (m) along the Itanga (black) and Ekolongouma (red) transects.

Once a ground surface estimation had been made for these sites, the difference between SRTM and the estimated ground surface (D; m) was calculated as follows:

$$D = E_{SRTM} - G \quad [2.2]$$

Where E_{SRTM} is the SRTM elevation (m a.s.l.).

Linear regression was then used to look for a relationship between mean tree height (H) and the difference between SRTM elevation and the estimated ground surface (D; m). The

statistical package R 3.0.1 (R Core Team, 2014) was used for this analysis and all other subsequent statistical analyses presented in this thesis.

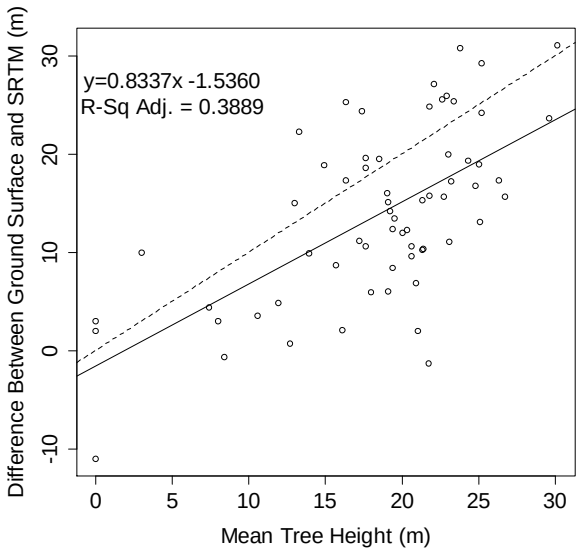

Figure 2.3. Relationship between mean tree height (H; m) and the difference (D; m) between the estimated ground surface (G; m a.s.l.) and SRTM (m a.s.l.; shown as a solid line) used to correct the SRTM DEM. Line equation and adjusted R-sq. value are shown. Dashed line shows a 1:1 relationship.

A significant ($p<0.001$) positive relationship was found between H and D (Fig. 2.3). Although H did not explain a lot of the variance in D, the regression equation was used to create a correction factor (CF; m) that was applied to the SRTM data at sites where the ASTER data had been less reliable:

$$CF = 0.8337 * H - 1.5360 \quad [2.3]$$

A ground surface estimate ($G2$; m a.s.l.) was then calculated at sample points along each of these transects by the following:

$$G2 = SRTM - CF \quad [2.4]$$

However, one unrealistic artefact of this approach was large dips in the estimated ground surface wherever there were very large mean tree height measurements. To try to create a more continuous and smoother ground surface, additional points were created every 0.001 degrees (ca. 11 m) along each transect. For these additional points ASTER and SRTM values were extracted in QGIS 2.4.0 and mean tree height estimates were assigned through linear interpolation of the actual mean tree height measurements using the R package Zoo (Zeileis and Grothendieck, 2005). Tree heights were then smoothed (using a smoothing window roughly equivalent to 1 km), again using the R package Zoo (Zeileis and

Grothendieck, 2005). A SRTM correction factor was then created for each point but this time the interpolated and smoothed mean tree height data replaced H in equation 2.3.

2.4.4 Laboratory Methods

2.4.4.1. Definition of Peat

In this study peat is defined as a soil with an OM content ≥65% and a minimum depth of 30 cm, sensu Page et al. (2011). Samples which did not fit this definition were excluded from the laboratory analyses.

2.4.4.2. Loss on Ignition

To determine the OM content of the samples, the loss on ignition (LOI) method was used, whereby the mass lost from a sample during ignition is assumed to be due to the loss of OM. Depending on sample size, approximately 0.5 to 1 g of dried sample was placed in a crucible and dried in an oven overnight at 105°C. The samples were cooled in a dessicator, weighed, then placed in a furnace for four hours at 550°C (based on the recommendations of Heiri et al. (2001)). Samples were cooled in a dessicator before reweighing.

The OM content (OM; %) of the sample was calculated by the following equation:

$$OM = \left(\frac{(m_{105} - m_{550})}{m_{105}}\right) * 100 \quad [2.5]$$

2.4.5. Peat Depth Corrections

The true peat depth was taken as the point in the peat profile at which the OM content dropped below 65%. For the peat cores this was determined from the LOI results. For two cores the OM content dropped below 65%, but further down the core increased again. In these instances, this was viewed as a mineral intrusion and not the base of the peat profile; the base of the base of the peat profile was taken as the point where OM content dropped below 65% and did not increase again. At the 24 sample points where both a peat core and a depth measurement were taken, a comparison was made between the depth determined by LOI and the depth measured using the metal poles. Peat depth was overestimated by the pole method at 23 of the 24 sample points. Therefore I calibrated the pole method to the coring and LOI method to correct the pole-only peat depth measurements. A significant ($p<0.001$) positive relationship between both methods was found (Fig. 2.4; adjusted R-sq. 0.97), which was used to calibrate all pole-only measurements:

$$y = 0.88758x - 34.76248 \quad [2.6]$$

Where y is the corrected peat depth (cm) and x is the peat depth (cm) measured by the pole method.

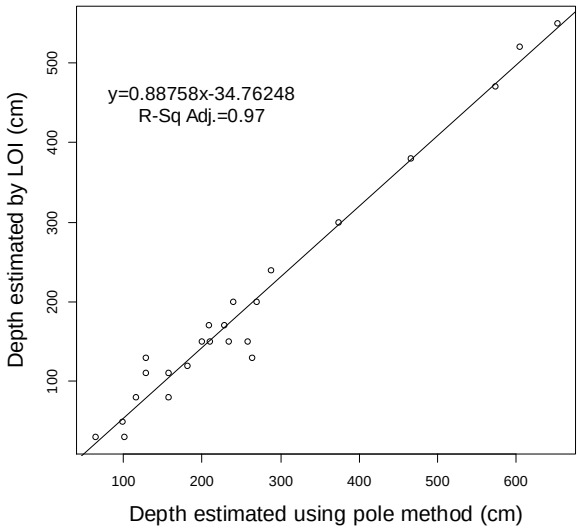

Figure 2.4. Relationship between peat depths estimated by the metal pole method and by LOI.

2.5. Results

2.5.1. Remote Sensing as a Methodology to Locate Peatlands within the Congo Basin

At eight out of eight sites, where peat accumulation was predicted from theory and remote sensing data, peat (≥65% OM, ≥30 cm depth) was found. At a ninth site, Moungouma, near the white-water Ubangui river, where I did not expect to find peat as nutrient levels were likely higher, no peat was discovered. Six main vegetation classes were encountered in the field: *terra firme* forest, seasonally flooded forest, hardwood swamp, *Raphia laurentii* palm dominated swamp, *R. hookeri* palm dominated swamp and savannah (Table 2.4). Only two were consistently associated with peat: hardwood swamp and *Raphia laurentii* palm dominated swamp. The *Raphia hookeri* palm dominated swamp was generally associated with peat, but not consistently. Savannah was not associated with peat, except on one occasion. *Terra firme* and seasonally flooded forest were never associated with peat.

Hardwood swamp forest (example shown in Fig. 2.5) was found at every site with the exception of Moungouma. The *Raphia laurentii* palm dominated swamp was found at Bondoki, the Centre, Ekolongouma, Ekondzo and Mbala. Typically it was often found further along the transects, away from the swamp margins. But in the case of Ekondzo and Mbala, there were small patches of this palm dominated swamp close to the margins of the swamp. It was found to form very distinctive monodominant patches, particularly at Ekolongouma (Fig. 2.6).

Table 2.4. Descriptions of vegetation classes encountered in the field and their association with peat.

Vegetation Class	Description	Associated With Peat?
Terra firme Forest	Generally limited in extent. Was most commonly found adjacent to the Ubangui River. Includes both primary and secondary vegetation. Dominated by dicots. Understorey frequently dominated by Marantaceae *Sarcophrynium* sp. Never or very rarely floods.	No
Seasonally Flooded Forest	Found to occur in transition between either savannah or *terra firme* vegetation and swamp vegetation. Dominated by dicots. Lianas often very abundant and sometimes dominate. Topographically very variable on a small scale, with a system of mounds and channels. Understorey is often confined to the mounds. Species such as *Guibourtia demeusei* and *Dialium pachyphilum* can often be found. Usually only floods in the major wet season.	No
Hardwood Swamp	Dominated by dicots. Trees often showing adaptations to wet conditions such as stilt and aerial roots and buttresses. Species commonly found across all sites include *Uapaca paludosa*, *Carapa procera, Symponia globulifera* and *Xylopia rubescens*. Myrasticaceae sp. was often abundant in the lower canopy.	Yes
Raphia laurentii Palm Dominated Swamp	*Raphia laurentii* dominant or monodominant swamp. The *Raphia laurentii* is a trunkless palm with fronds reaching up to 12-14 m in length. The swamp is more open than the hardwood swamp. Tree species present are the same as the hardwood swamp, but tree abundance is much less. Ferns are often abundant in the understorey.	Yes
Raphia hookeri Palm Dominated Swamp	*Raphia hookeri* dominated. *Raphia hookeri* forms a trunk and reaches heights of up to ca. 16 m. It appears to be associated with the presence of seasonal channels or old fluvial features.	Yes but not consistently and not associated with thick peat deposits.
Savannah	Grassland often dominated by *Hyparrhenia diplandra*. Distributed largely along river courses or near villages. Seasonally flooded in parts. Seasonally burned. Boundary between savannah and forest is very abrupt.	Generally no, but shallow, discrete peat deposits can be found in savannah streams.

The *Raphia hookeri* palm dominated swamp (example shown in Fig. 2.7) was consistently found within what were suspected to be old or seasonal channels. Whilst peat was often found under the *Raphia hookeri* palm dominated swamp, this vegetation class was not necessarily indicative of peat. However, at the Itanga, Makodi and Bondoki sites, even when patches of *Raphia hookeri* did not overlie peat, it was always found to be associated with a very organic soil, but one which did not meet the criteria used in this study to define peat i.e. the OM horizon was <30 cm thick. At Moungouma, however, there was no OM accumulation; a few centimetres of leaf litter and live roots overlay a clayey mineral

layer. Whilst the transects at Bondoki, Ekondzo, Itanga and Makodi all started in savannah, only at Itanga was peat found to be forming under savannah vegetation, within what appeared to be a channel flowing from the forest to the Likouala aux Herbes River.

True *terra firme* forest i.e. never inundated, was found only along the Bondoki, Bondzale, Mbala and Moungouma transects. Seasonally flooded forest was found along every transect except for Makodi and the Centre. Unless dried up channels were visible, it was often not obvious whether a forest was truly *terra firme* or was seasonally inundated. Local knowledge from field assistants had to be relied on to determine the type of forest in these instances. Once the transects had entered swamp forest, unless briefly traversing a channel system, no more patches of *terra firme* or seasonally flooded forest would be encountered along the transects. As an example Table 2.5 describes vegetation succession along the Bondoki transect (Appendix 1 to 8 describes the vegetation succession along the remaining eight transects).

Figure 2.5. Photo showing hardwood swamp. Centre, March 2014.

Figure 2.6. Photo showing *Raphia laurentii* palm dominated swamp. Ekolongouma, February 2012.

Figure 2.7. Photo showing *Raphia hookeri* palm dominated swamp occupying a channel which drains the swamps. Itanga, March 2013.

Table 2.5. Description of variations in land cover characteristics along the Bondoki transect.

Distance (m)	Vegetation Type	Vegetation Description	Flood Regime	Peat Present	Microtopography	Disturbance/ Anthropogenic Activity
0	S	Dominated by *Poaceae* sp.	Partially flooded in major wet season. Mounds remain above water level.	No	Gently undulating, but some mounds 1-2 m.	Seasonal anthropogenic burning.
250	SFF	No species obviously dominates.	Seasonally flooded in major wet season.	No	Undulating 1-2 m.	Ca. 10-20 m away from clearing created for small plantation, which will be burned before crops are planted.
500	TFF	Marantaceae *Megaphrynium* or *Sarcophrynium* sp. and *Laccosperm secundiflorum* dominate understorey.	No flooding.	No	Generally flat, but in places up to 1 m undulations.	Some minor tree fall.
1250	SFF	Marantaceae *Megaphrynium* or *Sarcophrynium* sp. and *Laccosperm secundiflorum* still present in understorey. Lianas are abundant. More palm species present. Signs of transition to wetter conditions. Pneumataphors present in places. At ca. 2000 m tree species with stilt roots, such as *Uapaca paludosa* and *Macaranga* sp. can be found.	Seasonally flooded.	No	Generally gentle undulations, but up to 1-2 m in places.	Some minor tree fall.
2500	HS	Trees such as *Uapaca paludosa* and *Carapa procera* present. Myrasticaceae sp. very abundant mid-canopy. *Palisota* sp. very common in understorey.	Seasonally flooded.	Yes	Gently undulating, with undulations up to 0.5–1 m.	Some minor tree fall.
3500	PS-RL	*Raphia laurentii* dominates forming lower canopy ca. 8 m. Tree species, including, but not limited to, *Uapaca paludosa, Symphonia globulifera*, *Carapa procera*, form higher canopy ca. 20 m. Myristicaceae sp. still present mid-canopy. Understorey mainly made up of ferns, *Palisota* sp. and *Cryptosperma senegalense*.	Seasonally flooded.	Yes	Flat with some < 0.5 m mounds where aerial roots are present.	Minor tree fall in places. Empty bullet cartridges found, showing forest is used for hunting by locals.

S-savannah, SFF-seasonally flooded forest, TFF- *terra firme* forest, HS-hardwood swamp, PS-RL-*Raphia laurentii* palm dominated swamp.

2.5.2. Peatland Topography

The ground surface of the eight peatland transects, estimated from the SRTM DEM corrected for canopy height, shows the peatland surface elevation to decrease slightly along five transects and increase along three transects (Fig. 2.8 A-H). Peatland surface elevation showed large fluctuations along all transects, with the Makodi transect having the largest maximum difference in peatland surface elevation of 18 m and Bondzale having the smallest maximum difference in peatland surface elevation of 9 m. Along the longest transect, the Centre (Fig. 2.8 C), there is a clear overall decrease in peatland surface elevation. The shorter distances of the other transects, combined with the large fluctuations in topography, make it difficult to identify trends in surface elevation with confidence. The high variability is most likely attributable to noise in the SRTM DEM and the ground surface along some transects being strongly influenced by tree height variation, despite efforts to reduce the effect of large variations in tree heights.

A)

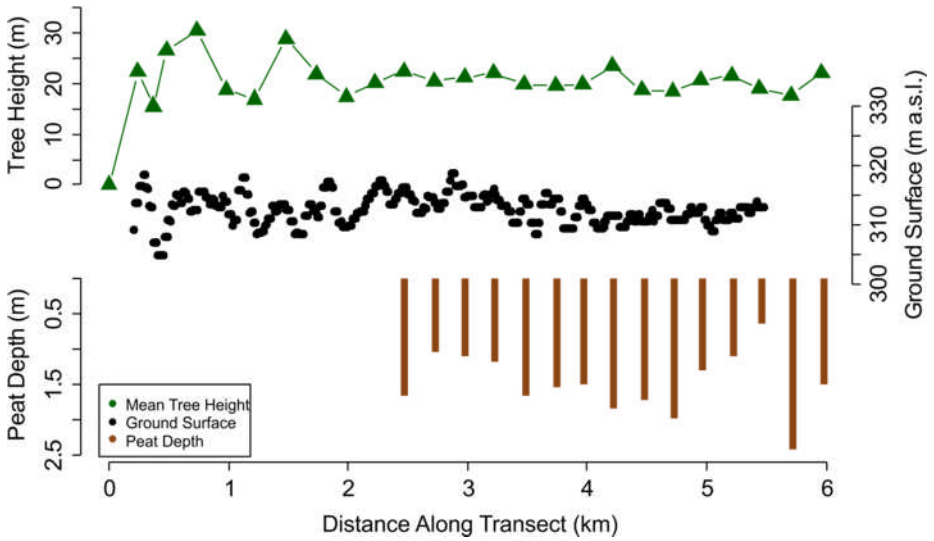

B)

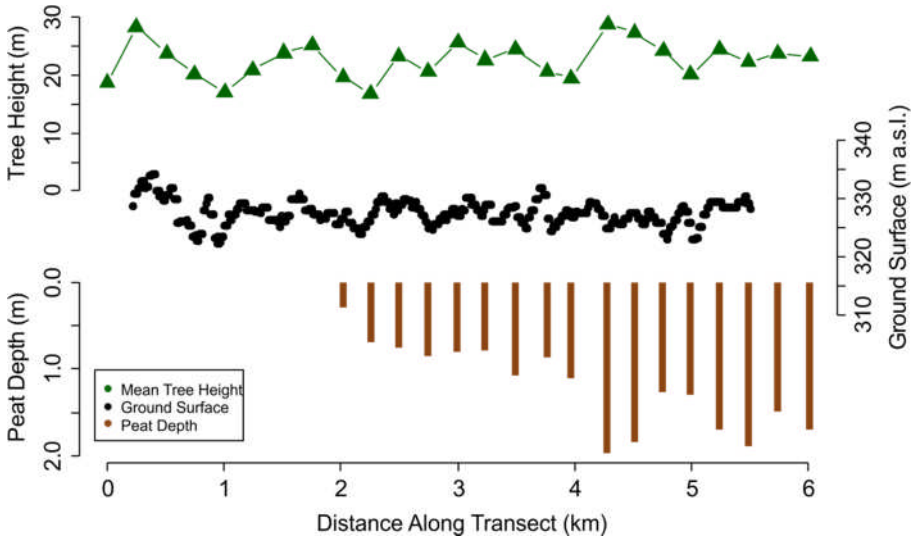
Tree Height (m)
0
10
20
30
Ground Surface (m a.s.l.)
310
320
330
340
Peat Depth (m)
0.0
1.0
2.0
Mean Tree Height
Ground Surface
Peat Depth
0
1
2
3
4
5
6
Distance Along Transect (km)

C)

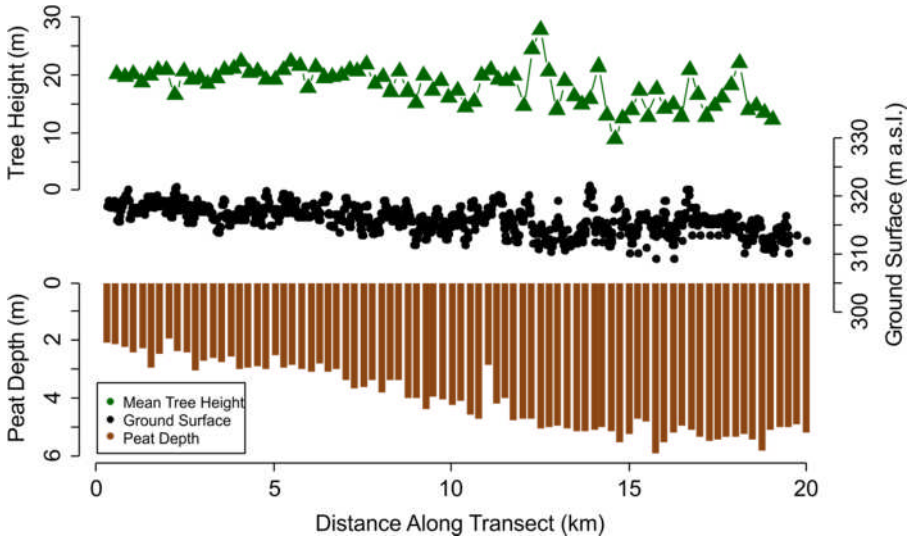
Tree Height (m)
0
10
20
30
Ground Surface (m a.s.l.)
300
310
320
330
Peat Depth (m)
0
2
4
6
Mean Tree Height
Ground Surface
Peat Depth
0
5
10
15
20
Distance Along Transect (km)

D)

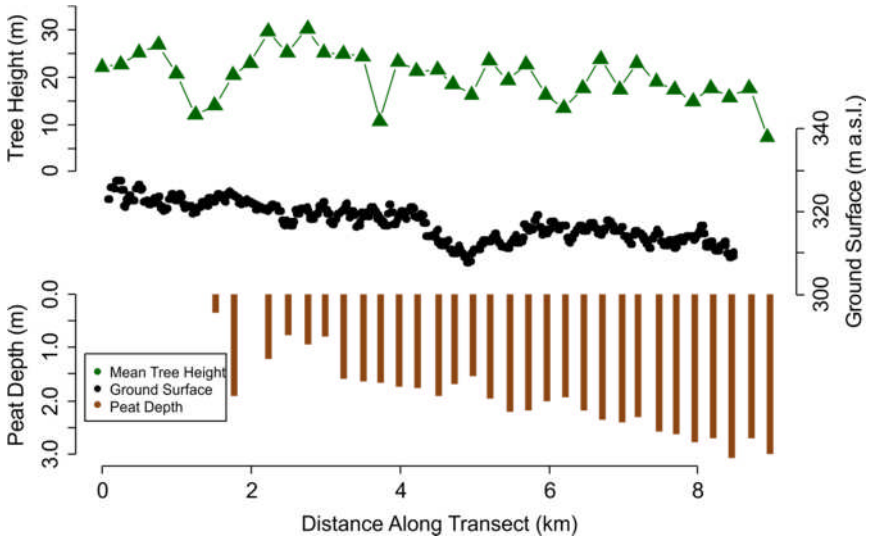
Tree Height (m)
0
10
20
30
Ground Surface (m a.s.l.)
300
320
340
Peat Depth (m)
0.0
1.0
2.0
3.0
Mean Tree Height
Ground Surface
Peat Depth
0
2
4
6
8
Distance Along Transect (km)

E)

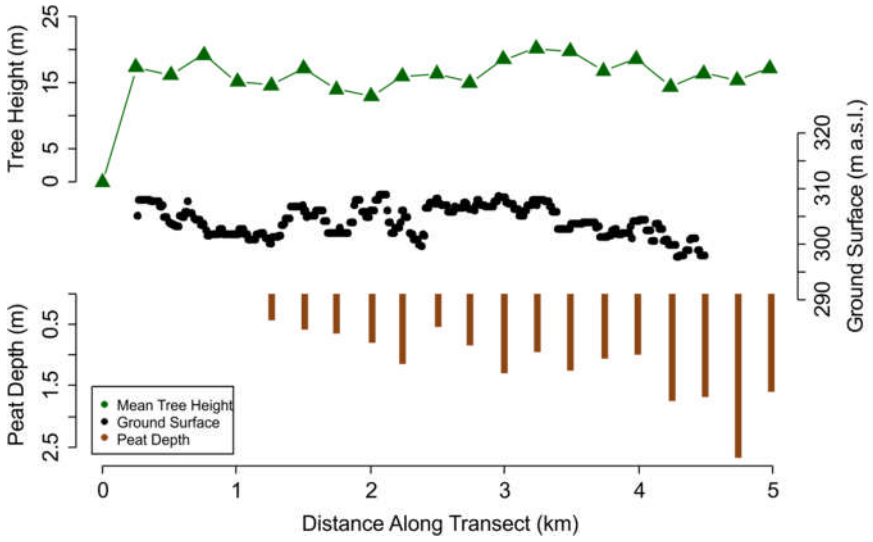
Tree Height (m)
0
5
15
25
Ground Surface (m a.s.l.)
290
300
310
320
Peat Depth (m)
0.5
1.5
2.5
Mean Tree Height
Ground Surface
Peat Depth
0
1
2
3
4
5
Distance Along Transect (km)

F)

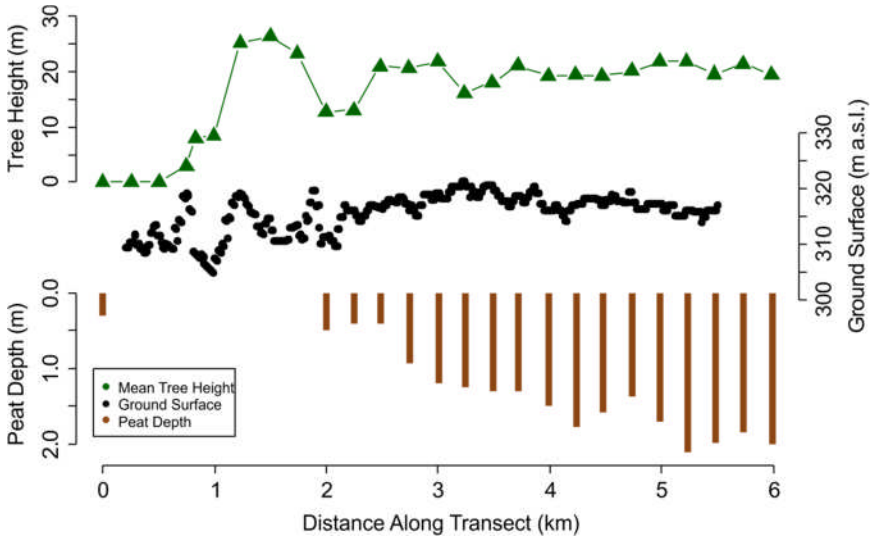
Tree Height (m)
0
10
20
30
Ground Surface (m a.s.l.)
300
310
320
330
Peat Depth (m)
0.0
1.0
2.0
Mean Tree Height
Ground Surface
Peat Depth
0
1
2
3
4
5
6
Distance Along Transect (km)

G)

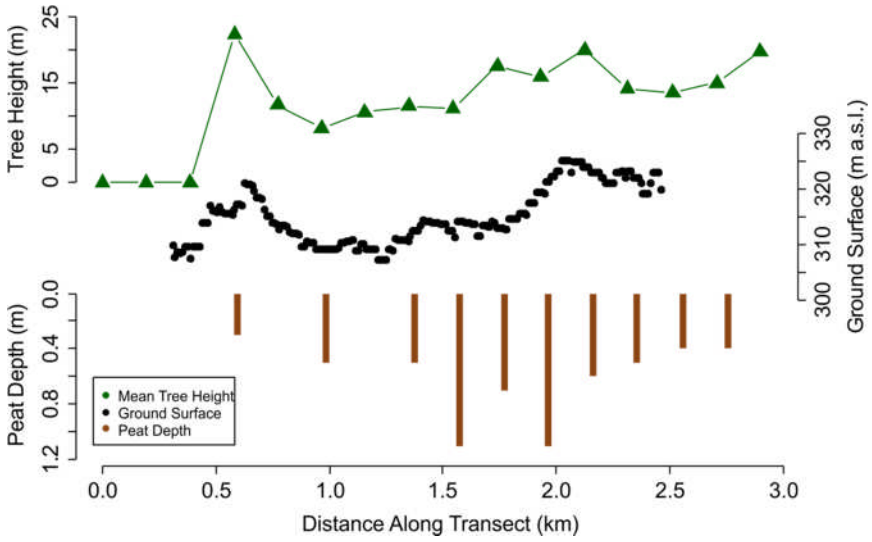

H)

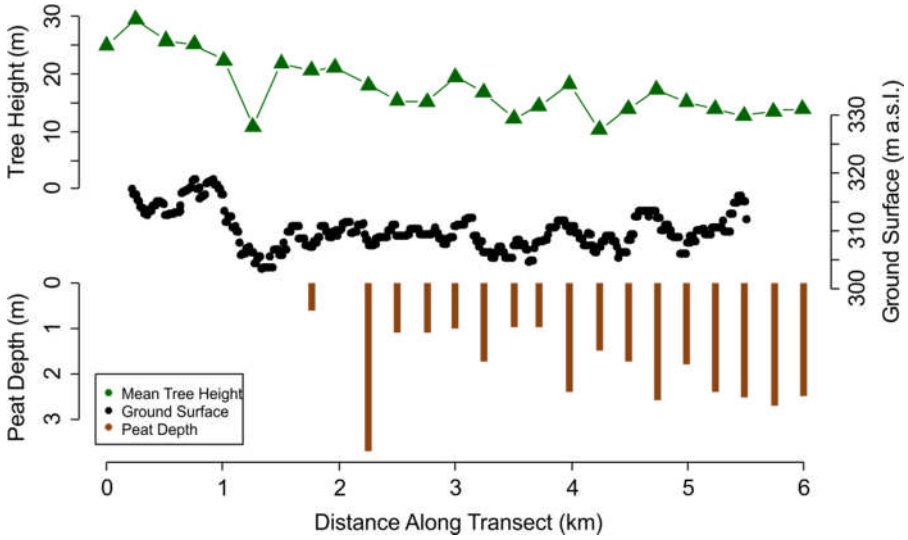

Figure 2.8. Along transect mean tree height (from *in situ* tree height measurements), estimated ground surface (SRTM DEM corrected for canopy height) and peat depth (determined through LOI measurements of peat cores and corrected depth measurements made using a metal probing pole) at A) Bondoki B) Bondzale C) Centre D) Ekolongouma E) Ekondzo F) Itanga G) Makodi H) Mbala.

2.5.3. Peat Depth

Across all sites, the mean (± st. dev.) peat depth under the three swamp vegetation classes (hardwood swamp, *Raphia laurentii* and *R. hookeri* palm dominated swamp) was 2.24±1.61 m. A maximum peat depth of 5.90 m was recorded along the Centre transect (Table 2.6). At the sites where peat was present there was a general trend of increasing peat depth with increasing distance from the swamp margin and as the Centre transect shows this trend continues to the midpoint of the interfluvial regions (Fig. 2.8 A-H).

Table 2.6. Peat depth measurements under swamp forest vegetation (Hardwood swamp, *Raphia laurentii* palm dominated swamp and *R. hookeri* palm dominated swamp) for each site.

Site	Min. (m)	Max. (m)	Mean (m)	St. Dev.	n
Bondoki	0	2.40	1.37	0.56	16
Bondzale	0	1.94	1.08	0.56	19
Centre	1.9	5.90	3.99	1.15	80
Ekolongouma	0.3	3.07	1.86	0.72	32
Ekondzo	0	2.65	1.08	0.66	17
Itanga	0	2.10	1.27	0.62	18
Makodi	0	1.20	0.52	0.44	18
Mbala	0	3.70	1.58	0.99	20
Moungouma	0	0	0	0	5
All	**0**	**5.90**	**2.24**	**1.61**	**225**

2.6. Discussion

2.6.1. Use of Remote Sensing to Identify Peatlands

Sampling across eight sites within the Likouala Department, ROC, confirmed that peat (≥65% OM, ≥30 cm) is present within the Cuvette Centrale. The presence (and absence) of peat (at one site), as predicted demonstrates the effectiveness of the methodology used to locate the peatlands. Remote sensing products, specifically Landsat TM and ETM+ imagery, have been used previously to identify new peatland field sites in other regions of the tropics (Lähteenoja et al., 2009b, Draper et al., 2014). However in these instances, some knowledge of the spectral signature associated with peatlands in the region was known in advance. Here, with no previous knowledge of what vegetation types were associated with peat, the SRTM and PALSAR data in addition to the Landsat ETM+ data, meant the search for peat could be based on finding areas which were suspected to have environmental conditions favourable for peat accumulation, rather than relying on known associations between vegetation classes, their spectral characteristics and peat occurrence.

The use of multiple datasets is key to the success of the remote sensing method of site identification. Individually, each dataset can either indicate whether an area may be part of a depression (SRTM DEM), has a high radar reflectance (PALSAR) or is vegetated (Landsat ETM+, Google Earth), but based on one dataset alone it may be hard to sufficiently narrow down the search for sites potentially accumulating peat. For example, the vast majority of the Cuvette Centrale is forested and whilst differences in forest vegetation are detectable from the Landsat

ETM+ imagery, without radar or topographical data, it can be difficult to make assumptions about the hydrology of the forest and therefore the likelihood of peat accumulation.

Whilst the remote sensing method was used successfully to identify the first two field sites despite little idea of ground conditions, there are limitations to what can be known from remote sensing data in advance of arrival in the field, with the most obvious example being, whether or not peat accumulation is actually occurring. A further example given earlier, is whether the depressions visible in the SRTM DEM are real changes in elevation or are attributable to canopy traits. Therefore having some regional knowledge is preferable and improves the effectiveness of the method. For example, knowing that the Ubangui river has high nutrient levels meant, that despite the Moungouma site being identified as a series of vegetated old meanders, likely liable to flooding, it was hypothesised to have higher decomposition rates and would therefore not accumulate peat. Likewise, it was not known until after the first fieldtrip what the changes in vegetation communities visible in the Landsat ETM+ or Google Earth imagery actually corresponded to. Once this was known, areas where the vegetation cover looked similar to the sites confirmed to have peat, could be targeted.

Many countries in Africa are reported to contain peatlands (see sections 1.3.10 to 1.3.14, Chapter 1). However, a lot of the information available is non-quantitative and the specific location of many of Africa's peatlands seems unknown. Given that the remote sensing products used here to locate peatlands in the Cuvette Centrale are freely available, a similar methodology could be adopted to help identify other poorly known areas of peatland in Africa.

2.6.2. Peatland Vegetation

Peat occurrence within the Cuvette Centrale was shown to be associated with at least four different vegetation communities. The most important vegetation communities were hardwood swamp and *Raphia laurentii* palm dominated swamp, because they were consistently associated with peat formation, were the most extensive in area and were associated with the deepest peat. Whilst the *R. hookeri* palm dominated swamp was often associated with peat, it was not found above thick peat deposits and was limited in extent. Peat formation under savannah seems to be relatively rare, with peat found at only one sample point in the savannah. With four out of the nine transects incorporating savannah vegetation, this was not due to failing to sample that vegetation type. A lack of canopy cover probably means that evapotranspiration (ET) rates in the savannah are extremely high and unless there is a constant supply of water, as there was in this instance in the form of a stream, conditions will be too dry for OM accumulation. Additionally, the savannahs of the Cuvette Centrale are maintained by burning which will also

limited OM accumulation by removing aboveground vegetation and possibly any OM accumulated since the previous burn.

Table 2.7. Wetland classes (excluding open water classes) featured in vegetation maps of the Congo Basin/ Cuvette Centrale derived from classifications of remote sensing data.

Study	Wetland Classes	Description
De Grandi et al. (2000a)	Swamp Forest	Not specifically stated but implied that this is periodically inundated forest.
	Inundated Forest	Not specifically stated but implied that this is permanently inundated forest.
De Grandi et al. (2000b)	Swamp Forest	No specific description or definition given.
Mayaux et al. (2002)	Permanently Flooded Forest	Frequent floods and soils with poor drainage. The upper canopy layer (up to 45m in some cases), composed of a small number of species, is quite homogeneous compared to the lowland rain forest. Flooded even in dry season.
	Periodically Flooded Forest	As above but not flooded in dry season.
	Swamp Grassland	Areas where extended flooding and poor drainage conditions prevent the tree growth.
Vancutsem et al. (2009)	Edaphic forest	Closed (>65%) broadleaf semi-deciduous high (14–30 m) forest on permanently or temporarily flooded land.
	Aquatic grassland	Closed (>65%) tall (0.8–3 m) grassland on permanently or temporarily flooded land.
	Swamp grassland	Closed (>65%) tall (0.8–3 m) grassland on waterlogged soil.
Gond et al. (2013)	Swamp forests located in the Congo Basin	No specific description or definition given.
	Swamp located at the valley bottom	No specific description or definition given.
Betbeder et al. (2014)	EVI 1	Forests subjected to seasonal flood pulse, located alongside rivers.
	EVI 2	Forests subjected to stable water levels, average elevation of 304 m and a maximum canopy height of 20 m.
	EVI 3	Forests subjected to seasonal short lasting flood pulses, with low amplitude, an average elevation of 306 m and a maximum canopy height of 30 m.

The vegetation classes defined here are broad but are more descriptive than the vegetation classes adopted in the most recent maps of the Cuvette Centrale vegetation cover (derived from classifications of remote sensing data; Table 2.7). Being principally based on observations from satellite data, as opposed to ground data, the classes do not include information on species

composition or underlying substrate. In terms of wetland classes sometimes the maps only include a single all-encompassing "swamp forest" class (De Grandi et al., 2000b). When multiple swamp forest classes are included they are distinguished by their perceived inundation period (De Grandi et al., 2000a, Mayaux et al., 2002, Betbeder et al., 2014) rather than their species compositions. However it is not clear what the permanently flooded and seasonally flooded forest classes, which are included in some of the maps, equate to in terms of the classes defined in this study. In this study no vegetation type encountered in the field was permanently flooded; although the hardwood swamp and palm dominated swamp classes have high water tables throughout the year, the water table is not permanently at or above the surface. Two of the maps also include grassland wetland classes (Mayaux et al., 2002, Vancutsem et al., 2009). In this study, only one savannah class is defined and encompasses both seasonally flooded and rarely flooded savannah. Whilst this class could be subdivided further, there did not seem much reason to do this for the purpose of this study as savannah was not found to be indicative of peat whether seasonally flooded or not. Secondly, at the sites where savannah was present, the occurrence of flooding was highly variable over very short distances and unless visited during periods of inundation, it was not apparent whether the savannah was seasonally flooded or not.

More descriptive information on the Cuvette Centrale vegetation can be found in older work by Lebrun and Gilbert (1954) (cited in Richards (1996)) and Evrard (1968) and many (although not all) vegetation classes defined in this study have an equivalent in the classifications of Lebrun and Gilbert (1954) and Evrard (1968). The classification of Lebrun and Gilbert (1954) (summarised in Table 1.1, Chapter 1) is based principally on inundation period rather than specific species associations, but does give a brief description of substrate beneath the vegetation. They describe a "*forets periodiquement inondees*" which is emerged the majority of the time and has very little OM accumulation. The equivalent classification in this study would be seasonally flooded forest, which does not accumulate peat due the infrequency of flooding. Lebrun and Gilbert (1954) do not specifically mention palms in their classes but describe two channel vegetation classes, "*forets riveraines*" and "*forets ripicoles colonisatrices*", both of which are described as having modest OM accumulation. Being associated with channels, the *Raphia hookeri* palm dominated swamp class of this study could fall under either of these two classes. They also mention a permanently flooded "*forets marecageuses*" (swamp forest), which could incorporate both the hardwood swamp and *Raphia laurentii* palm dominated swamp.

Evrard (1968) primarily focuses on vegetation associations, but for some classes a brief description of inundation frequency and soil type is given. With *Guibourtia demeusii* commonly found in the seasonally flooded forest of this study, this class seems very close to Evrard's (1968) "Seasonally flooded *Oubanguia africana- Guibourtia demeusii* association", which is

described as having a limited understorey. Although neither *Entandrophragma palustre, Coelocaryon botryoides* or *Rothmannia megalostigma* were recorded in any of the swamp forest plots, Evrard's (1968) mature swamp forest *Entandrophragma palustre-Coelocaryon botryoides-Rothmannia megalostigma* association, under which peaty soils accumulate, can probably be considered to be the equivalent of the hardwood swamp class of this study. Evrard's (1968) "*Raphia laurentii association*" is almost certainly the same as the *Raphia laurentii* palm dominated swamp of this study. He describes them as forming extensive stands on hydromorphic soils and mentions that ferns are common in the understorey, which fits with the findings of this study. Evrard (1968) also mentions a "*Raphia sese association*" associated with channels and meanders. Although identified here as *Raphia hookeri, R. sese* and *R. hookeri* have very similar characteristics, such as the curled black trunk fibres (Fig. 2.9) and both species are associated with channels and can be found to co-occur (Hughes and Hughes, 1992). It is possible, given the similarities, that *Raphia sese* has been misidentified here as *R. hookeri*. Even if correctly identified, given the similar environmental niches that the two palms occupy, it seems likely that Evrard's (1968) *Raphia sese* association is either the same as or very similar to the *Raphia hookeri* palm dominated swamp of this study. Evrard (1968) describes the substrate under "*Raphia sese association*" as "muck", a mixture of sand and organic material, reaching depths of 1-2 m.

Figure 2.9. Photo showing curled black trunk fibres of *Raphia hookeri*, but which are also a feature of *R. sese*. Photo courtesy of Ian Lawson. Makodi, February 2012.

Both *Raphia laurentii* dominated swamp and *R. sese/ R. hookeri* dominant swamp are stated to be widespread throughout Central Africa, with both *R. sese* and *R. hookeri* reportedly a common

feature of channel networks in the DRC, Central African Republic and Cameroon (Hughes and Hughes, 1992). *Raphia laurentii* dominated swamps are reported in Equatorial Guinea, inland behind the Muni Estuary, and in Cameroon, largely in the south, where it is associated with valley bottoms (Hughes and Hughes, 1992). Like that seen at Ekolongouma, in both Cameroon and Equatorial Guinea *Raphia laurentii* is reported to form either pure stands or stands with very few tree species present, which, in Cameroon, can be up to 3 km across (Hughes and Hughes, 1992). Monodominance in forests can either indicate an early successional community or it can result from positive feedback mechanisms, driven by a combination of species-specific traits under low levels of disturbance (Peh et al., 2011). Monodominance in wetlands is also recorded in Central and South America (Lopez and Kursar, 2007, Parolin et al., 2002, Phillips et al., 1997, Urquhart, 1999) and in some instances is the result of a limited number of pioneer species able to establish themselves in what are often harsh environments (Parolin et al., 2002). Once established however, allogenic changes within these monodominant stands can permit the arrival of other species (Parolin et al., 2002). However, in Central America, palynological records show that *Raphia taedigera*, which forms extensive monodominant stands often overlying peat, is an early pioneer species of these peatlands, but one which is persistently dominant or common throughout the peatlands' development (Phillips et al., 1997, Urquhart, 1999). Therefore it is possible that *Raphia laurentii* monodominant swamps, being as widespread as they are, are the result of *Raphia laurentii* being better adapted than other species to the environmental conditions of Central African swamps. The success of *Raphia taedigera* in Central America is attributed to its ability to germinate under waterlogged conditions (Urquhart, 1999) and its tolerance of a wide range of nutrient statuses (Phillips et al., 1997). No mention is made of OM accumulation under the *Raphia laurentii* swamps in Cameroon or Equatorial Guinea (Hughes and Hughes, 1992), but if *Raphia laurentii*, like *R. taedigera*, can tolerate a wide range of nutrient statuses, then these *R. laurentii* monodominant swamps in Cameroon and Equatorial Guinea may not necessarily be indicative of peat, as a higher nutrient status may impede peat accumulation (Thompson and Hamilton, 1983).

2.6.3. Peat Depth and Topography

With a maximum peat depth of 5.9 m recorded, the depths measured at the eight peatland sites in this study were considerably shallower than the 30 m reported by Markov et al. (1988) for ROC peatlands and the 17 m reported by Evrard (1968) for the Cuvette Centrale. Whilst peat depths of up to 17 or 30 m may be possible, if they exist they are probably extremely rare, as stated by Evrard (1968). Furthermore I suggest that if these measurements are correct, they come from valley systems either within the Cuvette Centrale or perhaps more likely at higher altitudes within the Congo Basin, and do not originate from the large interfluvial basins studied

here. This is because this study has shown the peatlands to occupy extensive shallow interfluvial basins, whose topography cannot support peat depths of 17 to 30 m, unless the peatlands have developed into domed systems and as shown by the peatland topography estimates, this is not the case. Unless a specific location is provided for these 17 to 30 m depth measurements, allowing them to be replicated, I suggest that these measurements are not representative of and may not even come from the Cuvette Centrale peatlands. When considering peat depths reported for the two other main regions known to harbour extensive tropical peatlands, South East Asia and lowland Amazonia, the peatlands of the Cuvette Centrale are comparable to those of lowland Amazonia, but are shallower than South East Asian peatlands (Table 2.8). For a discussion of what this means in terms of peatland genesis between the three regions go to Chapter 5, section 5.6.5.

When reporting or comparing mean peat depth estimates, consideration should be given to how representative the estimated mean is of depth values across an individual peatland or a region as a whole. In particular there should be some thought of potential sampling bias. Few studies which involve peat coring achieve a completely random sampling design, mainly down to the logistics of traversing a wetland environment. In this study all transects, except one, start from outside the peatlands. Therefore there is a sampling bias whereby peatland margins are better represented than the peatland interiors. As the general trend was for peat depths to increase with increasing distance from the peatland margin, it is probable that the mean peat depth is over influenced by shallower peats.

Differences in methodology or how peat is defined is another reason why it is difficult to make absolute comparisons of depth values between studies. For example, Householder et al. (2012) measured peat depths along the Madre de Dios River, Peru, using a similar probing method to the one used in this study, but without applying a correction factor and as this study shows, this can lead to an overestimation of peat depth. Likewise, in studies where depth has been determined through coring, the criteria used for defining the base of the peat differs (e.g. a minimum OM content of 75% (Lähteenoja et al., 2009b)), is not stated (e.g. Jaenicke et al. (2008)) or the peat base was defined subjectively, for example by eye (e.g. Lähteenoja et al. (2009b)).

Table 2.8. Peat depths reported in the literature for lowland tropical peatlands.

Location	Data Source	Peatland Type	Peat Depth (m)	
			Mean (± st. dev.)	Max
Mukah Division, Sarawak, Malaysia	Melling et al. (2005)	Forested peatlands	4.8	NA
Sungai Sebangau catchment, Central Kalimantan, Indonesia	Page et al. (1999)	Mixed	7.8	>11
Pastaza-Marañon Foreland Basin, Western Amazonia, Peru	Draper et al. (2014)	Pole forest Palm swamp Open peatland	3.15±0.27 1.73±0.23 2.65±0.38	6.6 5.4 4.5
Madre de Dios River Basin, Western Amazonia, Peru	Householder et al. (2012)	NA	2.54±1.84	9
Likouala Department, Cuvette Centrale, ROC.	This study	Hardwood and palm dominated swamp	2.24±1.61	5.9

Peatland topography was difficult to assess. Conventional levelling techniques were not feasible over many kilometres and a differential GPS failed to give any meaningful results. The SRTM DEM corrected for *in situ* canopy height showed the Centre transect to have a clear overall decrease in elevation towards the interior. Four of the other transects showed a decrease in peatland surface elevation, but three showed an increase. However, I consider the peatland elevations along these transects not to be reliable; their short length and the unrealistically large fluctuations in elevation mean it is not possible to say with certainty what the true trend in peatland surface elevation is. The unreliable results for these transects are down to limitations of the method. The relationship between H and D used to correct the SRTM for canopy height, although significant, had a relatively low explanatory power. This could be for a number of reasons. Firstly, despite only using sites where ASTER corresponded reasonably well with mean tree height, noise in the ASTER data could still be contributing to the low R-sq. value. Secondly, this method assumes that canopy height has remained constant between the date of ASTER and SRTM data acquisition and between the date of SRTM data acquisition and the date of *in situ* tree height measurements. Tree fall was observed to occur along all transects. It is possible that, operating at a spatial resolution of 30 m, a small scale tree fall event could lead to discrepancies between H and D. Thirdly it assumes that the *in situ* tree heights measurements are a good representation of canopy height. Whilst efforts were made to try to measure the trees nearest to the transect and avoid for example, systematically selecting emergent trees, a sampling bias is still possible.

In South East Asia peatlands are domed by anything from 4 to 10 m (Jaenicke et al., 2008) and in Peruvian Amazonia by ca. 6 m (Lähteenoja et al., 2009a). In this study, noise fluctuations in the estimated ground surface frequently exceed 5 m and so if relatively small peat domes existed they could go undetected. However, Jaenicke et al. (2008), who used a similar methodology to determine peatland topographies in Indonesia, were still able to depict peat domes, even before corrections were made for the forest canopy, despite equal levels of noise in the SRTM DEM as found here for the Cuvette Centrale. Therefore, whilst it is not possible to completely rule out the presence of small peat domes, large peat domes, like those found in Indonesia and Amazonia, are not found in the Cuvette Centrale. The flat or slightly concave surface of these peatlands, as indicated by the Centre transect peatland surface elevation, combined with increasing peat depth with distance from swamp margins implies that these peatlands are occupying extensive shallow interfluvial basins.

2.7. Conclusion

Fieldwork in the Cuvette Centrale confirmed the presence of extensive lowland peatlands in Central Africa. The novel combination of remote sensing products to identify sites with environmental conditions favourable for peat accumulation prior to field verification proved successful and could potentially be used to identify other undocumented peatlands on the continent. Peat occurrence in the Cuvette Centrale is strongly associated with both hardwood swamp and *Raphia laurentii* palm dominated swamp and frequently associated with *Raphia hookeri* palm dominated swamp, thus providing a potential method for mapping these peatlands. *In situ* depth measurements showed the peat to be of modest depth, comparable with peatlands of lowland Amazonia and shallower than South East Asian peatlands. An SRTM DEM corrected for canopy height produced variable results but for the longest (20 km) transect there was a clear decrease in peatland surface elevation and therefore these peatlands are considered to be non-domed systems. The combined flat surfaces with the trend of increasing peat depth with distance from peatland margin, implies that these peatlands occupy extensive shallow interfluvial basins.

Chapter 3: Peatland Properties of the Central Congo Basin.

3.1. Abstract

Little data is available on the properties of tropical peatlands, with this being particularly true for African peatlands. It is now confirmed that underneath the swamp forests of the Cuvette Centrale, central Congo Basin, are extensive peat deposits. Here samples collected from eight peatland sites within the Likouala Department, Republic of Congo, Cuvette Centrale, are used to characterise these peatlands in terms of their basic peat properties; C and N concentrations, C/N ratios, organic matter content, bulk density, pH and electrical conductivity. The mean (± st. dev.) C and N concentration and C/N ratio of the peats were 58.4±5.8%, 1.2±0.6% and 59±28 respectively. Mean (± st. dev.) peat bulk density was 0.17±0.08 g cm^{-3} and mean OM content was 90.93±8.97%. Peatland ground or flood water had a mean (± st. dev.) pH of 3.24±0.20 and electrical conductivity of 171±36 µS cm^{-1}. When compared to published values from South East Asian and lowland Amazonian peatlands, the Cuvette Centrale appear to have slightly higher bulk densities, C concentrations and C/N ratios. It is suggested that this is largely a result of the Cuvette Centrale peatlands having undergone a greater degree of decomposition, leading to a more compact peat composed of a high proportion of recalcitrant, C enriched organic matter.

3.2. Introduction

Understanding of tropical peatland ecosystems and estimates of their C stocks are limited by a lack of *in situ* data (Lawson et al., 2015). Estimations of peatland C stocks require values for peatland extent and thickness, but also peat bulk density and C concentration. Unlike peatland extent, which can in many instances be obtained remotely (e.g. Draper et al., 2014), and peat depth which can be estimated from probing the peatland (e.g. Householder et al., 2012), estimates of peat bulk density and C concentration require samples to be taken. Obtaining sufficient bulk density and C concentration data is labour intensive and logistically difficult. For example Wahyunto and Suryadiputra (2008) estimate that to produce a 1:10000 map of the Sumatra and Kalimantan peatlands, with samples taken every hectare, would require a workforce of 2500 people each spending 20 days in the field. It is therefore of no surprise that this data are often not available for many regions of the tropics and estimates of C stocks have to rely on published values of peat bulk density and C concentrations obtained from other tropical peatlands. For many tropical countries Page et al. (2011) provide the sole estimate of peatland C stocks and use a single peat C concentration and bulk density estimate derived from South East Asian data. Whilst the dearth of data makes it necessary to substitute published data from other regions for *in situ* measurements, the situation is less than adequate because even within a region there can be considerable spatial variation in peat properties. For example mean bulk density for different peatland types in the Pastaza-Marañon, Peru, vary by up to 100% (Draper

et al., 2014). As data collection efforts have increased for tropical peatlands, there have been considerable revisions made to regional peatland C stock estimates, highlighting the value of this new data. For instance new estimates of peat depth and bulk density saw peatland C stocks for the Sumatran and Kalimantan areas of Indonesia being revised down by ca. 10 Pg C (Dommain et al., 2014) from their previous estimate of 33 Pg C (Wahyunto et al., 2003, Wahyunto et al., 2004).

In situ measurements of peatland properties not only improve peatland C estimates, but also give insight into the functioning of peatlands and highlight the similarities or diversity of these ecosystems across the tropics and also within individual regions. For example measurements of peat C/N ratios can indicate differences in organic matter (OM) inputs or degree of decomposition (Wust et al., 2003, Malmer and Holm, 1984, Kuhry and Vitt, 1996), OM content can indicate different depositional environments or the rate of OM accumulation relative to mineral deposition rates (Wust et al., 2003) and the pH and electrical conductivity (EC) of a peatland reflect the concentration of dissolved base cations present, which can signify differences in hydrological regime and also has implications for nutrient availability for vegetation communities (Shotyk, 1988, Theimer et al., 1994, Walter et al., 2015).

The location and extent of many African peatlands remains ambiguous; with the exception of a handful of sites across the continent (e.g. the highland peatlands of Burundi and Rwanda (Pajunen, 1996, Duese, 1966); the Okavango Delta, Botswana (McCarthy et al., 1989); peatlands of KwaZulu-Natal, South Africa (Ellery et al., 2012, Grenfell et al., 2010); Tritrivakely, Madagascar (Bourdon et al., 2000)), even less information is available on the properties of these peatlands and there appears to be no published bulk density values for African peatlands. This not only poses difficulties when estimating peatland C stocks for the continent, but also makes it hard to build up a clear picture of peatland ecosystem diversity and development across the continent. In the Cuvette Centrale, central Congo Basin, it is now confirmed that extensive, shallow, non-domed peatlands occupy interfluvial basins (Chapter 2). Their large extent means that the Cuvette Centrale is not only the most significant region of tropical peatland in Africa but is also one of the most significant regions of tropical peatland in the world (see Chapter 4). In this chapter I describe the Cuvette Centrale peatlands in terms of their peat C and N concentrations, C/N ratios, OM content, pH and electrical conductivity, with the purpose of placing the Cuvette Centrale peatlands in context with the two other major regions of tropical peatland occurrence, South East Asia and lowland Amazonia, and providing data from which new peatland C stock estimates for the Cuvette Centrale can be derived (Chapter 4).

3.3. Aims

The aim of this chapter is to characterise the peatlands of the Cuvette Centrale in terms of their peat properties. The objectives are to measure peat bulk density, OM content, C and N concentration and measure peatland surface pH and conductivity. A second aim is to establish whether these peat properties vary spatially, with the objective of using these relationships to estimate peatland C stocks across the Cuvette Centrale in Chapter 4.

3.4. Methods

3.4.1. Site Description

The data presented in this chapter comes from eight peatland field sites (Bondoko, Bondzale, Centre, Ekolongouma, Ekondzo, Itanga, Mbala and Makodi) and one non-peatland site (Moungouma) visited in the Likouala Department, Republic of Congo (ROC). For the field site locations see Fig. 2.1 (Chapter 2) and for their full descriptions see Table 2.5 (Chapter 2) and Appendix 1-8. For a description of the Likouala Department see Chapter 1, section 1.4. For methods relating to site selection and peat and vegetation sampling protocol refer to Chapter 2, section 2.4.

3.4.2. Sub-sampling of Peat Cores in the Field

During the first fieldtrip when Makodi and Ekolongouma Swamp were sampled, sampling for chemical analysis was done by sampling a 3 cm long slice every 10 cm down the peat profile e.g. samples were taken at 7-10 cm, 17-20 cm and so on. Sampling for bulk density was done by sampling a 7 cm long slice from each stratigraphic unit identified in the field. Samples for chemical analysis and bulk density were taken from the same cores. During the subsequent fieldtrips, when the remaining eight sites were sampled, the sampling strategy was simplified; the full peat profile was sampled in 10 cm long sections, which were used for both bulk density measurements and chemical analyses.

3.4.3. Surface pH and Electrical Conductivity

EC measurements of water can be used as a proxy for the concentration of total dissolved solids (TDS), with higher TDS tending to result in higher EC (Theimer et al., 1994) and pH can give an indication of the degree to which organic acids, produced during the decomposition of OM, have been neutralised by base cations (Berner and Berner, 1996). Together the two measurements give insight into the nutrient concentrations in the peatland and in non-peatland sites may indicate a reason as to why no peat has accumulated e.g. higher nutrient concentrations or pH have permitted higher decomposition rates. Therefore a conductivity meter (manufacturer: Horiba, Northampton, U.K., model: Twin Cond B-173) and pH meter (manufacturer: Hanna

Instruments, Leighton Buzzard, U.K., model: HI 9124 Waterproof Portable pH Meter) were used to take EC and pH measurements of the ground or flood water along each transect at each point a vegetation plot was established (see section Chapter 2, section 2.4.2.4). However, in non-swampland areas the water table was sometimes too low to permit a measurement. Both the pH and conductivity meter were calibrated every day before use. Conductivity and pH measurements at Makodi Swamp and Ekondzo Swamp and conductivity measurements at the Centre were prevented by equipment failures.

3.4.4. Bulk Density

In order to estimate peatland C stocks, one needs to know the mass of peat per unit volume i.e. the bulk density. To measure peat bulk density samples were weighed wet and then dried in the oven at 105°C for 24 hours (Rowell, 1994). Samples which were for both bulk density and chemical analyses were mixed thoroughly to ensure homogeny of the sample before a sub-sample was taken. The rest of the sample was then reweighed and dried in an oven at 105°C for 24 hours. Once cooled in a dessicator, samples were weighed again.

Dry bulk density (ρ, g cm^{-3}) of each sample was calculated using the following equation (adapted from Rowell (1994)):

$$\rho = \frac{m_{dry}}{V} \quad [3.1]$$

Where m_{dry} is the calculated dry mass (g) of the entire sample and V is the volume (cm^{-3}) of the core section that corresponds to that sample.

For samples which were subsampled m_{dry} was calculated by the following equation:

$$m_{dry} = m_{wet} - (m_{wet} * W) \quad [3.2]$$

Where m_{wet} is the wet mass (g) of the entire sample and W is the water content by mass of the sample expressed as a fraction.

W was calculated by the following equation:

$$W = m_{sub} - \frac{m_{dry}}{m_{sub}} \quad [3.3]$$

Where m_{sub} is the mass (g) of the subsample before drying.

3.4.5. Carbon and Nitrogen

Peat C and N concentrations were measured for use in total C stock estimates (Chapter 4) and to calculate C/N ratios to give insight into the OM lability and degree of decomposition. C and N

concentrations were measured for all peatland surface samples (0-10 cm) and for each of the eight peatland sites C and N concentrations were measured down core, every 10 cm, for the inner most core, or in the case of Makodi, the deepest core. At Ekolongouma additional down core C and N concentration measurements were made for four other cores. Samples for C and N analysis were dried at 40°C and were mill ground (manufacturer: Retsch (U.K.) Limited, Hope, Hope Valley, U.K., model: MM301 mixer mill) to 100 μm. C and N concentrations (wt%) were measured using an elemental analyser (manufacturer: Eurovector , Milan, Italy, model: EA3000 elemental analyser).

3.5. Results

3.5.1. Surface pH and Electrical Conductivity

Ground/flood water pH values ranged from 2.73 to 5.95. The mean peatland ground/flood water pH and EC (measurements without an ǂ in Table 3.1) was 3.24±0.20 (n=33) and 171±36 μS cm^{-1} (n=28) respectively. The Moungouma transect had noticeably higher pH levels and lower conductivity levels than the other transects (Table 3.1). With the exception of the Moungouma transect, where the pH generally increased towards the Ubangui River, there was no obvious trend in pH and EC along the transects.

Table 3.1. Ground/flood water pH and conductivity (µS cm $^{-1}$) along each transect †.

Bondoki	Distance (km)	0	0.37	1	2	3	4	5	6		
	pH	NA‡	NA‡	NA‡	NA‡	3.23	3.12	3.26	3.22		
	Conductivity	NA‡	NA‡	NA‡	NA‡	188	230	163	153		
Bondzale	Distance (km)	0	1	2	3	4	5	6			
	pH	NA‡	NA‡	3.31	3.29	3.07	3.38	3.07			
	Conductivity	NA‡	NA‡	126	153	167	143	210			
Centre	Distance (km)	4	8	12	16	20					
	pH	3.43	3.32	3.30	3.40	3.44					
	Conductivity	-	-	-	-	-					
Ekolongouma	Distance (km)	0	1	2	3	4	5	6	7	8	9
	pH	NA‡	NA‡	3.34	3.16	3.20	2.82	3.14	3.16	2.73	3.27
	Conductivity	NA‡	NA‡	147	198	196	210	220	210	195	189
Itanga	Distance (km)	0	0.83	1	2	3	4	5	6		
	pH	3.78	3.30‡	3.93‡	3.27	3.50	3.35	3.30	3.41		
	Conductivity	59	146‡	61‡	168	177	170	173	179		
Mbala	Distance (km)	0	1	1.25	2	3	4	5	6		
	pH	NA‡	NA‡	3.36	3.21‡	3.22	3.08	3.12	2.86		
	Conductivity	NA‡	NA‡	112	132‡	152	152	156	182		
Moungouma	Distance (km)	0	0.39	0.79	1.17	1.41	1.74	2.19	2.49		
	pH	3.89‡	NA‡	4.42‡	NA‡	4.78‡	4.88‡	5.95‡	5.69‡		
	Conductivity	43‡	NA‡	23‡	NA‡	14‡	36‡	29‡	29‡		

NA indicates that no measurements could be made owing to a lack of water.
†No data is shown for the Ekondzo transect due to equipment failures.
‡Mineral soil or organic soil <30 cm

3.5.2. Bulk Density

The mean peat bulk density was 0.17±0.08 g cm^{-3}, with values ranging from <0.01 to 0.51 g cm^{-3} (Fig. 3.1.). There were significant differences in peat bulk density between sites ($p<0.001$; Kruskal-Wallis rank sum test). Bondzale had the highest mean bulk density (0.26 g cm^{-3}); this was significantly higher than the mean bulk densities of the Centre and Ekondzo sites. The Centre had the lowest mean bulk density (0.11 g cm^{-3}), which was significantly lower than all sites except Ekondzo.

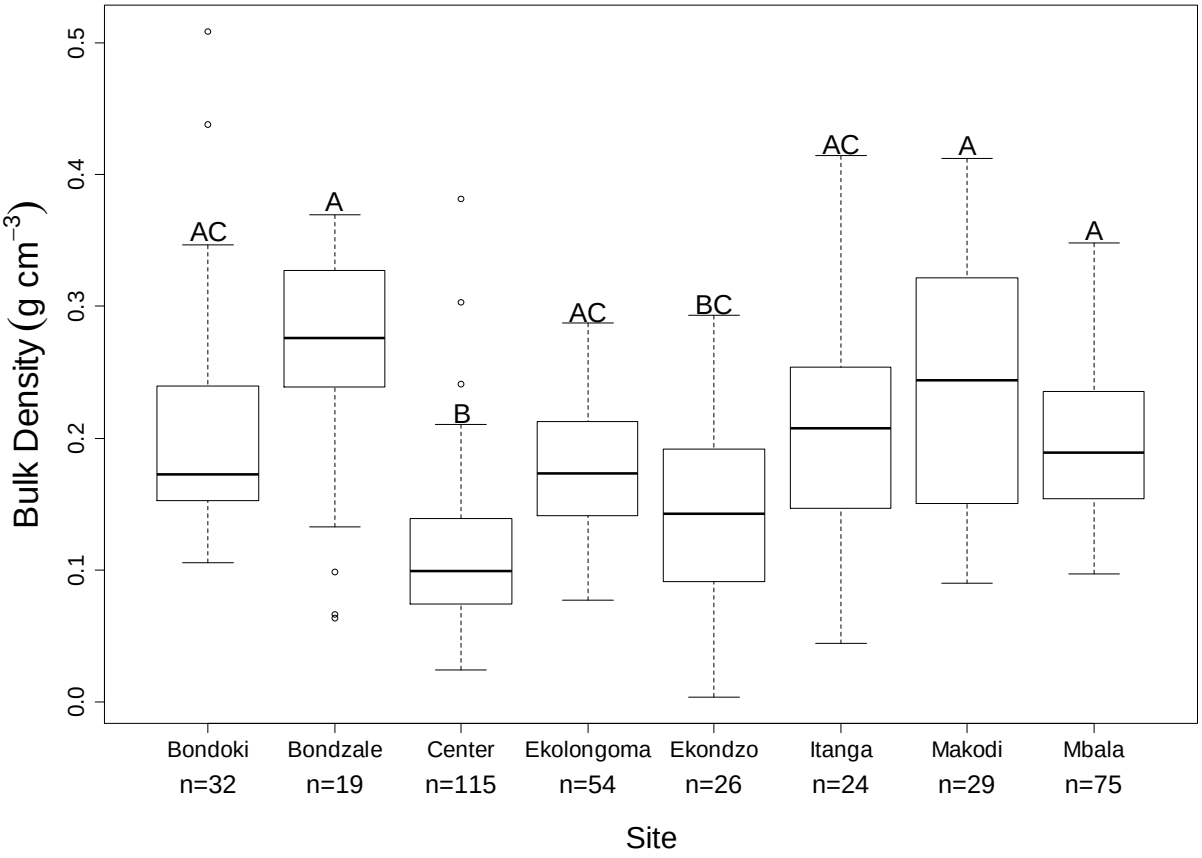

Figure 3.1. Boxplot of peat bulk densities for each site. The median is shown by the black line. The box shows the upper and lower quartiles. The bars show maximum and minimum values. Circles represent outlying values. Sites which do not share a common letter are significantly different ($p<0.05$, Kruskall-Wallis multiple comparison test).

Figure 3.2 shows bulk density variation down core and along each transect (due to a limited number of bulk density samples, the Makodi transect is not shown). All transects show a general pattern of low surface bulk densities and increasing bulk density values towards the base of the cores.

A)

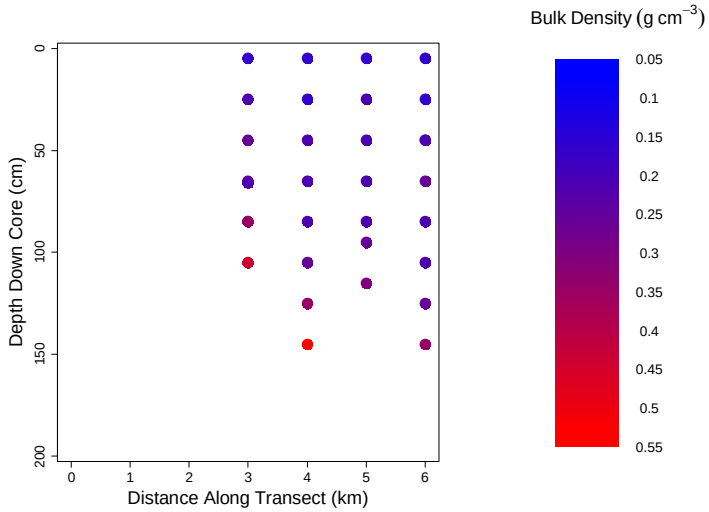
Depth Down Core (cm)
0
50
100
150
200
Distance Along Transect (km)
0
1
2
3
4
5
6
Bulk Density (g cm^{-3})
0.05
0.1
0.15
0.2
0.25
0.3
0.35
0.4
0.45
0.5
0.55

B)

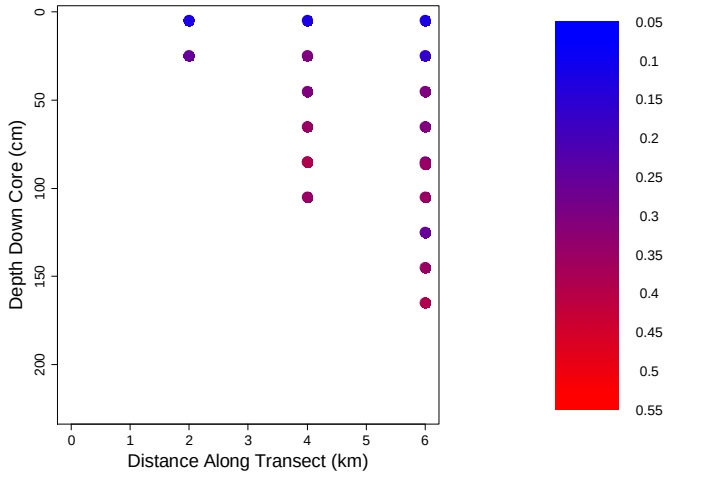
Depth Down Core (cm)
0
50
100
150
200
Distance Along Transect (km)
0
1
2
3
4
5
6
Bulk Density (g cm^{-3})
0.05
0.1
0.15
0.2
0.25
0.3
0.35
0.4
0.45
0.5
0.55

C)

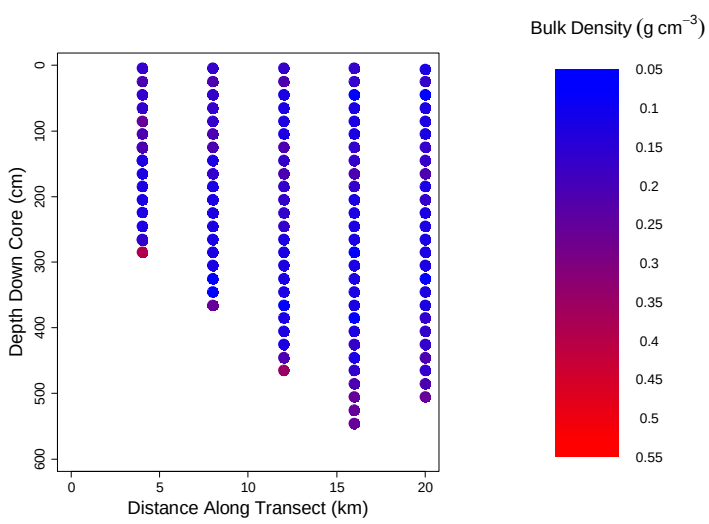
Depth Down Core (cm)
0
100
200
300
400
500
600
Distance Along Transect (km)
0
5
10
15
20
Bulk Density (g cm^{-3})
0.05
0.1
0.15
0.2
0.25
0.3
0.35
0.4
0.45
0.5
0.55

D)

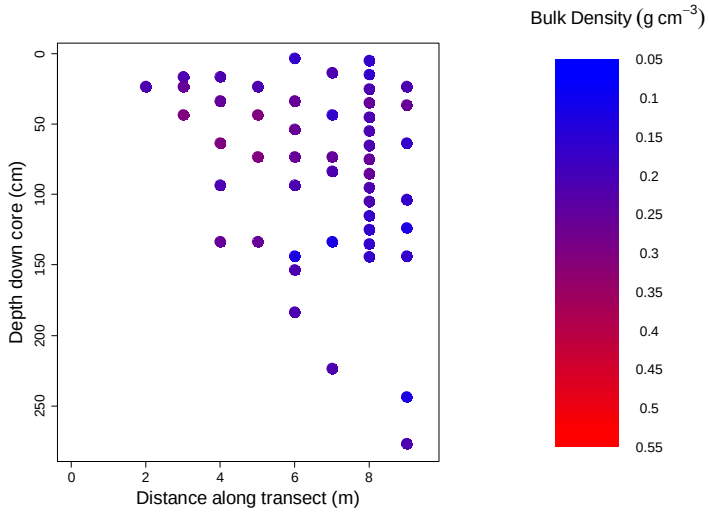
Depth down core (cm)
0
50
100
150
200
250
0
2
4
6
8
Distance along transect (m)
Bulk Density (g cm^{-3})
0.05
0.1
0.15
0.2
0.25
0.3
0.35
0.4
0.45
0.5
0.55

E)

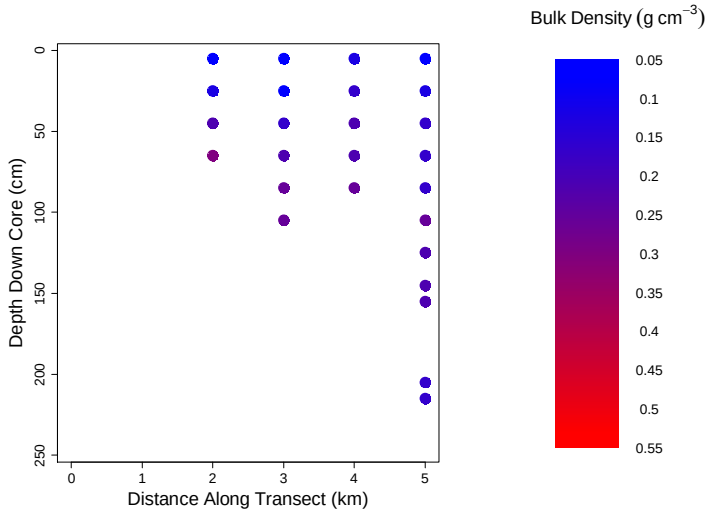
Depth Down Core (cm)
0
50
100
150
200
250
0
1
2
3
4
5
Distance Along Transect (km)
Bulk Density (g cm^{-3})
0.05
0.1
0.15
0.2
0.25
0.3
0.35
0.4
0.45
0.5
0.55

F)

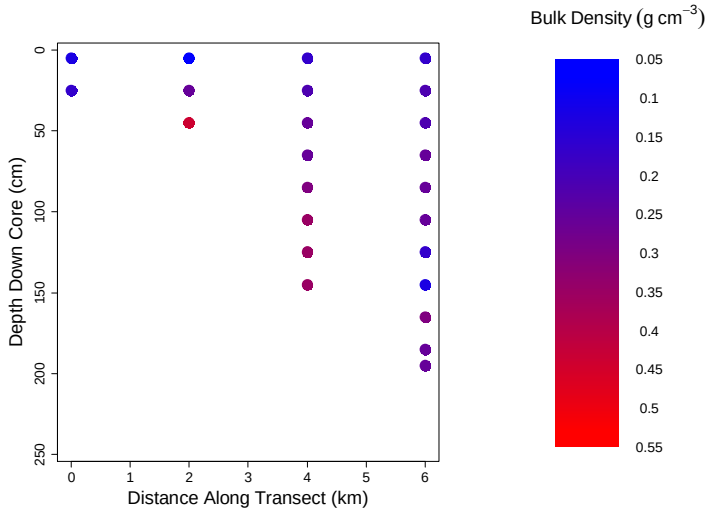
Depth Down Core (cm)
0
50
100
150
200
250
0
1
2
3
4
5
6
Distance Along Transect (km)
Bulk Density (g cm^{-3})
0.05
0.1
0.15
0.2
0.25
0.3
0.35
0.4
0.45
0.5
0.55

G)

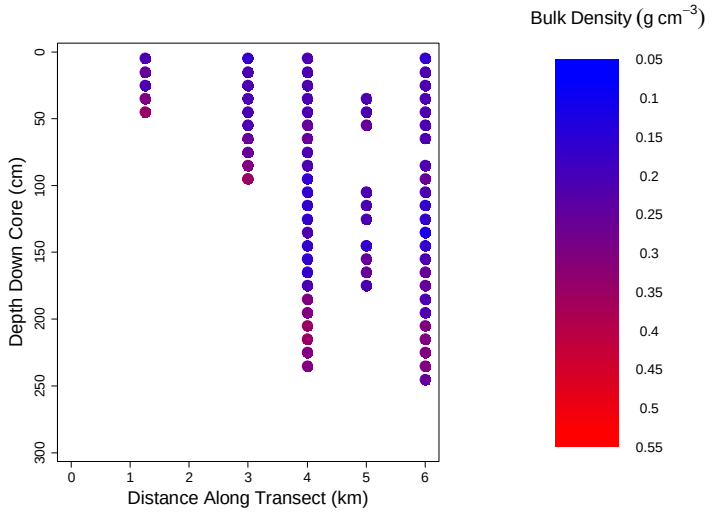

Figure 3.2. Peat bulk density variation down core along the A) Bondoki B) Bondzale C) Centre D) Ekolongouma E) Ekondzo F) Itanga G) Mbala transect.

Linear regression was used to investigate whether there were any relationships between peat bulk density and the following: peat OM content and total core depth. A significant negative ($p<0.001$) relationship was found between peat bulk density and OM content (Fig. 3.3) and a significant ($p<0.001$) negative relationship between total core depth and mean bulk density for each core (Fig. 3.4). A One-way ANCOVA which showed a significant relationship between bulk density and depth down core which differed between sites and cores ($F(83, 284)=8.248$, $p<0.001$; Table 3.2), had a higher explanatory power than the two linear regression models (R.sq. adj.=0.62).

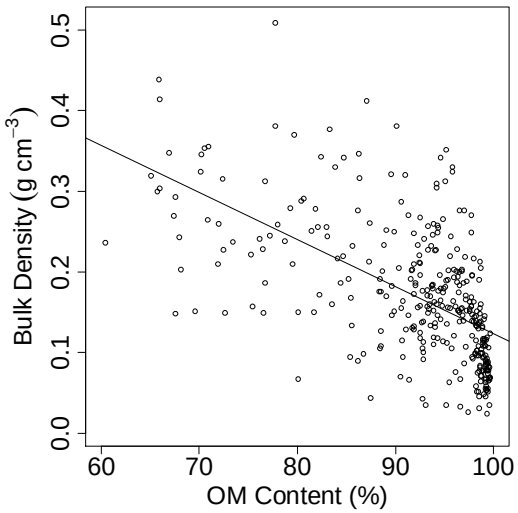

Figure 3.3. The peat bulk density plotted against OM content (%).The solid line is the best-fit regression (adjusted R-sq.=0.35; p<0.001; y=-0.006x+0.706).

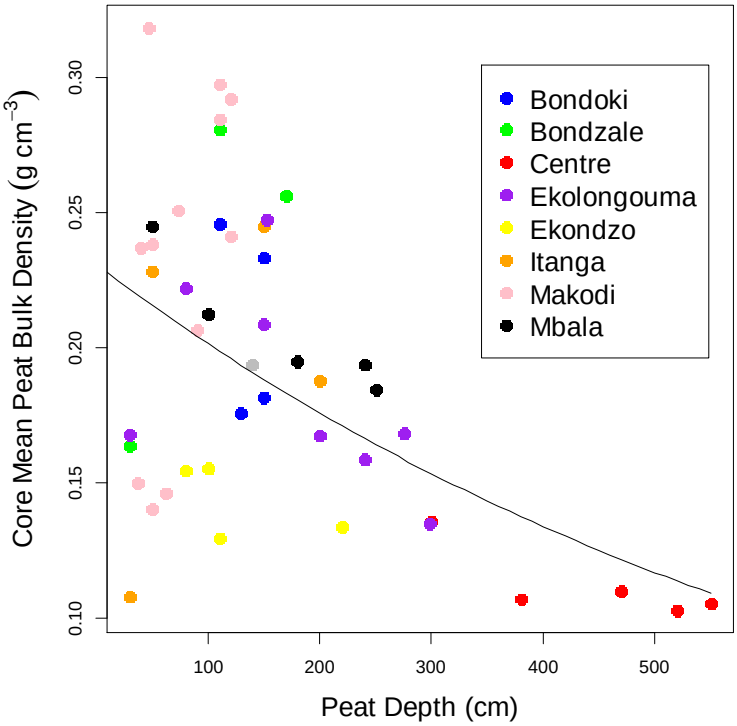

Figure 3.4. Mean core peat bulk density plotted against total core peat depth. The solid line is the best-fit regression (adjusted R-sq.=0.29; p<0.001; $y=e^{-0.001x-1.465}$). Different colours represent different sites.

Table 3.2. Output from a One-way ANCOVA of where bulk density is the dependent variable, site and core are the two factors and depth down-core is the covariate.

Term	F Statistic	p Value
Site	48.4	<0.001
Core	2.1	<0.001
Depth	28.7	<0.001
Site*Depth Interaction	19.3	<0.001
Core*Depth Interaction	3.2	<0.001

3.5.3. Organic Matter Content

The overall mean peat OM content was 90.9±9.0%, with a maximum value of 99.7% and a minimum of 65.1%. The peat OM content was significantly different between sites (p<0.001; Kruskal-Wallis rank sum test). The Centre was the site with the highest mean OM content of 96.4%, which was significantly higher than all other sites. Makodi was the site which had the lowest mean OM content of 81.4%, which was significantly lower than all sites except Bondzale and Ekondzo (Fig. 3.5).

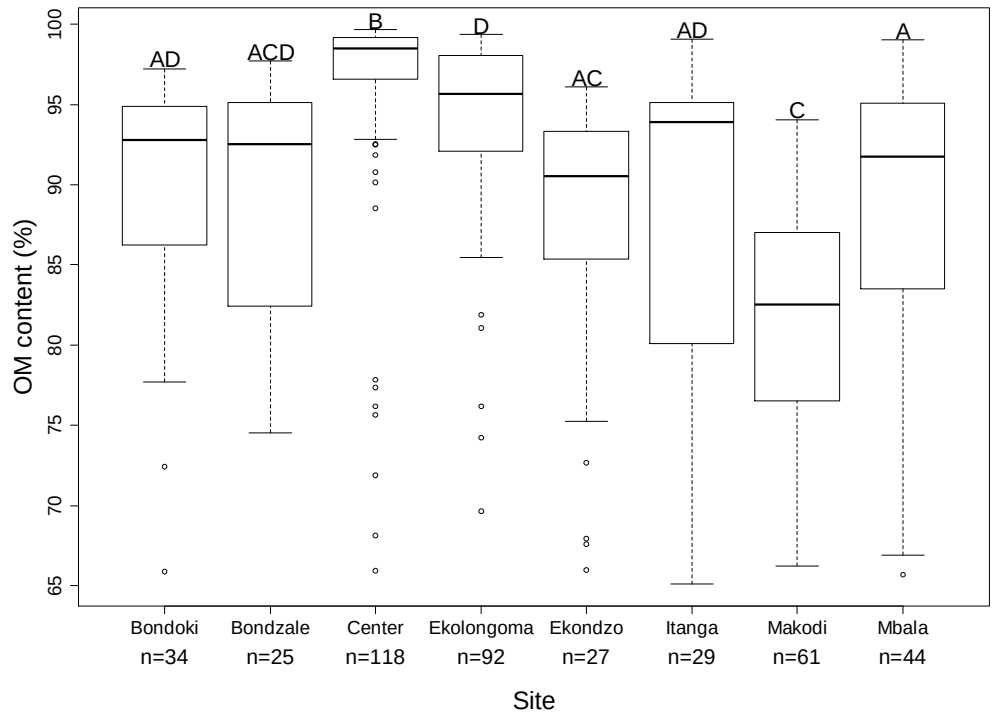

Figure 3.5. Boxplot of peat OM contents for each site. The median is shown by the black line. The box shows the upper and lower quartiles. The bars show maximum and minimum values. Circles represent outlying values. Sites which do not share a common letter are significantly different ($p<0.05$, Kruskall-Wallis multiple comparison test).

3.5.4. Carbon and Nitrogen

Mean peat C concentration from all samples from all sites was 58.4±5.8%, with values ranging from 42.3 to 73.1%. With a mean peat C concentration of 61.1%, Ekolongouma was the site with the highest mean peat C concentration, whilst Makodi had the lowest mean of 51.2%. A Kruskall-Wallis rank sum test showed the mean peat C concentration at Ekolongouma to be significantly ($p<0.001$) higher than at Makodi and Ekondzo (Fig. 3.6). No other sites were significantly different from one another.

The overall mean peat N concentration was 1.2±0.6% and ranged from 0.4 to 4.3%. Makodi had the highest mean peat N concentration of 1.8% and Ekolongouma had the lowest mean N concentration of 1.1%. Kruskall-Wallis rank sum test showed these two sites to be significantly different ($p<0.001$; Fig. 3.6). No other sites had significantly different mean peat N concentrations.

The mean peat C/N ratio was 59±28 and ranged from 13 to 180. Ekolongouma was the site with the highest mean C/N ratio of 70 and Makodi was the site with the lowest peat C/N ratio of 35. A Kruskall-Wallis rank sum test showed Ekolongouma to have a significantly higher mean peat C/N ratio than the Centre, Ekondzo and Makodi ($p<0.001$; Fig.3.6). Both Bondzale and

Ekolongouma had exceptionally high maximum C/N ratios. At both sites there were several peat samples which returned C/N ratios greater than 100.

A)

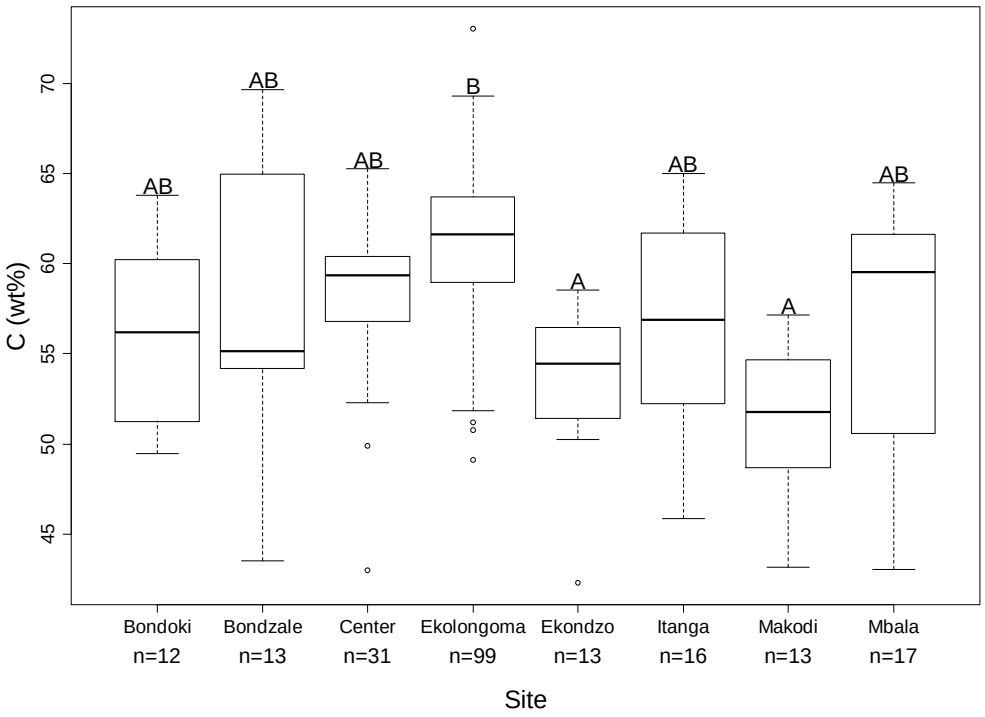

B)

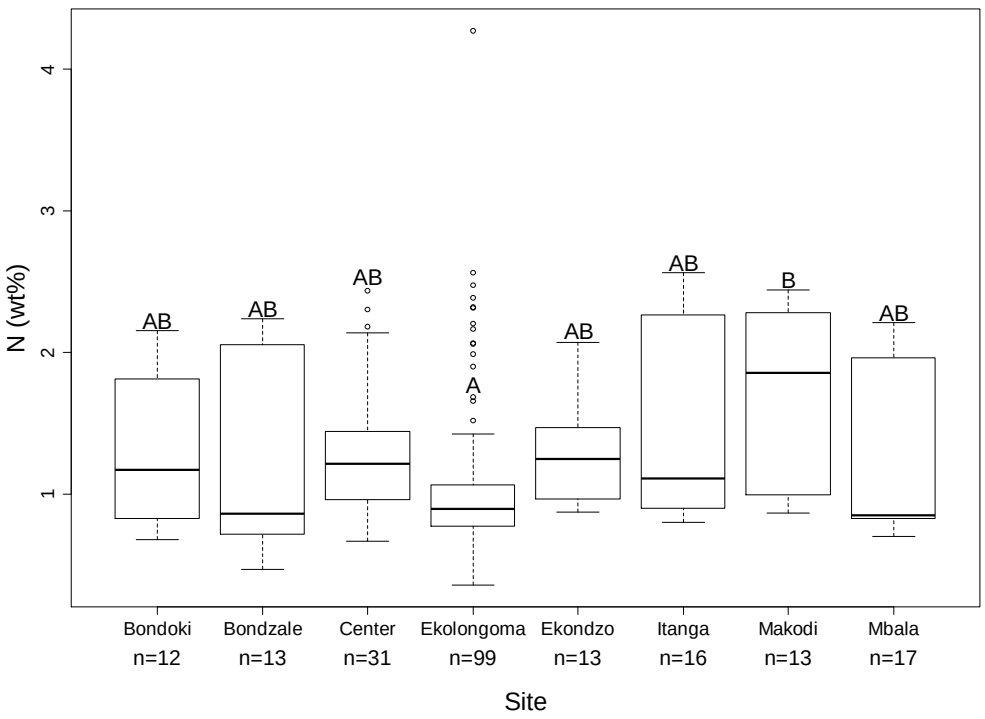

C)

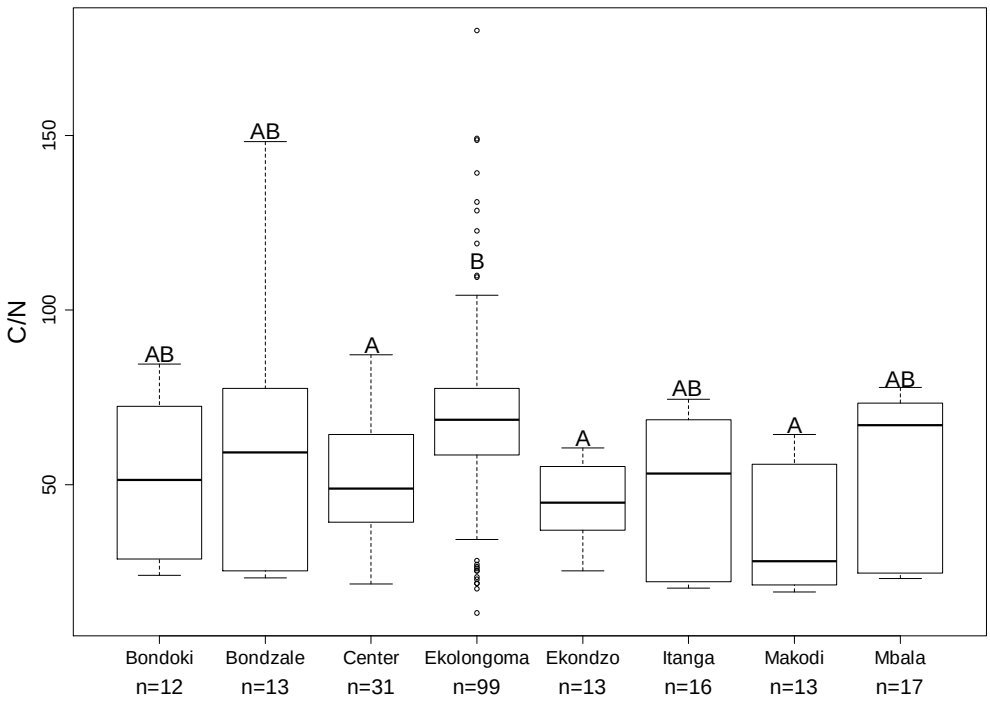

Figure 3.6. Boxplot of A) peat C concentrations (%) B) peat N concentrations (%) C) peat C/N ratios for each of the eight peatland sites. The median is shown by the black line. The box shows the upper and lower quartiles. The bars show maximum and minimum values. Circles represent outlying values. Sites which do not share a common letter are significantly different ($p<0.05$, Kruskall-Wallis multiple comparison test).

Figure 3.7 shows peat C and N concentrations and peat C/N ratios down profile for the inner most (or in the case of Makodi, the deepest) core from each of the eight sites where peat was found. All cores show an initial increase in peat C concentrations and C/N ratios with increasing depth down core and a decrease in peat N concentrations. Towards the base of the peat profile, the majority of cores (excluding Ekolongouma and Makodi cores) show a decrease in peat C concentrations.

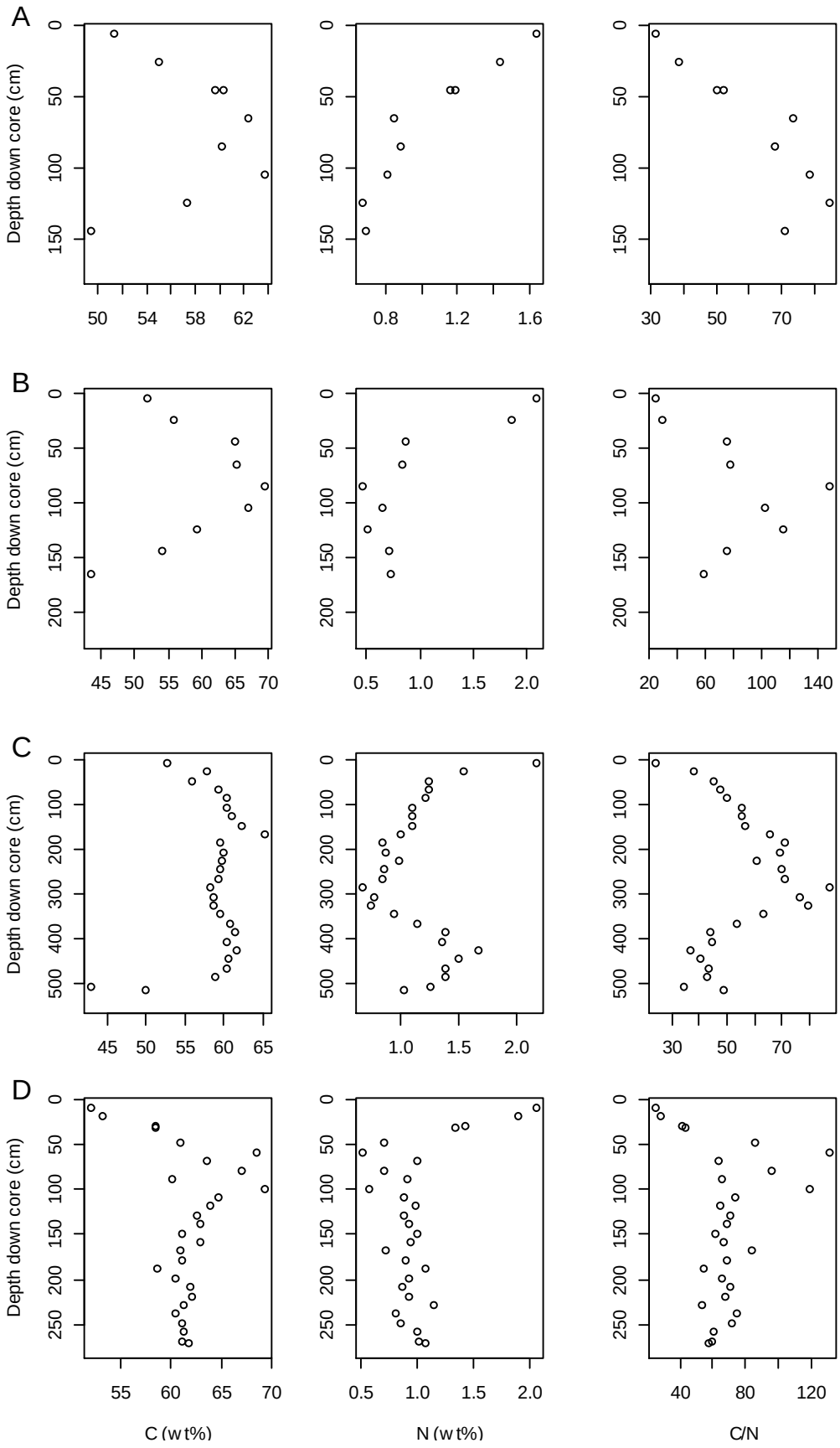

Figure 3.7. Peat C and N concentrations and C/N ratios down core for A) Bondoki 6 km B) Bondzale 6 km C) Centre 20 km D) Ekolongouma 9 km.

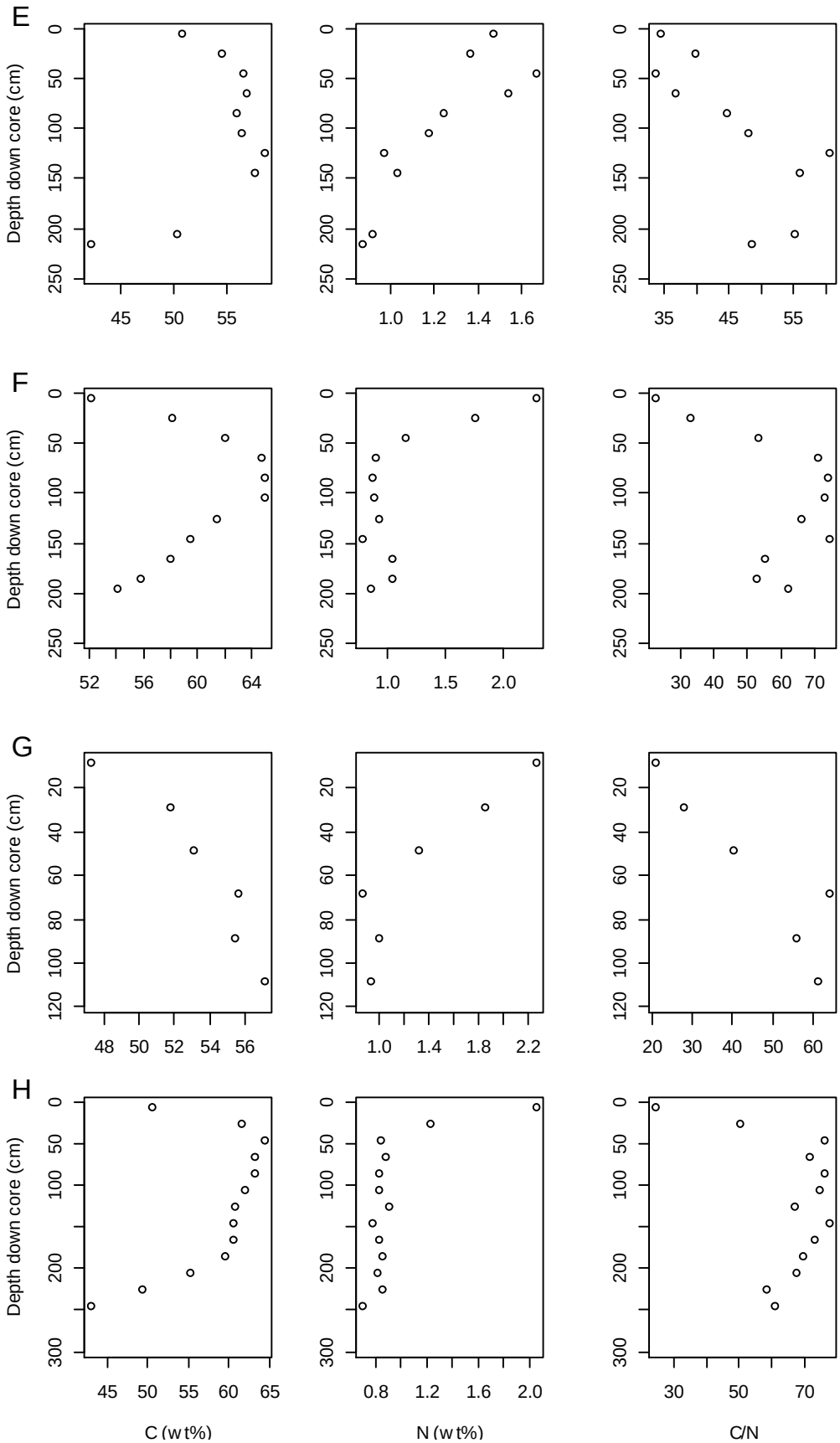

Figure 3.7. Continued. E) Ekondzo 5 km F) Itanga 6 km G) Makodi deepest core (not on transect) H) Mbala 6 km.

Results from linear regression analysis found peat C concentration to have a significant p<0.001) exponential relationship with OM content (Fig. 3.8). No significant (p=0.15) relationship was found between peat C concentrations and peat bulk density (Fig. 3.9). However, peat bulk density was found to have a significant (p<0.001) positive relationship with peat C/N ratios (Fig. 3.10), although the R-squared adjusted value was low (R-Sq. Adj.=0.19).

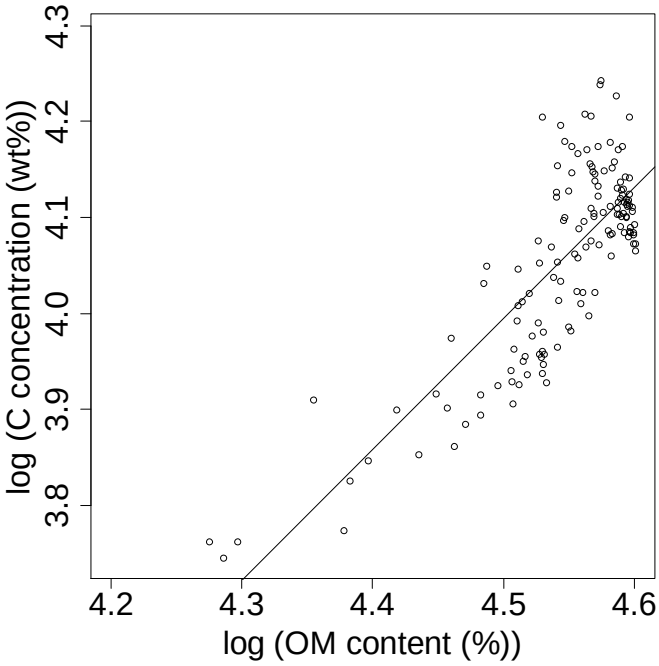

Figure 3.8. A log-log plot of peat C concentration plotted against LOI. The solid line is the best-fit regression (adjusted R-sq.=0.66 p<0.001; y=1.367x-2.156).

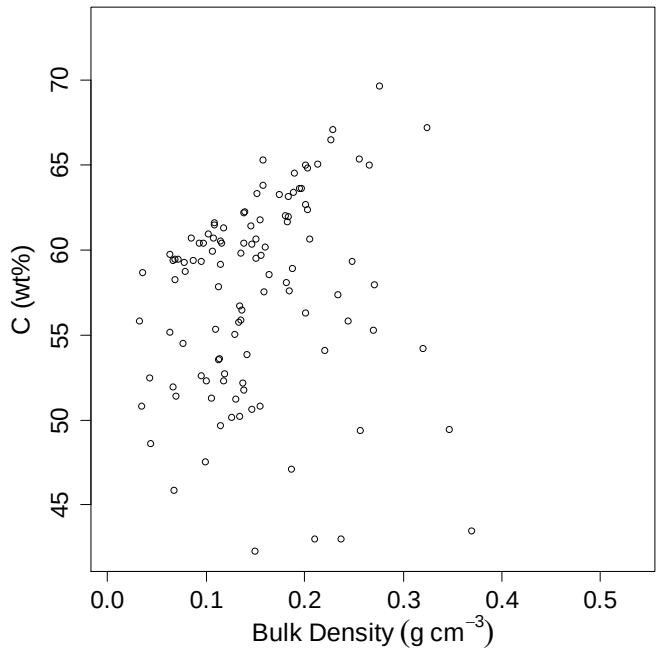

Figure 3.9. Peat C concentration plotted against peat bulk density.

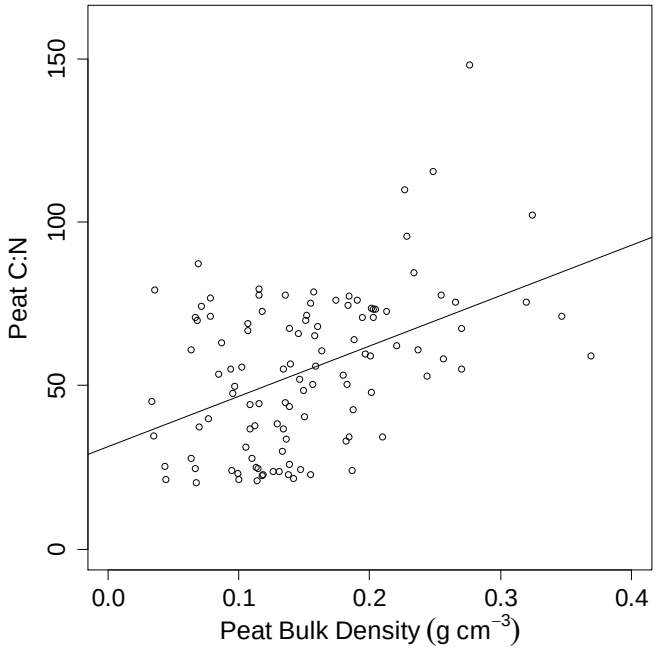

Figure 3.10. Peat C/N ratios plotted against peat bulk density. The solid line is the best-fit regression (adjusted R-sq.=0.19; p<0.001; y=153.665x+31.584).

3.5.5. Peat Properties Under Different Vegetation Types

To discern whether there was any difference in peat characteristics under the different swamp vegetation types, peat cores were divided into those which came from areas of hardwood swamp and those which came from palm dominated (both *Raphia hookeri* and *R. launrentii*) swamp and the mean bulk density values of the two vegetation classes were compared. Mean peat bulk density for hardwood swamp (0.16±0.09 g cm $^{-3}$, n=156) was significantly lower than the mean peat bulk density for palm dominated swamp (0.18±0.08 g cm $^{-3}$, n=217; p=0.01, Wilcoxon rank sum test). However, the significantly different mean peat bulk densities between the two vegetation types may be at least partially attributable to vegetation types coinciding with other factors such as peat depth. Therefore the peat bulk densities were split into different core depth groups. The mean peat bulk density for each vegetation type for that depth group was then compared. Of the depth groups for which there was a sufficient number of bulk density samples for both vegetation types to make a comparison, only on one occurrence was bulk density found to be significantly different between the two vegetation types (Table 3.3) and no vegetation type consistently had a higher mean bulk density than the other.

Table 3.3. Comparison of mean peat bulk densities for hardwood swamp and palm dominated swamp for corresponding peat core depths using Wilcoxon–Mann–Whitney test.

Core Depth (cm)	Hardwood swamp forest mean bulk density (g cm $^{-3}$)	n	Palm dominated swamp mean bulk density (g cm $^{-3}$)	n	P-value
0-50	0.23	5	0.22	14	p=0.89
51-100	0.18	9	0.20	21	p=0.50
101-150	0.25	32	0.21	47	p<0.01
151-200	0.22	21	0.18	19	p=0.17
251-300	0.14	18	0.16	23	p=0.10
501-550	0.11	28	0.10	26	p=0.86

When comparing mean peat C concentrations under the two vegetation types palm dominated swamp (58.9±5.6%) had significantly higher mean C concentrations than hardwood swamp (56.2±6.1; p=0.008; Mann-Whitney U test; Table 3.4). Peat N concentration was significantly higher under hardwood swamp (p<0.001; Mann-Whitney U test) and peat C/N ratios were significantly higher under palm dominated swamp (p=0.001; Mann-Whitney U test). It was not possible to compare C concentrations under the two vegetation types for different core depths because down core C concentration measurements were only made for the deepest cores along each transect. So to assess the possible influence of core depth on the mean peat C concentration, comparisons were made using only surface samples (Table 3.4). When only surface peat C concentrations were compared, no significant difference was found between the two vegetation types (p=0.22; Mann-Whitney U test). By contrast surface peat N concentrations were significantly different (p=0.04; Mann-Whitney U test). C/N ratios were not significantly different for the two vegetation types (p=0.12; Mann-Whitney U test).

Table 3.4. Mean peat C and N concentrations and C/N ratios under hardwood swamp and palm dominated swamp for all samples and surface samples only.

Sample Type	Vegetation Type	Mean C Concentration (%; ±St.Dev.)	Mean N Concentration (%; ±St.Dev.)	Mean C/N Ratio (±St.Dev.)	n
All	Hardwood Swamp	56.2±6.1	1.6±0.7	47.1±31.3	37
	Palm Dominated Swamp	58.9±5.6	1.1±0.5	61.8±26.9	176
Surface Only	Hardwood Swamp	52.3±2.3	2.3±0.2	23.5±2.3	19
	Palm Dominated Swamp	51.8±3.6	2.1±0.6	26.7±8.5	29

3.6. Discussion

3.6.1. Peatland Surface pH and Conductivity

Since all peatlands produce organic acids through the decomposition of OM, the pH of the peat is determined by the degree to which these acids are neutralised by bases, normally being brought into the peatland through groundwater or surface flow (Gorham et al., 1984). The low pH levels

found for the sites in this study demonstrate that base inputs into these peatlands are very low. The surface pH values are towards the lower end of the range reported for other tropical peatlands (Table 3.5). Typically peatlands with pH values this low tend to be ombrotrophic peatlands (e.g. Page et al., 1999, Lähteenoja et al., 2009a). Higher pH values can be an indication of minerotrophic conditions (e.g. Lähteenoja et al., 2013). However, whilst the low pH values of this study may be a sign of ombrotrophy, the pH values of the Likouala aux Herbes river have also been found to be very low (see Chapter 6, Table 6.8 and also Laraque *et al.* (1998)) as a result of high concentrations of organic acids originating from the swamp forests within its catchment (Mann et al., 2014). Therefore river water could enter the peatlands and a low pH could still be possible. There are few EC measurements reported for tropical peatlands, but when compared to the measurements of Page et al. (1999) for an Indonesian ombrotrophic peatland, the EC values of the Cuvette Centrale peatlands are noticeably higher (Table 3.5). However, in this instance this does not imply higher nutrient concentrations, but rather more acidic conditions in the Cuvette Centrale; in the peatland sites, the ground/flood water will contain high concentrations of organic acids and therefore high concentrations of H^+ ions, leading to a high EC (Gray, 2006, Rydin and Jeglum, 2006).

The Moungouma transect stands out as having noticeably higher pH levels, which increase with proximity to the Ubangui River, suggesting that the nutrient status of the old meanders along this transect are, at least in part, affected by the Ubangui white waters, resulting in higher nutrient levels, which might impede peat development by sustaining high microbial activity. The less acidic conditions of the Moungouma transect can also explain why the EC measurements along this transect are lower than the peatland sites, as there will be fewer H^+ ions in solution (Gray, 2006, Rydin and Jeglum, 2006).

Table 3.5.Tropical peatland surface pH and EC measurements.

Location	Study	Peatland Type/ Description	Mean pH (±St. Dev.)	Mean EC (±St. Dev; µS cm^{-1})	Notes
Maludam Peninsula, Sarawak, Malaysia	Anderson (1983)	Forested coastal	3.4±0.1	NA	pH of surface peat samples
Sungai Sebangau catchment, Central Kalimantan, Indonesia	Page et al. (1999)	Mixed swamp Mixed swamp Transitional forest Low pole forest Low pole forest	3.9±0.5 3.4±0.3 3.4±0.4 3.5±0.4 3.6±0.3	54±9 53±6 51±6 50±4 44±5	pH of peatland surface water
Pastaza-Marañón Foreland Basin, Western Amazonia, Peru.	Lähteenoja and Page (2011)	Forested Forested Forested Forested Forested floodplain Forested Open with *Mauritia flexuosa* palm *Mauritia flexuosa* palm swamp Open with *Mauritia flexuosa* palm *Mauritia flexuosa* palm swamp *Mauritia flexuosa* palm swamp	3.8±0.1 3.9±0.0 3.8±0.2 3.8±0.1 4.5±0.1 4.4±0.0 5.7±0.2 5.1±0.2 6.1±0.3 5.8±0.2 6.0±0.2	NA NA NA NA NA NA NA NA NA NA NA	pH of peatland surface water
Cuvette Centrale, Congo Basin, ROC	This Study	Forested	3.2±0.2	171±36	Peatland ground or flood water

3.6.2. Peat Bulk Density

The mean and maximum bulk density values for the Cuvette Centrale sites are generally higher than those reported for South East Asian and Amazonian peatlands (Table 3.6). Two factors determine the bulk density of peat: the density of the material which comprises the peat and how compact the peat is. The density of the material that comprises the peat is often strongly related to the proportion of OM to mineral matter; the higher the mineral content, the higher the bulk density (van Asselen et al., 2011, Parry and Charman, 2013). This can be seen when the peat bulk density values are plotted against OM content for the Cuvette Centrale samples (Fig. 3.3) and accounts for the increase in bulk density towards the base of the cores (Fig. 3.2). It also accounts for the relationship between core depth and mean core bulk density (Fig. 3.4); in shallower peat the proportion of the profile in transition to the underlying mineral layer will be greater than in deeper peats and therefore have a stronger influence on the mean bulk density for that peat profile. However, as the ANCOVA results show, the relationship between peat bulk density and depth down core varies between different localities. Additionally a higher mineral content cannot be the only factor behind the high bulk density values, as the mean OM content of the Cuvette Centrale peatlands is either only slightly lower or higher than the OM contents for

the South East Asian or lowland Amazonian peatlands respectively (Table 3.6) and the relationship between OM content and bulk density for the Cuvette Centrale peatlands had a relatively low explanatory power (R-sq. adj.=0.38).

The second cause of higher bulk densities in the Cuvette Centrale peats may be caused by the degree of compaction. During the decomposition process the original structure of the OM breaks down and OM particles consolidate, resulting in a denser, less porous peat (Clymo, 1984). In the field it was observed that the peat was very dark and well humified suggesting it had undergone a considerable degree of decomposition. Higher rates of decomposition, unless balanced by high rates of OM productivity, will result in low peat accumulation rates. Peat accumulation rates derived from radiocarbon dates, discussed in detail in Chapter 5, indicate that compared to South East Asian and lowland Amazonian peatlands, the Cuvette Centrale peatlands accumulate OM more slowly. The high mean C/N ratio of the Cuvette Centrale peatlands also support the idea of a high degree of decomposition; as fresh plant litter is added to the peat, the more labile compounds with low C/N ratios will decompose first leaving a higher proportion of more recalcitrant OM compounds, with higher C/N ratios (Tian et al., 1992, Chimner and Ewel, 2005, Ono et al., 2015).

The high water and OM content of peat, resulting in a high degree of compressibility and low cohesion, means that obtaining accurate bulk density measurements is more of a challenge than when sampling mineral soils, with both compaction and failure to recover the full sample being potential problems. However, it is considered unlikely that a sampling bias is the cause of the *higher* bulk densities. Here samples were taken with a Russian-style corer, which have been suggested, if biased, to systematically underestimate peat bulk density (Clymo, 1983). Furthermore, if large roots were encountered in the field, which the corer could not cut through, the sampling location had to be moved slightly to avoid these larger roots, leading to their exclusion from the core samples, and therefore some higher density samples.

Oven drying time and temperature are another possible source of bias in bulk density measurements, as any residual water will increase the apparent bulk density. Again, however, this is considered to be an unlikely cause of the higher Cuvette Centrale bulk density measurements, because all but one study in Table 3.5 adopted the same drying time and all studies adopted either the same or lower drying temperature than the one used in this study.

The differences in peat bulk density between sites could be attributable to both density of material and degree of compaction. The site with the lowest mean bulk density, the Centre, also coincides with the deepest peat and highest mean OM content and therefore a lower proportion of mineral matter in the samples most likely accounts for the low mean bulk density. At

Ekondzo however, the low mean bulk density is probably due to the fact that when sampling was carried out, the site was completely inundated. It was noted when walking along the transect that the surface of the peat appeared to be floating in parts. When one stood on the surface it would sink and displace water above the peat surface. If the surface layers of the peat expand or float during inundation this would result in an increase in peat depth and a decrease in bulk density and would explain the extremely low surface bulk density values recorded at Ekondzo. Continuous water table data from Bondoki suggests that this phenomenon occurs at other sites (see Chapter 6, section 6.6.7). The implication of this is that at some locations the peatlands have seasonally varying peat depths and bulk densities. This is not a new idea; seasonal decreases in bulk density associated with waterlogging have also been observed in northern peatlands (Price and Schlotzhauer, 1999). This phenomenon would have no impact on the estimation of C stocks (discussed in Chapter 4), as long as bulk density and peat depth measurements from a site are made in the same season.

The highest mean bulk density, at Bondzale, does not seem to be related to the OM content of the peat, with Bondzale having one of the highest mean LOI values, but it could be linked to higher rates of decomposition. Bondzale is located to the north of the other sites and therefore is at a slightly higher elevation in the Cuvette Centrale compared to the other sites (Chapter 2, Fig. 2.1). In general, considering a basin, water will flow from the highest to the lowest point, unless obstructed by an object. Therefore perhaps Bondzale experiences slightly better drainage than the other sites and therefore the OM is exposed to more oxidised conditions. Continuous water table measurements show that the water table at Bondzale dropped more than 80 cm below the surface in places, which is considerably greater than that measured at the other sites, as discussed in Chapter 6.

In summary, the peat bulk density of the Cuvette Centrale peatlands are higher than published values for other tropical peatlands. Whilst bulk density was related to mineral content, this relationship does not account for the higher bulk density values of the Cuvette Centrale peatlands compared to other tropical regions. Likewise, sampling biases are extremely unlikely to be the cause. Instead it is suggested that a higher degree of decomposition and therefore compaction is the cause, supported by the higher C/N ratios of the samples.

Table 3.6. Peat properties taken from the literature for lowland tropical peatlands in South East Asia and Amazonia.

Location	Data Source	Peatland Type	Mean Peat C Concentration (%)	Mean Peat C/N	Mean Peat Bulk Density (g cm^{-1})	Mean Peat LOI (%)
West Kalimantan, Indonesia	Anshari et al. (2010)	Undrained peatlands	53.4±3.2	63±25	0.09±0.03	95.9±9.2
Mukah Division, Sarawak, Malaysia	Melling et al. (2005)	Forested peatlands	47.8±0.9	27±1	0.15±0.0004	98.65
Central Kalimantan, Indonesia	Shimada et al. (2001)	Riverine Terrace Basin/Domed Marginal Floodplain	55.5±4.2 56.7±5.1 57.0±4.5 56.6±3.9 52.5±8.0	NA NA NA NA NA	0.12±0.0.3 0.12±0.03 0.10±0.02 0.09±0.03 0.14±0.04	NA NA NA NA NA
Pastaza-Marañon Foreland Basin, Western Amazonia, Peru	Draper et al. (2014)	Pole forest Palm swamp Open peatland	50.5±1.6 44.0±2.7 48.5±2.8	NA NA NA	0.08±0.01 0.10±0.01 0.05±0.02	NA NA NA
Pastaza-Marañon Foreland Basin, Western Amazonia, Peru	Lähteenoja and Page (2011)	Mixed	48.7±8. 7	30±10	0.08±0.05	87.21±14.30
Cuvette Centrale, Congo Basin, ROC	This Study	Forested	58.4±5.8	59±28	0.17±0.08	90.93±8.97

3.6.3. Peat C and N Concentrations

Carbon concentrations and C/N ratios for the Cuvette Centrale peatlands, like peat bulk density, are slightly higher than values reported for other tropical peatlands (Table 3.6). As explained, this is probably due to a high proportion of recalcitrant organic compounds with high C concentrations and C/N ratios (Tian et al., 1992). It could also be owing to the occasional presence of pyrogenic material. C/N ratios greater than 100 have been reported for charred plant material following slash and burn agriculture (Rumpel et al., 2007). Therefore the exceptionally high C/N ratios measured in some of the Bondzale and Ekolongouma samples are probably attributable to the presence of black carbon in the peat profile. Whilst these values will have a strong influence on the overall C/N mean, the ranges and means of C/N ratios from the other sites and the overall median (61) are still very high and support the idea of a high degree of decomposition. Analysis of the structure and composition of the OM in future work would help test this. Overall, sites generally did not have significantly different peat C concentrations. The significant difference between the site with the highest mean C concentration, Ekolongouma, and the two sites with the lowest mean C concentration, Makodi and Ekondzo, is probably a consequence of the suspected presence of black carbon in the Ekolongouma cores. This could also account for the significantly higher C/N ratios of the Ekolongouma site. The presence of pyrogenic material has also been suggested to be the cause of variations in mean C concentration for ombrotrophic peatlands in Kalimantan, Indonesia, with different studies sampling different sites with different fire histories (Lampela et al., 2014).

The initial increase in C concentration and decrease in N concentration with increasing depth and the resulting increase in C/N ratios seen in all cores, can be explained by the decomposition of OM through time, with the increasing loss of labile compounds, such as cellulose, with relatively low C/N ratios, and the persistence of more stable compounds such as lignin, with higher C/N ratios (Tian et al., 1992). This is the opposite trend to what has been observed in temperate and boreal peatlands; decreasing C/N ratios with depth (Malmer and Holm, 1984, Kuhry and Vitt, 1996). With C/N ratios showing a negative relationship with peat humification, both Malmer and Holm (1984) and Kuhry and Vitt (1996) attributed the down core trends to the loss of C during decomposition. Crucially, however, the peat in these two studies was largely composed of *Sphagnum* sp. remnants. Although not well-researched, there is evidence to suggest that even with high leaf litter inputs, tropical peatlands are largely comprised of roots and woody biomass, owing to the rapid decomposition of leaf litter under the warm, humid climates compared to the roots and woody biomass (Chimner and Ewel, 2005, Ono et al., 2015). Therefore, although leaf litter C concentrations and C/N ratios have also been found to decrease in tropical peatlands with increasing decay, it is the change in C concentrations and C/N ratios of the

root and woody biomass OM fraction that determines the peat C concentrations and C/N ratios. Both Chimner and Ewel (2005) and Ono et al. (2015) found C concentrations and C/N ratios of the root and woody biomass OM fraction to either remain constant or increase during decomposition.

The trend of decreasing C concentrations towards the base of the Cuvette Centrale cores, however, is almost certainly caused by an increase in mineral content and is seen in other tropical peatland profiles (Lawson et al., 2014, Lähteenoja et al., 2009b). As the results show (Fig. 3.8) the OM content of the peat strongly determines the C concentration, but this relationship starts to break down for high OM content samples. This could largely be down to differences in the degree of OM decomposition between the surface and lower down the peat profile, which will affect C concentration but not OM content.

The lack of a relationship between C concentration and bulk density is initially surprising. One would expect that if high bulk densities were a result of high mineral contents then there would be a negative relationship between C concentration and bulk density. However, as peats with a low mineral content decompose, the OM can consolidate (Clymo, 1984) and at the same time the proportion of recalcitrant C compounds can increase (Ono et al., 2015, Chimner and Ewel, 2005), resulting in a positive relationship between bulk density and C concentration. In a population that contains peats with both high and low mineral content and of varying degrees of decomposition, these two opposing relationships could to a degree cancel one another out resulting in no overall relationship between bulk density and C concentration. To add to this are the samples which are suspected to contain black carbon, whose presence will possibly be independent of both mineral content and degree of decomposition, or only weakly related (if enhanced fire and more humified peat both occur during drier intervals).

In summary, the peat C concentrations and C/N ratios of the Cuvette Centrale peatlands are slightly, but not significantly, higher than published values for other tropical peatlands. A higher proportion of recalcitrant, C enriched OM and pyrogenic compounds are considered the most probable explanation for this. Although the OM content of the peat largely determines the peat C concentration, the presence of these C enriched compounds mean that the C concentration of peats with a high OM content can be quite variable. It can also account for the lack of a relationship between peat bulk density and C concentration.

3.6.4. Relationship Between Vegetation and Peat Properties

Considering whether different vegetation types corresponded to different peat properties was based on the supposition that differences in vegetation reflect variation in environmental conditions, such as nutrient status and hydrology which correlate with

different peat properties. It was also thought possible that differences in OM structure and chemistry from the different vegetation types could drive some of the variation in peat properties. The initial finding that peat properties (bulk density, C and N concentrations and C/N ratios) differ significantly between hardwood swamp and palm dominated swamp appears to be attributable to confounding factors, rather than the overlying vegetation types, principally differing mean peat depth and fire occurrence at some sites. The association between *Raphia hookeri* palm and shallower peat deposits could account for the higher overall mean bulk density of the palm dominated swamp, but as the results show, when identical depths under the two different vegetation types were compared bulk density was not significantly different. Likewise the initial finding that peat under palm dominated swamp had significantly higher C concentrations and C/N ratios is probably because the palm dominated swamp incorporated most of the Ekolongouma samples, whose unusually high C concentrations and C/N ratios have been partially attributed to the presence of black carbon in the profile. When only surface samples were considered their C concentrations and C/N ratios were not significantly different between the two vegetation types.

The supposition that the two vegetation types may have different peat properties assumes constancy in the development of the peatland in terms of environmental conditions or vegetation cover, which is unrealistic. Whilst studies of other tropical peatlands have assigned different peat properties to different peatland vegetation communities (Draper et al., 2014), in the Cuvette Centrale it seems unjustified, as the spatial distribution of vegetation does not correlate with spatial variations in peat properties and any differences in OM inputs between the vegetation types seems to have a negligible effect on surface peat properties.

3.6. Conclusions

In situ measurements and analysis of samples taken from eight peatland sites across the Likouala Department, ROC, show that the Cuvette Centrale peatlands can be characterised as nutrient poor peatlands, with relatively high peat bulk densities, C concentrations and C/N ratios compared to other tropical peatlands. These peatlands have very low pH but high EC, indicating high concentrations of H^+ in solution and therefore low concentrations of base cations entering the peatlands. The higher bulk densities of the Cuvette Centrale peatlands cannot be accounted for by a higher mineral content alone and it is suggested that the higher peat bulk densities are due to the peat being at a more advanced stage of decomposition, leading to a higher degree of OM consolidation. The higher C concentrations and C/N ratios are then likely to largely be the result of a high proportion

of recalcitrant and C enriched OM, plus occasional black carbon presence indicating intermittent fires in some locations.

Chapter 4: Peatland Extent and Carbon Stocks in the Central Congo Basin.

4.1. Abstract

The Cuvette Centrale, the world's second largest tropical wetland, contains extensive, shallow and C dense peatlands. Tropical peatlands are known to play an important role in the global C cycle, acting as a C store, sink and sometimes source of C emissions**.** Like many tropical regions, the peatland C stock of the Cuvette Centrale is, however, essentially unknown, with previous estimates lacking *in situ* data. Here I combine remote sensing techniques with *in situ* data on peat characteristics from eight peatland sites in the Likouala Department, Republic of Congo (ROC), to provide the first estimate of peatland extent and C stocks based on ground data for the Cuvette Centrale. Peatland extent in the Cuvette Centrale, derived from supervised classifications of optical, radar and elevation data, is estimated to be 145,529 km^2 (95% CI, 134,720-154,732 km^2), making the Cuvette Centrale the most extensive tropical peat complex in the world. When combined with *in situ* measurements of the peat depth, bulk density and C concentration, the best estimate of peat C stocks is 30.2 Pg C (90% CI, 27.8-32.7 Pg C). This new estimate of peat C stocks is ten times higher than previous combined estimates for the DRC and ROC and more than 20 times higher than the estimated peatland aboveground C stocks (1.4 Pg C). When added to global estimates, my estimate for the Cuvette Centrale increases the tropical peat C stocks from 88.6 Pg C to 115.8 Pg C. Therefore, the peatlands of the Cuvette Centrale are of global importance.

4.2. Introduction

Owing to their high organic matter (OM) contents, peatlands are a globally significant C stock, storing an estimated 480 Pg C (Page et al., 2011). When a peatland has a net accumulation of OM, it acts as a C sink (Limpens et al., 2008). However, when disturbed, peatland ecosystems can be considerable sources of C emissions. As an extreme example, during the 1997 El Niño event, fires across Indonesian peatlands lead to the release of C emissions at a level that was equivalent to 13-40% of annual fossil fuel emissions (Page et al., 2002).

The United Nations (UN) Reduced Emissions from Deforestation and Degradation Plus (REDD+) programme is an initiative whereby developing countries can receive financial incentives to reduce greenhouse gas (GHG) emissions from deforestation or forest degradation or to enhance forest C stocks through sustainable management and conservation practices (Sukhdev et al., 2011). With peatlands now recognised as an important component in the global C cycle, under the UN REDD+ scheme participating

countries must now include any significant peatland C stocks in their C accounting (UNFCCC, 2012). However, in some countries a lack of quantitative data from peatland ecosystems is a serious obstacle to the inclusion of peatland C stocks in national inventories. This is particularly true for African countries where there is a large knowledge gap with regards to peatland location, extent and C stocks (see sections 1.3.10 to 1.3.14, Chapter 1). The latest estimates for Africa, based on extremely sparse data, suggest that the Republic of Congo (ROC) is the country with the most significant peatland C stocks on the continent at ca. 2.4 Pg C (Page et al., 2011). This combined with the 0.6 Pg C estimated to be stored in peatlands of the neighbouring Democratic Republic of Congo (DRC) suggest that the Congo Basin stores a total of ~3 Pg C in peatlands (Page et al., 2011). However, for both countries these estimates are based on ambiguous area and depth estimates taken from the grey literature (see section 1.3.13, Chapter 1) and C density values obtained from the literature for South East Asian peatlands (Page et al., 2011). Both the ROC and DRC are UN REDD+ partner countries (UN-REDD Programme Collaborative Online Workspace, 2015). Therefore it is of national interest to obtain estimates of peatland extent and C stocks founded on robust *in situ* data. Newly acquired ground data that I have collected from the extensive peatlands in the north of the ROC, in the Cuvette Centrale, provide this opportunity (see Chapter 2).

Peatland C stock estimates require values for four parameters; peatland area, peat depth, peat bulk density and peat C concentration. The first two components give the volume of peat, whilst the latter two give the C density of the peatland. The size, remoteness and difficult access of many peatland regions mean that mapping of peatland area is not always feasible from the ground. In many temperate and boreal regions land cover or soil maps are used to derive peatland area (Sheng et al., 2004, Buffam et al., 2010, Parry et al., 2012). However, in the tropics detailed maps are often not available. Remote sensing, therefore, offers the most effective solution to determining peatland extent over large, inaccessible areas. Differences in vegetation composition and structure, soil moisture content and topography have all been used to delineate peatlands from surrounding non-peatland areas using remote sensing data, whether through simple visual interpretation of remote sensing imagery (Jaenicke et al., 2008, Beilman et al., 2008) or more robustly through automated statistical classifications of remote sensing data (Draper et al., 2014, Householder et al., 2012, Lähteenoja et al., 2012).

Landsat Thematic Mapper (TM) and Enhanced Thematic Mapper (ETM+) have been commonly used to detect differences in vegetation that are known, via field measurements in a number of regions, to correspond with the presence or absence of peat (Lähteenoja et al., 2012, Householder et al., 2012, Draper et al., 2014). Synthetic Aperture Radar (SAR)

has also proved successful at detecting wetland areas (e.g. De Grandi et al., 2000b, Mayaux et al., 2002, Bwangoy et al., 2010). The high soil moisture contents of the soils and standing water for a lot of the year mean that swamp forests have much higher levels of backscatter in comparison to *terra firme* forests. If a wetland area is known to be peat-forming then areas of high reflectance are likely to be indicative of peat. Additionally, structural differences such as canopy height or openness can result in variations in reflectance, allowing SAR data to be used for distinguishing between different peatland vegetation communities (Draper et al., 2014). Whilst the Shuttle Radar Topography Mission (SRTM) digital elevation models (DEM) have been used to visually delineate domed South East Asian peatlands (Jaenicke et al. 2008), a classification using only SRTM data is unlikely to successfully depict peatlands. However, as peatlands are mostly likely to occur in low lying areas where water can accumulate, SRTM data can help to distinguish between low-lying swamp vegetation and higher altitude vegetation communities which may have similar spectral or reflectance signatures (Draper et al., 2014). Since a combination of all three datasets have been used to successfully identify individual peatland sites within the Cuvette Centrale (Chapter 2), these datasets are likely to be useful in the mapping of regional peatland extent across the world's second largest tropical wetland.

Once peatland extent is determined, the simplest calculation to estimate peatland C stocks is to multiple peatland area by mean values for depth, bulk density and C concentration (Draper et al., 2014). The accuracy of this method is dependent on the peat sampling obtaining an unbiased mean of each parameter and that the mean is the best description of the central tendency of the data distribution. There can also be covariation in peatland properties that may not be well represented using mean values. Therefore, if possible, it is preferable to account for these covariations, through models.

In this chapter I first estimate peatland extent within the Cuvette Centrale, Congo Basin, through the classification of radar, optical and elevation data to delineate different vegetation classes, of which hardwood swamps and palm-dominated swamp are known to be associated with peat from extensive fieldwork. I then estimate peatland C stocks for the Cuvette Centrale, based on the area estimates and my estimates of peat depth, peat bulk density and C concentration determined from *in situ* and laboratory measurements. This will assist both the ROC and DRC to better plan conservation and other initiatives with more robust information than has been available in the past.

4.3. Aims

The aim of this chapter is to use ground data from the recently discovered peatlands in the Likouala Department, ROC, to firstly determine the extent and spatial distribution of

peatlands within the Cuvette Centrale. The objective is to use ground truth points to classify multiple remote sensing datasets to produce a map of peatland spatial distribution and an estimate of peatland extent. The second aim is to estimate peatland C stocks within the Cuvette Centrale. The overall objective is to produce an estimate of peatland C stocks by combining the estimates of peatland extent with *in situ* measurements of peat depth, bulk density and C concentration.

4.4. Methods

In this section, I first provide a brief site description, before explaining the remote sensing methods used to estimate peatland extent. I then describe three different methods used to estimate peatland C stocks. Finally I describe the methods used to estimate aboveground C stocks in the peatlands.

4.4.1. Site Description

This chapter focuses on estimating peatland extent and C stocks for the entire Cuvette Centrale, Congo Basin (3.3°N to 4.9°S, 15.0°E to 25.6°E). For a description of the Cuvette Centrale see section 1.4, Chapter 1. The *in situ* measurements referred to in this chapter come from nine field sites (eight containing peat) visited in the Likouala Department, ROC. For the location of the field sites see Fig. 2.1 (Chapter 2) and for a description of the vegetation, peat occurrence, flood regime, microtopography and disturbance levels see Table 2.5 (Chapter 2) and Appendix 1-8. For methods relating to site selection and peat and vegetation sampling protocol refer to Chapter 2, section 2.4.

4.4.2. Peatland Area

Owing to the large size of the peatlands and the large geographical area being covered, classifications of remote sensing data using ground data are required to estimate peatland area across the Cuvette Centrale. This section describes the classification methods used to produce peatland area estimates.

Five land cover classes were used in the classifications: *terra firme*, hardwood swamp, palm dominated swamp, savannah and water (Table 4.1). These were based on six vegetation land cover classes observed in the field (Table 2.4, Chapter 2), as *terra firme* and seasonally flooded forest were not easily distinguishable from each other via remote sensing products and were therefore amalgamated into a single class, "*terra firme*". Similarly, the *Raphia laurrentii* and *R. hookeri* were not easily distinguishable from each other via remote sensing products and were therefore amalgamated into a single class, "palm dominated swamp".

Two of the classes were observed in the field to be strongly associated with the presence of peat: hardwood swamp forest and palm dominated swamp forest (Table 4.1). In the field hardwood swamp forest was consistently found to be associated with the presence of peat. *Raphia laurentii* palm dominated swamp forest was also consistently found to be associated with the presence of peat. However, the much rarer *Raphia hookeri* palm dominated swamp forest was found to be associated with the presence of channels or fluvial features, which were often, but not always containing peat. Therefore, although the palm dominated swamp class is assumed to denote the presence of peat, it will also represent small areas of swamp which do not contain peat. Conversely, for savannah, just one out of the 12 on-the-ground sample points contained peat. Therefore, in the classifications savannah is not considered to be simultaneous with peat presence, although it will also represent small areas which do contain peat.

Table 4.1. Classification land cover classes.

Land Cover Class	Description	Signifies Peat Presence?	Total No. of Ground Truth Points	No. of Ground Truth Points from Google Earth
Terra firme	Consists of the "*terra firme*" and "seasonally flooded forest" class described in Table 2.4, Chapter 2.	No	144	77
Hardwood Swamp	Consists of the "hardwood swamp" class described in Table 2.4, Chapter 2.	Yes	129	0
Palm dominated swamp	Consists of the "*Raphia laurentii* palm dominated swamp" and "*Raphia hookeri* palm dominated swamp" classes described in Table 2.4, Chapter 2.	Yes	101	0
Savannah	Consists of the "savannah" class described in Table 2.4, Chapter 2.	No	66	59
Water	Water bodies such as rivers or lakes.	No	76	69

Mapping the land cover classes requires ground truth data to train the algorithm and to assess the accuracy of the output. Ground truth points (a total of 278) were collected using a GPS (manufacturer: Garmin, Hampshire, U.K.; model: GPSmap 60CSx) over three field campaigns in the Likouala Department. Additional ground points, provided by Dr W. Hubau, for 33 points (28 for *terra firme*, 5 for hardwood swamp), collected using a GPS between 2008 and 2013, were obtained from the DRC to improve the spatial distribution of the ground truth points across the region. Further ground truth points were created for the savannah (59 points), *terra firme* (77 points) and water (69 points) classes using Google Earth, as these classes did not have a sufficient number of points from the ground data alone and were clear and unambiguous in Google Earth imagery. Coordinates were recorded along with a screen shot of the Google Earth image.

A combination of phased array L-band Synthetic aperture radar (PALSAR), Landsat Enhanced Thematic Mapper (ETM+) and Shuttle Radar Topography Mission (SRTM) remote sensing products were used successfully to identify previously undocumented peatlands within the Cuvette Centrale (see Chapter 2). Therefore similar PALSAR, Landsat ETM+ and SRTM products were selected for use in the classifications and are summarised in Table 4.2 and described in full below. All edits and creations of files from the original datasets, obtained from the providers, were done using ENVI 4.6.1. *(Exelis Visual Information Solutions, Boulder, Colorado)*.

Table 4.2. Remote sensing products used in the maximum likelihood classifications in this chapter.

Product	Description	Data Provider (Available From:)
PALSAR HV	A ca. 50 m resolution mosaic of mean PALSAR HV values from the years 2007-2010.	JAXA EORC (1997) (http://www.eorc.jaxa.jp/ALOS/en/palsar_fnf/data/index.htm)
PALSAR HH	A ca. 50 m resolution mosaic of mean PALSAR HH values from the years 2007-2010.	JAXA EORC (1997) (http://www.eorc.jaxa.jp/ALOS/en/palsar_fnf/data/index.htm)
PALSAR HV/HH	A ca. 50 m resolution mosaic HV/HH ratios created from the above mean PALSAR HV and HH mosaics.	JAXA EORC (1997) (http://www.eorc.jaxa.jp/ALOS/en/palsar_fnf/data/index.htm)
SRTM DEM	A 1-arc second SRTM DEM mosaic, resized to ca. 50 m resolution. Voids (i.e. extremely large negative numbers) present in the data were filled using ASTER Global Digital Elevation Model (GDEM) (version 2) 1-arc second data.	SRTM: USGS (2006) (http://earthexplorer.usgs.gov/) ASTER: NASA and METI (2011) (http://earthexplorer.usgs.gov/)
SRTM slope	A slope file calculated from the above SRTM DEM using the Topographic Modelling tool in ENVI 4.6.1, resized to ca. 50 m resolution.	SRTM: USGS (2006) (http://earthexplorer.usgs.gov/) ASTER: NASA and METI (2011) (http://earthexplorer.usgs.gov/)
Landsat ETM+ (bands 5, 4, 3)	A mosaic of the OSFAC ROC and DRC Landsat ETM+ (bands 5, 4 and 3) 60 m resolution mosaics resized to ca. 50 m resolution. Each band in the ROC mosaic is the median of the years 2000, 2005 and 2010. Each band in the DRC mosaic is a composite of the years 2005 to 2010.	OSFAC (2010) (http://osfac.net/index.php?option=com_k2&view=item&layout=item&id=532&Itemid=810&lang=en and http://osfac.net/index.php?option=com_k2&view=item&layout=item&id=531&Itemid=809&lang=en)

A four-year average (2007-10) ALOS PALSAR HH and HV 50 m resolution georeferenced mosaic was created for the entire Cuvette Centrale. Firstly an HH and an HV mosaic for each of the four years was created and then each of the eight mosaics were converted from raw digital numbers (i.e. values range from 0 to 255) to decibels (σ) using the following equation in Band Math (ENVI 4.6.1):

$$\sigma = 10 * (log_{10}(b1^2) - 83) \quad [4.1]$$

Where $b1$ is the HH or HV mosaic for each of the four years in digital numbers.

Secondly, each σ-mosaic was smoothed using an enhanced lee adaptive filter (Lopes et al., 1990) using the default 3x3 filter size to remove speckle. Across the four years there was clearly a temporal variation in backscatter signal and so it was decided that mean HH and HV values across the four years would be more representative of the region than any one individual year. Areas of inundated forest often have high proportions of HH backscatter owing to the double-bounce mechanism, whereby the radar signal is first reflected off the surface of standing water and then tree trunks. All forested areas, however, should have relatively high proportions of HV backscatter, owing to volume scattering by the forest canopy. Consequently lower HV/HH ratios were thought more likely to represent areas of swamp forest, than high HV/HH ratios. Therefore a new file of HV/HH ratios was created in Band Math using the following equation:

$$HV/HH = (10^{(\frac{b1}{10})})/(10^{(\frac{b2}{10})}) \quad [4.2]$$

Where $b1$ is the mean HV σ-mosaic and $b2$ is the mean HH σ-mosaic.

A georeferenced mosaic of SRTM 1-arc second (equivalent to 30 m) resolution elevation data (derived from X-band radar) was created for the entire Cuvette Centrale. Scenes which contained voids in the data (owing to SRTM data acquisition problems) were replaced with ASTER Global Digital Elevation Model (GDEM) (version 2) 1-arc second data.

Since topographic modelling indicated that the peatlands of the Cuvette Centrale are relatively flat (see Chapter 2, section 2.5.2) it was thought that slope data could help differentiate peatland from non-peatland areas, with low slopes more likely to be associated with peatlands and steeper slopes associated with river levees or higher ground supporting *terra firme* forest. From the new SRTM DEM file, slope was calculated using the Topographic Modelling tool using the default kernel size of 3. The resulting file was then converted to a byte file, whereby all slope values ≤25 were multiplied by 10 and all values >25 were given a value of 250, to reduce file size. Both the new SRTM DEM file and the SRTM slope byte file were reprojected to the same pixel resolution as the PALSAR mosaics using the Convert Map Projection tool, with the "Rigorous" method selected.

Pre-processed Landsat ETM+ mosaics, composed of bands 5, 4 and 3 resampled to a 60 m resolution, covering the entire ROC and DRC were obtained from OSFAC (2014). Each band in the ROC mosaic is the median of the years 2000, 2005 and 2010. Each band in the DRC mosaic is a composite of the years 2005 to 2010 (OSFAC do not specify how the composite was created). Subsets of the ROC and DRC mosaics were mosaicked together using colour balancing from the whole file to produce a mosaic for all three bands for the

Cuvette Centrale. The final Landsat mosaic was re-projected to the same pixel resolution as the PALSAR mosaics using the Convert Map Projection tool, with the "Rigorous" method selected.

Many methods are available to use training data and remote sensing data to produce a land cover classification map (Campbell and Wynne, 2011). However, the vastness of the Cuvette Centrale meant, that despite extensive fieldwork, on the ground coverage was still limited in extent relative to the size of the region. The main priority was therefore devising a method that produced reasonable confidence intervals for peatland extent. The selected method was a supervised maximum likelihood classification, which was run 1000 times to assess uncertainty. Maximum likelihood was chosen because the accuracies of initial maximum likelihood classifications were higher than classifications using other techniques. To reduce computational time, principal component (PC) transformations were used to convert the eight bands of remote sensing data (Table 4.2) to a byte file format without losing information contained in the original files. Of the eight bands of uncorrelated data variance produced, the first six were used in the maximum likelihood classifications. The seventh and eighth bands were not included as they contained little variance, most of which was attributable to noise in the original datasets.

For each of the 1000 classification iterations, two thirds of the ground truth points from each class were randomly selected for use as training data, with the remaining ground truth points assigned to test data. Each iteration produced a user's and producer's accuracy and an area estimate for each land cover class. The final output was 1000 estimates for each pixel of its land cover class, expressed as a percentage probability of the commonest allocated class. The best estimate of peatland area was taken as the median value of the combined palm dominated swamp and hardwood swamp area from the 1000 runs alongside the 90% CI (the 5th and 95th percentile). The overall accuracy of the peat probability map, and accuracy per class, was assessed as the percentage of total ground truth points assigned to the correct class.

4.4.3. Peatland Carbon Estimates.

I used three methods to estimate peatland belowground C stocks in the Cuvette Centrale. Firstly, I utilised the mean area of peatland from the 1,000 iterations and the mean of the *in situ* peat depth (see Chapter 2), mean peat bulk density and mean carbon concentration (see Chapter 3) measurements from all the available peat samples, as this is a simple method that has been utilised in other tropical peat studies (Draper et al., 2014). Secondly, I used a similar approach, but because there is evidence to suggest that bulk density and core depth are not entirely independent of one other, (see Chapter 3, section 3.5.2), I used a relationship between peat core mean bulk density and core depth for the *in situ* data to

assign each *in situ* peat depth measurement a modelled peat mass before scaling up. For the third approach I tried to account for the fact that the relationship between bulk density and depth may be spatially variable, therefore I used the output on an ANCOVA between bulk density, core and depth down-core (see Chapter 3, section 3.5.2). By using three techniques I assess whether the final estimate is method-dependent.

4.4.3.1. Method 1: Mean Values for each Component.

The peatland belowground C stock (BGC; Pg C) can be simply estimated by:

$$BGC = \frac{A * BD * C * D}{10^{12}} \quad [4.3]$$

Where A is the mean combined area of palm dominated swamp and hardwood swamp (m^2), BD is the mean peat bulk density (kg m^{-3}), C is the mean peat C concentration (expressed as a fraction) and D is the mean peat depth (m). However, to get a more robust estimate and to estimate confidence intervals for BGC, bootstrapping was used where each variable in equation 4.3, was randomly sampled with replacement from the original dataset to create a simulated dataset that was the same length as the original (BD: n=372; C: n=213; D: n=225). The mean values of the , BD, C and D simulated datasets were used in equation 4.3. This was repeated 10,000 times to give 10,000 estimates of BGC. The mean value of BGC is used as the best estimate and the 5^{th} and 95^{th} percentiles are used as the upper and lower confidence intervals.

To assess which variables were the source of most uncertainty in estimates of BGC, method 1 was re-run four more times, but for each run, only one of the variables in equation 4.3 was bootstrapped, whilst the other three variables were held at the mean values of the original datasets.

4.4.3.2. Method 2: Accounting for Depth-Bulk Density Relationships

Total core depth and the mean sampled bulk density per core were significantly negatively correlated (Fig. 3.4, Chapter 3). Although not strong (R-sq adj.=0.29), this relationship was used to apply a mean bulk density (BD; g cm^{-3}) to each depth (D; cm) measurement by the following:

$$BD = e^{-0.001D-1.465} \quad [4.4]$$

Each depth measurement was then assigned a peat mass (M; kg m^{-2}) by the following:

$$M = BD * D \quad [4.5]$$

Where BD is the mean core bulk density (kg m^{-3}) and D is the core depth (m).

BGC can then be estimated by the following equation:

$$BGC = \frac{A * M * C}{10^{12}} \quad [4.6]$$

Where the denotation of A and C are the same as in equation 4.3. To give a better estimate of BGC and to estimate confidence intervals, the same bootstrapping method used in method 1 was employed. Again the mean value of BGC is used as the best estimate and the 5th and 95th percentiles are used as the upper and lower confidence intervals.

4.4.3.3. Method 3. Accounting for Down-Core Bulk Density Relationships.

A One-way ANCOVA showed that there was a significant relationship between bulk density and depth down core and that this relationship was significantly different between cores ($F_{83, 284}$ =8.248, p<0.001; Table 4.3). When both core and depth down core are accounted for, over 60% of the variance in bulk density is accounted for (R-sq adj.=0.62). To incorporate this finding into estimates of total peatland C stocks, the following method was devised. Firstly, the ANCOVA regression equations were binned into five different core depth groups, to account for the dependency between regression slope and core depth (Fig. 4.1). The groups were as follows: <0.5 m depth, 0.51-1.00 m depth, 1.01-1.50 m depth, 1.51-2.00 m depth and >2.00 m depth. This was followed by a bootstrapping method whereby a simulated dataset of peat mass, of length equal to the original depth dataset, was created by randomly sampling depth values with replacement from the original dataset. For each depth value in the simulated dataset, peat mass was estimated by randomly sampling, with replacement, a regression equation from the corresponding depth bin. By doing so, dependencies between peat bulk density and mineral content are accounted for, preventing high bulk densities being ascribed to deep cores, but also weak or even no relationship between bulk density and depth for some cores are accounted for, which was not possible with Method 2. The mean of this simulated peat mass dataset forms M in equation 4.6. Again, A and C are the mean values of the simulated datasets, that are the same length as the originals, created by sampling with replacement. This process was repeated 10,000. Again the mean value of the 10,000 estimates BGC is used as the best estimate and the 5th and 95th percentiles are used as the upper and lower confidence intervals.

Table 4.3. Output from a One-way ANCOVA of where bulk density is the dependent variable, core is the factor and depth down-core is the covariate.

Term	F Statistic	p Value
Core	10.0	<0.001
Depth	28.7	<0.001
Core*Depth Interaction	6.0	<0.001

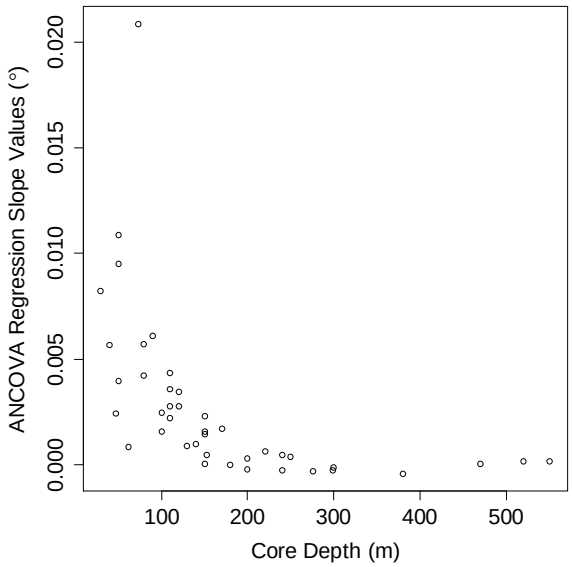

Figure 4.1. Regression slope values from an ANCOVA where square root bulk density is the dependent variable, core is the independent variable and depth down core is the covariate, plotted against total core depth.

4.4.3.4. Country Level Peatland Carbon Estimates

The output of the 1000 maximum likelihood classifications provided an area estimate for the entire Cuvette Centrale only and did not provide separate peatland area estimates for the ROC and DRC. Therefore estimates of peatland area for each country were obtained from the peatland probability map. Peatland belowground C stocks for the two countries were estimated from equation 4.6, using mean values of BD, C and D.

4.4.3.5. Study Region Carbon Estimates

To understand how spatial scale affects the C stock confidence interval estimation, C stocks were estimated for the 36,000 km^2 study region in the Likouala Department, ROC (shown in Fig. 1.4, Chapter 1), from where the ground data originates. The methods used to estimate C stocks for this region were the same as those used to estimate C stocks for the entire Cuvette Centrale (see sections 4.4.2., 4.4.3.1-4.4.3.3.).

4.4.4. Aboveground Carbon Stock Estimates.

The data used here for aboveground biomass and C estimates for the three forest classes were acquired *in situ* from 40 m x 20 m vegetation plots (palm dominated swamp: n=35; hardwood swamp: n=25; *terra firme*: n=11). See Chapter 2, section 2.2.3.5 for vegetation plot sampling methods. Aboveground biomass (AGB; kg) of each tree was calculated using the following equation taken from Chave et al. (2014):

$$AGB = 0.0673 * (\rho D^2 H)^{0.976} \quad [4.7]$$

Where ρ is the wood specific gravity (g cm^{-3}), D is the diameter (cm) of the tree and H is the tree height (m). Values for wood specific gravity were obtained from the Global Wood Density Database (Zanne et al., 2009), available from http://hdl.handle.net/10255/dryad.235. Species-level mean wood specific gravity was used where possible. If the tree was not identifiable to species level or the database did not contain any values for that species, a mean value for genus was used. If the genus was not available then a family mean was used. If the tree was not identified even to family level, a mean plot wood specific gravity was used. Tree height was measured using a laser hypsometer (manufacturer: Nikon, Kingston upon Thames, UK, model: Laser 550A S) in the field for a subset of stems (n=369). These were used to compute a height-diameter allometry for swamp and non-swamp vegetation height, allowing height to be estimated from diameter for trees with no height measurement within a plot. For the height-diameter allometry additional height and diameter data (stems: n=322), collected over the period January 2012 to June 2014 from separate vegetation plots within the Likouala Department, were obtained from Professor Simon Lewis, to produce a more robust height-diameter allometry. All height-diameter data was first separated into two vegetation groups: swamp and non-swamp. A 3-parameter Weibull-fit distribution, following Feldpausch et al. (2012), was then fitted to each group. I estimated swamp tree height (H; m) from tree diameter (D; cm) using:

$$H = 27.4142 - 18.0682 * exp(-exp(-7.7836) * D\text{^}2.1489) \quad [4.8]$$

For non-swamp tree height (H; m) from tree diameter (cm) I used:

$$H = 38.2080 - 32.8500 * exp(-exp(-4.8040) * D\text{^}1.3040) \quad [4.9]$$

All palms in the vegetation plots were of the genus *Raphia,* however no allometric equations have been developed for this genus, therefore family-level allometric equations taken from Goodman et al. (2013) were used to estimate the aboveground biomass (AGB) of any palms which had a measureable trunk. AGB estimates do not include the AGB of *Raphia laurentii* and juvenile *R. hookeri* present in the plots, because there was no trunk to measure. This inevitably leads to an underestimation of AGB in the palm dominated swamp plots. Height measurements of individual palms were made in some plots to be used in the estimation of mean canopy height. The inclusion of height in the allometric equations for palms has been shown to give considerably better estimates of AGB. Therefore if height was available, the following family-level allometric equation, which incorporates height, was used to estimate palm AGB (kg):

$$AGB^{0.25} = 0.55512 * ((dmf * D^2 * H_{stem})^{0.25}) \quad [4.10]$$

Where dmf is the dry mass fraction (g g^{-1}), D is the diameter of the palm trunk (cm) and H_{stem} is the height of the stem (m). There are no dry mass fraction values available for the genus *Raphia,* therefore the mean (0.37) of the species dry mass fraction values presented in Goodman et al. (2013) was used.

If no height measurement was available for an individual palm, the following family-level allometric equation, based on trunk diameter only, was used to estimate palm AGB(kg). Again a value of 0.37 was used for the dry mass fraction:

$$lnAGB = -2.0752 + \big(2.6401 * (\ln(D))\big) + (0.8426 * (\ln(dmf))) \quad [4.11]$$

Once the AGB of each tree or palm had been calculated, the AGB (kg) for all trees in a plot were summed to give the total AGB for each plot which was converted to Mg ha^{-1}. The carbon content of trees is, on average, 47% (Martin and Thomas, 2011), therefore the aboveground carbon stock (AGC) was assumed to be 47% of the AGB for each plot.

Estimates of total AGC for the palm dominated swamp and hardwood swamp were obtained by multiplying the mean area and mean plot AGC for the respective swamp class. Again to obtain a more robust estimate a bootstrapping method was applied whereby for both area and AGC, values were randomly sampled with replacement from the original dataset to create a simulated dataset that was the same length as the original. This was repeated 10,000 times to give 10,000 estimates of AGC for palm dominated swamp and hardwood swamp respectively. For each swamp class the mean value is used as the best estimate and the 5^{th} and 95^{th} percentiles are used as the upper and lower confidence intervals. Again country level estimates were made using an area estimate obtained from the peatland probability map and the mean value of AGC for each swamp class.

4.5. Results

4.5.1. Maximum Likelihood Classifications and Peatland Extent.

The 1000 runs of the maximum likelihood classification gives a best estimate of peatland area of 145,529 (90% CI 134,720-154,732) km^2 (Table 4.4). The areas within the Cuvette Centrale with the highest probability of being peat are located to the west of the Ubangui River in the interfluvial basins of the Likouala, Cuvette and Sangha Departments of the ROC and within the DRC the interfluvial basin between the Congo and Ubangui rivers, along the river valleys of the left bank tributaries of the Congo and in the Lac Tumba and Lac Mai-Ndombe region (Fig. 4.2). Hardwood swamp was found to be slightly more extensive than palm dominated swamp (790,042 km^2 vs. 66312 km^2). *Terre firme* was found to be the most extensive class within the region and savannah the least. Overall the

peat probability map had an accuracy of 84%, with individual class accuracies ranging from 73% for the *terra firme* class to 100% for the water class (Table 4.5).

Table 4.4. Land cover class area estimates from the 1000 maximum likelihood classifications.

Class	Area (km^2)		
	Median	Percentile	
		5th	95th
Water	34995	19676	56959
Savannah	26321	20924	35434
Terra firme	772378	750958	786766
Palm Dominated Swamp	66312	56899	74696
Hardwood Swamp	79042	68071	90469
Total Swamp Area	**145529**	**134720**	**154732**

Table 4.5. Overall accuracy and accuracy per class for the peatland probability map derived from the 1000 maximum likelihood classifications.

Class	Accuracy (%)
Water	100
Savannah	97
Terra firme	73
Palm Dominated Swamp	79
Hardwood Swamp	85
Overall	**84**

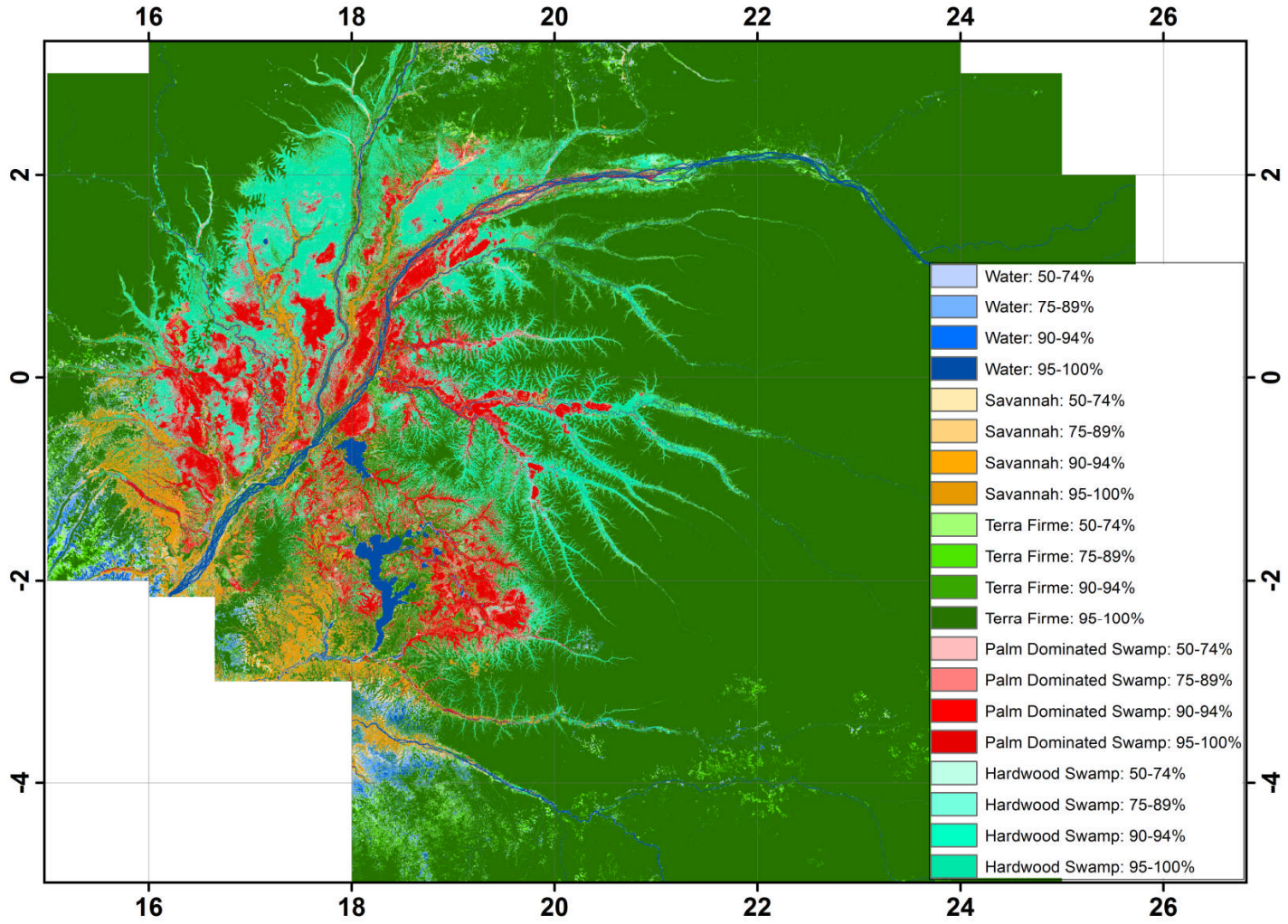

Figure 4.2. Peatland probability map derived from 1000 maximum likelihood classifications. Different colours and shades represent different land cover classes and levels of probability respectively (refer to legend). Palm dominated swamp and hardwood swamp denote the presence of peat.

4.5.2. Spectral Signature of Land Cover Classes

Mapping peatland extent from remote sensing data relies on specific land cover classes being associated with peat presence, but also that the different land cover classes have distinctively different reflective properties, allowing them to be differentiated from one another in the remote sensing datasets. When class ground truth point values were compared for each of the eight datasets, there were clear differences in the values associated with the five land cover classes. Equally, however, there was no one remote sensing dataset where all five land cover classes could easily be distinguished from one another (Fig. 4.3). The two peat classes, hardwood swamp and palm dominated swamp, had significantly different values from the three non-peat land cover classes for the following datasets: Landsat ETM+ B4 and B3, PALSAR HH and the SRTM DEM (Fig. 4.3). For Landsat ETM+ B4 the two peat classes' reflectance levels were significantly higher than water and savannah, but significantly lower than *terra firme*. For Landsat ETM+ B3, the reverse was true, with the two peat classes having significantly lower reflectance levels than water and savannah, but significantly higher than *terra firme*. For PALSAR HH, the two peat classes had significantly higher backscatter coefficients than all other classes. For the SRTM DEM the two peat classes had significantly higher elevations than water and savannah and significantly lower elevations than *terra firme*. Of these four datasets, the SRTM DEM was the only one where were palm dominated swamp and hardwood swamp were significantly different from one another, with palm dominated swamp having lower elevations than hardwood swamp. The two peat classes were also distinguishable from one another for the Landsat ETM+ B5, PALSAR HV and HV/HH ratio datasets. However, for these datasets one of the peat classes overlapped with a non-peat class. For the Landsat ETM+ B5 data palm dominated swamp reflectance levels were significantly higher than hardwood swamp and water reflectance levels, were significantly lower than savannah, but were not distinguishable from *terra firme*. For the PALSAR HV data the palm dominated swamp backscatter coefficients were significantly lower than hardwood swamp, significantly higher than water and savannah, but were not significantly different from the *terra firme* class. For the PALSAR HV/HH ratio data hardwood swamp was significantly higher than the palm dominated swamp and savannah, significantly lower than *terra firme*, but was indistinguishable from the water class. Like hardwood swamp, palm dominated swamp PALSAR HV/HH ratios were also significantly lower and higher than *terra firme* and savannah, respectively. For the SRTM slope data, the two peat classes had significantly lower and significantly higher slope values than *terra firme* and water, respectively, but were not significantly different from the savannah class.

There were also differences in the ranges of the ground truth point values for the different land cover classes. For example, the Landsat ETM+ B3, PALSAR HV, HH and HV/HH ratio

values for the water class were exceptionally large. The range of PALSAR HV and HH values for the savannah class were also large. Likewise, the *terra firme* class SRTM DEM elevations spanned a much wider range than any other class.

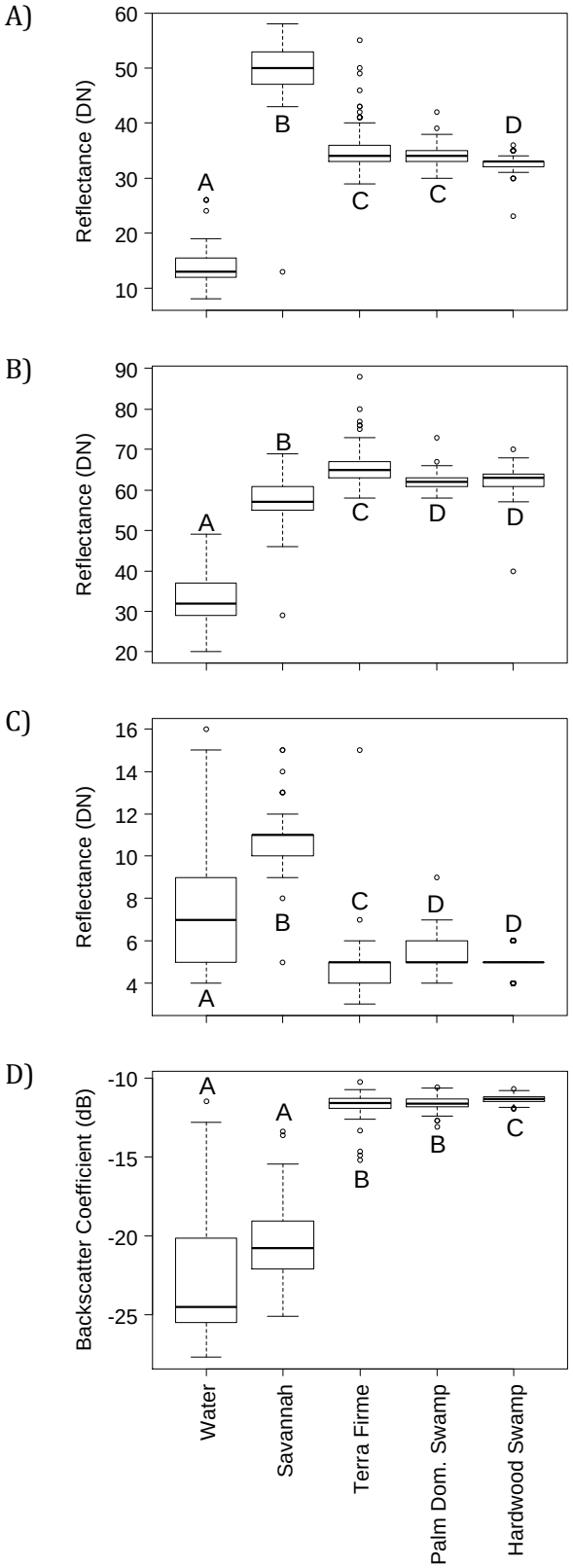

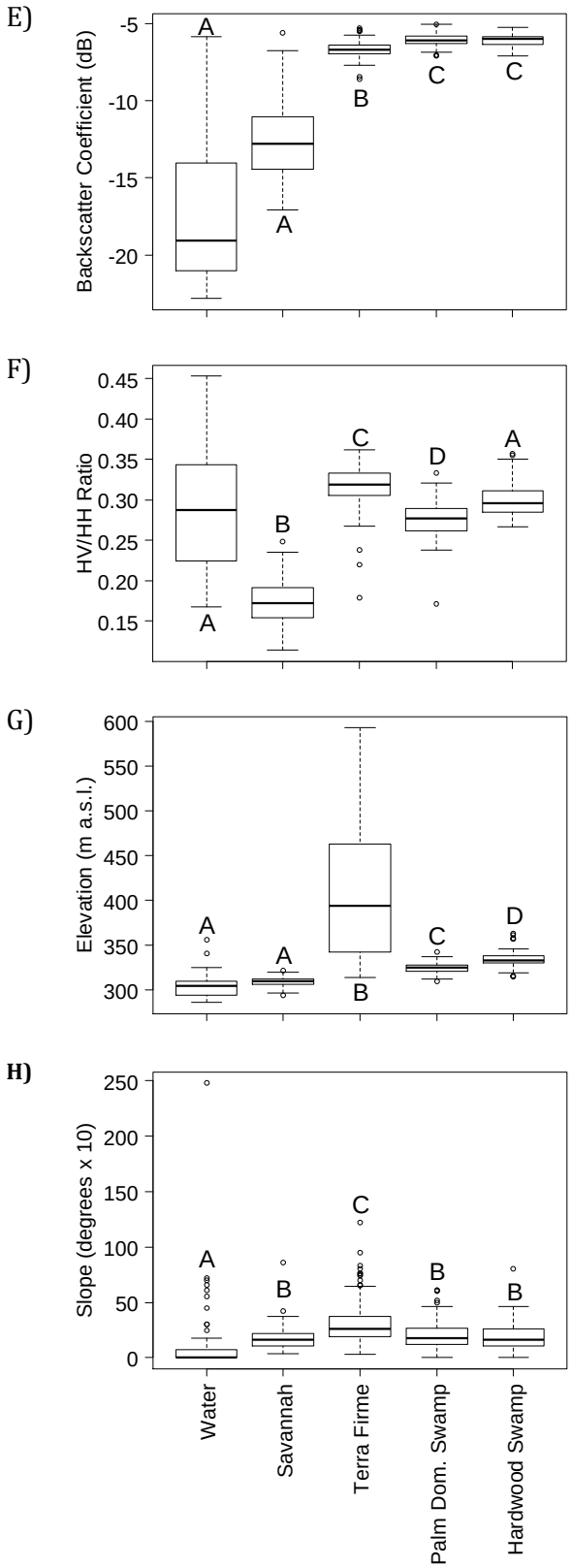

Figure 4.3. Boxplot of land cover class ground truth point values for A) Landsat ETM+ B5 B) Landsat ETM+ B4 C) Landsat ETM+ B3 D) PALSAR HV E) PALSAR HH F) PALSAR HV/HH ratio G) SRTM DEM H) SRTM slope. The median is shown by the black line. The box shows the upper and lower quartiles. The bars show maximum and minimum values. Circles represent outlying values. Land cover classes which do not share a common letter have significantly different ground truth point mean values for the respective dataset ($p<0.05$, Kruskall-Wallis multiple comparison test).

4.5.3. Belowground Peatland Carbon Stock Estimates

Belowground peatland C stock best estimates, produced by the three different methods, were similar and ranged from 30.2 to 32.7 Pg C (Table 4.6). Method 1, which used mean values for each component in equation 4.3, produced the highest belowground peatland C stock estimate, whilst method 3, which used the results of an ANCOVA, where bulk density was the dependent variable, core was the independent variable and depth down core was the covariate, to model variations in peat mass down core, produced the lowest. The range and uncertainty in belowground peatland C stocks was highest under method 3 and lowest under method 2. At a country level, using the peatland extent from the peat probability map and mean values of peat depth, bulk density and C concentration, the ROC and DRC peatland belowground C stocks are an estimated 12.2 Pg C and 20.2 Pg C respectively.

Table 4.6. Peatland belowground C estimates for the three different methods used to estimate peat C stocks.

	Peatland Belowground C (Pg C)		
Output	**Method 1**	**Method 2**	**Method 3**
Best Estimate (mean)	32.7	31.6	30.2
Range	28.8 to 37.0	29.5 to 33.8	24.8 to 37.0
Lower CI (5th percentile)	31.2	30.7	27.8
Upper CI (95th percentile)	34.2	32.6	32.7

Of the four variables used to estimate peatland belowground C stocks, peat depth was by far the most variable, followed by bulk density (Table 4.7). Variations in peat C concentrations were considerably lower and variations in area estimates were lower still. Sensitivity analysis revealed that peat depth was the largest source of uncertainty in peatland belowground C stocks and bulk density the second largest. Uncertainty in the peatland belowground C stock resulting from variations in area and C were less than 1 Pg C (Fig. 4.4).

Table 4.7. Mean, standard deviation and standard deviation expressed as a percentage of the mean for the four variables used in estimating peatland belowground C stocks.

Variable	Mean	St. Dev.	St. Dev. (%)
Area (km^2)	145,189	6462	4
Depth (m)	2.24	1.61	72
Bulk Density (g cm^3)	0.17	0.08	49
C (%)	58.4	5.8	10

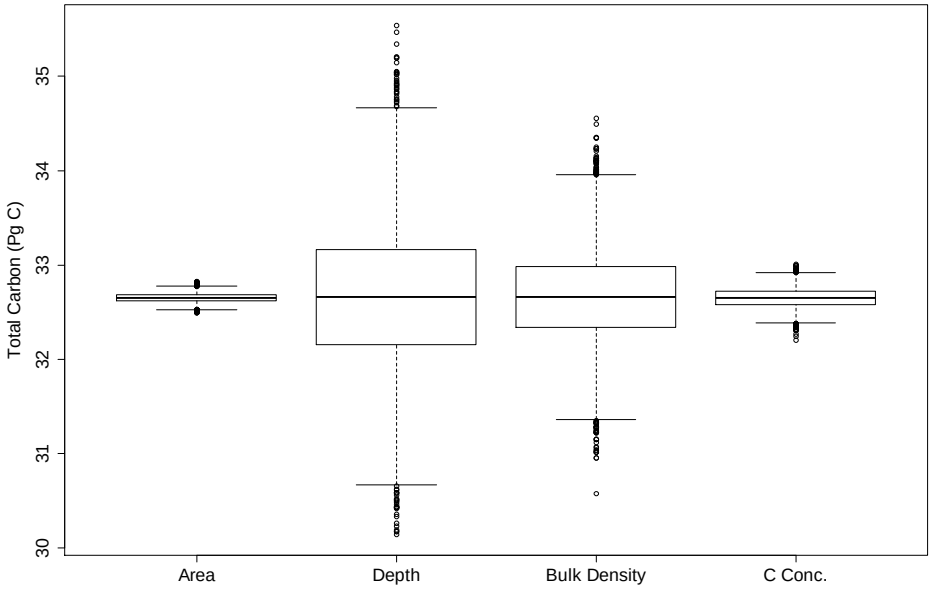

Figure 4.4. Boxplot of sensitivity analysis, whereby only one component of the peatland belowground C estimates was bootstrapped, whilst the three other variables were held constant. X-axis labels refer to the bootstrapped variable. The median is shown by the black line. The box shows the upper and lower quartiles. The bars show maximum and minimum values. Circles represent outlying values.

Belowground peatland C stock best estimates for the study region, produced by the three different methods, ranged from 4.9 to 5.3 Pg C (Table 4.8). Like the C stock estimates for the entire Cuvette Centrale, the 90% CIs were less than ±10% of the best estimates for the three methods. The study region peatland area estimate 90% CIs were also within ±10% of the best estimate (median: 23,626 km^2; 90% CI 22,485-24,999 km^2).

Table 4.8. Study region peatland belowground C estimates for the three different methods used to estimate peat C stocks.

	Peatland Belowground C (Pg C)		
Output	**Method 1**	**Method 2**	**Method 3**
Best Estimate (mean)	5.3	5.2	4.9
Range	4.8-5.9	4.7-5.6	4.1-5.9
Lower CI (5th percentile)	5.1	5.0	4.5
Upper CI (95th percentile)	5.6	5.3	5.3

4.5.4. Aboveground Peatland Carbon Stock Estimates

The estimated mean (± st. dev.) AGC for the palm dominated swamp was 66.4±50.7 Mg C ha^{-1} (n=35) and was significantly lower than the estimated mean (± st. dev.) AGC of the hardwood swamp, 122.5±50.8 Mg C ha^{-1} (n=25; $p<0.001$, One-Way ANOVA and post hoc Tukey test; Fig. 4.5). The mean (± st. dev.) AGC of the *terra firme* forest was 105.7±57.5 Mg C ha^{-1} (n=11) and was not significantly different from either the palm dominated swamp and hardwood swamp AGC estimates ($p=0.05$).

Across the Cuvette Centrale the palm dominated swamp and hardwood swamp combined store an estimated 1.4 (90% CI 1.3-1.5) Pg C, which is only 4.3-4.6% of the belowground peatland C stocks (30.2-32.7 Pg C). The majority of this AGC (69%) is stored in hardwood swamp (Table 4.9). At a country level an estimated 0.6 Pg C is stored in the aboveground peatland vegetation for the ROC, of which an estimated 0.2 Pg C is in palm dominated swamp and 0.4 Pg C is in hardwood swamp. In the DRC an estimated 0.9 Pg C is stored in the peatland above ground biomass, with 0.3 Pg C stored in palm dominated swamp and 0.6 Pg C in hardwood swamp. When combined with belowground peat C stocks, the ROC and DRC peatlands are estimated to store 12.6 Pg C and 21.1 Pg C respectively.

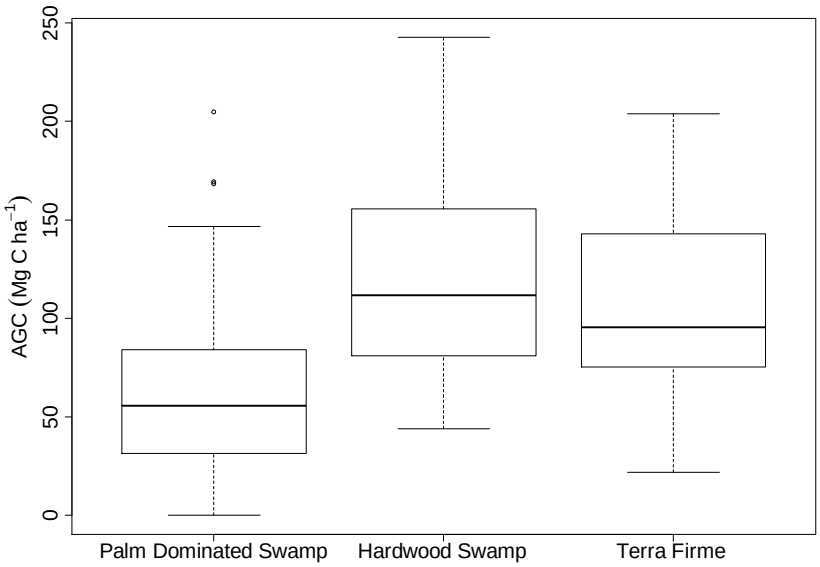

Figure 4.5. Boxplot of AGC for palm dominated swamp and hardwood swamp. The box shows the upper and lower quartiles. The bars show maximum and minimum values. Circles represent outlying values.

Table 4.9. Peatland total aboveground C for palm dominated swamp and hardwood swamp

Output	Total AGC (Pg C)	
	Palm Dominated Swamp	Hardwood Swamp
Best Estimate (mean)	0.4	1.0
Range	0.3 to 0.6	0.8 to 1.1
Lower CI (5th percentile)	0.4	0.9
Upper CI (95th percentile)	0.5	1.0

4.6. Discussion

4.6.1. Peatland Area

4.6.1.1. Peatland Area Estimates for the Cuvette Centrale

The peatland extent of the Cuvette Centrale is estimated to be 145,529 km^2. Previous estimates have mostly been based on histosol extent estimates taken from the

FAO/UNESCO (1971-1978) 1:5,000,000 Soil Map of the World and assumptions of peat existence (see Fig. 1.3 and 1.4, Chapter 1). My estimate of peatland extent is considerably larger than the combined FAO/UNESCO (1971-1978) histosol extent for the ROC and DRC (3,370 km^2) and the most recent combined estimate of maximum peatland extent for the ROC and DRC (26,177 km^2; Page et al., 2011), the origin of which is unclear (see Fig. 1.2 and 1.3, Chapter 1). The source of information for the Soil Map of the World is also ambiguous and does not appear to be based on extensive ground data (see Chapter 1, section 1.3.13). Therefore my estimate of peatland extent in the Cuvette Centrale is the first to be based on *in situ* measurements and is likely to be much more robust.

Independent estimates of the wetland extent of the Cuvette Centrale, derived from classifications of remote sensing data, exceed the estimated peatland extent of this study (ranging from 230,000 to 359,556 km^2; Betbeder et al., 2014, Bwangoy et al., 2010), with the exception of Mayaux et al. (2004), who estimate a combined wetland extent for the ROC and DRC of only 9360 km^2. It is not surprising that these wetland extent estimates exceed my peatland extent estimate, as the estimate of Bwangoy et al. (2010) includes areas beyond the Cuvette Centrale and incorporates areas of savannah and, along with the estimate of Betbeder et al. (2014), areas of seasonally flooded forest, which, although are seasonal wetlands, are not associated with peat according to the findings of this study. Like the previous peatland extent estimates, wetland maps of the Cuvette Centrale are seldom based on ground data and have either been derived from unsupervised classifications, i.e. the algorithm was not trained (Vancutsem et al., 2009, Betbeder et al., 2014), or supervised classifications based on visual interpretation of aerial photographs or maps (Bwangoy et al., 2010, Mayaux et al., 2002, Bwangoy et al., 2013).

When compared to peatland extent estimates for other regions of the tropics, the Cuvette Centrale likely contains the world's most extensive tropical peatland complex. South East Asia is estimated to have ca. 248,000 km^2 of peatland, but this is distributed across mainly the Sumatra, Borneo and New Guinea islands and the Malaysian Peninsular (Page et al., 2011) and therefore is not confined within one specific region. Furthermore, the Cuvette Centrale peatland complex is today largely intact, whereas deforestation, drainage and fire mean that the extent of South East Asian peatlands is in rapid decline (Hooijer et al., 2010). In terms of the largest peatland extent for individual countries, the new estimates for the Cuvette Centrale, mean that worldwide, the DRC ranks fifth, behind Russia, Canada, Indonesia and the U.S.A and the ROC ranks ninth behind the aforementioned countries plus Finland and Sweden (Joosten, 2009).

4.6.1.2. Peatland Area Uncertainty

Qualitatively, the peatland probability map seems reasonable, as it depicts well known land marks such as Lac Télé, Lac Tumba, Lac Mai-Ndombe and the ridge of *terra firme* that stretches from the Likouala aux Herbes to Lac Télé. Similarly, the spatial distribution of land cover classes fits with observations made in the field, such as large areas of savannah boarding the Likouala aux Herbes and thin strips of *terra firme* forest boarding the Ubangui. Likewise, the distinctive patch of palm dominated swamp at Ekolongouma, first observed from Google Earth, is clearly visible on the map. The overall accuracy of the peatland map was 84%. The accuracy of the water and savannah classes was extremely high, while the lower accuracies of the *terra firme*, hardwood swamp and palm dominated swamp can be attributed to the natural transitions between these three forest classes and the fact that there was not always a clear distinction between the ground truth point values of these three classes for each of the eight datasets (Fig. 4.3).

The peatland probability map is one of only two classifications of the Cuvette Centrale which has incorporated ground data in the validation process (the other being Bwangoy et al., 2010).The majority have relied solely on vegetation maps and high resolution imagery (Mayaux et al., 2002, De Grandi et al., 2000b, Betbeder et al., 2014, Bwangoy et al., 2013, Vancutsem et al., 2009). Likewise, whilst some studies present classification accuracy levels (e.g. Vancutsem et al., 2009, Bwangoy et al., 2010, De Grandi et al., 2000b), many do not and no confidence intervals are presented for any of the classification derived wetland area estimates for the Cuvette Centrale (presented in Table 1.4, Chapter 1). Therefore, making direct comparisons between the accuracy of the peatland probability map with previous classifications is not possible. However, although the land cover class names may differ, the general distribution of wetland classes is similar between the peatland probability map and previous classifications.

I used a method which involved 1000 runs of a maximum likelihood classification, described in section 4.4.2., to estimate peatland area CI's. An alternative method is to use a single classification and use the results of the classification confusion matrix (a table of false/true negatives/positives for test ground truth data) to estimate confidence intervals, as detailed by Olofsson et al. (2013) and recently used to estimate CIs for area estimates of a Peruvian peatland complex (Draper et al., 2014). However, my method has a number of advantages over the method of Olofsson et al. (2013). Firstly by resampling of ground truth points for each of the 1000 classifications, the influence of individual ground truth points on the area and CI estimates are reduced. This is particularly useful when the ground truth dataset is relatively small. Secondly, the Olofsson et al. (2013) method is designed so that smaller CIs are achieved when the number of ground truth points is

proportional to the size of the landscape and to the area of each land cover class i.e. as the "known" area of the landscape increases, confidence in the area estimate increases. For unknown, remote or inaccessible areas, where ground truth data is limited, i.e. areas where remote sensing is most needed for mapping landscapes, class CIs can be very high. Whilst the high CIs reflect the want of more ground data, they can also be unrealistic e.g. the CIs can range from negative to greater than the extent of the landscape being classified. My method produces more realistic CIs and does not severely penalise land cover area estimates for large and/or inaccessible regions. Finally, rather than solely providing an overall uncertainty, the peatland probability map highlights areas where the uncertainty is greatest for each class i.e. a spatial distribution of uncertainty. This can be used to guide future sampling on the ground to improve confidence in area estimates and maps of the land cover class in question.

4.6.1.3. Spectral Signature of Land Cover Classes

For no single remote sensing product were all five land cover classes distinctly separable (Fig. 4.3) and no single dataset was the most useful for depicting all five classes. However, by using multiple products it was possible to take advantage of a range of characteristics associated with each land cover class to provide a unique spectral signature of each land cover class. This matches the finding of Draper et al. (2014), who, when mapping lowland peatlands of Peruvian Amazonia, found that using a combination of optical, radar and elevation data provided improved separation of different land cover classes, than when any of these products were used individually.

The association between the Landsat ETM+ reflectance levels and the different classes were largely as expected. Reflection of longer infrared wavelengths tends to be controlled by soil and leaf moisture contents, with higher moisture levels leading to lower levels of reflectance (Campbell and Wynne, 2011). Therefore, it is unsurprising that, in band 5, operating in the mid infrared region of the electromagnetic spectrum (USGS, 2014), the water class had the lowest mean reflectance value and savannah had the highest and that the hardwood swamp had a significantly lower mean reflectance value than *terra firme* forest. It is surprising, however, that the *terra firme* forest and palm dominated forest did not have significantly different mean reflectance values. However, it is perhaps possible that the wetter conditions of the palm dominated swamp are counteracted by the lower biomass levels resulting in an overall lower absorbance by leaf water.

For Landsat ETM+ band 4, detecting in the near infrared (NIR) region (USGS, 2014), the higher reflectance of the three forest classes compared to the savannah vegetation could be attributable to higher leaf area index (LAI) in the forest classes. The internal structure of leaves tend to strongly reflect NIR radiation (Campbell and Wynne, 2011) and higher

LAI values have been found to be associated with higher NIR reflectance for temperate coniferous forests (Spanner et al., 1990). It is not clear why reflectance values of the *terra firme* class were significantly higher than the two swamp classes, but one possibility could be a higher LAI (Spanner et al., 1990). Another possibility could be the presence of water in the swamps, as water absorbs NIR radiation (Campbell and Wynne, 2011). This also explains the lower reflectance values for the water class.

The absorbance of red light by chlorophyll and open water (Campbell and Wynne, 2011) can explain the low levels of reflectance across all classes for band 3, which detects in the visible red region (USGS, 2014). The slightly higher levels of reflectance for the savannah class could again be attributable to a lower LAI (Spanner et al., 1994). The large range of reflectance values for the water class could be attributable to different water depths and perhaps also different sediment loads. The water class ground truth points were from a mixture of lakes and black and white water rivers and whilst varying sediment loads are thought to be better detected by bands measuring in the NIR region (Ritchie et al., 1990, Ma and Dai, 2005, Doxaran et al., 2002, Wang et al., 2009), bands operating in the visible red region have also been able to detect different sediment levels in water bodies (Froidefond et al., 1991, Dekker et al., 2002, Islam et al., 2001, Zhou et al., 2006). Likewise in shallow waters, the close proximity to the surface of the substrate at the bottom of the water body can increase the degree of reflectance (Ackleson and Klemas, 1987, Bustamante et al., 2009).

The ability of SAR L-band to penetrate forest canopies and interact with the forest floor means that it is considered particularly useful for mapping wetlands (Hess et al., 2003, Jung et al., 2010a, Mayaux et al., 2002, Bwangoy et al., 2010, Bwangoy et al., 2013, Betbeder et al., 2014, Alsdorf et al., 2007). Typically flooded forests have higher HH backscatter than non-flooded forests, due to what is known as the double bounce mechanism (Richards et al., 1987, Hess et al., 1990). Less dense canopy cover, but still a high presence of trunks means that palm swamps can have particularly high HH backscatter (Hess et al., 2003). The lack of a difference between the mean HH backscatter values for the three forest classes in this study is therefore hard to explain. If the PALSAR data for each year was acquired during one of the wet seasons, it could be that the inclusion of seasonally flooded forest in the *terra firme* forest class has resulted in a higher mean HH backscatter value for this class. However, if *terra firme* and seasonally flooded forests do have distinctly different HH backscatter signals, then one might expect the *terra firme* forest class to have a much wider range of values. However the range of HH values for this class is similar to the two swamp forest classes. But perhaps the lack of a difference between the HH backscatter of the *terra firme* forest and swamp classes is not

that unusual. Although Hess et al. (2003) found there to be clear differences between the L-band HH backscatter signal of *terra firme* forest, flooded forest and flooded palms in central Amazonia, they also noted that there were a number of classes which overlapped in terms of HH backscatter, including wetland and non-wetland classes. For this reason, they recommended, that whilst SAR data is useful in the mapping of wetlands, it should not be relied on solely when classifying a landscape.

Although there was no difference between the mean HH and HV backscatter, the significantly different HV/HH ratios shows that there are some differences between the backscatter signals of the three forest classes, with *terra firme* forest depolarizing the signal (i.e. it changes the orientation of the electromagnetic signal) the most and palm dominated swamp the least. The more open canopy of the palm dominated swamp could mean there is less volume scattering of the signal as it passes through the canopy compared to the other two forest classes and the presence of water on the forest floor of the two swamp classes would mean that a higher proportion of the signal is returned in a like-polarized mode compared to the *terra firme* forest class (Hess et al., 2003).

The much lower HH and HV backscatter values for both the savannah and water classes are not surprising. The smooth surface of water bodies mean that most of the signal is reflected away from the antenna via specular reflectance leading to low HH and HV values (Silva et al., 2008). The low stature of grasses means that a lot of savannah vegetation will appear transparent in L-band (Silva et al., 2008). The lack of volume scattering by the vegetation means little of the signal is reflected back towards the antenna. For both HH and HV, these two classes had a much wider range of reflectance than the three forest classes. The heterogeneity of the savannah class could be attributable to a number of things. Firstly, although the grassland vegetation should be largely undetectable at L-band, patches of higher biomass, such as areas where shrubs are present, or taller grasses will increase the proportion of signal directed back towards the antenna (Hill et al., 1999). Secondly, Menges et al. (2004) found in their study on the effects of fire on SAR backscatter in an Australian savannah, that whilst the removal of grass through burning did not affect the backscatter signal, changes in soil properties such as soil moisture content did. Therefore, the patches of burned savannah in the Cuvette Centrale could be contributing to the high variability in SAR backscatter. Finally, during the wet seasons parts of the savannah become inundated, creating a mosaic of flooded and non-flooded savannah. This should affect the backscatter signal from this class but perhaps not always in a predictable way. Depending on vegetation height and density there can either be an increase in specular backscatter or an increase in double bounce backscatter when herbaceous vegetation becomes inundated (Silva et al., 2008). Water level height also

affects which mechanism prevails. Yuan et al. (2015) looked at the relationship between PALSAR L-band backscatter and water level changes in both forested and herbaceous wetlands in the south of the ROC. For the herbaceous wetlands they found that as the area became inundated, the backscatter signal increased, which they attributed to an increase in double-bounce backscattering. But as water levels rose further the backscatter signal began to decrease. The authors proposed that this is a result of increased specular backscattering, as the vegetation becomes almost entirely submerged. With different levels of vegetation height and flood height across the savannah regions, this could be the biggest cause of the backscatter variability in this class. Similarly the presence of herbaceous vegetation along water ways has been suggested to increase backscatter from water bodies, even at L-band (Horritt et al., 2003, Mason et al., 2007). Therefore, vegetation could be contributing to some of the water class variability, particularly if there are occasionally trees lining the river banks. Likewise, surface water roughness caused by wind and rain events can increase backscatter from lakes or rivers (Mason et al., 2007).

Like the Landsat ETM+ bands, the SRTM DEM values associated with the five land cover classes were mostly as expected, with the swamp, water and savannah classes associated with low elevations and *terra firme* forest associated with higher elevations. The association of water with low elevations is largely self-explanatory. The association of savannah with low elevations is partly attributable to the fact that savannah is largely maintained by anthropogenic fire (Posner et al., 2009) and since the majority of the Cuvette Centrale's human population are concentrated along rivers, there is often a coincidence of savannah with rivers and therefore lower elevations. Additionally, operating at X and C-band, the SRTM radar signal is only able to partially pass through forest canopies (Weydahl et al., 2007, LaLonde et al., 2010). Therefore, when an area is forested the SRTM radar measures somewhere between the forest floor and the top of the canopy, whereas in savannah the SRTM radar should measure the ground. The result is that savannah regions which are adjacent to forests of the same elevation will appear to have lower elevations (LaLonde et al., 2010, Weydahl et al., 2007). This artefact of SRTM could also account for the lower elevations associated with palm dominated swamp compared to hardwood swamp. The more open, lower stature of the canopy in palm dominated swamp could lead to a perceived lower elevation in the DEM. The difference in elevation between the swamp forest classes and the *terra firme* class may be explained, in part, by the same artefact, but also by the fact that areas of low elevation in the landscape are more likely to be accumulating water and are therefore more likely to host swamp vegetation, whereas areas of higher ground, with better drainage are unlikely to be able to support swamp vegetation.

The topographical uniformity of the low lying areas of the Cuvette Centrale and the lack of any peat domes can explain the low slope angles associated with the palm dominated swamp and hardwood swamp. The much lower slope angles associated with water can be explained by the flat surface of many water bodies and rivers and the distribution of savannahs along river flood plains can account for the low slope angles associated with this class. The association of *terre firme* forest with large slope angles is almost certainly the result of *terre firme* forest occupying higher elevations where the topography is more varied.

In summary, there is no one unique characteristic, detectable from a single remote sensing dataset, which can be used to distinguish the two peatland vegetation classes from other land cover classes and each other. Instead it is a combination of characteristics, detectable only when using multiple remote sensing products, which allow the peatland vegetation classes to be delineated.

4.6.2. Estimating Peatland C stocks

The three methods used to estimate the total peatland C stock produced very similar results, with best estimates being 32.7, 31.6 and 30.2 Pg C for methods 1, 2 and 3 respectively. Method 1, which used bootstrapped means of area, bulk density, depth and C concentration, produced the largest value, near symmetrical CIs and the second largest range (8.2 Pg C difference; Table 4.5). This method does not account for dependencies between variables and this is probably the cause of the slightly higher C estimate using this method. For example, there is evidence that shallower cores tend to have a higher bulk density than deeper cores (Fig. 3.4, Chapter 3), presumed to be the result of a higher mineral content. Therefore, if bulk density measurements from shallower cores have a strong influence over the mean, using this mean in combination with mean depth derived from both shallow and deep cores, may lead to an overestimated peatland C stock.

Method 2 accounts, at least in part, for the bulk density-depth relationship by applying an exponential relationship (equation 4.4) between mean peat bulk density and core depth to estimate peat mass per depth measurement. This method produced the second highest estimate of peat C stocks, near symmetrical CIs and the smallest range (4.3 Pg C difference; Table 4.5). Parry and Charman (2013) used a similar method to estimate peatland C stocks in an upland UK blanket bog. However, the explanatory power of this relationship in my dataset was low (R-sq. adj.= 0.29) and therefore the use of this relationship leads to an unrealistic narrowing of peat bulk density variation. This, therefore, explains the lower confidence intervals of the method 2 estimate.

Method 3 has the advantage that, by making use of multiple linear regressions between bulk density and depth down core, it accounts for dependencies between peat bulk density and mineral content, but also allows for no relationship to exist (i.e. a slope value of zero). By binning the regression equations into different depth equations it also accounts for the fact that relationships between depth down core and peat bulk density are dependent on total peat depth. Therefore this prevents high bulk densities being ascribed to deep cores. Overall, it is felt that method 3 is a better reflection of spatial variations in bulk density across a peatland. However, whilst mineral content can have a strong influence on bulk density, other factors such as OM composition, degree of peat decomposition and consolidation mean that even when OM content is constant, peat bulk density can vary by more than a factor of two (Lawson et al., 2015). Neither methods 2 nor 3 account for bulk density variation attributable to these factors, but being highly spatially variable both within and between peatlands, adequately accounting this could be difficult and would certainly require a much larger dataset. Therefore one advantage of method 1 is that, by using a mean value, the variation in bulk density driven by unknown factors, is at least incorporated into the C estimates. However, the problem of not accounting for dependencies between variables, which could result in an overestimation of peatland C stocks, means that the more conservative 30.2 Pg C estimate of method 3 is preferred.

The relatively small confidence intervals for peatland total C estimates, obtained from bootstrapping, are not necessarily a reflection of the true uncertainty in the peatland C stock estimates, but instead reflect the fact that once a certain sample size is achieved, resampling of that sample will not result in large variations in the estimated mean. Uncertainty estimates obtained through bootstrapping therefore rely on the assumption that the sample is an unbiased representation of the population (Manly, 1997). However the sampling design of this study was not random and therefore cannot be said to be unbiased. Achieving a non-biased sampling design in a location such as the Cuvette Centrale is logistically difficult and unless one has access to a helicopter (e.g. Beilman et al. (2008), Mackenzie River Basin, Canada) is a problem faced by most studies of remote or expansive peatlands. While the lack of random sampling is a key limitation of this study, my work being based on extensive field data is an improvement on the guesswork of other studies attempting to estimate peat C stocks in the Cuvette Centrale (Page et al., 2011). One particular weakness is that, whilst this study used a number of ground truth points from the DRC in the classification of the remote sensing data, no peat property data was available from the DRC. The relatively small C stock CIs estimated for the 36,000 km^2 study region increase confidence in the equally small CIs for the Cuvette Centrale C stock estimates. However, obtaining data from the DRC and other, unsampled, regions in the ROC should be the focus of future studies of the Cuvette Centrale peatlands. This would

greatly improve confidence in any estimates of peatland extent and C stocks for the Cuvette Centrale, by reducing the assumption that data from a relatively small area of the Cuvette Centrale is representative of the entire region.

When considering the individual variables from which peatland C stock estimates are derived, the finding that peat depth followed by bulk density are the largest sources of uncertainty is consistent with the findings of previous studies (Parry and Charman, 2013, Buffam et al., 2010, Draper et al., 2014). With peat depth as the source of largest uncertainty, future work within the Cuvette Centrale should concentrate on obtaining as many peat depth measurements as possible from as wide an area as possible. For large peatlands, such as those found in the Cuvette Centrale, there is probably a tendency for peat depth to be underestimated as a result of a sampling bias, favouring sampling towards the peatland edge, where depths tend to be shallower. However, whilst increasing the number and distribution of peat depth measurements may increase the confidence in a peat depth estimate, it may not reduce the level of estimated uncertainty by a large amount. This is because even within a single peatland depth can vary considerably, even over distances of a just a few meters (Parry et al., 2012). If peat depth varies in a systematic way, then modelling of peatland geometry may improve confidence in estimates of peatland volume than by using a mean peat depth and area estimate (Buffam et al., 2010). The sites visited in the Cuvette Centrale showed a systematic increase in peat depth from the peatland margins towards the interior. Therefore modelling peat depth, based on a distance from peatland margin was initially considered. However, in order to do this, each unit of peatland within the landscape requires an estimate of a definitive edge. But the reality is that boundaries between classes in the peat probability map are diffuse. This reflects a reality that the transition between peatland and non-peatland can be gradual. Therefore defining a peatland edge requires some arbitrary decisions to be made (e.g. Jaenicke et al., 2008). Since many studies, especially in temperate and boreal regions, obtain peatland area and boundaries from pre-existing maps (e.g. Parry et al., 2012, Buffam et al., 2010), which they assume to be without error, assumptions made in determining peatland boundaries are seldom acknowledged or discussed (an exception being Sheng et al. (2004)). More importantly, whilst the Cuvette Centrale peatlands within the ROC appear to be occupying shallow basins, a large proportion of the peatlands on the DRC side appear to more closely follow river networks. Therefore, based on the limited information to date, it does not seem justified to model peatland depth across the Cuvette Centrale. Again this highlights the need for further sampling of peat depth, using the peatland probability map as a guide.

The main causes of variation in bulk density have been discussed above and it has been suggested that a larger data set may permit spatial variations in bulk density to be modelled more effectively than in methods 2 and 3. The finding that uncertainty attributable to peat C concentrations was so low as to be almost negligible is consistent with other studies (Draper et al., 2014, Buffam et al., 2010, Parry and Charman, 2013). In general peat C concentration does not vary considerably and will lie somewhere between 50 to 60% (Lawson et al., 2015). Dependencies between peat C concentration and other variables, such as bulk density and OM content can exist (Lawson et al., 2015). However, as the sensitivity analysis shows, trying to incorporate these correlations in peatland C stock estimates will not substantially improve estimates. However, this does not mean that measuring peat C concentrations is without merit, as slight differences do exist between peatlands and can give an interesting insight into the chemical properties of the C pool i.e. a higher C concentration suggests a higher proportion of lignin in the OM pool or the presence of black carbon (Lawson et al., 2015).

The low levels of uncertainty ascribed to area reflect the reasonably consistent output from the 1000 classifications. The true uncertainty associated with the area estimates will be larger depending on how representative the sampling is of the region. An additional source of uncertainty is the use of vegetation class to denote the presence of peat. As stated, the palm dominated swamp class incorporates *Raphia hookeri* palm dominated swamp, which although largely associated with peat, is not consistently associated with peat. To try to account for this, zero peat depth measurements under swamp vegetation were included in the peat depth dataset. However, there is no way of knowing whether the proportion of sample points under *Raphia hookeri* which were found not to have peat is characteristic of the region as a whole. Furthermore, the similar spectral properties of the two *Raphia* species, means there is no way of knowing what proportion of the palm dominated swamp the *Raphia hookeri* palm dominated swamp constitutes. Although, based on observations made in the field and reports of the typical distribution of these two palms throughout Central Africa (Hughes and Hughes, 1992; see Chapter 2, section 2.4.2.), the vast majority of the palm dominated swamp is probably *Raphia laurentii* dominated palm swamp, with *R. hookeri* palm dominated swamp being more limited in extent and confined to seasonal or old channel networks.

The estimated 30.2 Pg C (90% CI, 27.8-32.7 Pg C; method 3) stored in the peatlands of the Cuvette Central, are the first estimates for this region based on ground data and far exceed any previous combined estimates for the ROC and DRC (3 Pg C; Page et al., 2011). The discrepancies between the estimate of this study and the previous estimate is due to the past small assumed area extent (6219 km^2 vs 145,529 km^2) and lower peat bulk density

using data from South East Asia (0.05 g cm^{-3} vs 0.09 g cm^{-3}). The assumed C concentrations (56%; Page et al., 2011) , again from South East Asia, was slightly lower than the mean C concentration of this study (58.4 %), however, the difference is so small that the effect on total C stock estimates is near to insignificant. Conversely, peat depth was assumed to be greater (7.5 m in ROC; 4 m in DRC) than the mean peat depth of this study (2.24 m), owing to unverifiable reports that peat depth in the Cuvette Centrale can reach exceptional depth (e.g. 30 m; Markov et al. (1988)). The Cuvette Centrale peatlands are characterised by shallow peats of high bulk density covering an exceptionally large area. This highlights the importance of having *in situ* measurements when estimating peatland C stocks, as the extrapolation of data from one region to another may not be valid.

The DRC and ROC have estimated peatland C stocks of 20.2 Pg C and 12.2 Pg C respectively. These national tropical peatland C stocks are surpassed only by Indonesia, which has an estimated 57.4 Pg C (Page et al., 2011). In terms of regional tropical peatland C pools, the Cuvette Centrale falls in behind South East Asia, whose tropical peatlands contain an estimated 68.5 Pg C (Page et al., 2011), but is considerably larger than the estimated tropical peatland C pool for the whole of South America (estimated to be 9.7 Pg C; Page et al., 2011). The global significance of this peatland C estimate from the Cuvette Centrale is therefore clear and when incorporated into the latest estimates in Page et al. (2011), increases the African tropical peatland C stock from 6.9 to 34.1 Pg C, an increase of 394%, and increases the global tropical peatland C stock from 88.6 Pg C to 115.8 Pg C, an increase of 31%. This study highlights the possibility that current estimates of tropical peatland extent and C stocks may be substantially underestimated for a number of regions. The lack of information on African peatlands as a whole (see sections 1.3.10 to 1.3.14, Chapter 1) may mean current estimates of peatland extent and C storage for the continent could increase further as more data is obtained. Likewise, given the many sources of uncertainty discussed before, as more data is obtained from the Cuvette Centrale, the current estimates presented here may be revised up or down. Regions from which an increase in the African peatland C stock may come are the Okavango Delta, Botswana and the Sudd, South Sudan, which are some of Africa's largest wetlands, covering areas of 10,000 km^2 and 16,500 km^2 respectively (Hughes and Hughes, 1992). The Okavango Delta has long been confirmed to harbour peat deposits (McCarthy et al., 1989, Ellery et al., 1989, Cairncross et al., 1988), reaching up to at least 3 m in depth (Cairncross et al., 1988) whilst the Sudd reportedly contains peat deposits in places (IMCG, 2011). No attempts have been made to quantify belowground C stocks in these wetlands. Both wetlands being much smaller than the Cuvette Centrale, the C stocks will not be as large, but they may still be important. For example, even if just 1 or 2 Pg C are contained within these wetlands, this would not be inconsequential, especially if one considers that a

country such as the UK is estimated to have a total peatland C stock of 3 Pg C (Lindsay, 2010).

At the same time as some tropical peatland C stocks remain unaccounted for in some regions, rapid C losses from tropical peatlands are occurring, primarily in South East Asia, with an estimated 0.54 Pg C yr^{-1} lost through deforestation and drainage (Grace et al., 2014) and, in years of particularly wide spread fires, possibly as much as 2.2 Pg C lost through peat combustion (Page et al., 2002), with the 2015-16 El Niño event predicted to result in the second largest peat fire C emissions on record (Mooney, 2015). However, a paucity of measurements, mean that the true level of C losses from South East Asian peatlands is uncertain (Couwenberg et al., 2010). Possible peatland C losses from other regions of the tropics are even more uncertain. Therefore, it seems likely that there will be multiple revisions to the tropical peatland C pool as more data is acquired both from regions where research on peatlands is already established and regions which are yet unaccounted for.

4.6.3. Aboveground Peatland C Stocks

The 1.4 Pg C estimated to be stored in the AGB of the Cuvette Centrale peatlands brings the total C stock of these ecosystems to 31.6 Pg C. The more than 20-fold difference between belowground and aboveground C stocks emphasises the importance of these peatlands and the need for peatland C pools to be adequately accounted for in national C inventories. The significantly higher AGC of the hardwood swamp compared to the palm dominated swamp is partially attributable to a greater number of trees per plot in the hardwood swamp. However, these differences are exacerbated by the exclusion of *Raphia laurentii* and juvenile *R. hookeri* from the AGB estimations, as they do not meet the 10 cm diameter at breast height (1.3 m) criteria, leading to a lower AGC estimate for the palm dominated swamp. In areas where *Raphia laurentii* dominate, these palms are likely to be the largest source of OM input to the peatlands. Therefore future work should attempt to quantify the AGB of *Raphia laurentii* stands.

Compared to an estimate of AGC for Central African tropical forests (202 Mg C ha^{-1}), derived from the mean AGB for Central African tropical forest (430 Mg ha-1; Lewis et al., 2013), the mean AGC of the *terra firme* plots in my study is surprisingly low. This could be due to the inclusion of seasonally flooded forest within this class, which has previously been noted for its lower stand density compared to *terra firme* forest (Lebrun (1936a) cited in Richards (1952)). When the two classes are separated the mean AGB of the *terra firme* only increases marginally from 106 to 122 Mg C ha^{-1}. The swamp AGC estimates are also lower than estimates of swamp AGC (151 Mg C ha^{-1}) derived from AGB estimates for the region (322 t ha-1; Lewis et al., 2013). The AGB estimates of Lewis et al. (2013) are all

derived from forest plots of 0.2 ha or bigger. Therefore it is possible that the small plot size used in this study has led to an underestimation of AGC across all classes and aboveground C stocks of the peatlands. In conclusion, the 1.4 Pg C stored in the peatlands AGB is likely to be a conservative estimate.

4.7. Conclusions

To quantify peatland extent within the Cuvette Centrale a method was devised whereby ground data were used to run maximum likelihood classifications of eight remote sensing products, including optical, radar and elevation data. Following 1000 reruns of the classification, the resulting peatland probability map shows the Cuvette Centrale, with 145,529 km^2 of peat, to be the most extensive tropical peatland complex in the world. Both the DRC and ROC, therefore rank within the top ten countries in the world in terms of peatland extent. Combining these area estimates with *in situ* measurements of bulk density, carbon concentration and peat depth give a total peatland C stock for the Cuvette Centrale of 30.2 Pg C, with approximately 20.2 Pg C being found within the DRC and 12.2 Pg C in the ROC. When aboveground C stocks are included the total C stock for the peatland ecosystem increases to 31.6 Pg C. The peatland C estimate greatly surpasses previous estimates of the tropical peatland C pool for the region, based on a series of assumptions and no *in situ* data, of 3.0 Pg C (Page et al., 2011). At a country level, the DRC and ROC tropical peatland C stocks are exceeded only by those of Indonesia (57.4 Pg C; Page et al., 2011). The new Cuvette Centrale peatland C stocks increase global tropical peatland C stocks from 88.6 Pg C (Page et al., 2011) to 115.8 Pg C. Therefore, the peatlands of the Cuvette Centrale are of global importance. While this is the first field-based estimate of peatland extent and C stocks, using 228 GPS ground truth points, 225 peat depth, 372 bulk density and 213 C concentration measurements of peat over an area of ca. 36,000 km^2, the vastness of the Cuvette Centrale means that the estimates here should be considered as a first estimate requiring further refinement in the future via explorations of other regions within the Cuvette Centrale, guided by the peatland probability map.

Chapter 5: Peatland Initiation and Development in the Central Congo Basin

5.1. Abstract

The Cuvette Centrale, Congo Basin, contains the largest extent of tropical peatland in the world. They are estimated to store 30.2 Pg C, making them a globally significant C pool. Understanding the historical development of these peatlands is fundamental to being able to identify future threats to the persistence of this C pool. Here radiocarbon dates and humification analysis of peat samples were used to determine the timing of peat initiation and peat accumulation through time across seven sites in the Likouala Department, ROC, Cuvette Centrale. Basal peat radiocarbon dates ranged from 10555 to 7175 cal yrs BP, indicating peat initiation began in the early Holocene at most of the seven sites. The onset of wetter climatic conditions at the start of the African Humid Period (AHP) is considered the most likely cause of peat initiation in the Cuvette Centrale. Age-depth models suggest that a hiatus in peat accumulation occurred sometime between ca. 7000 and 2000 cal yrs BP, which the humification analysis suggests was associated with higher peat decomposition rates. Although the timing of this event is not well constrained, it is tentatively ascribed to the AHP termination. Following this hiatus peatland accumulation rates resumed, suggesting that over the last ~2 millennia, the Cuvette Centrale peatlands have acted as a C sink. The early Holocene date of peat initiation and the modest depths (mean depth of 2.24±1.61 m) of the Cuvette Centrale peatlands, contrast with the deeper South East Asian peatlands of a similar age and the lowland Amazonian peatlands of similar depth but of younger, Late Holocene ages. This highlights the heterogeneity of peatland development across the tropics. Such heterogeneity is most likely a result of differences in precipitation, topography and the frequency of disturbance events.

5.2. Introduction

The Cuvette Centrale, Congo Basin, is one of the world's largest tropical wetlands (Keddy et al., 2009). Historically overlooked, it is now known to harbour the largest extent of tropical peatland, estimated to store ca. 30.2 Pg C, meaning these peatlands are a globally significant belowground C pool. Central Africa is second only to South East Asia in terms of tropical peatland C stocks (Page et al., 2011). Knowing how and when the peatlands of the Cuvette Centrale formed is important for identifying potential threats to this ecosystem and for implementing good land management practices. With this knowledge in place it may be possible to avoid poor land management choices often seen in South East Asia, leading to dramatically declining C stocks in that part of the world (Hooijer et al., 2010).

Peatland initiation can occur through three processes; terrestrialisation, paludification and primary mire formation (Ruppel et al., 2013, Charman, 2002). Terrestrialisation is when a water body becomes gradually infilled by OM (Ruppel et al., 2013, Charman, 2002), whereas paludification and primary mire formation is when OM accumulation occurs in a terrestrial environment. More specifically, paludification is the accumulation of OM following a change in environmental conditions which results in a terrestrial environment becoming waterlogged (Ruppel et al., 2013, Charman, 2002). Primary mire formation occurs when OM accumulates on a newly exposed wet mineral soil (Ruppel et al., 2013). The latter process is most commonly found along uplifting coastal regions and glacial landscapes (Ruppel et al., 2013) and is therefore unlikely to be of importance in the Cuvette Centrale. Although not specifically relating to the initiation of peatlands, the term "lateral expansion" is important when considering peatland formation. Lateral expansion is the lateral spread of peatlands once initiation has begun. It is permitted through the alteration of water tables in areas adjacent to the peatlands, normally from increased runoff from the peatlands themselves, causing these areas to become waterlogged (Charman, 2002, Ruppel et al., 2013). Lateral expansion can follow on from any of the three peatland initiation processes.

Based on studies elsewhere, the factor(s) leading to peat initiation in the Cuvette Centrale likely relate to changes in geomorphology and/or climate. The origin and geological history of the Cuvette Centrale is not well understood (Buiter et al., 2012, Kadima et al., 2011). Being located within an intracratonic basin by definition implies an unknown origin but also a degree of seismic inertia (Buiter et al., 2012). Despite this, a series of north-east, south-west trending faults and horsts have been identified in the Cuvette Centrale, against what is otherwise a landscape with very little topographic variation (Master, 2010). It has been proposed that these faults and horst are the cause of the unusually straight courses which the rivers take through this landscape and are also possibly the cause of a number of lakes with remarkably shallow geometries in the region by acting as a slight damn behind which water can pool (Master, 2010)(see Chapter 1, section 1.3.2. for a fuller discussion). Therefore theoretically these faults and horsts may have provided the prerequisites for peat accumulation by impeding drainage within the landscape.

Since the Last Glacial Maximum (LGM) Central Africa has experienced two phases of increased humidity. Firstly during the glacial-interglacial transition (~15 to 12 k yrs BP) when the cool and dry conditions of the LGM (Maley and Brenac, 1998, Bonnefille and Chalie, 2000, Elenga et al., 1994, Kiage and Liu, 2006) gave way to warmer and wetter conditions (Burrough and Thomas, 2013, Shanahan et al., 2015, Kiage and Liu, 2006,

Bonnefille and Chalie, 2000). This new climatic phase was on a continental scale and is referred to as the African Humid Period (AHP). The termination of the AHP, marked by aridification across Africa, began around 5500 yrs BP, but had a latitudinally staggered onset, with regions below 15° N not experiencing reductions in precipitation until as late as 2500-4000 yrs BP (Shanahan et al., 2015). In Central Africa some palynological records in lake and swamp sediments suggest that by ca. 2000 yrs BP wetter conditions were re-established within the region (Maley and Brenac, 1998). However, studies indicate that forests, which contracted during the AHP termination, were still expanding until ca. 950 to 490 yrs BP (Ngomanda et al., 2005, Elenga et al., 1996, Vincens et al., 1999, Elenga et al., 1994), suggesting a later onset of wetter conditions. Therefore either the onset of the AHP or the more recent change in precipitation could have contributed to peat initiation within the Cuvette Centrale.

Radiocarbon dating of the peat profile offers a way of determining when and how peat initiated and how the peatland has developed since initiation (Charman, 2002). The approximate timing of peat initiation can be obtained through basal peat radiocarbon dates, which can then be interpreted in light of other dated events or chronological environmental records. If multiple basal dates are available, inferences can be made from the spatial pattern of dates as to the process of peat formation (Charman, 2002). For example if basal dates become progressively younger from the interior of the peatland to the margins, this suggests either paludification or lateral expansion (Charman, 2002). Radiocarbon dates down profile provide insight into peat development through the estimation of peat accumulation, with changes in accumulation rates indicative of a change in environmental conditions, primarily hydrology, leading to either increased accumulation or increased decomposition (Korhola et al., 1995). If dated at a high enough resolution timings of changes in accumulation rates can be reasonably well constrained. Additionally down profile humification analysis can provide a proxy chronology of peatland surface hydrology, with more humified peat indicating drier surface conditions (Roos-Barraclough et al., 2004).

In this chapter I present the results of radiocarbon dating of basal peats, which I use to determine the timing and possible causes of peat initiation in the Cuvette Centrale. Radiocarbon dating and humification analysis of down core peat samples are also presented and used to establish how peat accumulation within the Cuvette Centrale may have varied through time.

5.3. Aims

The aims of this chapter are firstly to determine the timing of peat initiation in the Cuvette Centrale and secondly to identify the main factors which drove peat initiation. The

objectives are to use radiocarbon dating of basal peats to determine the timing of peat initiation and then to identify possible causes of peat initiation which would coincide with these dates. Thirdly the aim is to determine whether peat accumulation has been constant through time. The objective is to use down core radiocarbon dating to construct age depth models of the peat profile to construct a picture of peat accumulation through time.

5.4. Methods

5.4.1. Site Description

The data presented in this chapter comes from seven field sites visited in the Likouala Department, Republic of Congo (ROC); Bondoko, Bondzale, Ekolongouma, Ekondzo, Itanga, Mbala and Makodi. For the field sites locations see Fig. 2.1 (Chapter 2) and for their full descriptions see Table 2.5 (Chapter 2) and Appendix 1-8.

5.4.2. Radiocarbon Dating and Age Models

Nine basal dates were selected for radiocarbon accelerator mass spectrometry (AMS) to date peat initiation and to estimate long-term peat and carbon accumulation rates. Three of these samples were basal dates from the same site (Ekolongouma; 4 km, 7 km and 9km cores) to assess any spatial gradients in age, or alternatively whether peat initiation commenced simultaneously across a wide area. It should be noted that at the 9 km sample point the last ~25 cm of the core could not be recovered and that the sample selected for dating was the deepest sample recovered. The remaining six samples came from the deepest core from each of the following sites: Bondzale, Bondoki, Ekondzo, Itanga, Makodi and Mbala (samples from the Centre had not been collected at the time of radiocarbon dating). An additional 13 AMS dates were obtained for down core peat samples for the three Ekolongouma cores (4 km: n=2; 7 km: n=2; 9 km: n=9), which were used for calculating age depth models of peat accumulation through time. For radiocarbon AMS dating bulk peat samples sieved at 200μm to remove any fine roots, which would give a younger radiocarbon age than the peat matrix, were used. Whilst it is preferable to date material that is unlikely to have migrated up or down the peat profile (e.g. macrofossils, seeds, wood fragments), the peat was too humified for this to be possible. The bulk peat samples were then sent to the NERC Radiocarbon Facility, East Kilbride. There samples were pretreated by digesting in 1M HCl at 80°C for 8 hours and then washed free from mineral acid with deionised water before being digested in 0.5M KOH at 80°C for 2 hours. The digestion was repeated using deionised water until no further humics were extracted. The residue was then rinsed free of alkali and digested in 1M HCl at 80°C for 2 hours before being rinsed free of acid, dried and homogenised. The total carbon in a known mass of the pre-treated sample was recovered as CO_2 by heating with CuO in a sealed quartz

tube. The gas was then converted to graphite by Fe/Zn reduction, which was then dated by AMS using a 5 MV and 250kV National Electrostatic Corporation AMS system.

Radiocarbon age calibration and age depth models (linear interpolation) were conducted using the R package clam (version 2.2) (Blaauw, 2010) and its default calibration curve, INTCAL13 (Reimer et al., 2013).

The long-term rates of carbon accumulation (LORCA) were calculated by the following equation (taken from Korhola et al. (1995)):

$$L = A * C \quad [5.1]$$

Where L is the LORCA (g C m^2 yr^{-1}), A is the dry mass accumulation (g m^2 yr^{-1}) and C is the carbon concentration expressed as a fraction. For C the mean C concentration of the peat core was used. The 7 km Ekolongouma core lacked sufficient C concentration measurements, so the mean of all C concentration measurements for the Ekolongouma site was used. Dry mass accumulation (A; g m^2 yr^{-1}) was calculated with the following equation:

$$A = r * \rho * 1000 \quad [5.2]$$

Where r is the net rate of height accumulation (mm yr^{-1}) of the peat i.e. the accumulation rate and ρ is the peat bulk density (g cm^{-3}). For ρ the mean bulk density of the peat core was used. Values for r were calculated using the following equation:

$$r = \frac{h}{t} \quad [5.3]$$

Where h is the height of accumulated peat (mm) i.e. the peat thickness and t is the time of accumulation (years). Values for t were calculated with the following equation:

$$t = y_1 - y_2 \quad [5.4]$$

Where $y_1$is the age of the base of the peat profile (calibrated years Before Present (cal yrs BP)) and y_2 is the age of the peat surface (cal yrs BP). y_1 was taken to be the median of the age range of highest posterior probability for the basal sample and y_2 was taken to be the year of sample collection.

5.4.3. Peat Humification Analysis

Humification analysis was carried out on the three Ekolongouma cores for which radiocarbon dates were obtained. It was thought that humification analysis, a proxy for surface wetness, would help with the interpretation of age depth models for these three cores. For example, if low accumulation rates coincided with more humified peat, it would imply that the low accumulation rates were a result of an increase in decomposition and therefore drier conditions.

The down core sampling resolution for humification analysis was every 10 cm for the full peat core. Samples were already pre-dried (40°C) and ground to 100 µm using a MM301 mixer mill. Approximately 0.02 g of each sample was put into solution with 10 ml of NaOH (8%), shaken, then placed in a water bath at 95°C for an hour. Samples were then topped up to 20 ml with deionised water, shaken, left to stand for an hour then shaken again before being filtered through a Whatman no. 1 filter paper. Samples were then diluted at 1:1 ratio with deionised water. Colorimetric analyses of the samples were carried out using a spectrophotometer (manufacturer: Hach, Loveland, Colorado, U.S.A, model: DR/2010) at a wavelength of 550 nm. For each sample three readings of absorbance were taken. The average of the three readings is reported in the results section.

5.5. Results

5.5.1. Radiocarbon Dates

Five of the nine basal peat samples submitted for dating returned early Holocene ages, with median age estimates ranging from 10555 to 8545 calibrated years Before Present (before AD 1950; cal yrs BP) and three returned mid-Holocene ages, with median age estimates ranging from 8165 to 7175 cal yrs BP (early Holocene and mid-Holocene are defined as the periods 11700 to 8200 yrs BP and 8200 to 4200 yrs BP, sensu Walker et al. (2014)). The Ekondzo core returned a late Holocene date (defined as the period 4200 yrs BP to present, sensu Walker et al. (2014)) of 2110 cal yrs BP (Table 5.1).

Table 5.1. AMS Radiocarbon results for the 9 peat samples sent for analysis. Only the calibrated age ranges with the highest posterior probability are presented.

Site	Distance Along Transect (km)	Depth (m)	^{14}C Age	Error (1σ)	Calibrated Age (cal yrs BP) (2σ) Median	Range
Bondoki	6	1.40-1.50	7352	38	8165	8033-8216 8242-8253 8256-8304
Bondzale	6	1.60-1.70	6817	39	7648	7585-7708
Ekolongouma	4	1.47-1.50	8484	41	9499	9450-9537
Ekolongouma	7	2.37-2.40	9091	39	10239	10190-10297 10329-10340 10355-10372
Ekolongouma	9†	2.70-2.73	9340	41	10555	10428-10465 10481-10679
Ekondzo	5	2.10-2.20	2147	35	2139	2005-2027 2036-2183 2199-2203 2234-2305
Itanga	6	1.90-2.00	8575	46	9539	9481-9629 9649-9651
Makodi	*	1.17-1.20	6239	39	7175	7017-7125 7149-7257
Mbala	6	2.40-2.50	7765	38	8545	8446-8604

†Last ~25 cm of peat profile could not be recovered. This is the deepest sample recovered.
*The deepest core at Makodi was selected for radiocarbon dating, which was a core taken adjacent to the transect rather than along the transect.

The AMS radiocarbon dates from the base, midsection and upper parts of the three Ekolongouma cores and the resulting age-depth models showed an early rapid period of peat accumulation (~7000 to 10,000 cal yrs BP), a slower period, with the possibility of a hiatus in peat accumulation (~2000 to 7000 cal yrs BP) and then a recent period of rapid peat accumulation (since ~2000 cal yrs BP; Table 5.2; Fig. 5.1). With only three dates for two of the cores, periods of increased and decreased peat accumulation rates are poorly constrained. The additional AMS radiocarbon dates for the deepest Ekolongouma core failed to further constrain these periods because a number of the dates were inverted. This may indicate a hiatus or period of slow accumulation or the results are caused by a disturbance to the peat profile at a later date.

Table 5.2. AMS Radiocarbon results for the mid-core peat samples from the three Ekolongouma cores.

Distance Along Transect (km)	Depth (cm)	^{14}C Age	Error (1σ)	Calibrated Age Ranges (cal yrs BP) (2σ)	
				Median	Range
4	0.57-0.60	2649	37	**2766**	2739-2808 2814-2844
	1.07-1.10	7652	42	8443	8389-8524 8527-8538
	1.47-1.50	8484	41	9499	9450-9537
7	0.57-0.60	2547	37	2630	2493-2599 2609-2639 2680-2752
	1.17-1.20	7600	38	8400	8348-8453
	2.37-2.40	9091	39	10239	10190-10297 10329-10340 10355-10372
9	0.57-0.60	1571	35	1466	1389-1539
	0.67-0.70	1754	38	1662	1562-1740 1756-1781 1798-1806
	0.77-0.80	1720	35	1627	1556-1707
	0.87-0.90	702	36	663	561-595 635-694
	0.97-1.00	4811	37	5520	5470-5561 5567-5606
	1.27-1.30	4251	37	4833	4649-4672 4699-4759 4807-4870
	1.67-1.70	6354	39	7289	7176-7218 7239-7337 7352-7416
	1.97-2.00	7662	39	8450	8398-8539
	2.37-2.40	7993	40	8870	8663-8666 8716-9007
	2.70-2.73	9340	41	10555	10428-10465 10481-10679

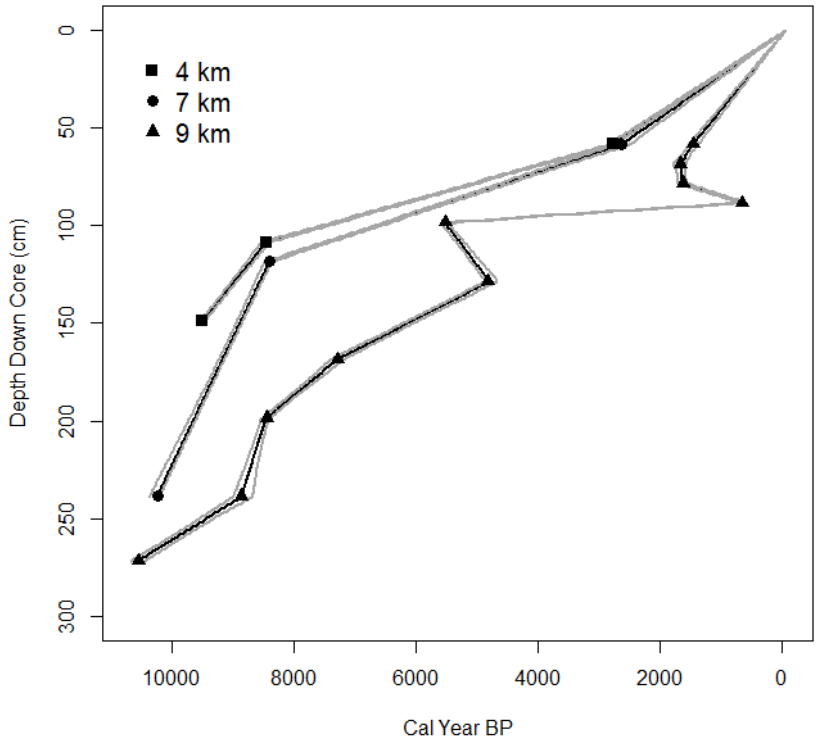

Figure 5.1. Linear age-depth models for the Ekolongouma cores at 4 km 7 km and 9km created using the AMS radiocarbon dates presented in Table 5.2. The black line represents the age depth model, the grey shading represents the 95% confidence intervals, and the black symbols represent the median of the calibrated age range for the dated samples.

Peat accumulation rates ranged from 0.16 to 0.29 mm yr^{-1} and 0.16 to 0.21 mm yr^{-1} for the peat cores with early Holocene and mid-Holocene basal dates respectively. For the Ekondzo core, with a late Holocene basal date, the estimated peat accumulation rate was much higher at 0.99 mm yr^{-1}. The apparent long-term rate of carbon accumulation (LORCA) for the early Holocene peat cores ranged from 19.95 to 33.10 g C m^2 yr^{-1} and for the mid-Holocene peat ranged from 18.40 to 32.88 g C m^2 yr^{-1}. For the Ekondzo core the LORCA was 69.37 g C m^2 yr^{-1}.

Table 5.3. Average peat accumulation rates and LORCA for each core with a radiocarbon dated basal sample. The additional mid-core dates available for the Ekolongouma cores were not used in the calculation of accumulation rates or LORCA. Therefore each value represents the overall average rate for that core.

Site	Distance Along Transect (km)	Depth (m)	Time Period (cal yrs BP)	Accumulation Rate (mm yr^{-1})	LORCA (g C m^2 yr^{-1})
Bondoki	6	1.40-1.50	8125 to -63	0.18	18.40
Bondzale	6	1.60-1.70	7647 to -63	0.21	32.88
Ekolongouma	4	1.47-1.50	9494 to -62	0.16	19.95
Ekolongouma	7	2.37-2.40	10244 to -62	0.23	22.89
Ekolongouma	9	2.70-2.73	10580 to -62	0.26	20.40
Ekondzo	5	2.10-2.20	2110 to -63	0.99	69.37
Itanga	6	1.90-2.00	9555 to -63	0.20	22.96
Makodi	-	1.17-1.20	7203 to -63	0.16	20.89
Mbala	6	2.40-2.50	8525 to -63	0.29	33.10

To test whether different peat depths across the study region are a product of differences in accumulation rates or differences in time since peat initiation, linear regression was used to look for relationships between basal sample depth and basal median age estimate and peat accumulation rates. The median age estimates for the basal samples showed a significant ($p=0.04$) positive relationship with sample depth (Fig. 5.2) and an even stronger significant ($p=0.002$) positive relationship was found between peat accumulation rates and the basal sample depth (Fig. 5.3). Linear regression was also used to test whether the LORCA across the study region are mainly a product of peat accumulation rates, but no significant relationship was found ($p=0.15$).

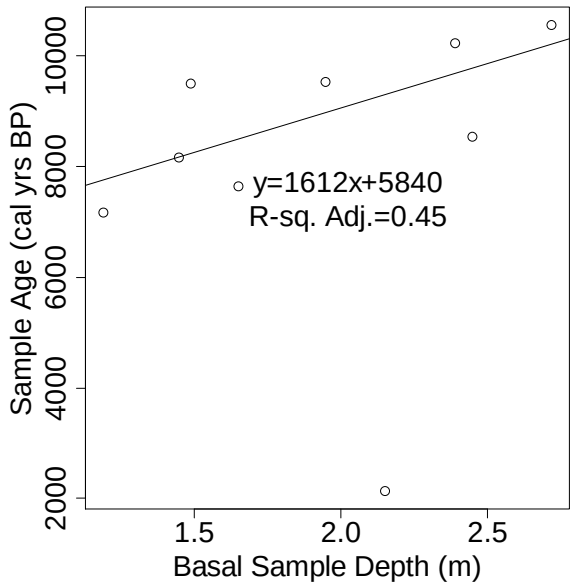

Figure 5.2. Basal peat median age estimates plotted against basal peat sample depth. The line equation and R-sq adjusted value from a linear regression are shown. The Ekondzo sample was excluded from the analysis.

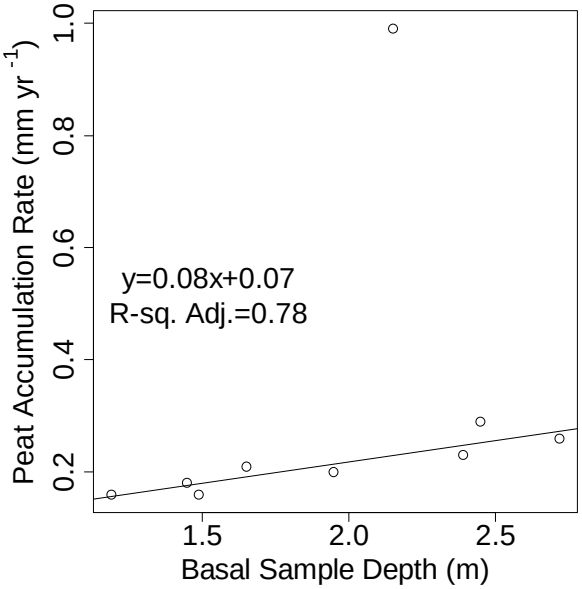

Figure 5.3. Peat accumulation rates plotted against basal peat sample depth. The line equation and R-sq adjusted value from a linear regression are shown. The Ekondzo sample was excluded from the analysis.

5.5.2. Humification Analysis

Of the three Ekolongouma cores for which humification analysis was carried out, the 4 km and 9 km cores, showed similar down core patterns in the degree of peat humification. Initially there are only small fluctuations in absorbance from the surface downwards, before an abrupt change mid-core to higher absorbance values, reflecting much more humified peat (Fig. 5.4). For both cores these higher absorbance values occur over ca. 60 cm section of the core. Further down the cores absorbance values decrease again. In the 7

km Ekolongouma core values are much more variable and there are no distinctive, sudden changes in absorbance, as seen in the other two cores.

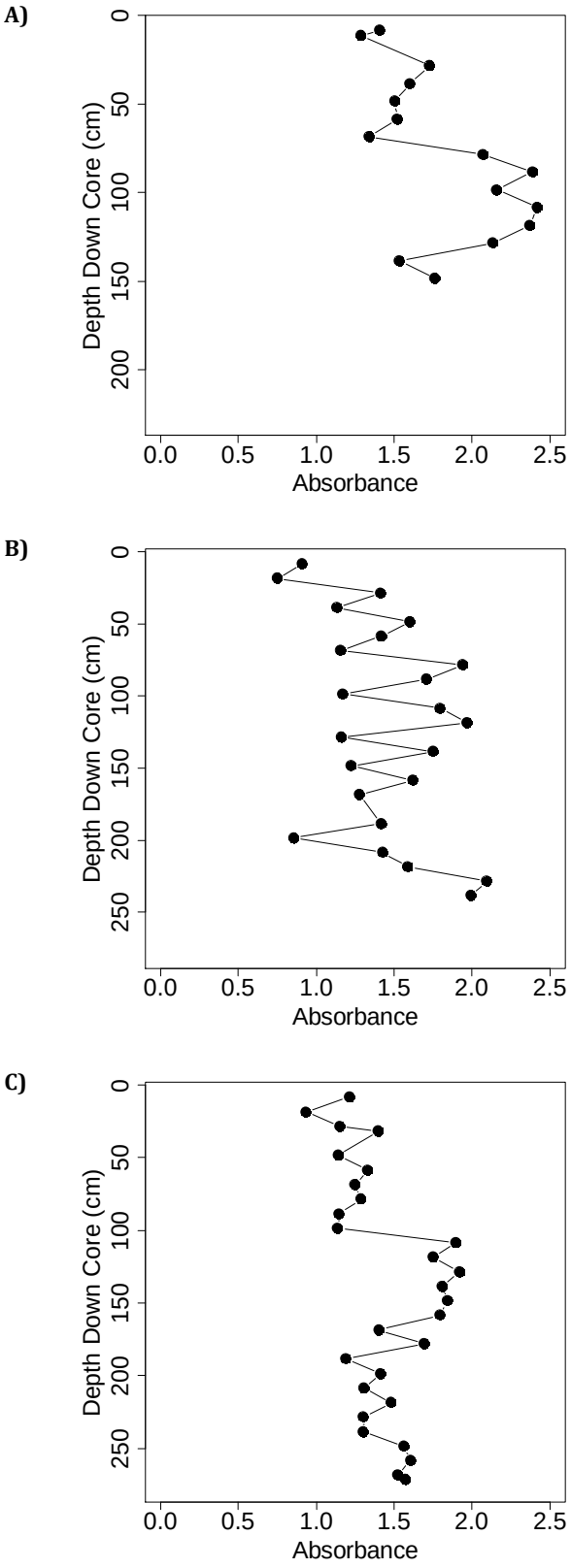

Figure 5.4. Down core absorbance recorded by spectrophotometer for the Ekolongouma cores at A) 4 km B) 7 km C) 9 km. Higher absorbance values represent higher degrees of humification.

5.6. Discussion

5.6.1. Peatland Initiation

The early Holocene and very beginning of the mid-Holocene basal ages across all sites, with the exception of Ekondzo, discussed in section 5.6.4, suggests that a change in regional environmental factors led to the onset of peat formation in the Cuvette Centrale, as opposed to more site-specific factors. The most parsimonious interpretation is that, given the timing of peat initiation, the onset of peat formation in the Cuvette Centrale was a result of a change to wetter climatic conditions during the AHP. Whilst the eight basal dates span a period of ca. 3400 years, this does not negate climate induced peat initiation. Boreal peatlands whose initiation is also linked to climatic change at the onset of the Holocene, show similar or larger spreads in basal dates (Weckstrom et al., 2010, Makila and Moisanen, 2007). Therefore the spread of peatlands by paludification or lateral expansion can take thousands of years. According to Elenga et al. (1994), swamp forest re-expansion in the south of the ROC, Plateaux Batéké, began around 13,000 cal yrs BP. The oldest basal date from this study was 10,555 cal yrs BP from the deepest Ekolongouma core, but as previously stated, the lowest 25 cm of organic material could not be recovered and so the true date of peat initiation at this point will be somewhat earlier. As an approximate estimate, obtained using the average peat accumulation rate for this core (0.26 mm yr^{-1}), peat initiation could be ca. 960 years earlier than the dated sample. However the date of peat initiation across the region is probably older still. As shown, deeper peats in the Cuvette Centrale tend to have older basal dates (Fig. 5.2) and peat depth is greater towards the centre of the peatland (Chapter 2), which has not yet been radiocarbon dated. Therefore the timing of Cuvette Centrale peat initiation may be more in line with the timing of southern ROC swamp forest re-expansion than the data initially suggests.

Determining the exact process of peatland formation is difficult with relatively few basal dates and with only one site, Ekolongouma, having multiple basal dates. Primary mire formation can be ruled out for this region as there is no volcanic activity or tectonic uplift to create new terrestrial surfaces. This leaves terrestrialisation and paludification as the two possible mechanisms. The Cuvette Centrale peatlands have been shown to occupy extensive shallow basins (Chapter 2). It could be that these peatlands formed through the terrestrialisation of water bodies occupying these basins or that these basins were terrestrial environments which became waterlogged permitting paludification. If terrestrialisation was the mechanism then the three basal dates from Ekolongouma which are progressively younger towards the swamp edge, could be the result of lateral expansion of the peatland following terrestrialisation. However, across all the peat cores

there were no unambiguous lake sediments at the base of the cores, which would be expected if terrestrialisation had occurred. Secondly, peat initiation occurred at a time when the regional climate became wetter and lake levels across Africa were rising (Cole et al., 2009, Junginger and Trauth, 2013, Junginger et al., 2014). Terrestrialisation tends to be more common when conditions become drier, leading to a drop in lake levels, which allows aquatic vegetation to encroach further into the lake creating a supply of OM inputs (Ruppel et al., 2013). Therefore terrestrialisation does not seem likely. The spatial gradient in the Ekolongouma basal dates and the timing of peat initiation would fit with a paludification scenario. It is unknown how old the interfluvial basins which the peatlands occupy are, or whether they were ever aquatic environments. However I suggest that prior to the Holocene they were terrestrial environments which, with the onset of wetter conditions at the start of the AHP became waterlogged owing to their lack of drainage, which led to peat initiation. Under this scenario, the deeper peats towards the centre of the basins would be older because water would first accumulate at the lowest point in the basin, which was found to be the case (Fig. 5.2).

5.6.2. Peat Accumulation Through Time

The peat accumulation rates across all sites (again excepting Ekondzo) are generally lower than typically found across the tropics (Sorensen, 1993, Lähteenoja et al., 2009b). This could be a result of constantly low accumulation rates or periods of faster accumulation interspersed with periods of zero or even negative accumulation. The Ekolongouma age-depth models suggest that a hiatus in peat accumulation has occurred, sometime after 7000 cal yrs BP and before 2000 cal yrs BP, after which peat accumulation has resumed. However, the inverted dates of the 9 km Ekolongouma core means there is some ambiguity surrounding the idea of a hiatus, which is discussed in section 5.6.3. A period of increased aridity around 3000 yrs BP in Central Africa is documented in a number of palaeo records (Maley and Brenac, 1998, Elenga et al., 1994, Elenga et al., 2001, Ngomanda et al., 2009, Hubau et al., 2015). Termed the “third millennium BP rainforest crisis”, this period is now thought to be part of the latitudinally staggered termination of the AHP (Shanahan et al., 2015, de Menocal, 2015), documented in a number of palaeorecords across Africa (Amaral et al., 2013, Costa et al., 2014, Junginger and Trauth, 2013, Junginger et al., 2014). A reconstruction of regional climate over the last 3000 years from dust deposits in a lake sedimentary sequence, located north-west of this study region, in the Nouabalé-Ndoki National Park, suggests that following this period of increased aridity, regional humidity increased again around 2000 yrs BP in the north of the ROC (Brncic et al., 2007). The humification analysis data suggest that the hiatus in peat accumulation was associated with increased decomposition of the peat. This could be consistent with drying and oxidation of the peat, leading to a net loss of OM. The lower degree of humification in

the top section of the peat cores indicate a decrease in peat decomposition and imply an increase in surface wetness. Therefore a plausible scenario is that peat accumulation, which commenced with the onset of the AHP, was interrupted by the AHP termination, with the peatlands possibly even experiencing a period of decomposition. When wetter conditions resumed ca. 2000 yrs BP, peat accumulation was able to continue. However, with the timing of the hiatus poorly constrained by two of the age-depth models and one age-depth model having date inversion, more radiocarbon dates are needed to be confident in this scenario. Whilst there are no radiocarbon dates for the top 50 cm of the peat cores, the resumption of peat accumulation from ~2000 cal yrs BP indicates that the Cuvette Centrale peatlands have over the past 2 millennia acted as a C sink.

The higher average accumulation rates of the deeper cores could be explained by the fact that deeper peats are found towards the centre of the basins; being lower than the peatland margins, during drier periods water tables in the centre of the basin will be maintained for longer than at the peatland margins. This means that the peatland margins are exposed to oxic conditions for longer leading to lower accumulation rates. The lack of a relationship between peat accumulation rates and LORCA can probably be attributed to differences in peat bulk density and C concentration between sites (Chapter 3).

5.6.3. Radiocarbon Date Inversions

The inversions in chronology of the Ekolongouma 9 km core, occurring between 67 cm and 130 cm, could have been caused either by contamination of the samples either during fieldwork or in the laboratory, or by material with either a younger or older ^{14}C age entering the peat profile. Whilst it cannot be completely ruled out, efforts were made to reduce contamination during field or lab work. Given that the inverted dates are spread over different drives of the corer and different sample batches for radiocarbon dating, which contained samples which did not return unusual dates, it seems unlikely that this is the cause. Therefore the latter explanation is preferred. Given that these peatlands are forested, they are not simply accumulating OM from the surface, but will be receiving younger OM inputs from tree roots at various points in the profile, leading to a younger bulk sample age (Wüst et al., 2008, Walker, 2005). The younger age of sample 87-90 cm is most probably due to the bulk sample containing younger root material. The inversion between sample 97-100 cm and 127-130 cm is possibly owing to contamination by older OM. There is evidence to suggest that Ekolongouma has experienced periodic flood events (see Chapter 6, section 6.6.11). From photos taken of the cores in the field, what appear to be traces of mineral material at ~97-100cm, as well as other points in the peat profile can be seen (Fig. 5.5). Therefore the inversion at this point could be due to older OM having been washed into the peat profile. However with a measured OM content of 97% (see

Chapter 2 section 2.2.4.2. for methods) and with no significant peak in cation concentrations at this point (see Fig. 6.19, Chapter 6) if there was a flood event, not a lot of material was brought into the peatland. Alternatively it could be down to a disturbance in the peat profile either at the time of deposition or subsequently. As for the overlap of ages between samples 67-70 cm and 77-80 cm, this can be attributed to a slight plateau in the calibration curve resulting in overlapping age ranges for these two samples (Table 5.2).

Whilst the radiocarbon date inversions mean there is some ambiguity surrounding the hiatus hypothesis, it could also be seen as evidence for a hiatus. In a study comparing radiocarbon dates obtained from different OM fractions of a Central Kalimantan peat core, Wüst et al. (2008) found that discrepancies in radiocarbon dates were greatest for samples which had come from a section of the core which had experienced very low or negative peat accumulation rates. They suggested that low or negative accumulation rates allow a greater degree of mixing of older material with younger material and a greater degree of disturbance of the surface OM layers, as they reside at the surface for longer.

Figure 5.5. A section of the Ekolongouma 9 km core. The red box highlights points in the profile where mineral intrusions can be seen.

5.6.4. Peat Initiation and Accumulation at Ekondzo

The markedly younger basal age of the Ekondzo site compared with the other sites is unexpected, but could be possible. If the age depth models from Ekolongouma can be trusted, then peat initiation at Ekondzo (2036-2183 Cal yrs BP) took place at approximately the same time that peat accumulation rates *increased* at Ekolongouma, thus coinciding with the recommencing of humid condition in the region (Brncic et al., 2007). Peat initiation at Ekondzo could therefore be linked to the onset of humid conditions in the late Holocene, but this explanation does not account for two things. Firstly, why peat did not initiate at Ekondzo in the early Holocene? It could be that peat did initiate in the early Holocene, but then was completely desiccated during the "3rd millennium BP rainforest crisis", but this would imply much higher rates of decomposition at Ekondzo than at any other site. The second problem with a peat initiation date of 2036-2183 Cal yrs BP, is the inferred rate of peat accumulation. Whilst the average accumulation rate for the Ekondzo core of 0.99 mm yr^{-1} is by no means high for a tropical peatland, it is difficult to explain why peat accumulated so much faster at Ekondzo than the other sites studied here, where

average accumulation rates range from 0.16 to 0.29 mm yr^{-1}. Therefore the most parsimonious explanation is that the Ekondzo basal sample has been contaminated by younger material and does not reflect the true age of the material. However basal dates from the other Ekondzo cores would help confirm (or refute) this.

5.6.5. Distinctions in Lowland Peatland Formation Across the Tropics

Peat depth is the combined product of rate of peat accumulation and the time since peat initiation. When compared to the other two main regions of lowland tropical peatland occurrence, the peat depths of the Cuvette Centrale are shallower (mean of 2.24 m) than those of South East Asia (with means of ca. 8 m reported for some sites; Page et al. (1999)), but of similar depth to lowland Amazonian peatlands (with reported mean depths ranging from1.7 to 3.2 m; Householder et al. (2012); Table 2.8, Chapter 2). When basal ages of the three regions are compared, the South East Asian inland peatlands tend to be either early or mid-Holocene age (Dommain et al., 2011), similar to the Cuvette Centrale peatlands, or occasionally older, dating back to the late Pleistocene (Anshari et al., 2001, Wüst et al., 2008, Page et al., 2004). Lowland Amazonian peatlands, on the other hand, tend to be much younger, dating to the late Holocene (Roucoux et al., 2013, Lähteenoja et al., 2009b). These different combinations of depth and date of peatland initiation indicate distinct modes of peatland formation across the tropics. In South East Asia, high rainfall has permitted high accumulation rates and the formation of domed systems. Although fluctuations in moisture levels and base level, related to sea level change, have caused instabilities in peat accumulation, the long term persistence of climatic conditions favourable for peat accumulation have led to peatlands that are of considerable depth and age (Dommain et al., 2011, Dommain et al., 2014, Page et al., 2010). In lowland Amazonia, high rainfall permits fast accumulation rates, but being located on dynamic river floodplains, the peatlands are vulnerable to fluvial erosion or burial (Lähteenoja et al., 2009b, Lähteenoja and Roucoux, 2010). Their fast accumulation, but short existence, results in peatlands of moderate depth but of young age. In the Cuvette Centrale, the radiocarbon dates suggest that suitable climatic conditions for peat accumulation commenced in the early Holocene. Located away from the rivers in interfluvial basins and the unusual lack of river meandering across the region, possibly linked to the containment of rivers by fault lines (Master, 2010, Kadima et al., 2011), means these peatlands have not experienced disturbance from fluvial processes. However, unlike in South East Asia, longevity has not led to the formation of deep or domed peatland systems (Chapter 2). Whilst the Cuvette Centrale peatlands have undergone periods of zero or negative peat accumulation, tentatively linked to the AHP termination, this alone cannot account for the lack of doming in these peatlands, as domed South East Asian peatlands also show signs of peat degradation in response to late Holocene climatic events (Dommain et al., 2014,

Dommain et al., 2011). In order for domed systems to develop, high rainfall is required to allow OM accumulation above the influence of the water table (Rydin and Jeglum, 2006). Annual rainfall for the Likouala Department is ca. 1700 mm yr^{-1} (Samba and Nganga, 2012). This compares with annual rainfalls of 2000-3500 mm yr^{-1} reported for lowland Amazonian peatland regions (Householder et al., 2012, Lähteenoja et al., 2009b) and 2000-4000 mm yr^{-1} for South East Asian peatland regions (Dommain et al., 2011). Therefore I suggest that the lack of doming in the Cuvette Centrale peatlands is due to the generally drier climate of this region compared to South East Asia or lowland Amazonia. This would mean that once these shallow interfluvial basins have filled up with peat, peat depth cannot increase further unless the regional climate becomes significantly wetter.

5.7. Conclusions

Radiocarbon dating of basal samples suggests that peat initiation in the Cuvette Centrale occurred in the early Holocene, likely in response to the onset of wetter climatic conditions across the region during the African Humid Period (AHP). Although constrained by a limited dataset, age-depth models constructed from radiocarbon dates from one site suggest a possible hiatus in peat accumulation. This is supported by a coincident increase in peat decomposition. The timing of this hiatus links it to the termination of the AHP, which had a widespread and substantial impact on forest and aquatic ecosystems across Africa (Amaral et al., 2013, Vincens et al., 2010, Junginger and Trauth, 2013, Junginger et al., 2014, Vincens et al., 1999, Maley and Brenac, 1998, de Menocal et al., 2000, Elenga et al., 2001, Elenga et al., 1994).

When considering the age and depth of the Cuvette Centrale peats, they show a development history distinct to those of South East Asia and lowland Amazonia. In South East Asia, longevity and high accumulation rates have resulted in deep peat deposits of considerable age (Dommain et al., 2011, Dommain et al., 2014, Page et al., 2010). In lowland Amazonia, despite high accumulation rates, peatland development is curtailed by fluvial erosion or burial, meaning that peatlands are of a relatively young age and modest depth (Roucoux et al., 2013, Lähteenoja et al., 2009b). In the Cuvette Centrale, the peatlands are of similar age to those of South East Asia, but are of depths similar to lowland Amazonian peats. I suggest that this is owing to the drier climate of Central Africa, preventing the development of domed systems and the gentle topography of the Cuvette Centrale being unable to accommodate deep peats.

Chapter 6: Central Congo Basin Peatland Hydrology

6.1. Abstract

Within the Cuvette Centrale, Congo Basin, peat has been accumulating since the early Holocene. Both peat initiation and accumulation is thought to have been determined by regional precipitation levels. However, it is not clear whether waterlogging in the peatlands, essential for the continued accumulation of organic matter (OM), is solely down to rainfall or whether the rivers of the region, which run adjacent to the peatlands, also play a role in maintaining peatland water tables. Here multiple approaches are adopted to determine whether the Cuvette Centrale peatlands are rain fed (i.e. ombrotrophic) systems or whether they receive additional water inputs (i.e. are minerotrophic systems) from river flood waters. The first approach uses a year of *in situ* continuous water table measurements from four peatland sites within the Likouala Department, ROC, Cuvette Centrale in combination with remote sensing rainfall estimates (TRMM) to determine whether rises in peatland water tables can be accounted for by rain fall alone. For the second approach geochemical data is used to assess possible sources of peatland inundation; the geochemistry of surface peat and OM samples, from nine sites, are compared with the geochemistry of rainwater samples and samples from an adjacent white water and black water river. The final approach uses microscopy to determine the composition of surface peat inorganic material to give insight into its potential origin. No river flood events were detectable in the water table time series and rises in water tables were of a magnitude that could be accounted for by rainfall alone. However, a recharge signal detectable in the water tables is suggestive of a ground water influence. Low cation concentrations in the surface of the peatlands imply rain fed systems and a lack of flooding from the white water river. However geochemical data was inconclusive as to whether or not the black water river contributes to peatland inundation, for the reason that the geochemistry of this river is determined by the dominance of swamp forests within its catchment. Inorganic material present in the surface peats was largely of biological origins and those of non-biological origin were of silt-size (≤20 μm), implying that inorganic material originates from within the peatlands or via aeolian deposition. The Cuvette Centrale peatlands cannot be confirmed as ombrotrophic systems, as the peatlands may be in receipt of groundwater, and possibly some black river water, but the evidence does suggest that these systems are heavily dependent on rainfall with little mineral inputs, and hence are ombrotrophic-like peatlands.

6.2. Introduction

Peat accumulation is dependent on the maintenance of waterlogged, anoxic conditions to ensure OM accumulation exceeds decay (Charman, 2002, Rydin and Jeglum, 2006).

Distinctions are made between peatlands whose water tables are wholly or partially maintained through terrestrial water sources e.g. a stream or ground water, which are termed minerotrophic and peatlands whose water tables are maintained through precipitation alone, which are termed ombrotrophic (Charman, 2002, Rydin and Jeglum, 2006). Ombrotrophic and minerotrophic peatlands not only differ in their hydrology, but often in their mineral status. The chemical and physical weathering of rocks and sediments by terrestrial water sources mean that peatlands which are in receipt of fluvial or ground water flow tend to have a higher mineral content than those which receive nutrients solely from atmospheric deposition (Gorham, 1961). It is because of this that the concentrations of cations are frequently used as an indicator of peatland hydrological status, particularly Ca concentrations. Since atmospheric deposition of Ca tends to be lower than ground water or river Ca concentrations, low peat Ca concentrations are often indicative of ombrotrophy (Verhoeven, 1986, Gorham and Pearsall, 1956). Likewise, Ca/Mg ratios have been used to detect ombrotrophic conditions; Ca/Mg ratios higher than those of rainwater imply an additional source of Ca other than atmospheric deposition (Lähteenoja et al., 2009a, Weiss et al., 2002, Muller et al., 2006). In addition to detecting the present day hydrological conditions, down core cation concentrations have been used to detect both changes in hydrological status over the development of the peatland i.e. a change from initial minerotrophic conditions to ombrotrophy or to detect events in the peatlands history such as periods of increased dust deposition or flood events (Muller et al., 2006, Weiss et al., 2002).

In the Likouala Department, Republic of Congo (ROC), Cuvette Centrale, peatlands occupy large shallow interfluvial basins (Chapter 2). Peat initiation and accumulation are thought to be closely linked to changes in Holocene regional rainfall (Chapter 3). Present rainfall in the region is ca. 1700 mm yr^{-1} (Samba and Nganga, 2012), which compared to the two other major regions of tropical peatland occurrence, South East Asia and lowland Amazonia, is relatively dry (e.g. rainfall in the Pastaza-Marañon foreland basin in the Peruvian Amazaon is >3000 mm yr^{-1}; Marengo et al. (1998)). Passing through the wetlands of the Cuvette Centrale are both white water rivers, i.e. rivers with high ionic concentrations and low particulate organic matter (POC) and dissolved organic carbon (DOC) concentrations, and black water rivers, i.e. rivers with low ionic concentrations and high DOC and POC concentrations. Within the Likouala Department the two major rivers of the region, the Ubangui and the Likouala aux Herbes, are a white water and black water river respectively. Not only do these rivers differ in their chemistry, but also in their discharge, with the Ubangui having a considerably larger discharge (average annual discharge over the period 1951-93, measured at Bangui, Central African Republic: 3800 $m^3 s^{-1}$) than the Likouala aux Herbes (average annual discharge over the period 1951-93,

measured at Botouali, Likouala Department: 281 $m^3 s^{-1}$). These two rivers run adjacent to the peatlands of the Likouala aux Herbes, and the water chemistry of both rivers are to varying degrees determined by the peatlands (Mann et al., 2014, Laraque et al., 2009). However it is unclear whether these two rivers contribute to the inundation of the peatlands. Satellite data suggest that the swamp hydrology is largely independent of the regions river hydrology (Jung et al., 2010b, Lee et al., 2011), but this is yet to be confirmed through *in situ* measurements.

In this chapter I use three different approaches to determine whether the Ubangui and Likouala aux Herbes rivers contribute to peatland inundation or whether rainfall alone is responsible for peatland water table levels. For the first approach I use a full year of *in situ* peatland water table measurements in combination with remote sensing estimates of regional rainfall to determine whether river flooding is necessary to account for measured increases in water table. For the second approach I use measurements of cation concentration in surface peat and OM samples and in river and rainwater samples to link peatland geochemistry to one of the regional water sources. Down core peat geochemical data is also used to determine whether the peatlands have previously experienced river flooding. The final approach uses microscopy to determine the composition of surface peat inorganic material to give insight into its potential origin.

6.3. Aims

The aim of this chapter is to determine whether the Cuvette Centrale peatlands are ombrotrophic or minerotrophic systems. The objectives are firstly to use continuous water table measurements and remote sensing estimates of regional rainfall to determine whether increases in peatland water tables can be accounted for by rainfall alone or whether additional inputs are required. Secondly, the objective is to compare surface peat geochemistry with regional rainfall and river water geochemistry to determine whether the peatlands geochemistry can be linked to one of the aforementioned water sources. A third objective is to use down core peat geochemical data to assess the likelihood of past flood events. The final objective is to use microscopy to determine the proportion of surface peat mineral material of biological or non-biological origin and, to determine whether the mineral particles are of silt or sand size. It is hypothesised that fluvial action would be required for the transportation of sand sized inorganic mineral material.

6.4. Methods

6.4.1. Site Description

The data presented in this chapter comes from nine field sites visited in the Likouala Department, ROC; Bondoko, Bondzale, Centre, Ekolongouma, Ekondzo, Itanga, Mbala,

Makodi and Moungouma. For the field sites locations see Fig. 2.1 (Chapter 2) and for their full descriptions see Table 2.5 (Chapter 2) and Appendix 1-8. For methods relating to site selection and peat and vegetation sampling protocol refer to Chapter 2, section 2.4. Additionally this chapter presents water chemistry data from rainwater samples collected across the Likouala Department and from the two main rivers within the Likouala Department, the Ubangui, a white water river and the Likouala aux Herbes, a black water river, both of which are right bank tributaries of the Congo River. For a site description of the Likouala Department see Chapter 1, section 1.4.

6.4.2. Continuous Water Table Measurements

6.4.2.1. Pressure Transducer Installation

To obtain continuous peatland water table measurements, which could later be used to compare peatland water table rises with estimates of regional rainfall, 14 pressure transducers (manufacturer: Solinst, Georgetown, Cananda, model: Levelogger Edge) were installed across four sites, Bondoki, Bondzale, Ekolongouma and Itanga (Table 6.1.), between February and April 2013. Of the four sites, two were adjacent to the Ubangui River (Bondzale and Ekolongouma) and two were adjacent to the Likouala aux Herbes River (Bondoki and Itanga; Figure 6.1). The pressure transducers were also distributed across two of the peatland vegetation types; *Raphia laurentii* palm dominated swamp and hardwood swamp. At the Bondoki site one pressure transducer was also installed in seasonally flooded forest to give insight into flooding patterns in a non-peatland area (Table 6.1). Pressure transducers were suspended below the peatland surface inside perforated plastic tubes, at a known depth thought likely to be below the minimum water table level (Fig. 6.2). The pressure transducers record a combination of water and atmospheric pressure; to obtain water pressure alone, atmospheric pressure needs to be subtracted from the measurement. Therefore at each of the four sites two aboveground pressure transducers (manufacturer: Solinst, Georgetown, Cananda, model: Barologger Edge) were installed to measure atmospheric pressure only. These were installed at points along the transect that insured each belowground pressure transducer was no more than 1 km away from an aboveground pressure transducer, which is within the 30 km radius specified by the manufacturer for accurate barometric compensation. Installation involved hanging the pressure transducers from trees inside a small perforated tube for protection, well above flood height level. Both above- and belowground pressure transducers were set to record pressure measurements every 20 minutes. Between March and May 2014 the data was downloaded from each pressure transducer. Once the data was downloaded, Solinst Levellogger Software 4 was used to subtract atmospheric pressure from the belowground pressure measurements using the data from the nearest aboveground

pressure transducer. Using the same software pressure measurements were converted into water table levels (WT; m above (+) or below (-) surface), based on equation 6.1 and corrected for depth below surface of the pressure transducer:

$$WT = \frac{P}{\rho * g} \quad [6.1]$$

Where P is the water pressure (kPa), ρ is the water density (g ml^{-1}) and g is gravity (m s^{-2}).

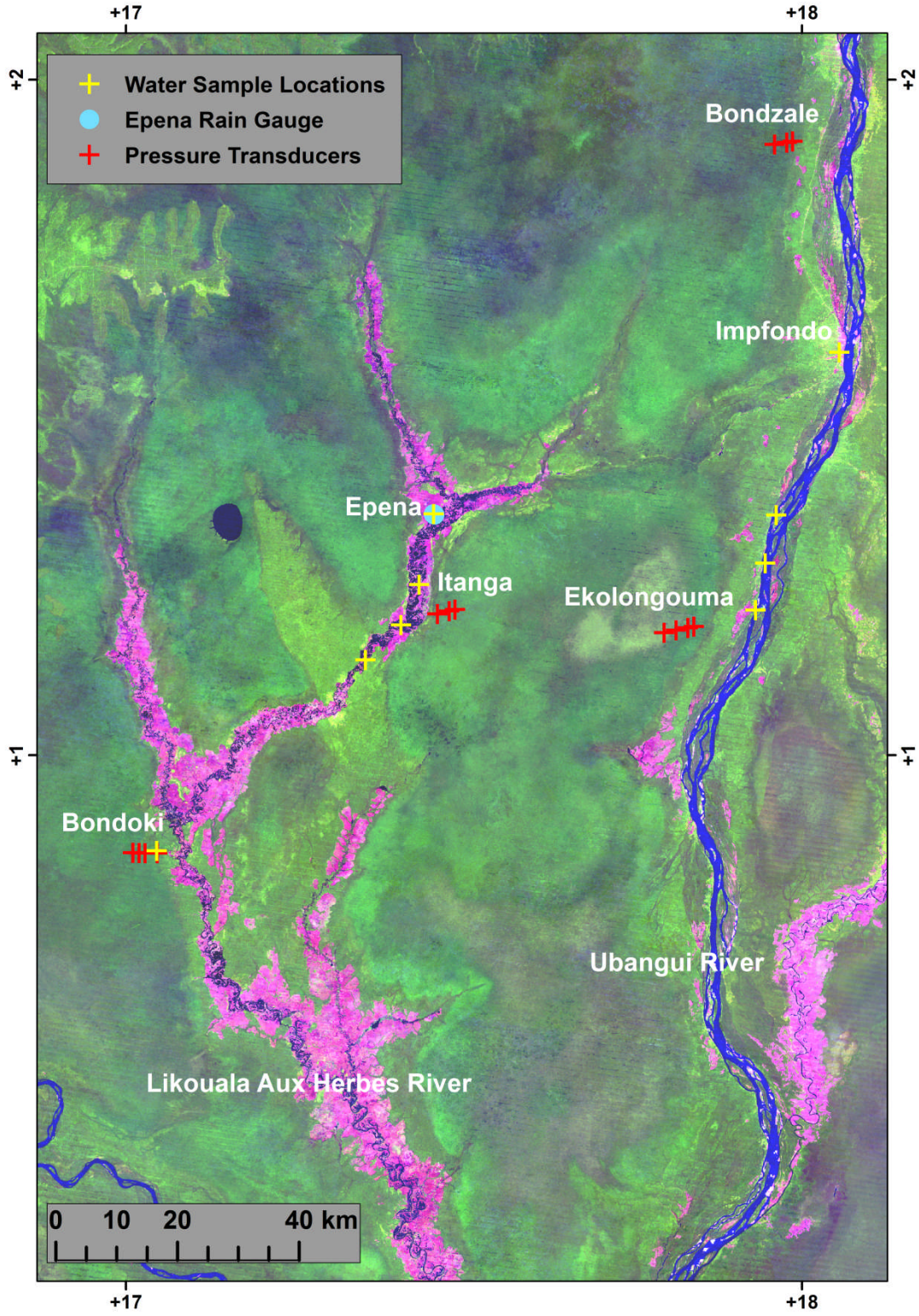

Figure 6.1. OSFAC Landsat ETM+ ROC mosaic showing the study region within the Likouala Department. Forested regions appear green, savannahs appear pink and rivers and lakes appear blue to very dark blue. The locations of the two main rivers of the region, the Likouala aux Herbes and the Ubangui, are shown along with the location of the river and rainwater sampling points (yellow crosses), the 14 continuous water table measurement sample points (red crosses) and the Epena rain gauge station (blue circle).

Table 6.1. Distribution of belowground pressure transducers across sites and along transects.

Site	Point of Installation Along Transect (km)	Vegetation Type	Peat Depth (m)
Bondoki	2 4 5 6	Seasonally Flooded Forest Palm Dominated Swamp Palm Dominated Swamp Palm Dominated Swamp	0 1.50 1.30 1.50
Bondzale	3 4 6	Hardwood Swamp Hardwood Swamp Hardwood Swamp	0.80 1.10 1.70
Ekolongouma	4 5 7 9	Palm Dominated Swamp Palm Dominated Swamp Palm Dominated Swamp Palm Dominated Swamp	1.50 1.53 2.40 2.99
Itanga	3 5 6	Hardwood Swamp Hardwood Swamp Hardwood Swamp	1.20 1.70 2.00

A)

B)

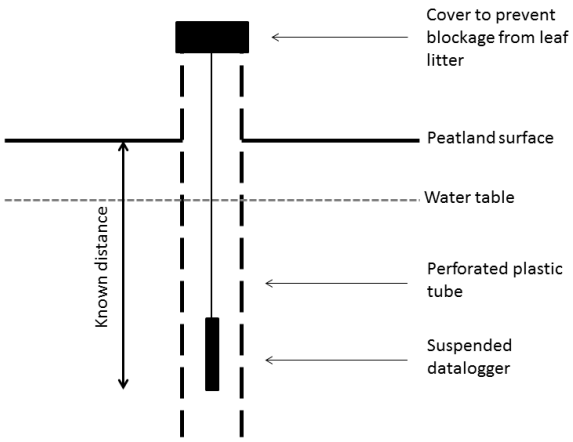

Figure 6.2. A) Pressure transducer installed in the field. B) Schematic showing pressure transducer suspended inside perforated tube in the peatland.

6.4.2.2. Data Analyses

If river flooding was involved in peatland inundation then it was hypothesised that flood waves entering the peatland should be detectable in the water table time series. Therefore each time series was plotted (using R 3.0.1) and visually inspected to look for any sudden, large magnitude rises in water table.

It was also hypothesised that if a river flood event occurred, water table levels would increase at a greater rate than that possible from a rain event alone. Therefore the rate of change in water table height (RC; mm min^{-1}) was calculated across all the time series by the following equation:

$$RC = (b - a)/20 \quad [6.2]$$

Where a is the water table height (mm) at the start and b is the water table height (mm) at the end of the 20 minute time interval. Any RC values too large to be attributable to a rain event would signal a flood event. However, consideration had to be given to what is known as the specific yield of the peat, whereby a given quantity of rainfall will not equate to the same rise in the water table when the water table is below the peat surface, but instead leads to a much larger rise as demonstrated in Fig. 6.3 (Shah and Ross, 2009), with the magnitude of the rise being dependent on the available pore space and connectivity. Therefore RC values were excluded from this analysis if the water table was below the peatland surface at the beginning or end of the 20 minute period. The maximum RC values recorded at each sample point were then converted to mm hr^{-1}.

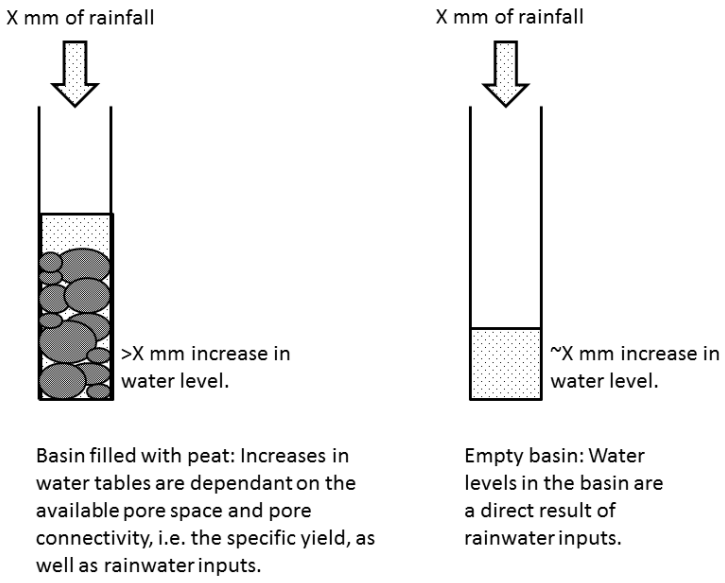

Figure 6.3. Schematic showing why the specific yield of peat would result in increases in water table height that are greater than the rainwater input.

Similarly, I calculated the total monthly cumulative increase in the water table (CIWT) at each location, for comparison with rainfall estimates. It was thought that if the peatlands receive water from precipitation alone, then over a set time period the CIWT should approximately equal estimates of total rainfall for that location over the same period. The monthly CIWT was calculated by summing all increases in water table per month for each location. However the datasets were dominated by very small, high frequency fluctuations, which appeared to be occurring on a daily basis and were suspected to be linked to evapotranspiration (ET) (see section 6.5.1 and 6.6.3). The summing of this effect over the period of a month meant that it made up a considerable proportion of the estimated CIWT.

To confirm whether these fluctuations were cyclical and on what frequency, spectral analysis was carried out in R 3.0.1. To avoid any low amplitude cyclical patterns being obscured by large scale events, spectral analysis was carried out on segments of each time series where there were no large increases in water table. These segments were also detrended to account for the steady drop in water table levels, which followed any large increase in water table. The spectral analysis results were used to determine the size of the smoothing window used (24 hours) to remove the low amplitude, high frequency signal from the water table time series. Smoothing of the time series was done using the R package Zoo (Zeileis and Grothendieck, 2005). Once the time series were smoothed, new monthly CIWT were calculated. To avoid the problem of specific yield CIWT values were only considered for months where the water table was consistently above the peatland surface. Monthly CIWT values were then compared with rainfall estimates from the Tropical Rainfall Meansuring Mission (TRMM) 3B43 datasets (spatial resolution: 0.25°x25°; temporal resolution: monthly; available from: http://gdata1.sci.gsfc.nasa.gov/daac-bin/G3/gui.cgi?instance_id=TRMM_Monthly). Since TRMM has been known to underestimate precipitation in heavy rain storms (Bajracharya et al., 2015, Habib et al., 2009, Mehran and AghaKouchak, 2014), daily rain gauge data (courtesy of WCS Congo) recorded at Epena, a village in the Likouala Department (shown in Fig. 6.1) was also obtained to assess the reliability of TRMM data for the region.

For an estimate of peatland drainage the monthly cumulative decrease in water table (CDWT) was calculated for each location by summing all decreases in water table. Again this was done only for months where the water table was consistently above the peatland surface. Given that drainage is likely to be a gradual process and the aim was to consider total drainage, CDWT was calculated using the unsmoothed time series. To determine to what degree ET is responsible for water loss from the peatlands, CDWT values were compared with ET values for the Congo Basin taken from the following studies: Matsuyama et al. (1994), Rodell et al. (2011) and Lee et al. (2011).

6.4.3. Peatland Metal Cation Concentrations

Typically if a peatland is minerotrophic it will have higher cation concentrations than an ombrotrophic peatland, because of the interaction the water has had with the ground surface prior to arrival at the peatland. Therefore if rivers flood peatlands, the chemical signature of the river waters should be detectable in the surface peats. For every location of every transect where peat was found selected cation concentrations (Al, Ca, Fe, K, Mg, Mn, Na, Pb, Ti) in surface peat samples were measured using inductively coupled plasma optical emission spectrometry (ICP-OES). OM surface samples from areas under swampland, where no peat was present, were also selected for analysis, including surface

samples from the Moungouma transect, where *Raphia hookeri* palm dominated swamp was present but was not associated with peat presence, and also surface samples from the swamp margins of other transects, where organic soils were present but did not meet the 30 cm depth criterion to be classed as peat.

In addition, from each of the eight peatland sites the deepest core was selected for down core ICP-OES analysis, at a sampling resolution of every other 10 cm (e.g. 0-10 cm, 20-30 cm). Such down core cation concentrations could detect flood events during the peatlands development.

Samples and three blanks per batch were first pre-treated with 3 ml of concentrated nitric acid and then digested with hydrofluoric acid to break down the OM. For this approximately 0.1 g of dried (40 °C) sample was digested with 1 ml 60% $HClO_4$ and 7 ml 40% HF for 2 hours on a hot plate. Following this, 1 ml of H_2SO_4 was added to the solution and heated again to drive off the $HClO_4$. The solution was then filtered into a 100 ml volumetric flask and diluted to volume (Allen, 1989).

Total metal cation concentrations in the solution were then measured by ICP-OES (manufacturer: Perkin Elmer, Waltham, Massachusetts, U.S.A, model: Optima 5300 DV; manufacturer: Thermo Fisher Scientific Inc., Waltham, Massachusetts, U.S.A, model: iCAP 7400 radial). For each sample, the mean concentration of the three blanks for that batch was subtracted from the measured sample concentration for each cation.

Whilst absolute metal cation concentrations can give an indication of nutrient status, metal cation ratios can act as a chemical signature which can be used to trace potential sources of cations to the peatlands. Several studies have compared peat Ca/Mg ratios to those of rainwater to determine whether a peatland is ombrotrophic or not (Lähteenoja et al., 2009a, Weiss et al., 2002, Muller et al., 2006). Therefore Ca/Mg ratios were calculated for the surface samples for the comparison with rain and river water samples (see section 6.4.4).

6.4.4. River and Rainwater Chemistry

For comparison with the peatland surface chemistry results, all water sources considered to be a possible cause of peatland flooding were sampled for ICP-OES analysis. Water samples were collected at three points along the Ubangui River and the Likouala aux Herbes River between April and May 2014. Rainwater samples from three different rain events occurring in different localities were collected over the same period. Sampling locations were marked with a GPS (manufacturer: Garmin, Hampshire, U.K.; model: GPSmap 60CSx) and are shown in Fig. 6.1. Following sample collection vials were wrapped in aluminium foil and stored in a cool dark room until transportation back to the U.K.

where they were promptly analysed for total metal concentrations (Al, Ca, Fe, K, Mg, Mn, Na, Pb) using an ICP-OES (manufacturer: Perkin Elmer, Waltham, Massachusetts, U.S.A, model: Optima 5300 DV). Like the surface peat/OM samples, Ca/Mg ratios were calculated for each water sample. At the time of sampling a pH measurement was taken for each sample using a pH meter (manufacturer: Hanna Instruments, Leighton Buzzard, U.K., model: HI 9124 Waterproof Portable pH Meter). Electrical conductivity was not measured due to an equipment failure.

6.4.5. Loss on Ignition Residues

Peat mineral material can either be of biological or non-biological origin. Non-biological silt-sized grains (≤20 μm) can enter the peatland either via atmospheric deposition or through surface water transportation. Sand-sized grains (>20 μm), however, require more energy for transportation and therefore are usually an indication of surface water transportation. Biological mineral material usually originates from within the peatland, with plant phytoliths, sponge spicules and diatoms being a common source of biological mineral matter in peats (Lopez-Buendia et al., 2007, Wust and Bustin, 2003). It was hypothesised that if the peatlands were ombrotrophic systems, the mineral material present in the surface peats would be predominantly of biological origin and any non-biological mineral material would be of silt-size. High levels of sand-sized non-biological material would indicate minerotrophic systems. Therefore loss on ignition (LOI; method: 550°C for 4 hours; Heiri et al. (2001)) residues from surface peat samples from seven peatland sites (Bondoki, Bondzale, Centre, Ekolongouma, Ekondzo and Mbala) and residues from surface OM samples from a swamp site with no peat accumulation (Moungouma) were examined under a microscope to determine the origin of the mineral matter. LOI residues were mounted in silicon oil and examined at up to x 400 magnification.

The first 50 pieces of mineral matter were counted under the microscope along a transect within the slide and were given a category based on their origin. Non-biological mineral material were defined either as silt or sand. Mineral matter smaller than 10 μm was not counted owing to the fact it is difficult to tell the origin of pieces so small; an exception to this was palm phytoliths which were often <10 μm but easily identifiable.

6.5. Results

6.5.1. Water Table Data

Twelve pressure transducers across four sites recorded continuous water table levels for at least 12 months of the year (time series vary due to differing installation and retrieval dates). At two sample points recording was interrupted; at the Itanga 5 km sample

location there is a six week gap (9th April to 22nd May 2013) owing to interference from a panther and at the Ekolongouma 7 km sampling location data is only available from the 20th February to the 4th May 2013 due to human interference.

There was no clear relationship between peatland vegetation type (palm dominated versus hardwood swamp) and water table height relative to the peat surface (minimum, maximum or mean), although sample sizes are small (Table 6.2). There was also no relationship between peatland vegetation type and the proportion of time peatlands were inundated or had water tables near the surface. Likewise, peat depth and distance along each transect did not seem to be related to water table levels. Water tables in the swamp interior were not consistently higher or lower than at the swamp margins and the greatest peat depths did not always correspond with the highest mean or maximum water table level or the longest inundation period.

Although only one seasonally flooded forest was monitored (Bondoki, 2 km), indicative differences could be seen. The seasonally flooded forest had the lowest mean and minimum water table level and the proportion of time with which the water table was within 10 cm of the surface was lower than for the peatland sample points (Table 6.2). However, the seasonally flooded forest had a maximum flood height similar to the peatland sites and the proportion of time for which this point was inundated was similar to the peatland sites along the same transect.

Plotted as time series, all of the water table records show a similar pattern of sharp rises followed by a much slower fall in water table height, with the non-peat site showing the most extreme fluctuations (Fig. 6.4). No clear flood wave events, where river waters enter the system, were seen. Within three of the four sites, the water table at the different sample locations along the transect followed similar patterns and seemed to respond to events simultaneously (Fig. 6.4. B-D). However at the Bondoki site, at two locations the water table plateaued once it had reached the peatland surface, whilst at the other peatland location the water table continued to rise and fall (Fig. 6.4. A). In the seasonally flooded forest, water tables also showed periodic plateauing, but this was when the water table was well below the surface.

Table 6.2. Water table (WT) data and peatland characteristics along the Bondoki, Bondzale, Ekolongouma and Itanga transects for the time period of 6th April 2013 to 30th March 2014. Negative WT values represent a water table below the ground surface.

Site	Transect Distance (km)	Water Table Level (m) Mean (±St. Dev.)	Min.	Max	Time Proportion WT is at Surface or Inundated (%)	Time Proportion WT is Greater than 10 cm below the Surface (%)	Vegetation Type	Peat Depth (m)
Bondoki	2	-0.35±0.34	-1.06	0.22	25	33	Seasonally Inundated Forest	0
	4	-0.10±0.16	-0.41	0.23	29	45	Palm Dominated	1.50
	5	-0.09±0.10	-0.37	0.02	28	61	Palm Dominated	1.30
	6	-0.09±0.09	-0.37	0.04	7	62	Palm Dominated	1.50
	Site Mean (excluding seasonally flooded forest)	**-0.09±0.01**						
Bondzale	3	0.14±0.16	-0.24	0.43	79	94	Hardwood Swamp	0.80
	4	0.08±0.15	-0.30	0.35	67	84	Hardwood Swamp	1.10
	6	-0.09±0.27	-0.84	0.26	55	62	Hardwood Swamp	1.70
	Site Mean	**0.04±0.12**						
Ekolongouma	4	0.00±0.10	-0.24	0.19	52	78	Hardwood Swamp	1.50
	5	0.04±0.09	-0.20	0.22	61	94	Hardwood Swamp	1.84
	9	0.08±0.07	-0.14	0.24	86	99	Palm Dominated	3.00
	Site Mean	**0.04±0.04**						
Itanga	3	0.02±0.09	-0.29	0.18	63	92	Hardwood Swamp	1.20
	5	0.07±0.07	-0.16	0.22	81	99	Hardwood Swamp	1.70
	6	0.00±0.09	-0.28	0.17	57	88	Hardwood Swamp	2.00
	Site Mean	**0.03±0.04**						
All	**Mean** (excluding seasonally flooded forest)	**0.01±0.06**						
	Palm dominated Swamp Mean	**-0.05±0.09**						
	Hardwood Swamp Mean	**0.03±0.07**						

A)

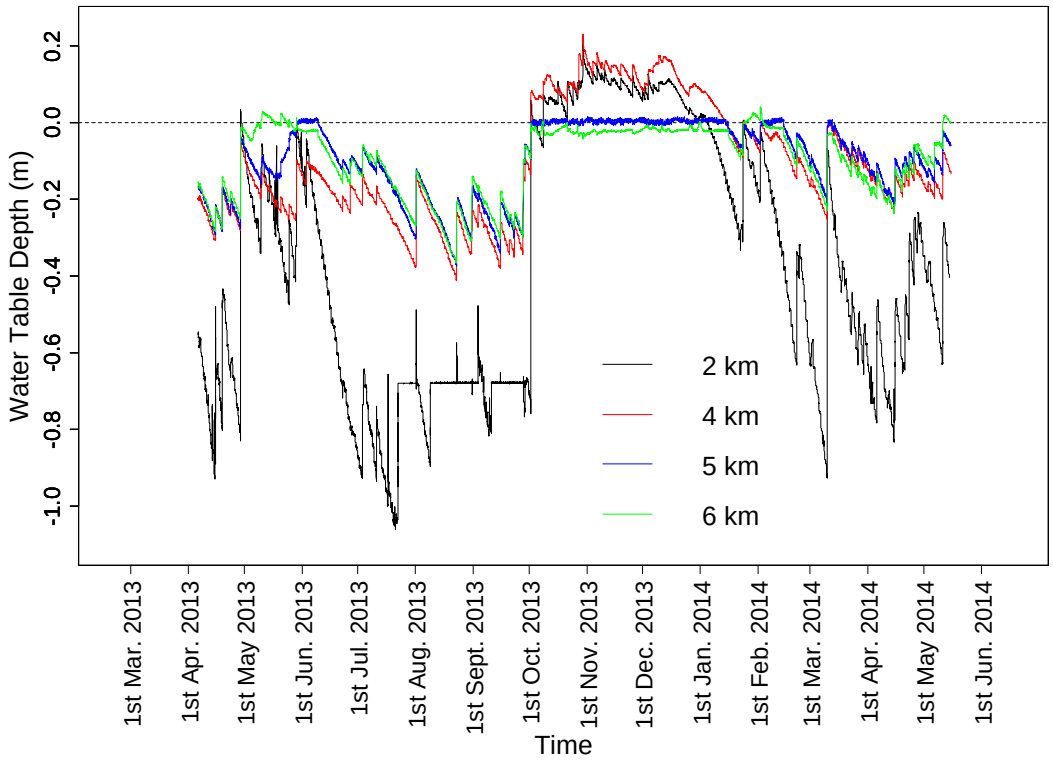
Water Table Depth (m)
0.2
0.0
-0.2
-0.4
-0.6
-0.8
-1.0
2 km
4 km
5 km
6 km
1st Mar. 2013
1st Apr. 2013
1st May 2013
1st Jun. 2013
1st Jul. 2013
1st Aug. 2013
1st Sept. 2013
1st Oct. 2013
1st Nov. 2013
1st Dec. 2013
1st Jan. 2014
1st Feb. 2014
1st Mar. 2014
1st Apr. 2014
1st May 2014
1st Jun. 2014
Time

B)

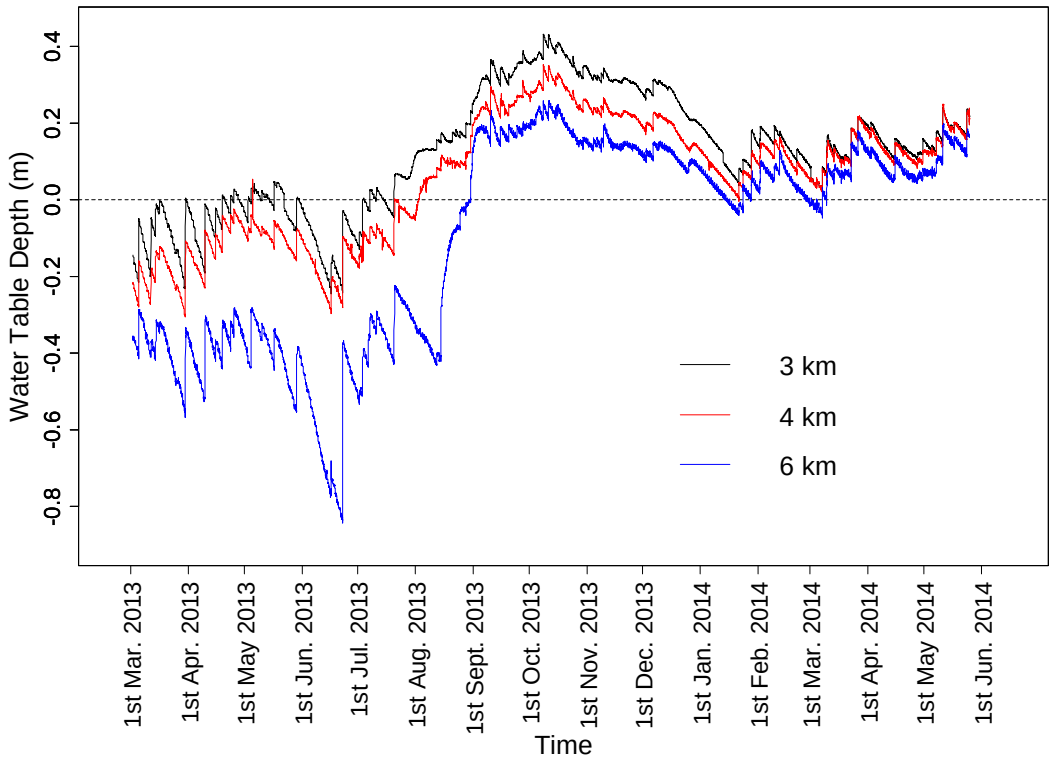
Water Table Depth (m)
0.4
0.2
0.0
-0.2
-0.4
-0.6
-0.8
3 km
4 km
6 km
1st Mar. 2013
1st Apr. 2013
1st May 2013
1st Jun. 2013
1st Jul. 2013
1st Aug. 2013
1st Sept. 2013
1st Oct. 2013
1st Nov. 2013
1st Dec. 2013
1st Jan. 2014
1st Feb. 2014
1st Mar. 2014
1st Apr. 2014
1st May 2014
1st Jun. 2014
Time

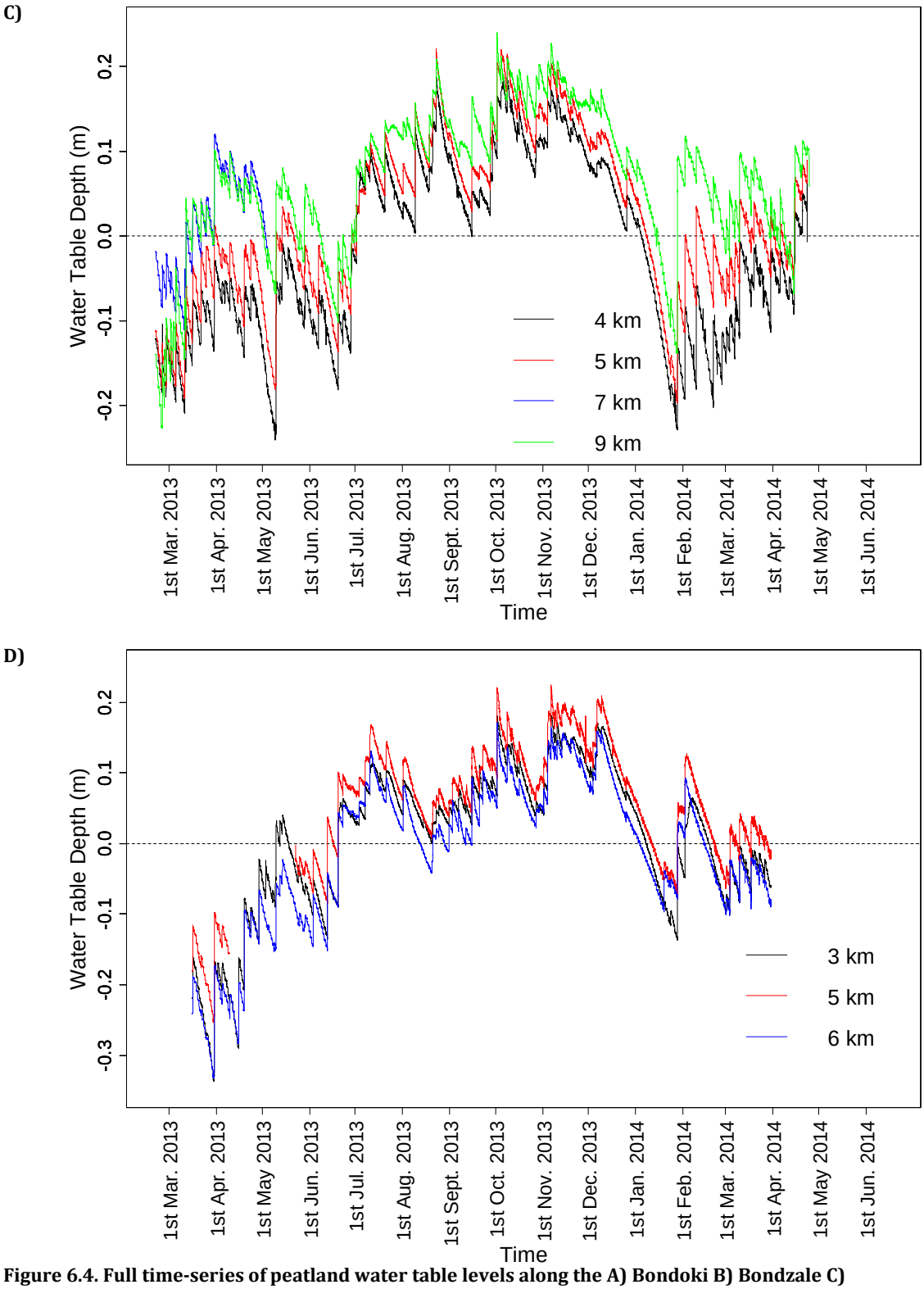

Figure 6.4. Full time-series of peatland water table levels along the A) Bondoki B) Bondzale C) Ekolongouma D) Itanga transect. Panel A also shows the full time-series of the Bondoki seasonally flooded forest water table levels (2 km; black line).

The maximum *RC* values ranged from 11 to 210 mm hr^{-1} (i.e. 0.18 to 3.5 mm min^{-1}), with the maximum *RC* value being recorded at Bondzale 3 km on the 23rd March 2014 (Table 6.3). The low maximum *RC* values recorded at the Bondoki 5 km and 6 km locations are due to the plateauing of water tables once at the peatland surface. All but two maximum

RC values coincided with a TRMM rain event; at the time of the Bondoki 5 km and the Itanga 5 km maximum RC values TRMM measured zero rainfall.

Table 6.3. Maximum positive rate of change (RC; mm hr^{-1}) in water table levels as recorded by the pressure transducers, across all location at the four sites.

Site	Location (km)	Time	Date	Rate (mm hr^{-1})
Bondoki	2	14:40	21-Oct-13	173
	4	14:20	27-Oct-13	79
	5	10:20	15-Oct-13	11
	6	04:00	02-Feb-14	27
Bondzale	3	01:40	23-Mar-14	210
	4	01:40	23-Mar-14	161
	6	01:40	23-Mar-14	104
Ekolongouma	4	07:40	09-Aug-13	114
	5	21:20	25-Dec-13	106
		09:20	30-Mar-13	123
	9	09:00	30-Mar-14	130
Itanga	3	21:40	01-Oct-13	92
	5	21:00	28-Nov-13	126
	6	22:00	01-Oct-13	115

Spectral analysis confirmed that the low amplitude, but high frequency fluctuations seen in all the time series (Fig. 6.5 shows examples of this) was cyclical with a recurrence period of approximately one day (Fig. 6.6). There were a few sample points which showed an additional signal with a 12 hour recurrence frequency. Despite detrending the sections of time series, the non-linear decline in water tables meant that many power spectral density diagrams still showed lower frequency, higher amplitude cycles which are partially obscuring the signals occurring at frequencies of 12 or 24 hours. A 12 hour cyclical signal which mirrored that of the pressure transducers was also seen in all the barologger atmospheric pressure time series (Fig. 6.7), suggesting that the 12 hour signal is related to atmospheric pressure.

Figure 6.5. Low amplitude, high frequency noise visible in a subsection of the water table time series for the sample point closest to the swamp interior at the following sites: A) Bondoki B) Bondzale C) Ekolongouma D) Itanga

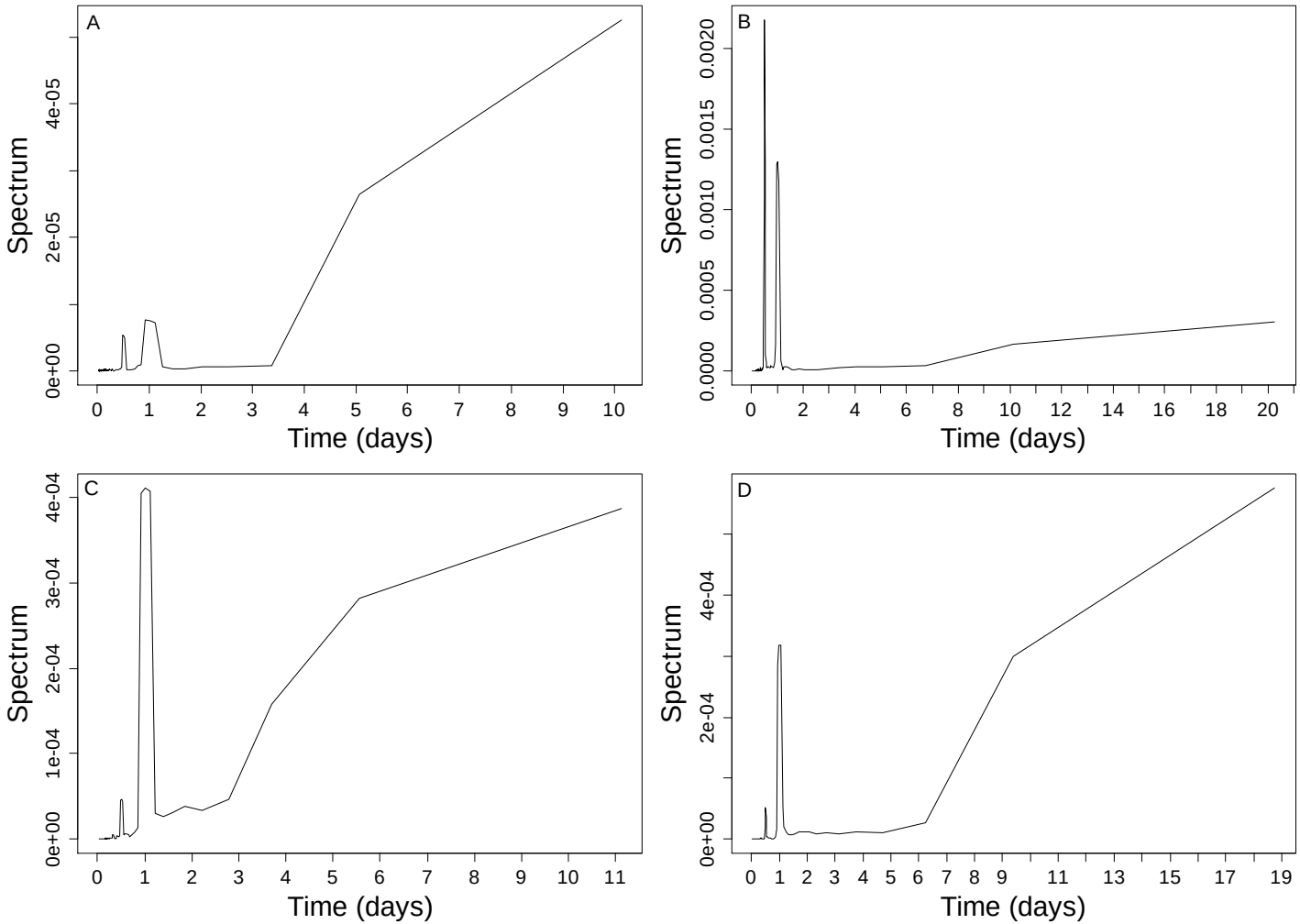

Figure 6.6. Power spectral diagrams from the spectral analysis of the water table time series subsections shown in Fig. 6.5 for A) Bondoki B) Bondzale C) Ekolongouma D) Itanga.

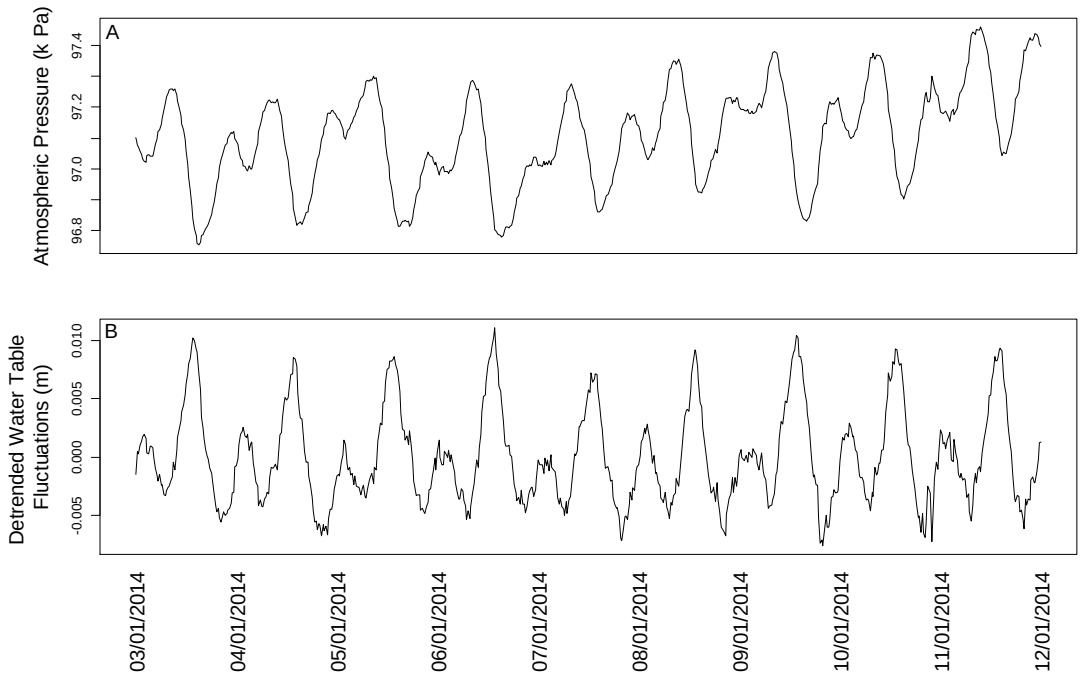

Figure 6.7. A) Barologger atmospheric pressure measurements at Bondzale 5 km. B) Detrended water table fluctuations measured by pressure transducer at Bondzale 6 km.

When the water table time series were smoothed to remove the background signal, a significant ($p<0.001$) exponential relationship was found between the monthly cumulative increase in water table (CIWT) values and TRMM monthly rainfall (Fig. 6.8). However the strength of this relationship was low (adjusted R-sq. value of 0.25). Of the 56 observations, TRMM was greater than the CIWT value in 40 instances and in the remaining 16 instances CIWT was higher than TRMM (Fig. 6.8). Of these 16 instances where CIWT values were greater than TRMM, ten came from the Bondzale site and were from the months December 2013 to April 2014, which as discussed below, was a period when ground conditions were particularly wet at Bondzale. When water table levels were visually compared with TRMM daily accumulated rainfall, rises in water tables often coincided with TRMM rain events, but there were instances where TRMM recorded a rain event but no rise in water table was observed and vice versa (see Fig. 6.9 for an example), showing a disparity between the two datasets. When comparisons were made between TRMM and rain gauge monthly rainfall for Epena village, there was a significant ($p=0.03$) positive relationship between the two datasets, but the low adjusted R-sq. value shows that TRMM measurements do not closely match rainfall measurements on the ground (Fig.6.10).

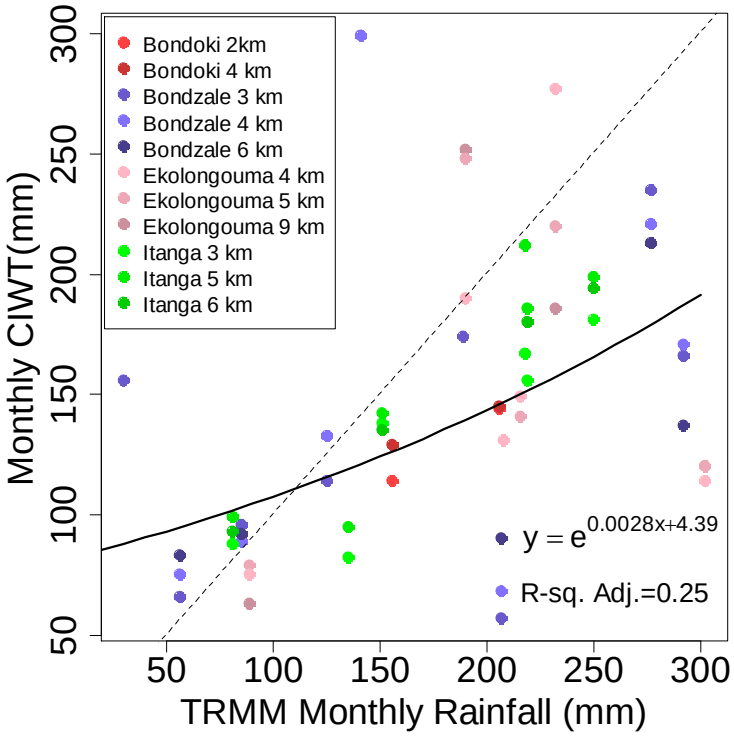

Figure 6.8. Relationship between monthly CIWT (for months when the water table is consistently above the peat surface) and TRMM monthly rainfall (solid line). Line equation and adjusted R-sq. value are shown. Dashed line shows a 1:1 relationship.

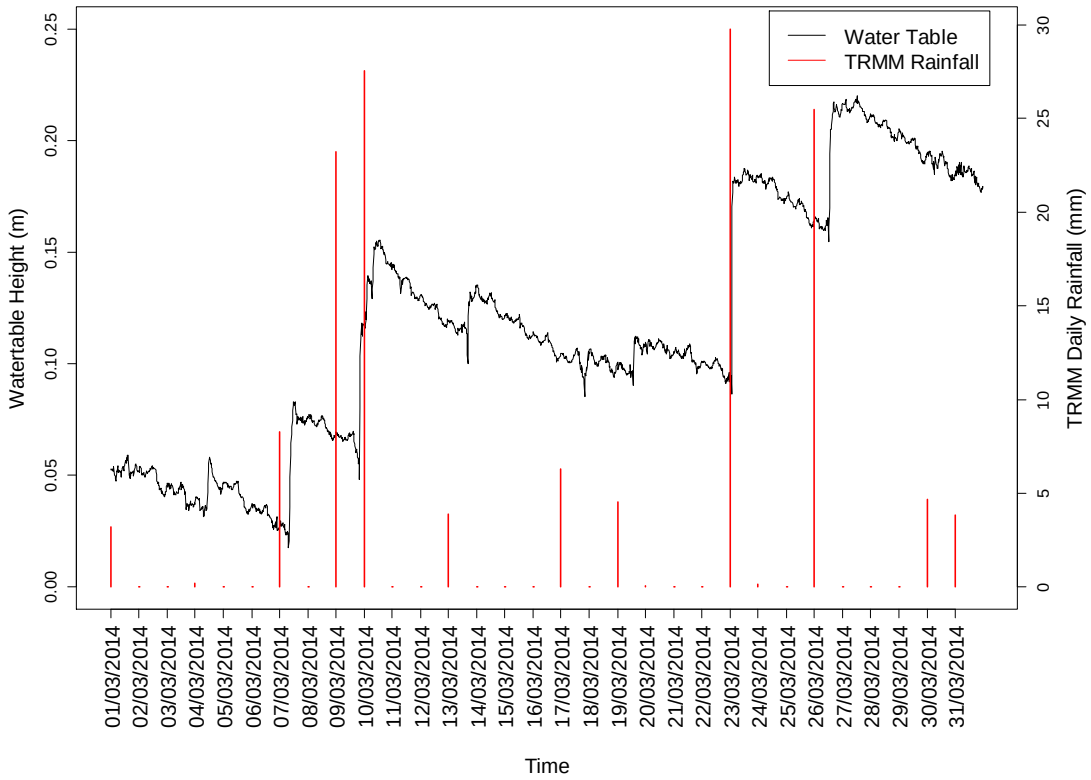

Figure 6.9. March 2014 water table time series for the 4 km Bondzale location and TRMM daily rainfall estimates for the Bondzale region.

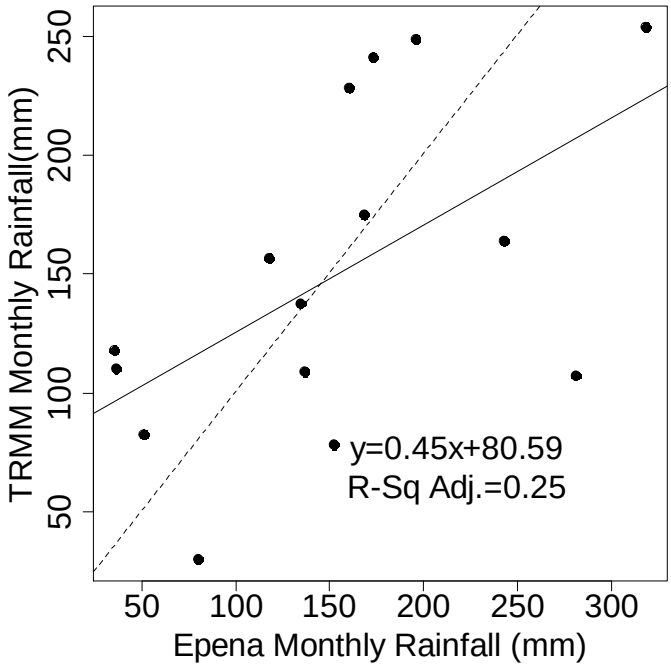

Figure 6.10. Relationship between TRMM monthly rainfall and rain gauge monthly rainfall (solid line) for Epena village for the time period of February 2013 to April 2014. Line equation and adjusted R-sq. value are shown. Dashed line shows a 1:1 relationship.

Owing to the timing of fieldwork, data was downloaded from the pressure transducers after slightly more than one year. The peatlands from February to May 2014 were wetter than in the equivalent period in 2013, particularly at Bondzale. This was also apparent whilst in the field; even areas of seasonally flooded forest, which contain no peat and had been completely dry in the same season the previous year, were inundated, sometimes reaching waist height. However, the rain gauge data from Epena showed that for the months of February to April 2013 and February to April 2014, rainfall was very similar, with a total of 468 mm over this period in 2013 and 455 mm in 2014. TRMM monthly rainfall estimates, on the other hand, suggest rather surprisingly that for this period, 2013 was generally wetter (487 mm), than 2014 (326 mm). TRMM data also shows 2013 to be wetter than 2012 for both the small and major wet seasons (Fig. 6.11).

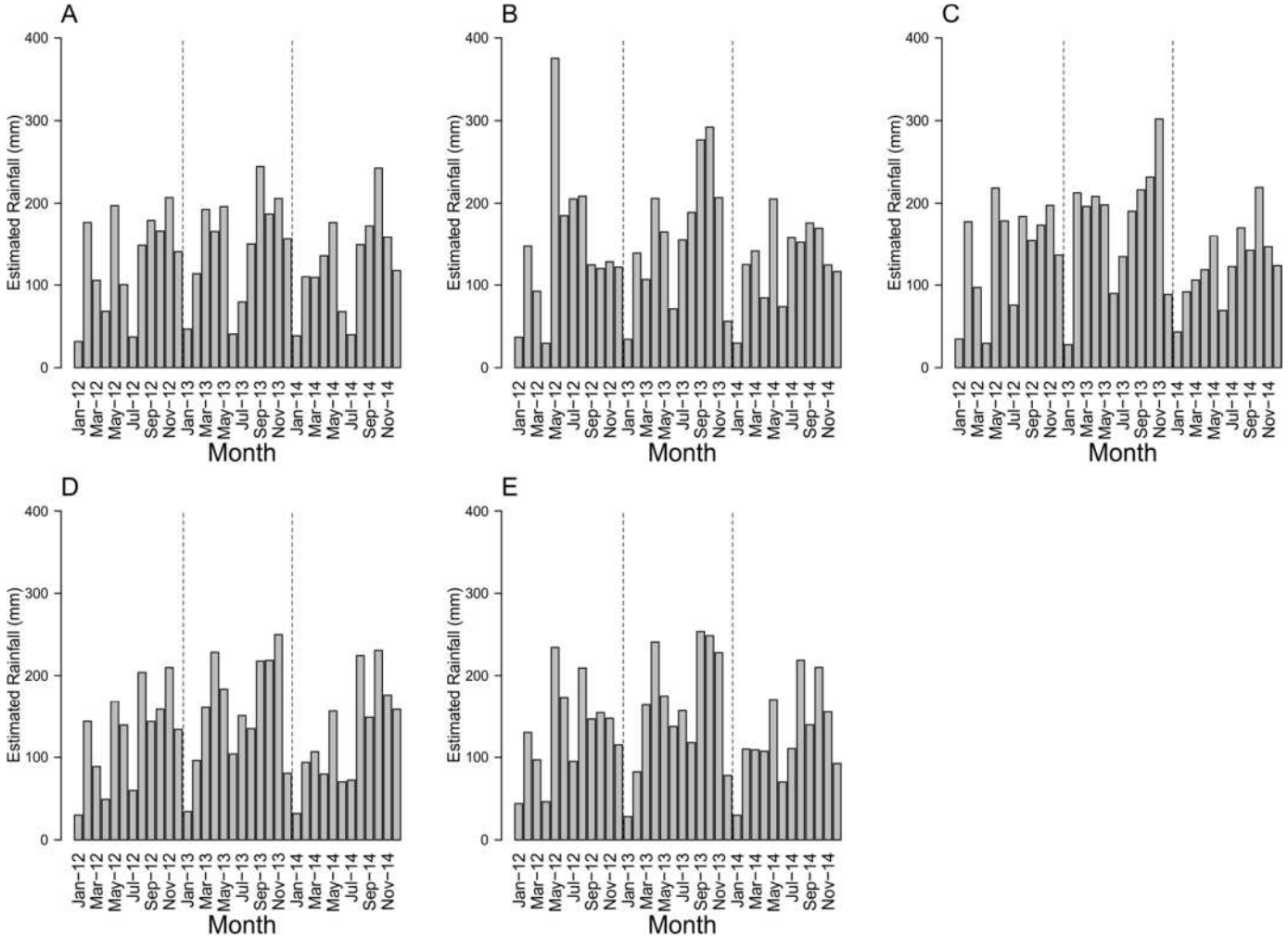

Figure 6.11. TRMM monthly rainfall estimates over the period of Jan. 2012 to Dec. 2014 for A) Bondoki B) Bondzale C) Ekolongouma D) Itanga E) Epena village. Dashed vertical lines are used to separate the different years.

When monthly cumulative decreases in water table (CDWT) were compared with estimates of ET taken from the literature for the Congo Basin (Table 6.4), ET values could not account for the majority of water lost from the peatlands. For the Matsuyama et al. (1994) estimates ET was almost always less than half the CDWT value and for the Rodell et al. (2011) and Lee et al. (2011) estimates, ET the majority of the time was less than a third of the CDWT value (e.g. Fig. 6.12).

Table 6.4. Monthly evapotranspiration (ET) estimates for the Congo Basin derived from three studies: Matsuyama et al. (1994), Rodell et al. (2011) and Lee et al. (2011).

	ET estimates (mm)		
Month	**Matsuyama et al. (1994)[1]**	**Rodell et al. (2011)[2]**	**Lee et al. (2011)[3]**
January	80	98	130
February	80	88	117
March	120	98	130
April	160	95	126
May	200	98	130
June	160	95	126
July	120	98	130
August	160	98	130
September	240	95	126
October	240	98	130
November	200	95	126
December	160	98	130

[1] Longitudinally averaged monthly ET estimates for the Congo Basin, for different latitudes. ET was assumed to be the residual difference between precipitation and vapour flux convergence values. The values presented here are corresponded to the study sites' latitudes.

[2] ET estimates for the Ubangui River basin which were calculated using a satellite and ground observation based water budget. Rodell et al. (2011) present ET seasonal variations in a graph but these were illegible, so values presented here are derived from the daily mean value.

[3] Annual ET estimates for the Cuvette Centrale derived from a variation of the Penman-Monteith equation. Values presented here were calculated using the annual estimated ET value for a 3°×3° area covering the region of this study.

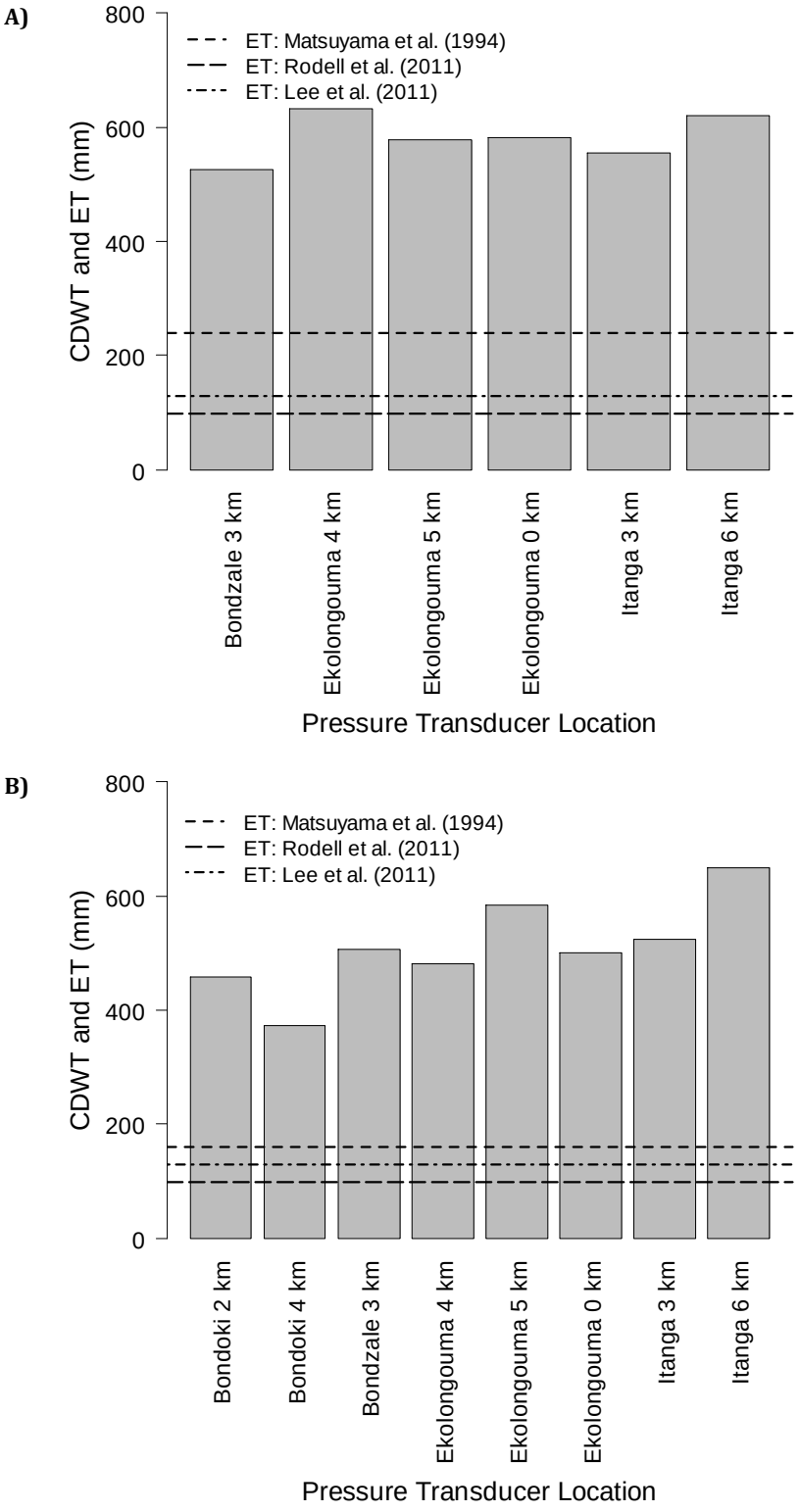

Figure 6.12. Bar plot of CDWT for all location where water tables were consistently above the peatland surface for A) October 2013 and B) December 2013. ET estimates from the three studies (Matsuyama et al., 1994, Rodell et al., 2011, Lee et al., 2011) are shown as horizontal dashed lines.

6.5.2. River and Rainwater Characteristics

The three types of water samples showed significantly different pH levels ($p<0.001$, One-Way ANOVA; Table 6.5): Ubangui River water had a near neutral pH, whilst the rainwater of the region was slightly acidic and Likouala aux Herbes River water was extremely acidic. The metal cation concentrations (mg l^{-1}) amongst the three water types differed in

their absolute concentration levels as well as the order of their relative concentrations (Table 6.5). The Ubangui River water samples could be characterised by significantly higher concentrations of Ca, Mg, Na and K than the rainwater or Likouala aux Herbes samples ($p<0.05$, One-Way ANOVA and a post hoc Tukey test), whilst the Likouala aux Herbes river water samples showed significantly higher concentrations of Fe, Al and Mn ($p<0.05$, One-Way ANOVA and a post hoc Tukey test). The rainwater samples generally showed significantly lower concentrations of cations than the two rivers ($p<0.05$, One-Way ANOVA and a post hoc Tukey test). However, rainwater Al concentrations were not significantly lower than the Ubangui and rainwater K concentrations were not significantly lower than the Likouala aux Herbes. The order of mean cation concentrations for the Ubangui River was Ca>Mg>Na>K>Fe>Al>Mn (Pb below detectable limits). For the Likouala aux Herbes River it was Fe>Al>Ca>Na>K>Mg>Mn (Pb below detectable limits) and for rainwater was K>Ca>Na>Mg>Al>Mn>Fe (Pb below detectable limits). The rainwater had the most variable Ca/Mg ratios and the highest mean Ca/Mg ratio (Fig. 6.13), whilst the Ubangui River had the lowest mean Ca/Mg ratio, however there was no significant difference between the Ca/Mg ratios of the three water sources ($p>0.05$, one-way ANOVA). Therefore, whilst the three water sources differ in their absolute cation concentrations, the Ca/Mg ratios, which are sometimes used to determine the source of peatland water inputs (Weiss et al., 2002, Lähteenoja et al., 2009a), were not distinguishable between the three sources.

Table 6.5. River and rainwater pH and cation concentrations from the Likouala Department. Mean values which do not share a common letter are significantly different (p<0.05, One-Way ANOVA).

Sample	Location Description	pH	Temp. (°C)	Metal Concentration (mg l^{-1})						
				Al (Ra)	Ca (Ax)	Fe (Ax)	K (Ax)	Mg (Ax)	Mn (Ax)	Na (Ra)
Rain-01	Bondoki	5.50	26.8	0.004	0.097	0.000	0.313	0.039	0.003	-0.002
Rain-02	Epena	4.75	25.0	0.021	0.207	0.004	0.271	0.043	0.004	0.230
Rain-03	Impfondo	4.81	24.6	0.017	0.079	0.004	0.272	0.015	0.008	0.103
	Mean	**5.02a**	**-**	**0.014a**	**0.128a**	**0.00a**	**0.285a**	**0.032a**	**0.005a**	**0.111a**
	St. Dev.	**0.42**	**-**	**0.009**	**0.069**	**0.003**	**0.024**	**0.015**	**0.002**	**0.116**
LIK-01	Downstream	3.86	31.3	0.552	0.673	1.564	0.327	0.170	0.018	0.473
LIK-02	Middle	3.79	31.0	0.572	0.557	1.542	0.329	0.168	0.018	0.488
LIK-03	Upstream	3.75	31.2	0.612	0.364	1.496	0.282	0.158	0.017	0.371
	Mean	**3.80b**	**-**	**0.579b**	**0.531b**	**1.53b**	**0.313a**	**0.166b**	**0.018b**	**0.444b**
	St. Dev.	**0.06**	**-**	**0.030**	**0.156**	**0.03**	**0.026**	**0.006**	**0.001**	**0.064**
UBG-01	Downstream	7.39	26.0	0.054	4.294	0.090	1.295	1.887	0.001	1.690
UBG-02	Middle	7.34	25.9	0.037	4.409	0.055	1.280	1.882	0.000	1.744
UBG-03	Upstream	7.43	25.7	0.069	4.181	0.123	1.195	1.798	0.001	1.612
	Mean	**7.39c**	**-**	**0.053a**	**4.295c**	**0.09c**	**1.257b**	**1.856c**	**0.001c**	**1.682c**
	St. Dev.	**0.05**	**-**	**0.016**	**0.114**	**0.03**	**0.054**	**0.050**	**0.000**	**0.066**

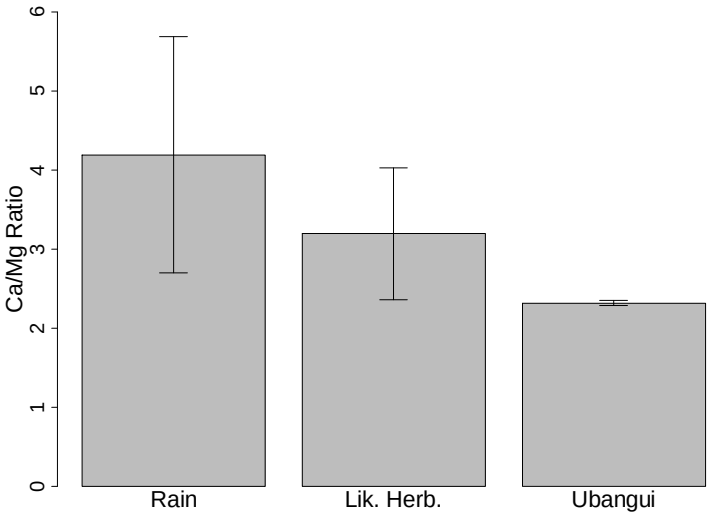

Figure 6.13. Mean Ca/Mg ratios for the rain, Likouala aux Herbes River and Ubangui River water samples. Error bars show the standard deviation.

6.5.3. Surface Peat and OM Metal Cation Concentrations

Of the metal cations measured (Al, Ca, Fe, K, Mg, Mn, Na, Pb, Ti) all nine sites showed low concentrations (mg kg^{-1}) in surface peat and OM samples, including the non-peatland site Moungouma (Figure 6.14). For all sites Al, followed by Fe, were present in the highest concentrations, with concentrations of Al being considerably higher than for any other cation. The relative order of concentration for the remaining cations differed between sites. In general there was no difference between the mean cation concentrations of the peatland sites. The exceptions to this are the Bondoki mean Ca concentration, which was significantly higher than Bondzale and the Centre ($p=0.047$ and $p=0.02$ respectively, One-Way ANOVA and a post hoc Tukey test), and the Bondoki mean Fe concentration, which was significantly lower than Itanga ($p=0.02$, One-Way ANOVA and a post hoc Tukey test). Although only two samples are available for Moungouma, these surface soil samples had much higher mean concentrations of Al, Fe, K, Na and Ti than any of the peatland sites; furthermore, the concentration of these cations in the Moungouma sample which came from the old meander closest to the present location of the Ubangui, were noticeably higher than in the sample taken further away from the Ubangui. Mean Ca/Mg ratios were not found to be significantly different between sites (One-Way ANOVA). All samples, including the Moungouma (non-peatland) samples (but excepting one sample from Ekolongouma) had Ca/Mg ratios lower than the mean rain and Likouala aux Herbes Ca/Mg ratios (Fig. 6.15). A few samples had Ca/Mg ratios higher than the mean Ca/Mg ratio of the Ubangui water samples. In summary, all sites had low cation concentrations, but cation concentrations of the non-peatland site, Moungouma, adjacent to the white water Ubangui, were higher than the peatland sites. All sites had Ca/Mg ratios, which overall were lower than the rain and river water Ca/Mg ratios. This coupled with the fact that the river and

rainwater samples did not have significantly different Ca/Mg ratios, means that ombrotrophic or minerotrophic conditions could not be determined from the Ca/Mg ratios.

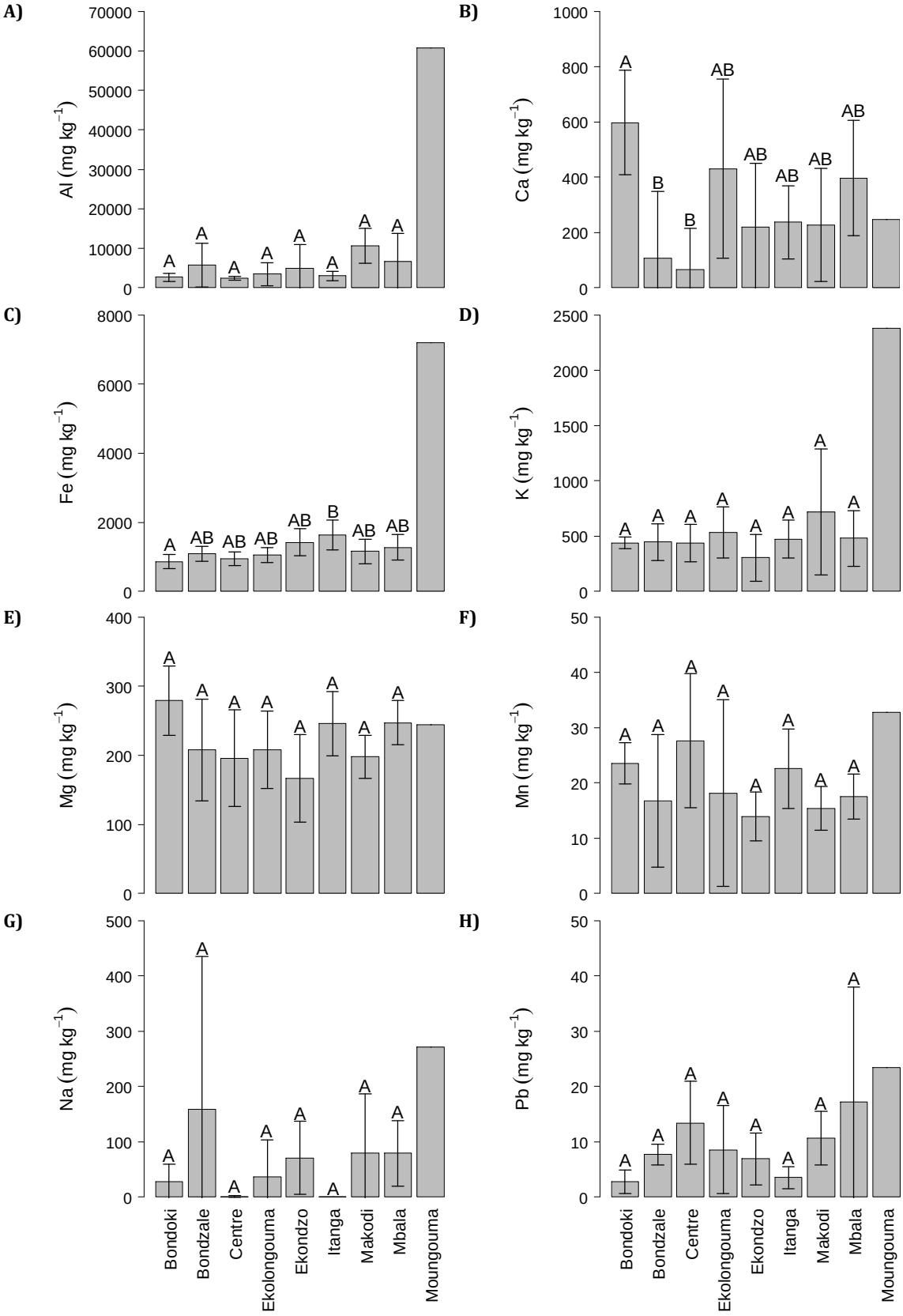

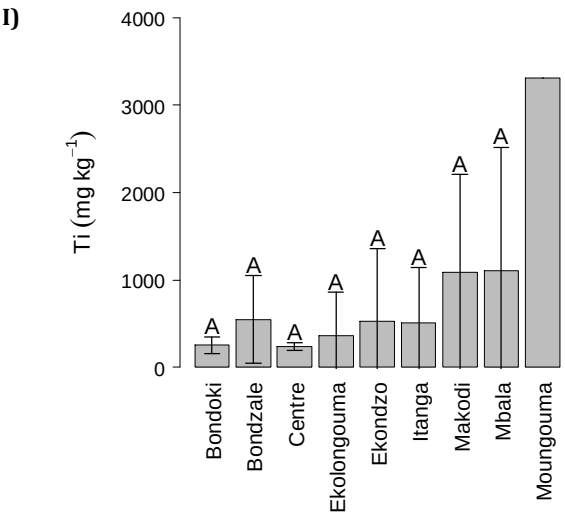

Figure 6.14. Surface peat and surface OM mean cation concentrations under swamp vegetation across the nine sites. Error bars represent the standard deviation. Means which do not share a common letter are significantly different ($p<0.05$, Kruskall-Wallis multiple comparison test (panel B;F-I) and ONE-WAY ANOVA (panel A;B-D)).

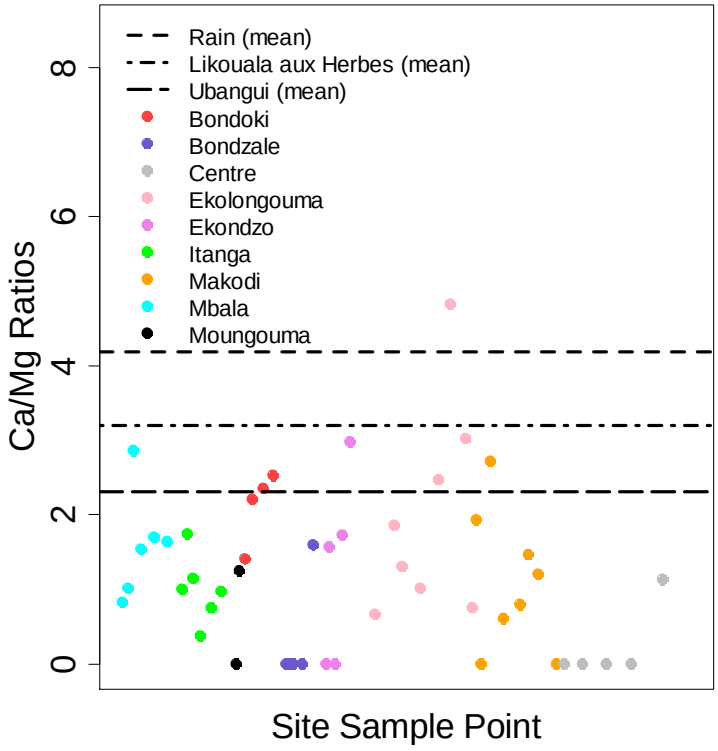

Figure 6.15. Surface sample Ca/Mg ratios for the nine transects. The mean Ca/Mg ratios of the rain, Likouala aux Herbes and Ubangui water samples are shown as dashed lines.

6.5.4. Peat Metal Cation Concentrations Down Core

From the analyses of the down core samples of peat metal cations (Fig. 6.16 to 6.23), some general patterns can be seen across a number of cores. Firstly Al and Ti concentrations seem to be correlated and increase towards the base of the cores. Fe, K, Mg and Mn all have relatively high surface values which decrease with increasing depth down core, before increasing again towards the base of the cores. Although a few cores show no

obvious pattern in Ca concentrations (e.g. Fig. 6.19, Fig. 6.21 and Fig. 6.22), the other cores show a decrease in concentration with increasing depth down core. Na concentrations are generally very low throughout the cores, although several cores show large spikes in Na concentrations. Pb concentrations are also generally low, though some cores show Pb concentrations increasing towards the base.

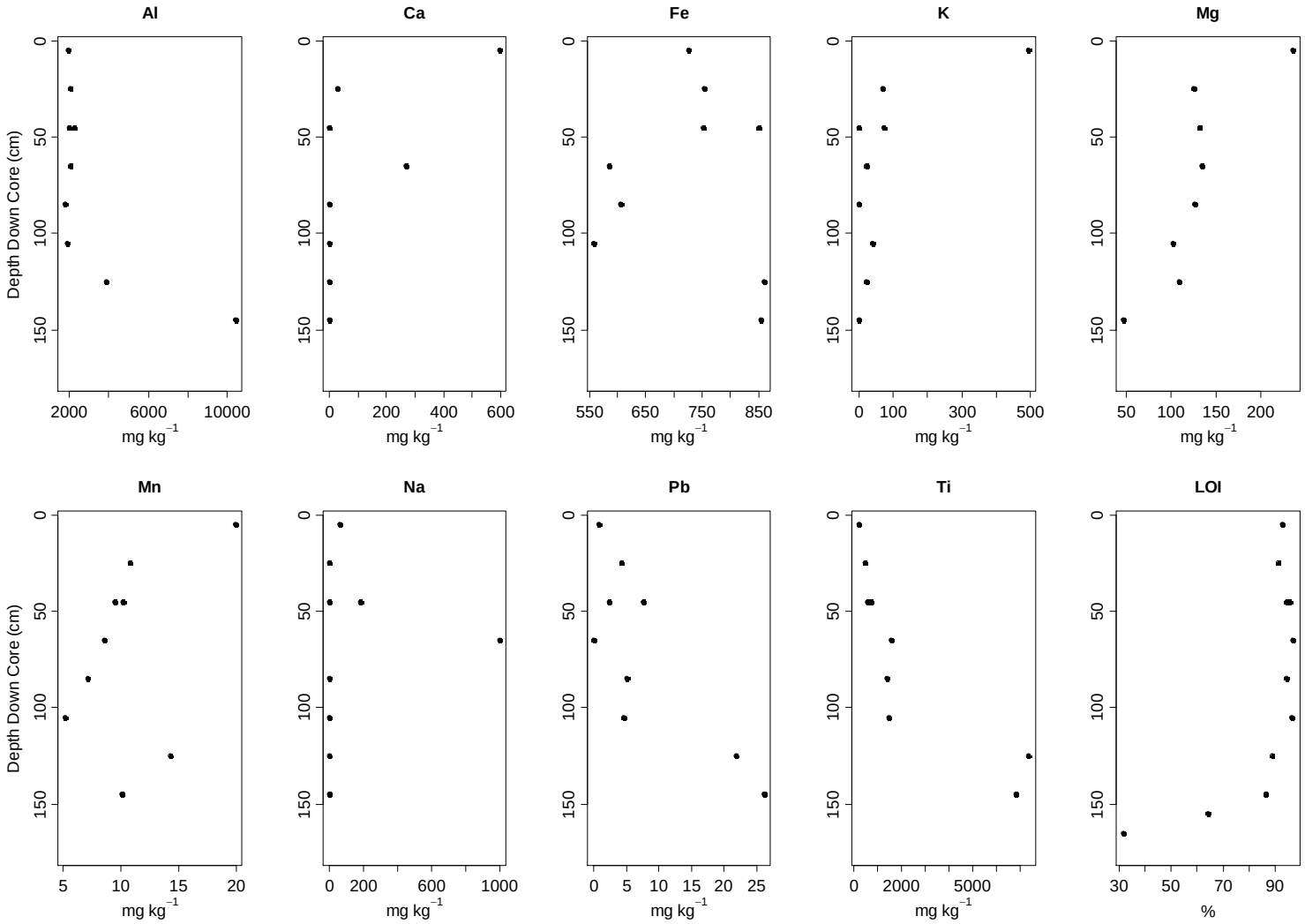

Figure 6.16. Down core cation concentrations and LOI values for the 6 km Bondoki core.

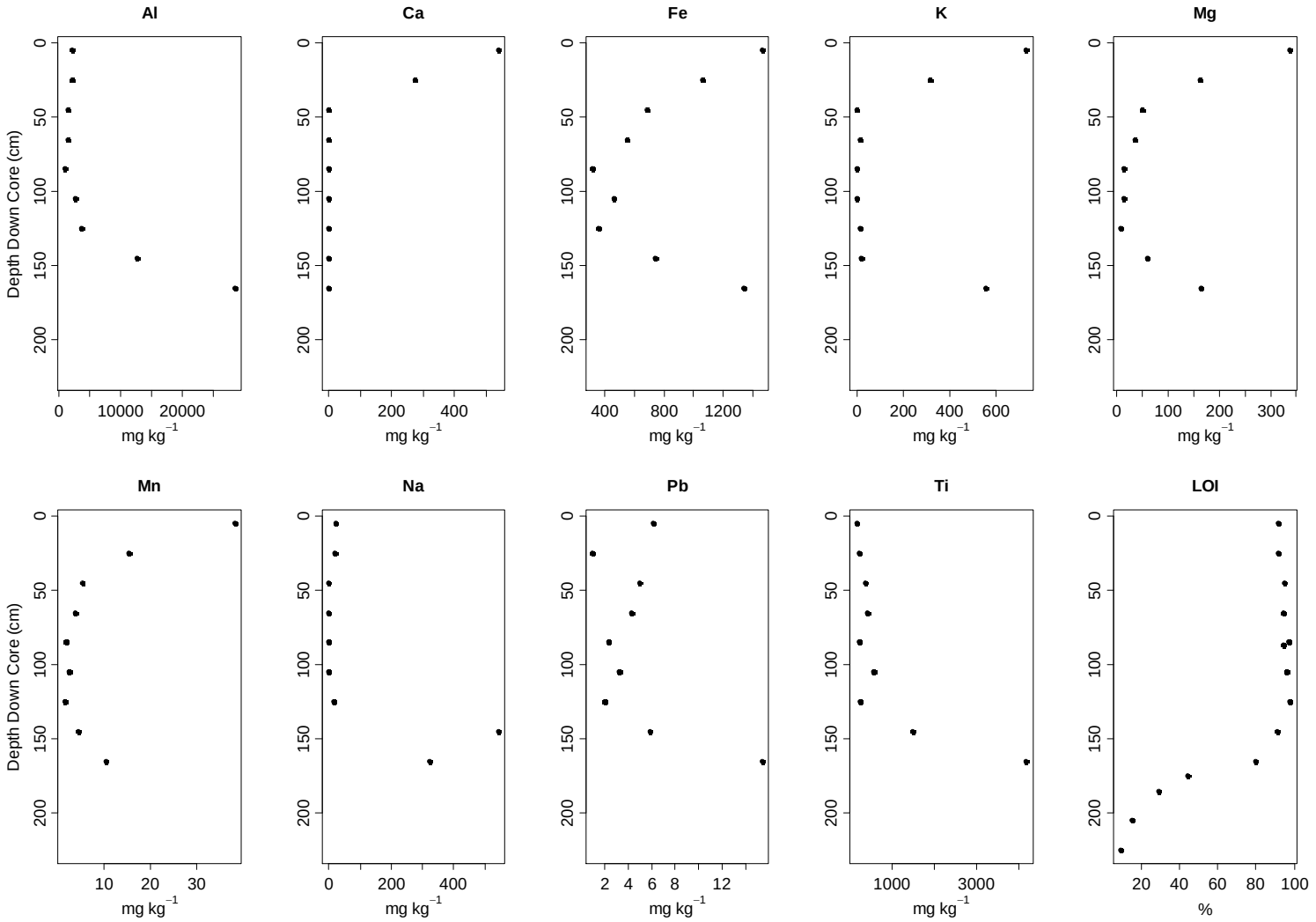

Figure 6.17. Down core cation concentrations and LOI values for the 6 km Bondzale core.

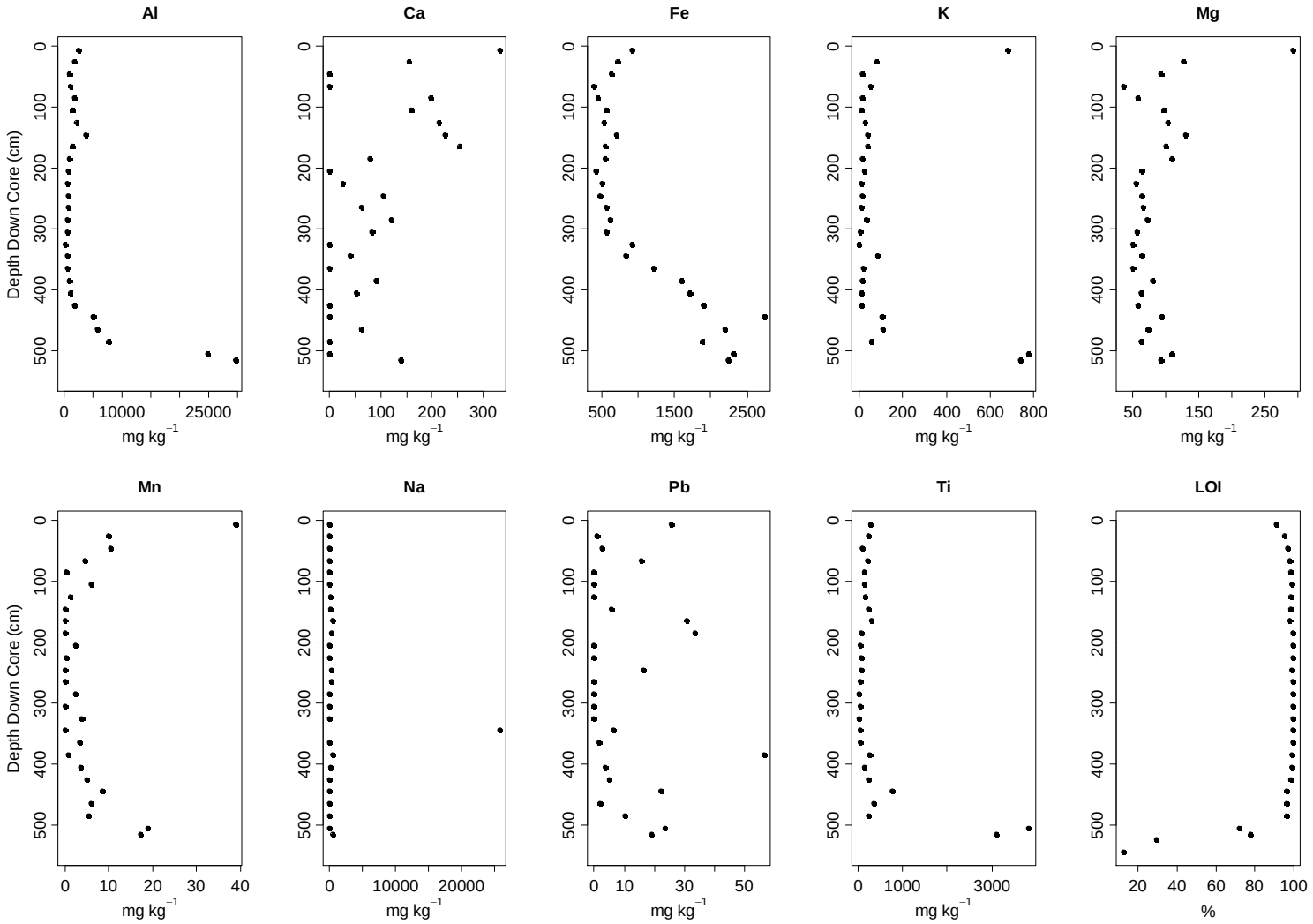

Figure 6.18. Down core cation concentrations and LOI values for 20 km Centre core.

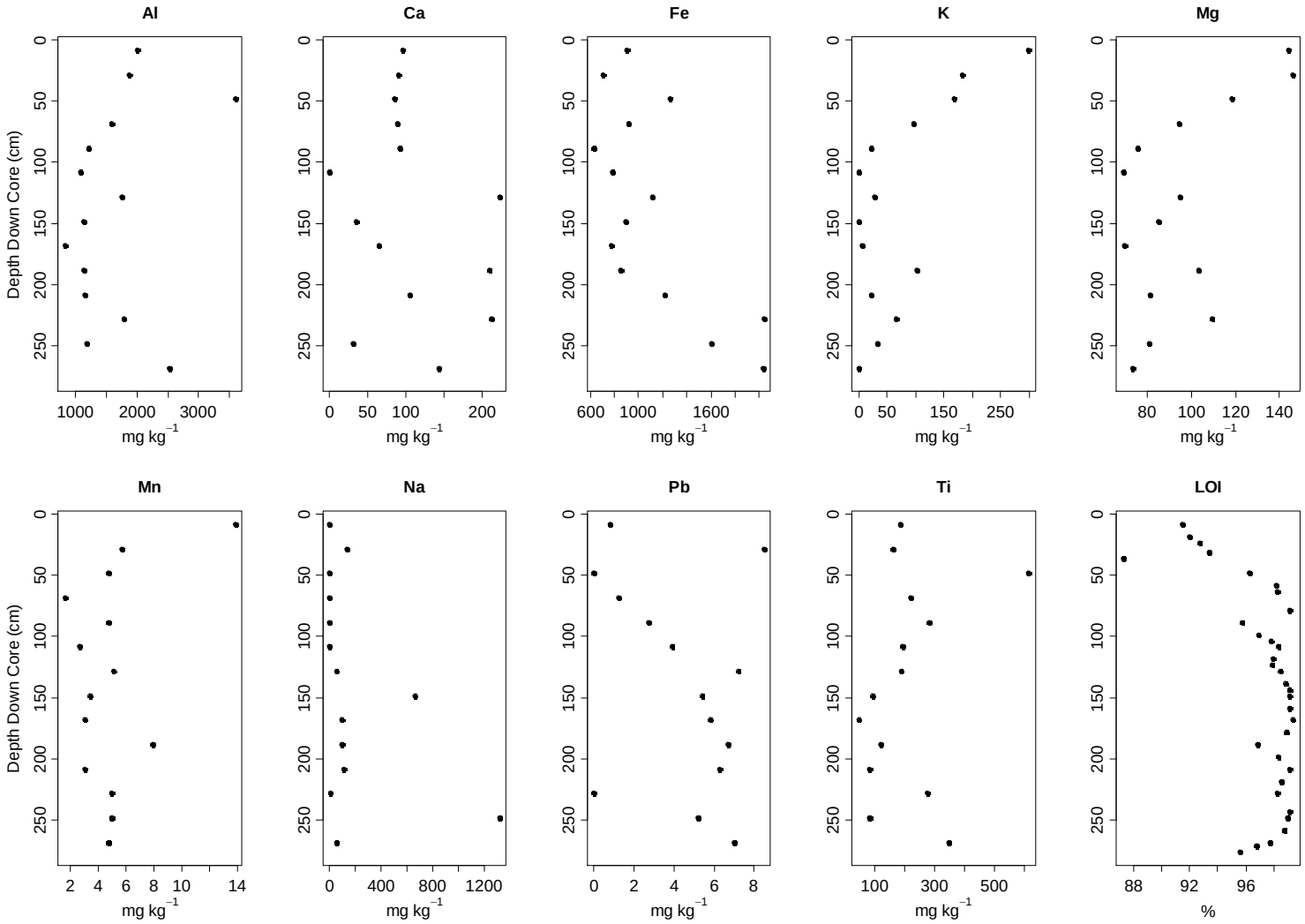

Figure 6.19. Down core cation concentrations and LOI values for the 9 km Ekolongouma core.

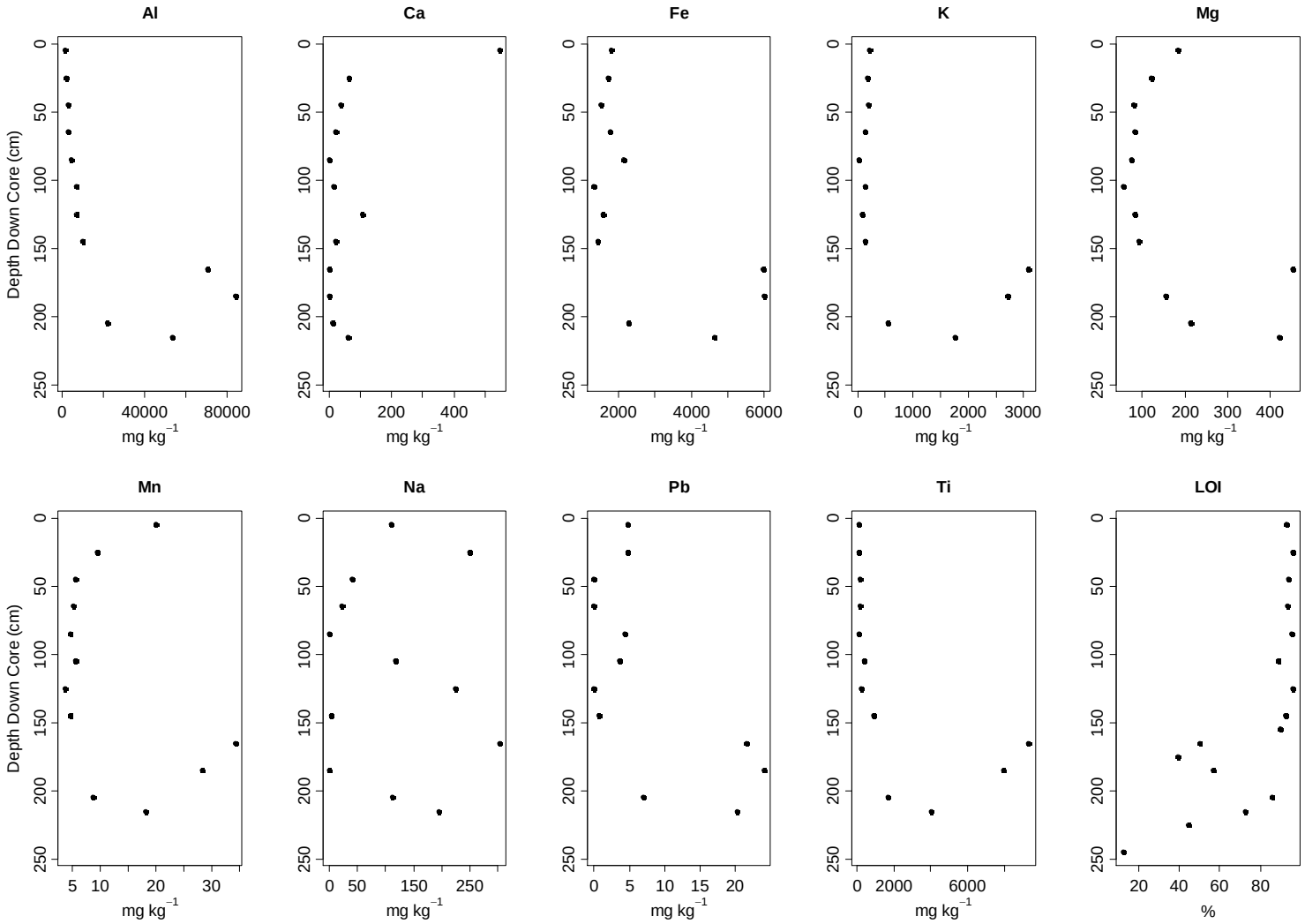

Figure 6.20. Down core cation concentrations and LOI values for 5 km Ekondzo core.

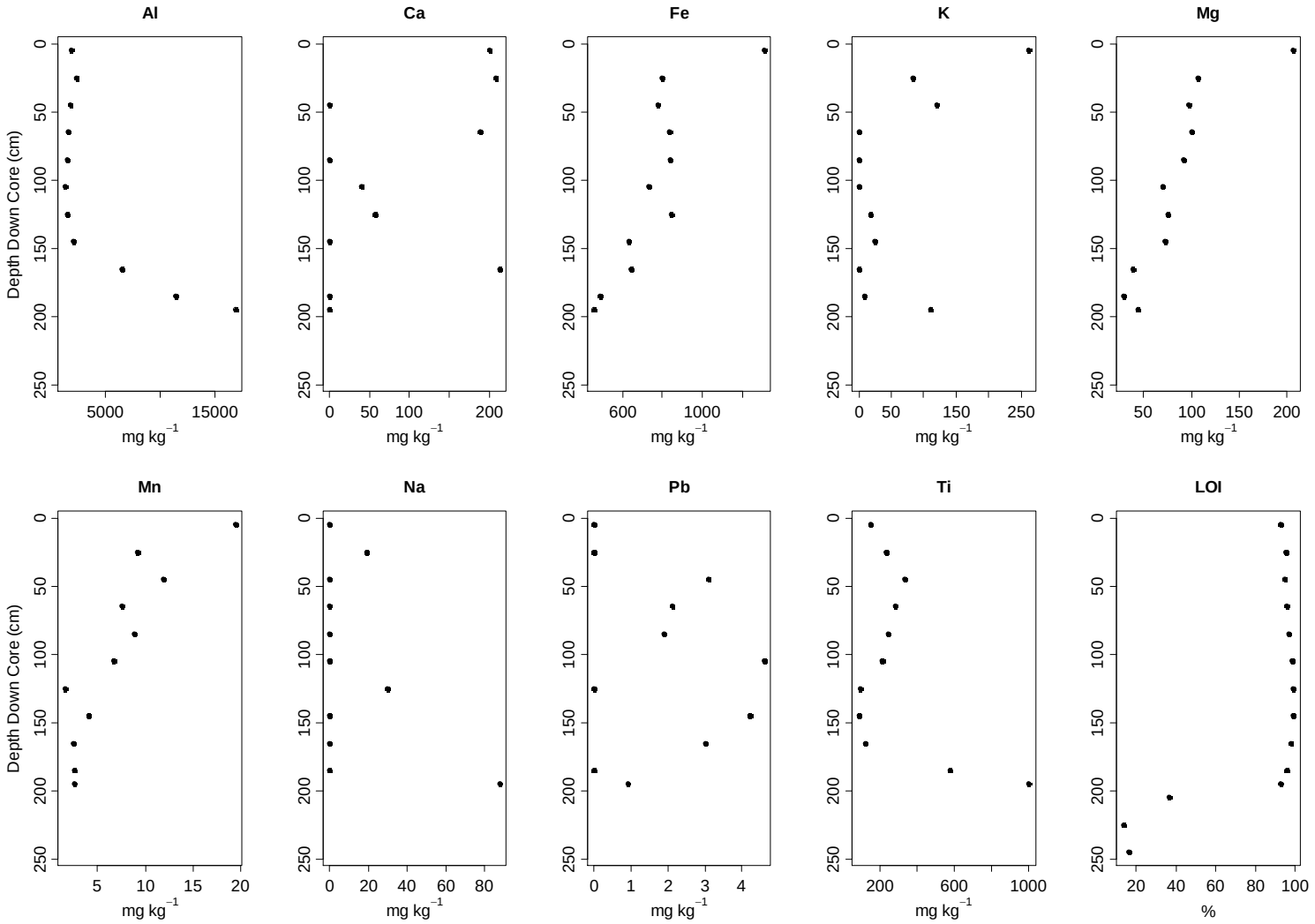

Figure 6.21. Down core cation concentrations and LOI values for the 6 km Itanga core.

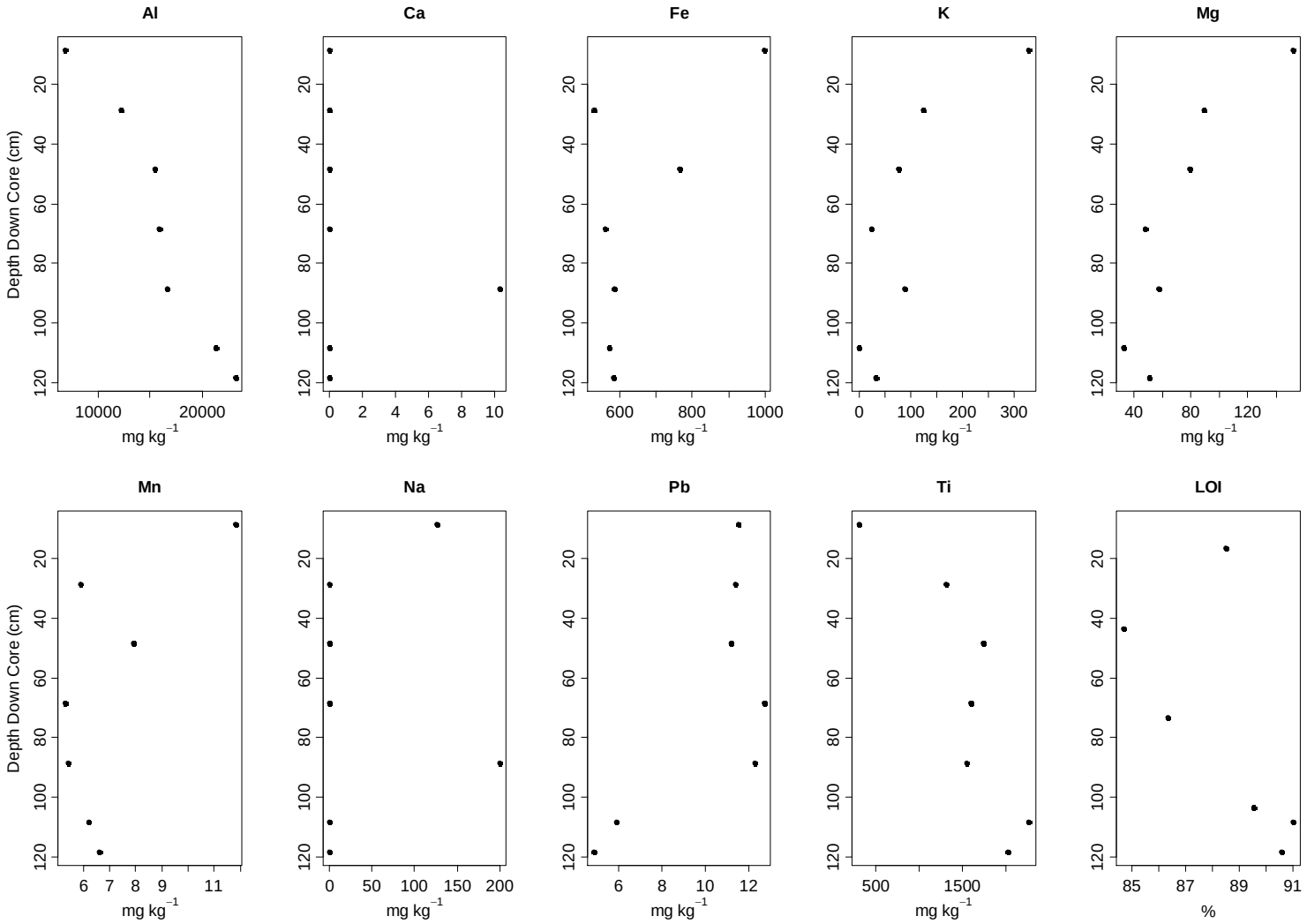

Figure 6.22. Down core cation concentrations and LOI values for the deepest Makodi core (not located along the transect).

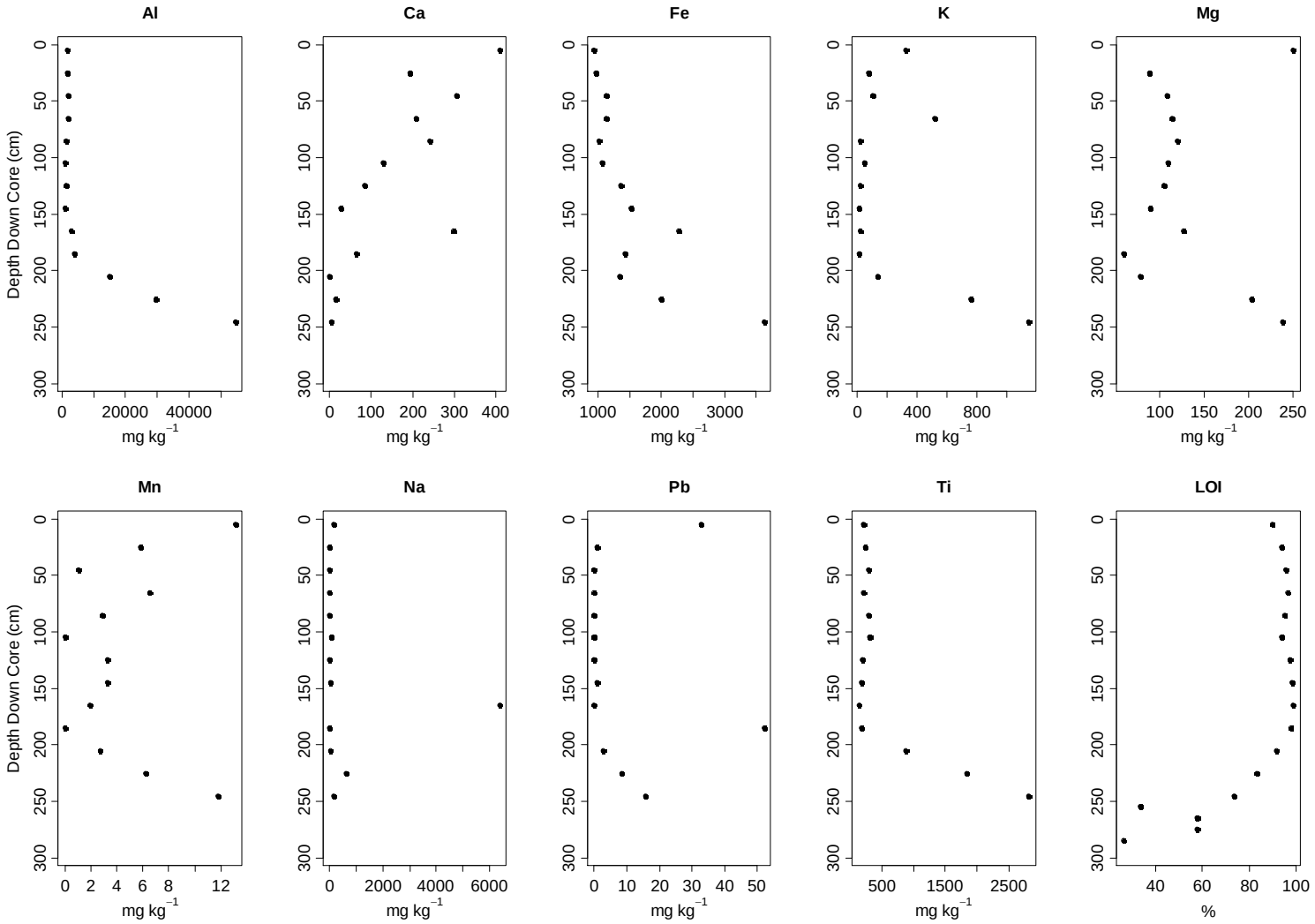

Figure 6.23. Down core cation concentrations and LOI values for 6 km Mbala core.

6.5.5. LOI Residues

The mineral matter present in peat surface samples was overwhelmingly of biological origin (Table 6.6). The majority of the biologically derived mineral matter was made up of plant phytoliths, whilst some samples were also found to contain pennate diatoms and sponge spicules. The non-biological mineral material present in the surface samples was almost entirely composed of silt sized grains (≤20 μm). Only two surface samples were found to contain sand sized grains (>20 μm); the Itanga 2 km sample (which was also unusual in not having a majority of mineral matter being of biological origin) and the Moungouma (non-peatland) 1.41 km sample.

Table 6.6. Origin of mineral material in surface and basal peat samples.

Site	Core (km)	Description	Depth (cm)	LOI (%)	Mineral Matter (%)	
					Biological	Non-Biological
Bondoki	3	Peat	0-10	92	96	4
	4	Peat	0-10	91	90	10
	5	Peat	0-10	93	100	0
	6	Peat	0-10	93	100	0
Bondzale	2	Peat	0-10	87	92	8
	4	Peat	0-10	95	98	2
	6	Peat	0-10	91	90	10
Centre	4	Peat	0-10	93	98	2
	8	Peat	0-10	94	100	0
	12	Peat	0-10	93	98	2
	16	Peat	0-10	93	96	4
	20	Peat	3-10	91	100	0
Ekondzo	2	Peat	0-10	93	88	12
	3	Peat (surface peat not recoverable)	NA	NA	NA	NA
	4	Peat	0-10	91	100	0
	5	Peat	0-10	93	100	0
Itanga	0	Peat: stream under savannah draining swamp.	0-10	80	86	14
	0.83	Not peat: stream under *Raphia hookeri* palm dominated swamp.	0-10	61	84	16
	2	Peat: stream under *Raphia hookeri* palm dominated swamp draining swamp	0-10	87	48	52
	4	Peat	0-10	95	90	10
	6	Peat	0-10	93	100	0
Mbala	1.25	Peat: stream draining the swamp under hardwood swamp.	0-10	84	92	8
	2	Not peat:	0-10	80	62	38
	3	Peat	0-10	88	96	4
	4	Peat	0-10	91	100	0
	6	Peat	0-10	90	100	0
Moungouma	0.78	Not peat: old meander under *Raphia hookeri* palm dominated swamp.	0-10	84	94	6
	1.41	Not peat: old meander under *Raphia hookeri* palm dominated swamp.	0-10	64	60	40

6.6. Discussion

6.6.1. Relationships Between Hydrology and Peat Depth and Vegetation

The differing vegetation communities overlying peat in South East Asia and Amazonia are considered to be driven largely by variations in hydrology and nutrient levels, the latter of which is often strongly linked to hydrology (Page et al., 1999, Draper et al., 2014). In this study however, and across all the fieldwork, there was no obvious difference in the water table regimes of areas under the two main vegetation communities associated with peat in the Cuvette Centrale (hardwood swamp and *Raphia laurentii* palm dominated swamp). Likewise there appears to be no discernible relationship between peat depth and water table regime; it might have been expected that areas of deeper peat were the result of higher water tables or longer periods of inundation, allowing higher rates of OM accumulation. Although unexpected, the apparent lack of a relationship between hydrology and vegetation and hydrology and peat depth could be genuine. As these peatlands appear to occupy large, shallow basins and have a flat surface (see Chapter 2), then one would expect that even as the peat got deeper towards the interior, the distance from the surface to the water table would remain approximately constant across the peatland (Fig. 6.24). Under this scenario the spatial distribution of different vegetation communities occupying the basin is unlikely to be linked to depth to water table.

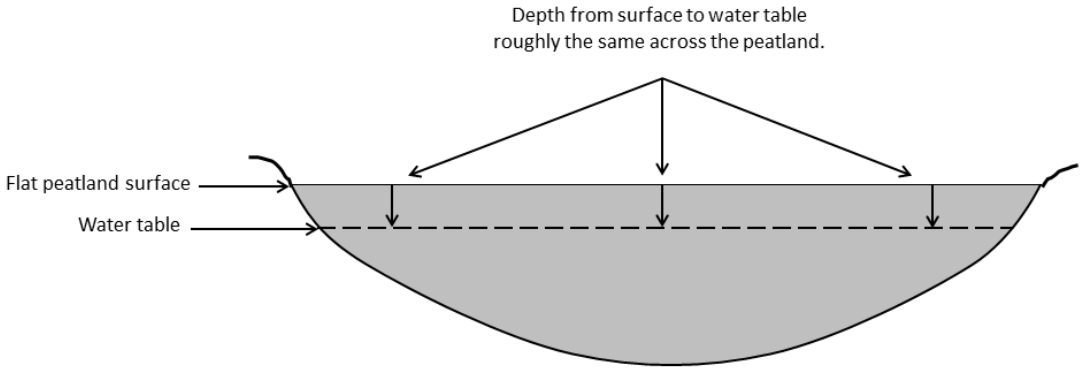

Figure 6.24. Schematic showing water table depth across a flat surfaced peatland occupying a basin.

Alternatively the lack of a relationship between the hydrology and vegetation or peat depth could be an artefact of the short time frame over which water table measurements were made or the peatland microtopography. As TRMM data suggests, 2013 may have been a wetter than typical year (Fig 6.11) and with only one full year's worth of water table measurements, any long term patterns cannot be detected. This last point is particularly important, because spatial patterns in vegetation communities and peat depth

are the result of long-term processes operating on decadal to millennial time-scales (Charman, 2002).

Any relationships between hydrology and vegetation and peat depth could be obscured by peatland microtopography. Peatlands often have a complex hummock-hollow microtopography and in forested tropical peatlands, buttressed trees and networks of aerial roots create mounds, whilst areas between trees are flat and uprooted trees can create deep hollows (Shimamura and Momose, 2005, Dommain et al., 2015). The pressure transducers were all installed away from trees in flat or small depressions. Even so the different dimensions of these small depressions will undoubtedly affect the measured water table height. Additionally there could also be small scale ponding caused by the presence of buttressed roots and woody debris nearby (Dommain et al., 2010).

6.6.2. Determining the Role of Rain and Rivers in Peatland Inundation

The lack of any flood waves observable in the peatland water table time series, such as the one recorded in a Peruvian lowland peatland (Fig. 6.25; Lawson et al., 2014) and the sharp rises followed by slower falls in water table height, considered symptomatic of rainfall events, indicates that for the time period over which measurements were made, there was no large scale river flood event. Likewise the RC values in water table height were of similar magnitude to published rainfall intensities (Table 6.7) and therefore could feasibly be the result of rainfall alone. The much lower RC values seen at the Bondoki 5 km and 6 km sample points are accounted for by the plateauing of water tables, discussed in section 6.5.7. The timing of the maximum *RC* values further supports the idea that they resulted from rainfall alone; many of the top ten *RC* values occurred outside of the major wet season (September to November) when river levels are below their banks. This includes the absolute maximum *RC* value of 210 mm hr^{-1}, which occurred at Bondzale on the 23rd of March 2014; a time when I was in the field in the Likouala Department and observed that neither the Ubangui nor the Likouala aux Herbes rivers had breached their banks. However, measurements of rain intensity are dependent on the time interval over which the measurement was made and this, therefore, makes it difficult to compare directly with published values, as none of the values presented in Table 6.7 were recorded over a 20 minute time period. With hindsight the ideal solution would be to record rainfall *in situ* at each of the four sites in time intervals that match the water table measurements. Furthermore the two approaches of visually looking for a flood wave and considering the magnitude of *RC* values, assume that a river flood event would result in a sudden and sizeable rise in water table height and this may not necessarily be the case.

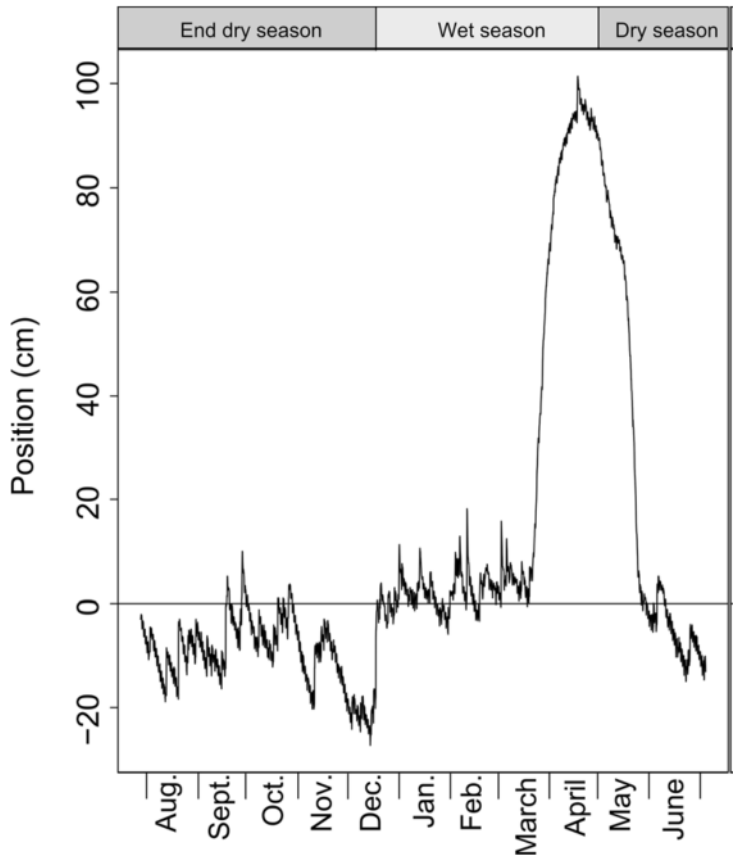

Figure 6.25. Peatland water table time series from Quistococha, a Peruvian lowland peatland, taken from (Lawson et al., 2014).

Table 6.7. Maximum rainfall intensities recorded in tropical regions taken from the literature.

Study	Location	Maximum rainfall intensity (mm hr^{-1})	Time interval (mins)*
Salako et al. (1995)	Okomu, southern Nigeria	240	7.5
Ojo and Olurotimi (2014)	Lagos, Nigeria	207	1
	Akure, Nigeria	180	1
Bidin and Chappell (2006)	Northeast Borneo, Malaysia	74	5
Krishnaswamy et al. (2012)	Western Ghats, India	72.5	30

*Time interval refers to the time period over which the rain intensity was measured. This is reported because rain intensity values are dependent on the time interval.

Overall the monthly CIWT were of similar magnitude to TRMM total monthly rainfall estimates. In particular, during the major wet season (September to November) when river flooding is most likely to occur, TRMM rainfall estimates were able to account for peatland water table increases. At Bondzale however, between December 2013 and April 2014, TRMM rainfall estimates could not account for the CIWT values and were sometimes as much as half the CIWT value. This could mean CIWT values were not solely the result of rainfall and there is an additional flooding source or that TRMM underestimated rainfall for these months and location. If the former, river flooding can be ruled out because the

rivers were observed to be below their banks at this time. With regards to the latter, the temporal and spatial resolution (0.25°x0.25°) of TRMM and the short lived, localised nature of some tropical rain events, mean a rain event could occur within the 0.25°x0.25° area but not pass over the sample point in question or a short duration rain event could occur within the 3 hour window without detection by TRMM. Evidence for this is firstly the relatively weak relationship between rainfall estimates for Epena village by rain gauge and TRMM (Fig. 6.10) where there are instances of one estimate being over 100% greater than the other, and secondly the occasional TRMM rain event which does not correspond to a rise in water tables or vice versa (as seen in Fig 6.9). The *RC* values, if attributable to rainfall, show there were particularly intense rain events at Bondzale in March 2014; if particularly intense rain events are occasionally not detected by TRMM this could lead to a substantial underestimation of rainfall. In other regions of the tropics it has been shown that without high frequency temporal measurements and a dense network of rain gauge stations, rainfall for a relatively small region will be underestimated (Sane et al., 2012, Bidin and Chappell, 2006). Once again, although difficult to obtain, *in situ* rain measurements would have greatly improved this analysis.

With only one year of data, river flood events which occur at a frequency of more than a year cannot be ruled out. Discharge records show the Ubangui to have high interannual variation and upstream in the Central African Republic, Ubangui floods events have an estimated return period of 7 to 35 years (Runge and Nguimalet, 2005). The Likouala aux Herbes has a less variable interannual discharge, however records dating back to the 1950s show that for the period 1960 to 1970 both the Unbangui and Likouala aux Herbes experienced a period of unusually high discharges (Laraque et al., 2001). Therefore flooding may occur occassionally. However even then, the rivers may still have little influence over peatland water tables. It is possible that if the peatlands and adjacent areas of savannah and seasonally flooded forest are already inundated due to rainfall, this may block any major influx of river water to the peatlands (Mertes, 1997).

Even if the peatlands experience periodic influxes of river waters, the lack of river flooding in the year of recorded data suggests the rivers do not help to maintain peatland water tables in the Cuvette Centrale. The idea that the hydrology of the swamps is not determined by the rivers of the region is not new. Lee et al. (2011) have shown, through the remote sensing of gravimetric and altimeter measurements, over the period January 2003 to December 2008, that the rise in Cuvette Centrale swamp water levels is greater than the stage rise in the rivers and swamp water levels are consistently above river levels, suggesting an independence between swamp water table levels and river stage. Additionally Jung et al. (2010b), who used altimeter measurements to characterise

floodplain features and flow patterns of the Cuvette Centrale and the Amazon wetlands, note that, unlike the Amazonian wetlands, there are very few channels connecting the swamps of the Cuvette Centrale to the rivers, limiting water movement between the two.

6.6.3. Semi-Diurnal and Diurnal Water Table Fluctuations

The semi-diurnal cyclical fluctuations recorded in the some of the water table time series and all the barologger time series are very similar to atmospheric pressure fluctuations attributable to atmospheric tides (Fig. 6.26). Atmospheric tides are caused by the moon's gravitational force and the sun's solar and gravitational force and result in semi-diurnal fluctuations in atmospheric pressure (Zurbenko and Potrzeba, 2013). However, for these to be recorded in the water table data must mean that some of the pressure transducers have not been properly compensated for atmospheric pressure. This could be due to a malfunctioning barologger or a problem with the software used to compensate the pressure transducers that result in a few of the water table time series still retaining some of the atmospheric pressure signal. To test for the former, a pressure transducer from the Bondzale transect which showed the semi-diurnal signal was compensated with the closet barologger and another further along the Bondzale transect, next to a pressure transducer which did not show the semi-diurnal signal. The two compensated signals both showed the semi-diurnal signal. When the atmospheric pressure measurements from the two barologgers were differenced, the maximum difference between the two was 0.11 k Pa and the mean was 0.03 k Pa. This compares to atmospheric pressure ranges of 1.52 k Pa and 1.57 k Pa recorded by the two barologgers. This suggests that, despite being 2 km apart, the two barologgers recorded similar atmospheric pressure values. Therefore, the semi-diurnal signal is not caused by a barologger malfunction, but seems to be owing to the software not fully compensating for atmospheric pressure for all pressure transducers. For the diurnal signal, there is no reason to believe that this is an artefact of the software and is therefore attributed to ET, as the minima occurs mid-afternoon when temperatures are at their highest and the ET potential should be highest. Detecting an ET signal in ground water measurements is not unusual and has been observed in other studies (e.g. White, 1932, Schilling, 2007, Wang et al., 2014).

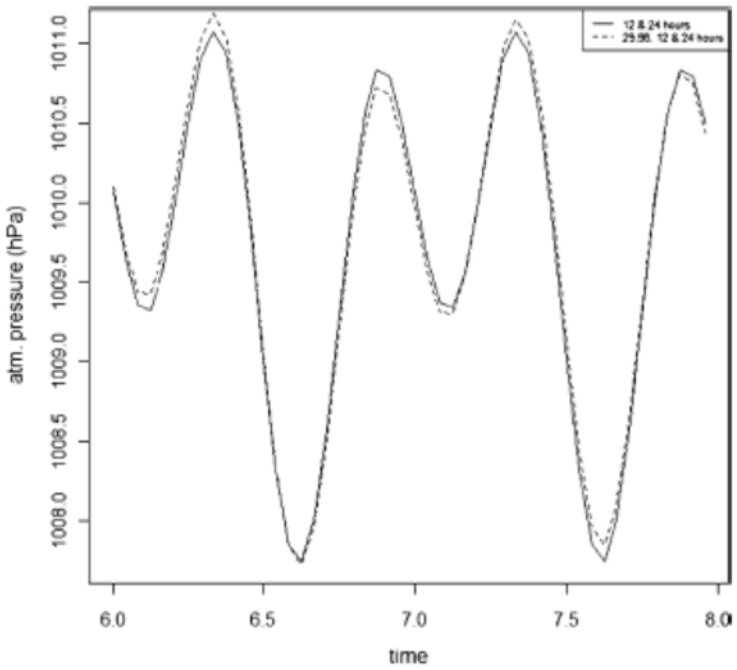

Figure 6.26. Atmospheric tides recorded in an atmospheric pressure time series presented in Zurbenko and Potrzeba (2013)

6.6.4. Peatland Groundwater Recharge

In a number of the water table time series, a slight increase can be seen in water table levels following the ET-driven daily water table minima (e.g. Fig. 6.5 C). This pattern is also seen in other studies (White, 1932, Wang et al., 2014, Schilling, 2007) and is attributed to water table recharge from ground water flow. In this study, if one assumes that the difference between monthly CIWT before and after the ET signal is removed is approximately equivalent to the rise in water tables attributable to ground water flow, then groundwater flow could account for 56-86% of total increase in water table. This ground water flow could either come from outside of the peatland or could be internal lateral flow within the peatland. For the former to occur a negative hydraulic head needs to exist within the peatland relative to the adjacent land. However, as mentioned earlier, Lee et al. (2011) demonstrated that river levels were consistently lower than the swamp water levels over the duration of their study. If so, this means a positive difference in hydraulic head exists between the peatlands and rivers and therefore implies that the direction of ground water flow is from the peatlands to the adjacent land rather than vice versa. If a peatland drainage outlet exists (which is thought to be the case in the Cuvette Centrale peatlands; see section 6.5.5) then there will also be a net lateral flow towards that drainage outlet, which may also account for the recharge. Likewise, complex microtopography and localised differences in ET, driven by variations in vegetation density, size and species, can produce highly variable hydraulic gradients across peatlands, which result in high spatial and temporal variations in internal groundwater

recharge (Drexler et al., 1999). However, this is an area that would benefit from further study.

To summarise, the peatland water table measurements do not detect major river flood events over the time period investigated and the data suggest that rainfall events can account for all sudden rises in water tables. However it is not clear from the water table data whether these peatlands are truly ombrotrophic, as there is still the possibility of infrequent river flood events not detected in the relatively short time series and that of ground water flow into the peatlands. Although, with regards to the latter, higher water levels in the peatlands than in the adjacent rivers suggest that water is more likely to flow from the peatlands to the adjacent land, which would mean the observed recharge is due to peatland internal flow.

6.6.5. Peatland Drainage

In the Cuvette Centrale water loss from peatlands can occur through three processes; ET, ground water flow or surface flow via channels. Being inherently difficult to measure, ET estimates are seldom based on direct measurements and different methods can produce very different values for the same region. For example Rodell et al. (2011) compared several modelled ET estimates for the Ubangui river basin; the mean daily ET estimates ranged from 2.11 to 4.53 mm day^{-1}. The ET estimates used here for comparison with the CDWT values also vary widely. Differences in spatial scales and location between studies within the Congo Basin will partially account for this, but it is also a sign that ET estimates over the basin are poorly constrained. As discussed earlier, an ET signal was detected in the water table time series. If specific yield data is available water table time series can be used to estimate ET by using the method of White (1932). In the future, specific yield data from the Cuvette Centrale would permit a more direct estimate of ET to be made, improving understanding of the hydrological balance of these wetlands. Despite the large variation, using any of the three ET estimates leads to the same conclusion; ET cannot account for the majority of water loss from the peatlands and therefore substantial drainage via ground water or channels must be involved.

Although the swamps of the Cuvette Centrale are relatively disconnected from the rivers of the region (Jung et al., 2010b), when travelling on both the Likouala aux Herbes and the Ubangui rivers, at various points small channels can be seen joining the rivers, which originate from the swamps. Furthermore, at a number of the field sites (e.g. Mbala, Bondoki, Itanga and Ekondzo), towards the swamp margins, there are a series of small or seasonal, slow moving, black water channels, some of which contain shallow peat deposits, which are clearly draining the swamps. Although small and few in number, these channels

could be responsible for the evacuation of a large proportion of the water from the peatlands.

Ground water flow could also partially account for peatland drainage. As mentioned previously, the proportion of water leaving the peatland via ground water increases during dry the seasons as channel levels drop (Mann et al., 2014). However, even during the dry season, the Likouala aux Herbes, if not the Ubangui, is probably fed to a large extent by surface flow from the peatlands, given its high OM; Johnson et al. (2006) showed that in Amazonian headwater catchments, DOC levels were an order of magnitude higher in overland flow than subsurface flows. Therefore it seems unlikely that the extremely high levels of DOM and POC in the Likouala aux Herbes River would occur if most of the water from the peatlands did not leave via channels.

6.5.6. Phenomena Affecting Magnitude of Below Surface Peatland Water Table Fluctuations

It was recognised early on that CIWT for months where the water table was below the peat surface could not be compared to TRMM rainfall estimates, owing to the specific yield of the peat, which causes water tables to rise disproportionately to the volume of water received. Although not considered at the time, there are at least two other phenomena which can cause similar effects. These are the Reverse Wieringermeer Effect and the Lisse Effect. The former causes an actual rise in water tables and occurs in soils, such as peatlands, which have large capillary fringes that extend to the surface. The limited pore space available in the capillary fringe for infiltrating water, results in rapid and large rises in the water table during rain events (Fig. 6.27; Jaber et al., 2006, Gillham, 1984, Miyazaki et al., 2012, Heliotis and Dewitt, 1987). The Lisee Effect, however, impacts not on the water table itself, but on water table measurements. Under high intensity rainfall, a seal of water can develop on the peatland surface trapping any air present in the unsaturated, vadose zone. As the surface water tries to infiltrate down into the peat, the pressure increases in the vadose zone, exerting a downward pressure on the water table. The pipes in which the pressure transducers were installed would not experience this increase in air pressure. Therefore the water would flow from the area of high pressure to low pressure leading to a rise in water table in the plastic pipes (Fig. 6.28; Weeks, 2002, Miyazaki et al., 2012, Heliotis and Dewitt, 1987). No examples were found in the literature of the Lisse Effect being observed in a tropical setting, but given the intensity of tropical rain events, it seems likely that the Lisse Effect is of even more relevance to tropical hydrological studies than those carried out in boreal or temperate regions.

Whilst specific yields, the Lisse Effect and the Reverse Wieringermeer Effect were not considered at the time of installation of the pressure transducers, it would have been

beyond the scope of this study to adequately account for them. For months when the water table is continuously above the peatland surface, these phenomena should no longer come into effect. However, this is not a long term solution to the problem, as this requires part of the dataset to be excluded from the analysis. Therefore future work should aim to find a way to estimate these phenomena, although the high spatial and temporal variation of these phenomena could pose a challenge (Shah and Ross, 2009).

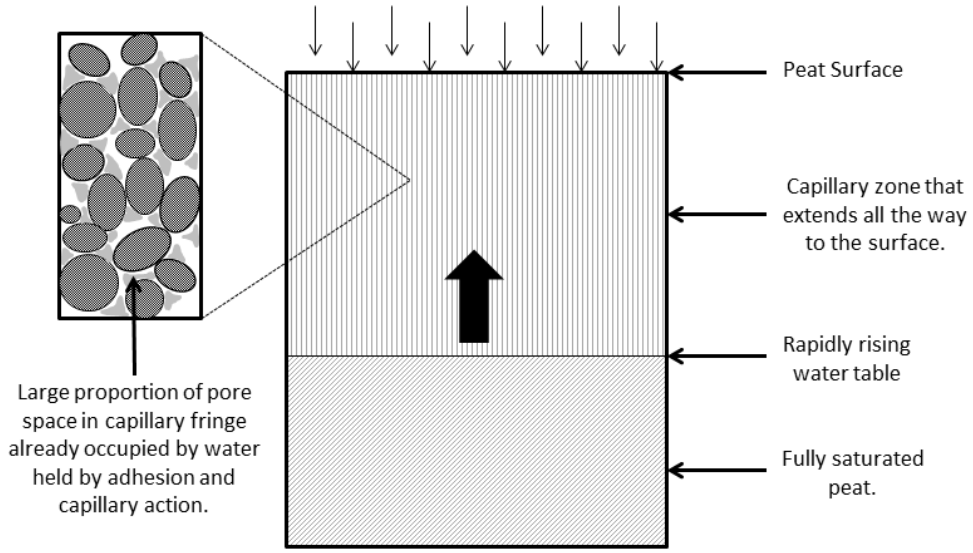

When water tables are shallow capillary fringes can extend all the way to the ground surface. The available pore space in the capillary fringe for infiltrating rain water can be limited, as pore space is already occupied by water held by adhesion and capillary action. Even under relatively light rainfall this can result in large and rapid increases in water table height.

Figure 6.27. Schematic showing the Reverse Wieringermeer Effect.

1. Intense rainfall seals the peatland surface preventing air escaping the vadose zone.
2. As surface waters slowly infiltrate down, pressure increases in the vadose zone.
3. The pressure gradient between the well and adjacent peat profile results in a rise in the water level in the well, whilst the water table remains virtually unchanged.

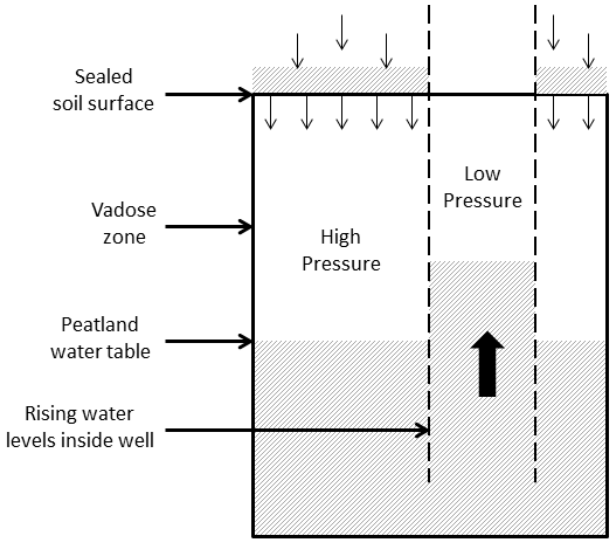

Figure 6.28. Schematic showing the Lisse Effect.

6.6.7. Oscillations in Peat Surface Elevation

The majority of peatland water tables showed similar patterns of sharp rises followed by gradual declines in water table. The Bondoki 5 km and 6 km water table time series, however, were unusual in that once water levels reached the peatland surface they did not change. I suggest that this is because the peatland surface began to float, and as the plastic pipes containing the pressure transducers were not fixed into the underlying mineral layer, they were free to rise and fall with the peatland surface. As water table measurements are relative to the peatland surface, if the peatland surface is oscillating with the water table, this results in no water table change being recorded. Floating peat surfaces were observed first hand in the field at Ekondzo, during a period when the site was completely inundated, although they were not observed directly at Bondoki. Floating peat surfaces have been reported for a number of higher latitude peatlands (e.g. Whittington et al., 2007, Whittington and Price, 2006, Fritz et al., 2008, Holm et al., 2000, Almendinger et al., 1986). The observed temporary nature of the phenomena is probably related to, what is known as, the compressibility of the peat (Fritz et al., 2008); initially as water tables drop, the peat surface will also drop, but eventually there will reach a point where the physical structure of the peat will prevent the peat surface from declining any further i.e. it will resist further compression. The lack of floating peat towards the margins of the peatland (shown by the lack of a plateau in the data at the Bondoki 4 km point) could be a result of higher bulk densities, higher mineral contents and lower porosity towards the peatland margins, resulting in reduced buoyancy (Holm et al., 2000). Additionally, the shallower peat may mean that the vegetation is more firmly rooted in the underlying mineral layer, helping to anchor down the peatland surface (Holm et al., 2000).

Since the pressure transducers were deliberately installed away from tree roots, it is hard to say whether seasonal oscillations in peat surfaces occur only in areas between trees or across the entire peat surface. Whilst the former seems more likely there is at least one measured instance of a forested peatland surface increasing in elevation with positive hydrological fluctuations (Almendinger et al., 1986). Changes in peatland surface elevation due to hydrologically induced swelling or floating are usually within the range of a few centimetres (Whittington and Price, 2006, Almendinger et al., 1986), although Fritz et al. (2008) report a maximum of 28 cm. Without having measured the phenomena directly it is not possible to say to what degree the peatland surface oscillates at Bondoki. However, if one considers that changes in water table levels at 4 km, 5 km and 6 km were of similar magnitudes in the months preceding October 2013 (Fig. 20), which is when the plateau in water tables began at 6 km and 5 km, then it seems reasonable to assume that the rises and falls in water table subsequently recorded at 4 km are of similar magnitude to the changes in surface elevation at 5 and 6 km. In October 2013 the water table reached a

maximum 23 cm centimetres above the surface at 4 km, whilst at 5 km and 6 km it was 1 cm and 4 cm below the surface respectively, suggesting that at 5 km and 6 km there was a maximum rise in surface elevation of ca. 23 cm.

In summary, there is good evidence to suggest that when inundated, in some locations within the Cuvette Centrale the surface peat layers float. This means that in some localities changes in peatland water table cannot be monitored via the method used here. It also means that for the areas which float, peat surface elevation, depth and bulk density (at least of the surface samples) are seasonally variable.

6.6.8. Water Table Time Series of the Seasonally Flooded Forest

Although the extreme rises in water table seen in the seasonally flooded forest initially appear too large to be from rainfall alone, rather than indicating river flooding, it is likely the result of some of the characteristic properties of the seasonally flooded forest. Unlike the adjacent peatlands, which have a relatively high hydraulic conductivity, the impermeable clay soils of the seasonally flooded forest will promote high surface run off in heavy rain events. Furthermore the seasonally flooded forests of the region tend to be much more topographically variable than the peatlands. Therefore it could be that during heavy rain events, the hole in which the pressure transducer was installed in the ground essentially acted like a drain, receiving all the local runoff from the surrounding mounds. The plateauing seen in the water table time series for the seasonally flooded forest is thought most likely due to an equipment malfunction. This is because, unlike the peatland sample points, there is no obvious mechanism to explain this phenomenon and the plateaux followed by very sharp spikes in water table level are suggestive of periods where the pressure transducer has failed to record changes in pressure, before recovering, giving rise to sharp spikes.

The lack of peat accumulation in the seasonally flooded forests of the Cuvette Centrale is because for the majority of the year water tables are well below the ground surface (as seen in Table 6.2) allowing the oxidation of OM. If water tables within the peatlands are maintained through rainfall, which the seasonally flooded forests are also in receipt of, the lower water tables of the seasonally flooded forest are a result of higher drainage rates, as demonstrated by the much faster decline in water table level in the seasonally flooded forest compared to the peatland sample locations along the Bondoki transect (Fig. 6.4 A). This is likely because of the slightly higher elevation of the seasonally flooded forest allowing it to sit above the regional water table for most of the year, except in extremely wet seasons when the regional water table rises.

6.6.9. River and Rainwater Characteristics

The cation concentrations of the river water samples were similar to other published values for the same two rivers and are consistent in that they show higher cation concentrations for the Ubangui, particularly Ca and Na, Mg and K, and lower concentrations for the Likouala aux Herbes River (literature summarised in Table 6.8). The rainwater samples are more variable, but these results and those of others show the regional rainwater to be slightly acidic, with low concentrations of cations (Table 6.8), as expected from an inland area with few anthropogenic impacts (Berner and Berner, 1996).

The differences in cation concentrations between the Likouala aux Herbes River and the Ubangui River reflect more obvious differences between the rivers and their catchments. Visually the two rivers differ markedly, the Ubangui being a white water river and the Likouala aux Herbes a black water river. This is the result of the two rivers draining two distinctly different hydrological basins. The Ubangui largely drains upland regions dominated by dry wooded savannah and semideciduous forest, where mechanical erosion is higher and there are relatively low levels of OM inputs (Coynel et al., 2005, Laraque et al., 2009). This explains the higher overall concentrations of cations and the particularly high concentrations of Ca, Na and Mg. The catchment of the Likouala aux Herbes however, is almost entirely covered in swamp forest and the very low hydraulic gradients of the Cuvette Centrale result in very low levels of mechanical erosion (Laraque et al., 2009). Like the other rivers which drain these swamplands, the chemical signature of the Likouala aux Herbes seems largely determined by the process of OM decomposition in the swamps (Mann et al., 2014). This is supported by the fact that the water chemistry of the Likouala aux Herbes is almost identical to that of Lac Tele, a lake with no major rivers flowing into it, whose water chemistry can only be the result of atmospheric deposition or the surrounding swamp forest (Table 6.8; Laraque et al., 1998). The high concentrations of humic acid produced in the swamps would explain the low pH of the Likouala aux Herbes water and would also account for the relatively high concentrations of solubilised Fe and Al (Berner and Berner, 1996). The water chemistry of the Ubangui is also affected by the swamp forests, albeit to a much lesser extent, with dissolved OM levels increasing and suspended and dissolved loads becoming diluted as it passes through the Cuvette Centrale (Laraque et al., 2009). However, as the data from this study shows the cation concentrations are still high as the Ubangui passes through the Cuvette Centrale and therefore one would expect, if this river contributed to flooding of the adjacent peatlands, it would be detectable in the geochemistry of the surface peats, which it is not. Since the Likouala aux Herbes geochemistry is governed by the swamps, using surface peat geochemistry to detect river flooding is of extremely limited use when considering peats adjacent to the Likouala aux Herbes.

The idea that metal ratios (as opposed to absolute concentrations) of peatland water sources should to a certain extent be reflected in the of metal ratios of the peat has been used both in Indonesia (Weiss et al., 2002) and Peru (Lähteenoja et al., 2009a) to determine whether a peatland is dominantly ombrotrophic or minerotrophic. In both these instances peat Ca/Mg ratios that fell in the range of rainwater Ca/Mg ratios were taken as a sign of ombrotrophy, whilst higher Ca/Mg ratios were a sign of minerotrophic conditions. The use of geochemistry as a way to determine river flooding from the Likouala aux Herbes has already been ruled out and the similar Ca/Mg ratios of the Likouala aux Herbes and rainwater is added confirmation to this. However, even Ca/Mg ratios from the Ubangui cannot be used to determine whether the peatlands are river flooded, as the Ubangui Ca/Mg ratios were lower than the rainwater Ca/Mg ratios of this study and fell within range of the global rainwater (Table 6.9). The Ubangui Ca/Mg ratios were also lower than the Likouala aux Herbes. One might have expected the white water river to have higher Ca/Mg ratios than the black water river. However, as mentioned, in addition to high Ca concentrations, the Ubangui water samples were also found to be high in Mg concentrations leading to a low Ca/Mg ratio. The fact that the Ubangui and Likouala aux Herbes river metal ratios were indistinguishable from global rainwater ranges and the regional rainwater samples, means this method cannot be used here to determine whether the peatlands are ombrotrophic or minerotrophic. It is therefore inadvisable to use this method without considering the geochemical signature of potential local water sources.

Table 6.8. Congo Basin water chemistry data from this study and others.

Sample	Study	Location	pH	Metal Concentration (mg l^{-1})						
				Al	Ca	Fe	K	Mg	Mn	Na
Rain	This Study	Likouala Department, ROC	5.02	0.014	0.128	0.00	0.285	0.032	0.005	0.111
	(Laraque et al., 1998)[1]	Enyelle, Likouala Department, ROC	-	-	0.544	-	0.168	0.330	-	0.057
	(Laraque et al., 1998)[1]	Moloundou, Cameroon	6.25	-	1.074	-	0.597	0.652	-	0.717
	(Laraque et al., 1998)[1,2]	Bonga, Cuvette department, ROC	6.15	-	0.711	-	0.254	0.431	-	0.080
	(Wirmvem et al., 2014)	Cameroon	5	-	0.9	-	1.1	0.4	-	0.3
Likouala Aux Herbes River	This study	Likouala Department, ROC.	3.80	0.579	0.531	1.53	0.313	0.166	0.018	0.444
	(Laraque et al., 1998)[1,2]	Likouala Department, ROC.	4.26	0.755	0.701	1.005	0.665	0.425	-	0.310
Ubangui River	This study	Likouala Department, ROC.	7.39	0.053	4.295	0.09	1.257	1.856	0.001	1.682
	(Probst et al., 1992)	Bangui, CAR	7.29	-	3.30	-	1.58	1.44	-	2.08
	(Dupre et al., 1996)[3] and (Negrel et al., 1993)[1,3]	Bangui, CAR	-	-	2.605	0.06	1.1	0.997	-	1.448
Lac Tele	(Laraque et al., 1998)[1,2]	NA	3.80	0.715	0.481	0.503	<DL	0.292	-	<DL

1. Data originally presented in μmol l^{-1}. 2. Mean of mulitple samples presented in paper. 3. Amalgamation the two papers results which are derived from the same water samples.

Table 6.9. Congo Basin water metal ratios from this study and others.

Sample	Study	Location	Ca/Mg
Rain	This Study	Likouala Department, ROC.	4.19
	Laraque et al. (1998)	Enyelle, Likouala Department, ROC	1.65
	Laraque et al. (1998)	Moloundou, Cameroon	1.65
	Laraque et al. (1998)	Bonga, Cuvette Department, ROC	5.82
	Berner and Berner (1996)	Global continental rainwater ranges.	2-6
Likouala Aux Herbes River	This Study	Likouala Department, ROC.	3.19
	Laraque et al. (1998)	Likouala Department, ROC.	1.65
Ubangui River	This study	Likouala Department, ROC.	2.31
	Dupre et al. (1996) and Negrel et al. (1993)	Bangui, CAR	2.61
	Probst et al. (1992)	Bangui, CAR	2.29

6.6.10. Determining Sources of Peatland Nutrient Inputs from Water and Peat Chemistry

The Cuvette Centrale peat surface metal ratios were all within the range of global rainwater or slightly under (Table 6.9). However, as discussed in section 6.5.9, this cannot be used in this region to infer whether the peatlands are ombrotrophic or minerotrophic. However the absolute concentrations of cations in the surface peats could still give an indication. When the peat surface cation concentrations from this study are compared to values for other tropical peatlands, it seems that in terms of Ca levels, the peatlands of the Cuvette Centrale are more similar to the ombrotrophic peatlands than the minerotrophic (Table 6.10). The other cations do not give a clear indication as to whether the Cuvette Centrale peatlands are more similar to ombrotrophic peatlands or not. This is either because the cation concentrations of the Cuvette Centrale peatlands lie between values reported for ombrotrophic and minerotrophic tropical peatlands, as is the case for Fe, or because the concentrations reported in the literature show no clear ombrotrophic/minerotrophic divide, as is the case for Mg and K (literature summarised in Table 6.10). Whilst the Likouala aux Herbes cannot be ruled out using the geochemical data, the particularly low levels of Ca, Mg and Na in the surface peats mean that the Ubangui is probably not a source of regular flooding to the adjacent peatlands.

One noticeable aspect of the Cuvette Centrale surface peat cation concentrations is the considerably higher Al concentrations relative to the other cations measured in the samples. Surface Fe levels, although not as high as Al, were also noticeably higher than the

other measured cations. One possible explanation for this is that the peatlands are in receipt of highly weathered clay minerals, which are rich in Al and Fe oxides, but poor in other, more easily weathered metals (Berner and Berner, 1996). Clay minerals may be deposited on the peatlands through flood waters or high levels of surface runoff from adjacent *terra firme* or seasonally flooded forests, which were observed in the field to overlie soils with high clay contents, which showed signs of iron precipitants in places. Alternatively Al and Fe enrichment could occur through dust deposits. A large proportion of aeolian deposition in Central Africa is of Sahelian or Saharan origin, the fine grained fraction of which is largely composed of clay minerals enriched in Al and Fe (Collins et al., 2013, Castillo et al., 2008, Roberts et al., 2001). If the dry mass accumulation rate of the peat is known, the dust deposition rate required to account for surface cation concentrations can be calculated (Sapkota et al., 2007). Using the median calibrated radiocarbon age of the 57-60 cm peat sample from the Ekolongouma 9 km core and the mean bulk density for the top 60 cm one can calculate the dry mass accumulation rate for the surface of this core using equations 5.2 to 5.4 (Chapter 5). If C in equation 5.1 in Chapter 5 is replaced with the surface Al and Fe concentrations, this gives an estimated Al and Fe dust accumulation rate of 0.145 g m^2 yr^{-1} and 0.065 g m^2 yr^{-1} respectively for the Ekolongouma 9 km sample point. Dust deposition rates reported in the literature for Central Africa are scarce, however, Landing et al. (1995) report Saharan dust cation deposition rates across Florida of 0.062 to 0.148 g m^2 yr^{-1} for Al and 0.032 to 0.104 g m^2 yr^{-1} for Fe. Therefore it seems reasonable to conclude that the high Al and Fe concentrations in the surface peats of the Cuvette Centrale may be the result of dust deposition and do not necessarily invoke the role of flood waters or high surface runoff.

Table 6.10. Cation concentrations of tropical surface peats taken from this study and the literature.

Study	Description	Cation Concentration (mg kg^{-1})						
		Al	**Ca**	**Fe**	**K**	**Mg**	**Mn**	**Na**
This study	Overall mean of the 8 peatland sites surface samples (ranges of surface sample means from the 8 peatland sites)	4944 (2403 to 10656)	286 (66 to 598)	1847 (860 to 1545)	689 (305 to 719)	221 (167 to 279)	21 (14 to 28)	80 (0 to 158)
Lähteenoja and Page (2011)	Ombrotrophic. Amazonia (range of means, samples from top 90cm)	NA	65 to 158	575 to 800	85 to 215	48 to 133	3 to 7	NA
Page et al. (1999)	Ombrotrophic. Central Kalimantan, Indonesian (range surface means under different vegetation).	NA	22 to 51	NA	120 to 135	21 to 40	NA	NA
Anderson (1983)	Coastal. Sarawak, Indonesia. Not specifically stated but implied to be ombrotrophic (25 km transect surface sample mean)	NA	331	NA	301	923	NA	237
Lähteenoja and Page (2011)	Minerotrophic. Amazonia (range of means, samples from top 90cm)	NA	1715 to 10250	2425 to 11525	305 to 5530	388 to 2770	44 to 248	NA
Lawson et al. (2014)	Minerotrophic. Amazonia (median, samples from top 150 cm).	1720	1430	1470	121	82	16	31

6.6.11. Down Core Cation Concentrations

Bioaccumulation of nutrients (Ca, Mg, Na and K) near the surface is a feature of South East Asian (Weiss et al., 2002) and South American peatlands (Lawson et al., 2014) attributed the overlying vegetation. This is also seen in the Cuvette Centrale samples. Similar Fe and Mn concentration patterns were also observed in South America (Lawson et al., 2014) and in the Cuvette Centrale. However, with neither Fe nor Mn being in high biological demand, Lawson et al. (2014) considered the bioaccumulation of these elements as an unlikely cause of the higher surface concentrations. Instead they suggest that more oxygenated conditions near the surface lead to reduced leaching of Fe and Mn. Lower down the profile, however, more anoxic conditions prevail. This, coupled with the low pH of tropical peatlands, means that Fe and Mn become highly soluble and are subsequently lost from the peat profile through leaching (Lawson et al., 2014). Therefore, the higher concentration of these cations in the surface of the Cuvette Centrale peatlands is not owing to higher deposition rates in more recent times.

The increase in most cations towards the base of the peat profiles coincides with, and can be explained by, an increase in mineral content, as shown by the decreasing LOI values. An increase in mineral content can also account for the peaks mid-profile in some of the cores. In the Ekolongouma 9 km core the peak in Al, Ti and to a lesser extent Fe, at ~48 cm coincides with a lower LOI value at this point in the peat profile (~9% less than the underlying horizon; Fig. 6.19). A photo of this core, taken in the field, shows horizontal banding of mineral material at this point. Two other cores (4 km and 5 km) from Ekolongouma have OM contents which briefly drop below 65% in the peat profile, suggestive of material having been washed into the peatland in a flood event. Therefore it seems that Ekolongouma has been subjected to periodic flooding through its development. Likewise the Ekondzo core shows peaks in most of the measured cations which coincides with OM contents less than 65% towards the base of the peat profile (160-200 cm), suggesting that during the early stages of peat development the Ekondzo site also experienced flood events. In the Centre 20 km core, the clear peak in Al, coincident with less pronounced peaks in Fe and Ti, at ca. 145 cm could be from a flood event. However, being situated in the centre of the peatland, ca. 22 km from the swamp margins, it is unclear whether mineral material could remain suspended in flood water this far into the peatland. Brncic et al. (2007) and Brncic et al. (2009) attribute spikes in Al, Fe and Ti concentrations in sediment profiles from the Nouabale´-Ndoki region, ROC, to increases in dust deposition during periods of increased aridity. It is possible that this peak in cation concentrations in the Centre peat profile is the result of increased dust deposition; concentrations down profile, especially Ti, which is known for its low mobility in peat profiles (Novak et al., 2011), are similar to the surface concentrations, which can be

accounted for through dust deposition (see section 6.5.10) and therefore, again, this does not necessarily imply a flood event. Furthermore, during a period of increased aridity, one would expect reduced peat accumulation rates, which will increase cation concentrations in the peat even without an increase in dust deposition (Weiss et al., 2002). Whilst the low cation concentrations at the surface of the Makodi core suggest a lack of flooding at the present day, the Al concentrations down core are much higher and point towards more minerotrophic conditions. This is not very surprising, given that Makodi was originally selected as a site because remote sensing imagery suggested it was an old fluvial feature in the landscape.

To summarise, bioaccumulation and reduced leaching could account for the higher cation concentrations in the top of the peat profiles and do not suggest flood events. Further down the cores peaks in cation concentrations in some cores, such as the Centre and Ekolongouma core could be accounted for by either increased dust deposition or decreased peat accumulation rates or both simultaneously. However, other cores show signs of past flood events during the peatlands' development.

6.6.12. Origin of Surface Inorganic Matter

The predominantly biological origin of inorganic matter in the peat surface shows that a large proportion of inorganic matter originates from within the peatland, rather than from an external source and indicates a lack of fluvial activity within the peatlands. The lack of sand sized grains in the surface peat LOI residues is consistent with the idea that atmospheric deposition is the main mechanism for mineral matter deposition in the peatlands. However, river flooding cannot be entirely ruled out on the basis of this last point, because the low gradients across the entire Cuvette Centrale constrain river suspended loads (Laraque et al., 2009) and it would be expected that during a flood event, any sand sized suspended load would be deposited out of solution near to the river banks. In summary, although river flooding cannot completely discarded, the size and origins of the surface peat inorganic matter favours ombrotrophic-like peatland systems.

6.7. Conclusions

A year of continuous water table measurements from four sites within the Likouala Department showed no visible signs of large scale flood events. Abrupt rises in the water table and total monthly increases in water tables were both of magnitudes that could be accounted for by rainfall alone. However a recharge signal was detected in the water table measurements. This could either be due to groundwater flow into the peatlands from the adjacent land or could be due to internal flow within the peatlands. At present neither can

be ruled out, but differences in the hydraulic head between the peatlands and the adjacent rivers may support the latter scenario.

Low cation concentrations in surface peats suggest that the white water Ubangui River can be ruled out as a regular source of flooding to the peatlands. The black water Likouala aux Herbes River, having a chemical signature which is determined by the dominance of swamp forest within its catchment, cannot be eliminated as a source of peatland inundation from the geochemical data. However, surface cation concentrations are of a level that could be accounted for through Sahel or Saharan dust deposition alone (Landing et al., 1995). This is supported by the lack of any course-grained inorganic material and the predominantly biological origin of the inorganic material in the surface peats. Down profile geochemical data suggests that whilst river flooding has occurred at some sites in the past, throughout most of the peatland sites it has been limited.

Since ground water flow to the peatlands and flooding from the Likouala aux Herbes cannot be discounted with the present data, the Cuvette Centrale peatlands cannot be said to be categorically ombrotrophic peatlands. However, their surface geochemistry and water tables which appear largely (if not wholly) dependent on regional rainfall, implies that functionally they are more similar to ombrotrophic systems than minerotrophic systems and terming them ombrotrophic-like systems appears a reasonable label.

Chapter 7: Conclusions

This thesis set out to address a major gap in scientific knowledge with regard to tropical peatlands and the Cuvette Centrale, the world's second largest tropical wetland. Overall, the general aims of this thesis were to confirm whether peatlands are present within the Cuvette Centrale, determine the characteristics of these peatlands, quantify their extent and C stocks and gain insight into their developmental history and how they function present day. In this final chapter, I first summarise the key findings of this thesis. I then go on to discuss some of the limitations of this work and possible directions future work on the Cuvette Centrale peatlands could take. Finally, I discuss the wider implications of the findings of this thesis.

7.1. Key Findings

Extensive fieldwork in the Likouala Department, Republic of Congo, between January 2012 and May 2014, covering 63.5 km of transect, confirmed that peat is found in the swamps of the Cuvette Centrale. With a maximum peat depth of 5.9 m recorded, the findings of this study did not corroborate previous claims that peat in the Cuvette Centrale can reach depths up 17 to 30 m (Markov et al., 1988, Evrard, 1968). However, peatland extent, estimated from a classification of multiple remote sensing products, based on associations between peat and specific vegetation types, was 145,529 km^2 (90% CI 134,720-154,732 km^2), making the Cuvette Centrale peatlands the largest single peatland complex in the world. This is considerably larger than the previous estimates on peatland extent based on grey literature estimates of histosols (Page et al., 2011). When peat depth, bulk density and C measurements are scaled up to the extent of the peatland, the estimated peat C stock of the Cuvette Centrale is 30.2 Pg C (90% CI 27.8-32.7 Pg C), a globally significant C stock and ten times higher than previous estimates (3 Pg C; Page et al., 2011). Therefore, this region is by far the largest tropical peatland C stock outside of tropical Asia. When added to the current best estimate of the global tropical peatland C pool, the central estimate increases from 88.9 Pg C (Page et al., 2011) to 115.8 Pg C.

Previous estimates of peatland C stocks place the Republic of Congo (ROC) as the country with the largest African C stocks, at 2.4 Pg C (Page et al., 2011). However, I estimate that the Democratic Republic of Congo (DRC) is the country with the largest African peat C stock, estimated at 20.2 Pg C, followed by the ROC with an estimated 12.2 Pg C. This places the DRC and ROC only behind Indonesia (57.4 Gt C), in terms of countries with the largest tropical peat C stocks in the world (Page et al., 2011). The discrepancy between my estimate and previous estimates of peat C stocks for the Cuvette Centrale are due to the much larger extent of this study, but is also due to differences in bulk density estimates. In this study the mean peat bulk density was 0.17±0.08 g cm^{-3}, whereas previous calculations

have used a bulk density value from South East Asian peatlands of 0.05 g cm^{-3} (Page et al., 2011). The higher bulk density found in this study is thought to be attributable to a higher degree of decomposition and therefore level of compaction. In support of this hypothesis are the relatively high C/N ratios, which is consistent with organic matter enriched in recalcitrant C compounds. This compaction is also thought to account for the marginally higher C concentration of the Cuvette Centrale peats (58.4±5.8%) compared to other tropical peatlands (ranging from ca. 44.0-57.0%; Table 3.6, Chapter 3).

Within the Likouala Department, the peatlands were found to cover almost the entire interfluvial regions. Although a number of difficulties were encountered when estimating peatland topography, a DEM corrected for canopy height indicated that the peatland surface is approximately flat. This, coupled with a gradual increase in peat depth from the margins towards the interior at most sites, indicates that the peatlands occupy extensive, shallow interfluvial basins. Radiocarbon peat basal dates indicate that peat development initiated in the early to mid-Holocene (with dates ranging from 10555 to 7175 cal yrs BP). Here I suggest that peat initiation was driven by the onset of wetter conditions at the start of the African Humid Period (from ~14.8 ka). Despite their longevity, the peatlands have reached only modest depths (mean: 2.24±1.61 m) and, as the corrected DEM indicates, have not developed into domed systems. This contrast with the inland peatlands of South East Asia and the lowland Amazonian peatlands, with both regions having examples of domed peatlands and with the former having initiated in the Late Pleistocene (Anshari et al., 2001, Wüst et al., 2008, Page et al., 2004) and early Holocene (Dommain et al., 2011), and have reached substantial depths (with means of ca. 8 m reported for some sites; Page et al. (1999)) and the latter which tend to be much younger (late Holocene) owing to peatland development being curtailed by fluvial erosion or burial (Lähteenoja et al., 2009b, Lähteenoja and Roucoux, 2010), but reaching moderate depths (with reported mean depths ranging from 1.7 to 3.2 m; Householder et al. (2012)). I suggest that the shallow depth and lack of peat domes, despite the longevity of the Cuvette Centrale peatlands, is owing to the gentle topography of the region being unable to accommodate deep peats and the drier climate of Central Africa, preventing the development of domed systems.

Although only available for one site, age depth models derived from down-core radiocarbon dates indicate a hiatus in peat accumulation occurring somewhere between ca. 7000 and 2000 cal yrs BP. Humification analysis shows that any hiatus at this time coincides with a higher degree of peat decomposition, implying drier conditions. Although poorly constrained, this hiatus is tentatively attributed to the African Humid Period (AHP) termination, now known to have commenced in Central Africa ca. 3000 yrs BP and is

widely documented in palaeorecords across the region (Maley and Brenac, 1998, Elenga et al., 1994, Elenga et al., 2001, Ngomanda et al., 2009, Hubau et al., 2015). Therefore, either intermittent, or an overall lower peat accumulation rate could account for shallower peat depths.

With only a limited number of radiocarbon dates available caution should be applied to any conclusions drawn. However, the picture emerging of peat initiation and development in the Cuvette Centrale is one where peat formation appears closely linked to precipitation levels. Comparisons between *in situ* peatland water table measurements and satellite-derived precipitation estimates alongside comparisons between surface peat geochemistry and river plus rainwater chemistry suggest that today the peatlands are dependent on rainfall for the maintenance of water tables, as opposed to river flood events. This agrees with the findings of previous remote sensing based studies (Lee et al., 2011, Jung et al., 2010b), which have suggested that the Cuvette Centrale wetlands are functionally very different from the likes of the Amazonian wetlands, in that the Cuvette Centrale wetlands appear hydrologically disconnected from the adjacent river, with few channels connecting the wetland to the hydrological networks (Jung et al., 2010a) and swamp water levels rising and falling independently of river levels (Lee et al., 2011).

Peatlands whose water tables are maintained solely by precipitation are referred to as ombrotrophic. However, here I avoid applying this term to the Cuvette Centrale peatlands, as the methods adopted and the short duration over which water tables were monitored, meant that ground water flows and river flood events with a > 1 year reoccurrence could not be ruled out. Yet even if they cannot be termed ombrotrophic, in terms of nutrient status the peatlands of the Cuvette Centrale are ombrotrophic-like, with very low surface pH levels and low concentrations of calcium, a cation commonly taken to indicate minerotrophic conditions when present in high concentrations.

7.3. Future Work

To a large extent this study accomplished the aims it set out achieve. However, for certain aspects of this work there are limitations which should be addressed in any future work. One of the most important findings of this work was the large peatland extent and size of the peat C stock. Whilst these estimates are the first for the region to be based on *in situ* measurements the ~40,000 km^2 area covered in sampling only forms a relatively small proportion of the vast Cuvette Centrale. Confidence in the peat probability map (Fig. 4.2, Chapter 4) and C stock estimates would be improved by sampling for peat in regions within the Cuvette Centrale currently unsampled. More specifically, the peat probability map should be used to locate areas of high peatland probability far from the current

sampling locations, as discoveries here will radically improve the mapping of peatlands. Therefore, this should be the main priority of any future work on these peatlands.

Peat depth was the largest source of uncertainty in the peat C estimates, therefore additional depth measurements should take priority in terms of C estimates. Bulk density and C concentration data were modest sources of uncertainty, so new measurements are of more limited use of the parameters used to estimate C stocks. By obtaining peat depth measurements from over the border in the DRC, where peatlands appear to occupy river valleys, in addition to interfluvial basins, would also help ascertain whether modelling of peat depth/volume is a possibility for the future.

Related to this last point, is the issue of determining peatland surface topography. Using the SRTM DEM corrected for canopy height clearly indicated that the peatland surface was flat along the longest transect, but for the other transects the results were highly variable and not reliable. Furthermore, *in situ* measurements using a differential GPS failed, most probably due to the canopy cover and poor satellite coverage, and, being forested, obtaining a clear line of sight over distances long enough to make traditional survey techniques practical, was not possible, and seems unlikely to be possible in the future. A future alternative to determine peatland topography would be the use of full waveform airborne LIDAR to obtain a DEM of ground height and tree height over large areas, which would allow the peatland surface topography to be mapped (Jaenicke et al., 2008).

With regards to understanding peatland initiation and development in the Cuvette Centrale, further radiocarbon dates would improve confidence in the interpretations made of the limited number of radiocarbon dates presented in this thesis. In particular, down-core radiocarbon dates from other sites would help determine whether the hiatus in peat accumulation, observed in the Ekolongouma cores, was truly region-wide. One question which was not clearly resolved from the radiocarbon dates was the process of peat formation (e.g. terrestrialisation or paludification). Increasing the number of basal dates from the Ekolongouma site and having multiple dates from the other sites, would help build up a better picture of the process of peatland initiation. Finally, although likely to be of early Holocene age, obtaining radiocarbon dates from the deepest core, which I collected at the midpoint between the Likouala aux Herbes and Ubangui rivers (Centre transect), would determine whether peat initiation in the region occurred at an earlier time than the current radiocarbon dates suggests.

Of all the objectives set during this study, the one which was least satisfactorily met was the use of continuous water table measurements and remote sensing estimates of regional rainfall to determine whether or not increases in peatland water tables can be accounted

for by rainfall alone or whether additional water inputs are required. This was due to a number of reasons: having only one year of water table data, the differences between the spatial and temporal resolution of the water table measurements and the TRMM rainfall estimates, plus a lack of any method to determine whether the recharge signal within the water table time series is owing to ground water flow into the peatland or the redistribution of ground water within the peatland, the former of which may also bring in new nutrients to the system. To improve our understanding of the contemporary maintenance of these peatlands I recommend additional data is collected to address these issues and improve the usefulness of the water table time-series, by firstly, using *in situ* measurements of rainfall to resolve the problem of the differing spatial and temporal resolution of rainfall estimates. Tipping-buckets connected to dataloggers have been used to measure rainfall *in situ* under tropical settings (Bidin and Chappell, 2006) and could offer a solution in the Cuvette Centrale. Secondly, although highly variable on small spatial and temporal scales (Shah and Ross, 2009), in the future intact samples could be taken with the specific purpose of estimating, if very approximately, specific yield (i.e. the change in water table which results from the drainage or input of water per unit volume per unit area; Fig. 6.3, Chapter 6). This would allow rises in water table to be compared to rainfall estimates for months when the water table was below the surface. Evapotranspiration (ET) estimates are much needed for the Congo Basin; specific yield estimates combined with the water table time series could permit more direct estimations of ET, than those estimated from the Penman-Monteith or water balance equations. However, with regards to determining whether ground water flow originates from outside the peatland or is the internal redistribution of ground water, it is not clear how this could easily be resolved.

Finally, as demonstrated in this thesis, remote sensing products can be used to identify environmental conditions suitable for peat formation. Therefore this methodology could be applied to other regions of Africa to optimise the search for peatlands, which like the Cuvette Centrale, are mentioned in the literature, but are not given a specific location. This could be a key step towards reducing further the uncertainty of African peat C stocks.

7.2. Implications

In the published literature there are at least 26 African countries which are cited as containing peatlands (Chapter 1). The large discrepancies between this study's estimate and previous estimates of peatland extent and C stocks for the Cuvette Centrale highlight how little is actually known about the distribution of African peatlands or the size of the peat C stock. Although it is extremely unlikely that there are any peatlands to be discovered which are anywhere near as large as those of the Cuvette Centrale, there is the

potential for other African peatlands to store C stocks which are important at either a national or regional scale (e.g. within the Okavango Delta).

The results of this thesis show that for both the ROC and DRC, peatlands store a very large proportion of the national C stocks. Both the ROC and DRC are United Nation's Reduced Emissions from Deforestation and Forest Degradation in Developing Countries (UN REDD+) partner countries (UN-REDD Programme Collaborative Online Workspace, 2015), which means that the two countries receive support from the UN REDD+ programme to set up national REDD+ strategies i.e. strategies to reduce greenhouse gas (GHG) emissions from deforestation or forest degradation or to enhance forest C stocks through sustainable management and conservation practices (Sukhdev et al., 2011). Such countries should then receive financial payments for any avoided GHG emissions or increase in C stocks. The UN REDD+ programme now requires partner countries to include any significant peatland C stocks in their C accounting (UNFCCC, 2012). However, a lack of *in situ* measurements is frequently a barrier to the inclusion of peatlands in national inventories (Murdiyarso et al., 2013). Therefore, being the first estimate of the Cuvette Centrale peat C stocks to be based on *in situ* measurements, the results of this thesis make a direct contribution to the required national C inventories of the ROC and DRC. The results, in particular the peatland probability map, also provide a basis on which the respective governments can plan REDD+ activities, which incorporate peatland ecosystems.

The swamps of the Cuvette Centrale currently experience little disturbance, but by highlighting the significance of these peatland ecosystems early on, scenarios such as those seen in South East Asia, where peatlands have experienced extensive degradation at the hands of oil palm and forest plantations and agricultural projects (Hooijer et al., 2010, Hooijer et al., 2012, Page et al., 2002, Hirano et al., 2014, Jauhiainen et al., 2012), can be avoided. In the Likouala Department, possible threats to the peatlands include the construction of roads to connect the communities along the Ubangui and Likouala aux Herbes rivers and the development of large scale agriculture or forestry activities, which would have a negative impact on the peatland hydrology. Indeed, oil palm plantations are already established, in what was once *terra firme* forest, in some locations in the Likouala Department (personal observation) and therefore the current lack of disturbance should not be seen to mean that action is not required to protect these ecosystems.

Whilst policies can be put in place to protect these peatlands from land use change, the results from this study suggest that peatland development is also sensitive to changes in regional precipitation levels (Chapter 5). Partly owing to the paucity of rain gauge stations across the Congo Basin, meaning that even present day rainfall patterns are poorly constrained across the region, and partly owing to the difficulties of predicting changes in

precipitation patterns in general (Washington et al., 2013), there is no clear consensus about how precipitation patterns will change under different emission levels across the Congo Basin (Cook and Vizy, 2012, Haensler et al., 2013, James et al., 2013, James and Washington, 2013). Therefore, it is unclear how these peatlands will be affected by future climate change. However, if precipitation levels drop or there is an increase in the intensity of dry seasons, this is likely to have a negative impact on the Cuvette Centrale peat C stocks.

The Cuvette Centrale peatlands, as well as being one of the most important tropical peatland C stocks globally, are also home to some of the world's highest concentrations of lowland gorillas (*Gorilla Gorilla gorilla*) and African forest elephants (*Loxodonta Africana cyclotis*) (Rainey et al., 2010, Fay and Agnagna, 1991). Lowland gorillas are listed as critically endangered and African forest elephants as vulnerable (WWF, 2015), but with the latter experiencing high hunting pressures in the Congo Basin (Maisels et al., 2013). Whilst there are a number of protected areas within the Cuvette Centrale (e.g. the Lac Tele Community Reserve, the Tumba-Lediima Nature Reserve), the majority of the region has no special legal protection. Although already a conservation priority for wildlife, the vast C stocks of this region provides a second incentive for the global conservation, development and scientific communities to work with the people of the Cuvette Centrale to pursue development pathways that substantially improve livelihoods while protecting this globally significant region of Earth.

References

ABERNETHY, K. A., COAD, L., TAYLOR, G., LEE, M. E. & MAISELS, F. 2013. Extent and ecological consequences of hunting in Central African rainforests in the twenty-first century. *Philosophical Transactions of the Royal Society B-Biological Sciences,* 368.

ACKLESON, S. G. & KLEMAS, V. 1987. Remote-sensing of submerged aquatic vegetation in lower Chesapeake Bay - a comparison of Landsat MSS to TM imagery. *Remote Sensing of Environment,* 22**,** 235-248.

ALLEN, S. E. 1989. Chemical Analysis of Ecological Materials. 2nd ed. Oxford, UK: Blackwell Scientific Publications.

ALMENDINGER, J. C., ALMENDINGER, J. E. & GLASER, P. H. 1986. Topographic fluctuations across a spring fen and raised bog in the Lost River Peatland, Northern Minnesota. *Journal of Ecology,* 74**,** 393-401.

ALSDORF, D., BATES, P., MELACK, J., WILSON, M. & DUNNE, T. 2007. Spatial and temporal complexity of the Amazon flood measured from space. *Geophysical Research Letters,* 34.

AMARAL, P. G. C., VINCENS, A., GUIOT, J., BUCHET, G., DESCHAMPS, P., DOUMNANG, J. C. & SYLVESTRE, F. 2013. Palynological evidence for gradual vegetation and climate changes during the African Humid Period termination at 13 degrees N from a Mega-Lake Chad sedimentary sequence. *Climate of the Past,* 9**,** 223-241.

ANDERSON, J. A. R. 1983. The tropical peat swamps of western Malesia. *In:* GORE, A. J. P. (ed.) *Ecosystems of the world. 4B. Mires: swamp, bog, fen and moor.* Amsterdam: Elsevier.

ANDRIESSE, J. P. 1989. Nature and Management of Tropical Peat Soils. *FAO Soils Bulletin,* 59.

ANKA, Z., SERANNE, M. & DI PRIMIO, R. 2010. Evidence of a large upper-Cretaceous depocentre across the Continent-Ocean boundary of the Congo-Angola basin. Implications for palaeo-drainage and potential ultra-deep source rocks. *Marine and Petroleum Geology,* 27**,** 601-611.

ANSHARI, G., KERSHAW, A. P. & VAN DER KAARS, S. 2001. A Late Pleistocene and Holocene pollen and charcoal record from peat swamp forest, Lake Sentarum Wildlife Reserve, West Kalimantan, Indonesia. *Palaeogeography Palaeoclimatology Palaeoecology,* 171**,** 213-228.

ANSHARI, G. Z., AFIFUDIN, M., NURIMAN, M., GUSMAYANTI, E., ARIANIE, L., SUSANA, R., NUSANTARA, R. W., SUGARDJITO, J. & RAFIASTANTO, A. 2010. Drainage and land use impacts on changes in selected peat properties and peat degradation in West Kalimantan Province, Indonesia. *Biogeosciences,* 7**,** 3403-3419.

AUCOUR, A. M., BONNEFILLE, R. & HILLAIRE-MARCEL, C. 1999. Sources and accumulation rates of organic carbon in an equatorial peat bog (Burundi, East Africa) during the Holocene: carbon isotope constraints. *Palaeogeography, Palaeoclimatology, Palaeoecology,* 150**,** 179-189.

AUCOUR, A. M., HILLAIRE-MARCEL, C. & BONNEFILLE, R. 1996. Oxygen isotopes in cellulose from modern and Quaternary intertropical peatbogs: implications for palaeohydrology. *Chemical Geology,* 129**,** 341-359.

BAIRD, A., MORRIS, P. J. & BELYEA, L. R. 2011. The DigiBog peatland development model 1: rationale, conceptual model, and hydrological basis. *Ecohydrology,* 5**,** 242-255.

BAJRACHARYA, S. R., PALASH, W., SHRESTHA, M. S., KHADGI, V. R., DUO, C., DAS, P. J. & DORJI, C. 2015. Systematic Evaluation of Satellite-Based Rainfall Products over the Brahmaputra Basin for Hydrological Applications. *Advances in Meteorology,* Article ID 398687.

BEADLE, L. C. & LIND, E. M. 1960. Research on the swamps of Uganda. *Uganda Journal,* 24**,** 84-98.

BEAUNE, D., FRUTH, B., BOLLACHE, L., HOHMANN, G. & BRETAGNOLLE, F. 2013. Doom of the elephant-dependent trees in a Congo tropical forest. *Forest Ecology and Management,* 295**,** 109-117.

BEEK, K. J., BLOKHUIS, W. A., DRIESSEN, P. M., VAN BREEMEN, N., BRINKMAN, R. & PONS, L. J. 1980. Problem Soils: Their Reclamation and Management. *Land reclamation and water management. Developments, Problems and Challenges. IRLI Publication.* Wageningen, The Netherlands: ISRIC.

BEILMAN, D. W., VITT, D. H., BHATTI, J. S. & FOREST, S. 2008. Peat carbon stocks in the southern Mackenzie River Basin: uncertainties revealed in a high-resolution case study. *Global Change Biology,* 14**,** 1221-1232.

BELYEA, L. R. & BAIRD, A. J. 2006. Beyond "The limits to peat bog growth'': Cross-scale feedback in peatland development. *Ecological Monographs,* 76**,** 299-322.

BERNER, E. K. & BERNER, R. A. 1996. *Global Environment: Water, Air and Geochemical Cycles.,* New Jersey, USA., Prentice-Hall Inc.

BETBEDER, J., GOND, V., FRAPPART, F., BAGHDADI, N. N., BRIANT, G. & BARTHOLOME, E. 2014. Mapping of Central Africa Forested Wetlands Using Remote Sensing. *IEEE Journal of Selected Topics in Applied Earth Observations and Remote Sensing,* 7**,** 531-542.

BIDIN, K. & CHAPPELL, N. A. 2006. Characteristics of rain events at an inland locality in northeastern Borneo, Malaysia. *Hydrological Processes,* 20**,** 3835-3850.

BLAAUW, M. 2010. Methods and code for 'classical' age-modelling of radiocarbon sequences. *Quaternary Geochronology,* 5**,** 1047-1059.

BLAKE, S., DEEM, S. L., MOSSIMBO, E., MAISELS, F. & WALSH, P. 2009. Forest Elephants: Tree Planters of the Congo. *Biotropica,* 41**,** 459-468.

BONNEFILLE, R. & CHALIE, F. 2000. Pollen-inferred precipitation time-series from equatorial mountains, Africa, the last 40 kyr BP. *Global and Planetary Change,* 26**,** 25-50.

BORD NA MONA 1980. Musisi Bog- Zaire Survey and Pilot Scheme. Unpublished.

BORD NA MONA 1985. Fuel Peat in Developing Countries. *World Bank Technical Paper No. 41.* Washington DC: The World Bank.

BORREN, W. & BLEUTEN, W. 2006. Simulating Holocene carbon accumulation in a western Siberian watershed mire using a three-dimensional dynamic modeling approach. *Water Resources Research,* 42.

BOTCH, M. S. & MASING, V. V. 1983. Mire Ecosystems in the U.S.S.R. *In:* GORE, A. J. P. (ed.) *Ecosystems of the World 4B: Mires: Swamp, Bog, Fen and Moor.* Oxford, UK: Elsevier Scientific Publishing Company.

BOUILLENNE, R., MOUREAU, J. & DEUSE, P. 1955. Esquisse écologique des faciès forestières et marécageux des bords du lac Tumba (Domaine de I'I.R.S.A.C., Mabali, Congo Belge). *Acad. Roy. Sci. Colon., Cl. Sci. Nat. Medic., Mem in-8°, N.S., III, 1., Brussels*.

BOURDON, S., LAGGOUN-DÉFARGE, F., DISNAR, J. R., MAMAN, O., GUILLET, B., DERENNE, S. & LARGEAU, C. 2000. Organic matter sources and early diagenetic degradation in a tropical peaty marsh (Tritrivakely, Madagascar). Implications for environmental reconstruction during the Sub-Atlantic. *Organic Geochemistry,* 31**,** 421-438.

BRANDT, J. S., NOLTE, C., STEINBERG, J. & AGRAWAL, A. 2014. Foreign capital, forest change and regulatory compliance in Congo Basin forests. *Environmental Research Letters,* 9.

BRNCIC, T. M., WILLIS, K. J., HARRIS, D. J., TELFER, M. W. & BAILEY, R. M. 2009. Fire and climate change impacts on lowland forest composition in northern Congo during the last 2580 years from palaeoecological analyses of a seasonally flooded swamp. *Holocene,* 19**,** 79-89.

BRNCIC, T. M., WILLIS, K. J., HARRIS, D. J. & WASHINGTON, R. 2007. Culture or climate? The relative influences of past processes on the composition of the lowland Congo rainforest. *Philosophical Transactions of the Royal Society B-Biological Sciences,* 362**,** 229-242.

BRODIE, J. F. & GIBBS, H. K. 2009. Bushmeat Hunting As Climate Threat. *Science,* 326**,** 364-365.

BUFFAM, I., CARPENTER, S. R., YECK, W., HANSON, P. C. & TURNER, M. G. 2010. Filling holes in regional carbon budgets: Predicting peat depth in a north temperate lake district. *Journal of Geophysical Research-Biogeosciences,* 115.

BUITER, S. J. H., STEINBERGER, B., MEDVEDEV, S. & TETREAULT, J. L. 2012. Could the mantle have caused subsidence of the Congo Basin? *Tectonophysics,* 514**,** 62-80.

BURROUGH, S. L. & THOMAS, D. S. G. 2013. Central southern Africa at the time of the African Humid Period: a new analysis of Holocene palaeoenvironmental and palaeoclimate data. *Quaternary Science Reviews,* 80**,** 29-46.

BURROUGH, S. L. & WILLIS, K. J. 2015. Ecosystem resilience to late-Holocene climate change in the Upper Zambezi Valley. *The Holocene,* 25**,** 1811-1828.

BUSTAMANTE, J., PACIOS, F., DIAZ-DELGADO, R. & ARAGONES, D. 2009. Predictive models of turbidity and water depth in the Donana marshes using Landsat TM and ETM plus images. *Journal of Environmental Management,* 90**,** 2219-2225.

BWANGOY, J.-R. B., HANSEN, M. C., POTAPOV, P., TURUBANOVA, S. & LUMBUENAMO, R. S. 2013. Identifying nascent wetland forest conversion in the Democratic Republic of the Congo. *Wetlands Ecology and Management,* 21**,** 29-43.

BWANGOY, J.-R. B., HANSEN, M. C., ROY, D. P., DE GRANDI, G. & JUSTICE, C. O. 2010. Wetland mapping in the Congo Basin using optical and radar remotely sensed data and derived topographical indices. *Remote Sensing of Environment,* 114**,** 73-86.

CAHEN, L. 1954. *Geologie du Congo Belge,* Liège, Vaillant-Carmanne.

CAIRNCROSS, B., STANISTREET, I. G., MCCARTHY, T. S., ELLERY, W. N., ELLERY, K. & GROBICKI, T. S. A. 1988. PALEOCHANNELS (STONE-ROLLS) IN COAL SEAMS - MODERN ANALOGS FROM FLUVIAL DEPOSITS OF THE OKAVANGO DELTA, BOTSWANA, SOUTHERN-AFRICA. *Sedimentary Geology,* 57**,** 107-118.

CAMPBELL, D. R. 2005. The Congo River basin. *In:* FRASER, L. A. & KEDDY, P. A. (eds.) *The World's Largest Wetlands: Ecology and Conservation.* Cambridge, UK: Cambridge University Press.

CAMPBELL, J. B. & WYNNE, R. H. 2011. *Introduction To Remote Sensing,* New York, The Guilford Press.

CASTILLO, S., MORENO, T., QUEROL, X., ALASTUEY, A., CUEVAS, E., HERRMANN, L., MOUNKAILA, M. & GIBBONS, W. 2008. Trace element variation in size-fractionated African desert dusts. *Journal of Arid Environments,* 72**,** 1034-1045.

CENTRE NATIONALE DE LA STATISTIQUE ET DES ETUDES ECONOMIQUES DU CONGO. 2016. *Population des Départements- Likuoala* [Online]. Centre Nationale de la Statistique et des Etudes Economiques du Congo,. Available: http://www.cnsee.org/index.php?option=com_content&view=article&id=135%3Apopdep&catid=43%3Aanalyse-rgph&Itemid=37&limitstart=9 [Accessed 16th February 2016].

CHARMAN, D. J. 2002. *Peatlands and Environmental Change,* Chichester, West Sussex, UK, John Wiley & Sons Ltd.

CHAVE, J., ANDALO, C., BROWN, S., CAIRNS, M. A., CHAMBERS, J. Q., EAMUS, D., FOLSTER, H., FROMARD, F., HIGUCHI, N., KIRA, T., LESCURE, J. P., NELSON, B. W., OGAWA, H., PUIG, H., RIERA, B. & YAMAKURA, T. 2005. Tree allometry and improved estimation of carbon stocks and balance in tropical forests. *Oecologia,* 145**,** 87-99.

CHAVE, J., REJOU-MECHAIN, M., BURQUEZ, A., CHIDUMAYO, E., COLGAN, M. S., DELITTI, W. B. C., DUQUE, A., EID, T., FEARNSIDE, P. M., GOODMAN, R. C., HENRY, M., MARTINEZ-YRIZAR, A., MUGASHA, W. A., MULLER-LANDAU, H. C., MENCUCCINI, M., NELSON, B. W., NGOMANDA, A., NOGUEIRA, E. M., ORTIZ-MALAVASSI, E., PELISSIER, R., PLOTON, P., RYAN, C. M., SALDARRIAGA, J. G. & VIEILLEDENT, G. 2014. Improved allometric models to estimate the aboveground biomass of tropical trees. *Global Change Biology,* 20**,** 3177-3190.

CHIMNER, R. A. & EWEL, K. C. 2005. A tropical freshwater wetland: II. Production, decomposition, and peat formation. *Wetlands Ecology and Management,* 13**,** 671-684.

CLULOW, A. D., EVERSON, C. S., PRICE, J. S., JEWITT, G. P. W. & SCOTT-SHAW, B. C. 2013. Water-use dynamics of a peat swamp forest and a dune forest in Maputaland, South Africa. *Hydrology and Earth System Sciences,* 17**,** 2053-2067.

CLYMO, R. S. 1983. Peat. *In:* GORE, A. J. P. (ed.) *Ecosystems of the World 4A: Mires: Swamp, Bog, Fen and Moor.* Oxford, UK: Elsevier Scientific Publishing Company.
CLYMO, R. S. 1984. The limits to peat bog growth. *Philosophical Transactions of the Royal Society of London Series B-Biological Sciences,* 303**,** 605-654.
COLE, J. M., GOLDSTEIN, S. L., DEMENOCAL, P. B., HEMMING, S. R. & GROUSSET, F. E. 2009. Contrasting compositions of Saharan dust in the eastern Atlantic Ocean during the last deglaciation and African Humid Period. *Earth and Planetary Science Letters,* 278**,** 257-266.
COLLINS, J. A., GOVIN, A., MULITZA, S., HESLOP, D., ZABEL, M., HARTMANN, J., ROEHL, U. & WEFER, G. 2013. Abrupt shifts of the Sahara-Sahel boundary during Heinrich stadials. *Climate of the Past,* 9**,** 1181-1191.
COOK, K. H. & VIZY, E. K. 2012. Impact of climate change on mid-twenty-first century growing seasons in Africa. *Climate Dynamics,* 39**,** 2937-2955.
COSTA, K., RUSSELL, J., KONECKY, B. & LAMB, H. 2014. Isotopic reconstruction of the African Humid Period and Congo Air Boundary migration at Lake Tana, Ethiopia. *Quaternary Science Reviews,* 83**,** 58-67.
COUWENBERG, J., DOMMAIN, R. & JOOSTEN, H. 2010. Greenhouse gas fluxes from tropical peatlands in south-east Asia. *Global Change Biology,* 16**,** 1715-1732.
COYNEL, A., SEYLER, P., ETCHEBER, H., MEYBECK, M. & ORANGE, D. 2005. Spatial and seasonal dynamics of total suspended sediment and organic carbon species in the Congo River. *Global Biogeochemical Cycles,* 19.
CROSBY, A. G., FISHWICK, S. & WHITE, N. 2010. Structure and evolution of the intracratonic Congo Basin. *Geochemistry Geophysics Geosystems,* 11.
DALY, M. C., LAWRENCE, S. R., DIEMUTSHIBAND, K. & MATOUANA, B. 1992. Tectonic evolution of the Cuvette Centrale, Zaire. *Journal of the Geological Society,* 149**,** 539-&.
DE BOISSEZON, P., MARTIN, G. & GRAS, F. 1963. *Les sols du Congo*, 1:2000000. Brazzaville: ORSTOM.
DE GRANDI, G., MAYAUX, P., RAUSTE, Y., ROSENQVIST, A., SIMARD, M. & SAATCHI, S. S. 2000a. The Global Rain Forest Mapping Project JERS-1 radar mosaic of tropical Africa: Development and product characterization aspects. *IEEE Transactions on Geoscience and Remote Sensing,* 38**,** 2218-2233.
DE GRANDI, G. F., MAYAUX, P., MALINGREAU, J. P., ROSENQVIST, A., SAATCHI, S. & SIMARD, M. 2000b. New perspectives on global ecosystems from wide-area radar mosaics: flooded forest mapping in the tropics. *International Journal of Remote Sensing,* 21**,** 1235-1249.
DE HEINZELIN, J. 1963. Addendum to Transcript of Discussions. *In:* HOWELL, F. C. & BOURLIERE, F. (eds.) *African Ecology and Human Evolution.* Chicago: Aldine Publishing Company.
DE MENOCAL, P. B. 2015. Palaeoclimate: End of the African Humid Period. *Nature Geoscience,* 8**,** 86-87.
DE MENOCAL, P. B., ORTIZ, J., GUILDERSON, T. P., ADKINS, J., SARNTHEIN, M., BAKER, L. & YARUSINSKY, M. 2000. Abrupt onset and termination of the African Humid Period: rapid climate responses to gradual insolation forcing. *Quaternary Science Reviews,* 19**,** 347-361.
DEKKER, A. G., VOS, R. J. & PETERS, S. W. M. 2002. Analytical algorithms for lake water TSM estimation for retrospective analyses of TM and SPOT sensor data. *International Journal of Remote Sensing,* 23**,** 15-35.
DISNAR, J. R., STEFANOVA, M., BOURDON, S. & LAGGOUN-DÉFARGE, F. 2005. Sequential fatty acid analysis of a peat core covering the last two millennia (Tritrivakely lake, Madagascar): Diagenesis appraisal and consequences for palaeoenvironmental reconstruction. *Organic Geochemistry,* 36**,** 1391-1404.
DOMINIK, J. & STANLEY, D. J. 1993. Boron, beryllium and sulfur in Holocene sediments and peats of the Nile Delta, Egypt - their use as indicators of salinity and climate. *Chemical Geology,* 104**,** 203-216.

DOMMAIN, R., COBB, A. R., JOOSTEN, H., GLASER, P. H., CHUA, A. F. L., GANDOIS, L., KAI, F.-M., NOREN, A., SALIM, K. A., SU'UT, N. S. H. & HARVEY, C. F. 2015. Forest dynamics and tip-up pools drive pulses of high carbon accumulation rates in a tropical peat dome in Borneo (Southeast Asia). *Journal of Geophysical Research-Biogeosciences,* 120**,** 617-640.

DOMMAIN, R., COUWENBERG, J., GLASER, P. H., JOOSTEN, H., NYOMAN, I. & SURYADIPUTRA, N. 2014. Carbon storage and release in Indonesian peatlands since the last deglaciation. *Quaternary Science Reviews,* 97**,** 1-32.

DOMMAIN, R., COUWENBERG, J. & JOOSTEN, H. 2010. Hydrological self-regulation of domed peatlands in south-east Asia and consequences for conservation and restoration. *Mires and Peat,* 6**,** 1-17.

DOMMAIN, R., COUWENBERG, J. & JOOSTEN, H. 2011. Development and carbon sequestration of tropical peat domes in south-east Asia: links to post-glacial sea-level changes and Holocene climate variability. *Quaternary Science Reviews,* 30**,** 999-1010.

DOWNEY, N. J. & GURNIS, M. 2009. Instantaneous dynamics of the cratonic Congo basin. *Journal of Geophysical Research-Solid Earth,* 114.

DOXARAN, D., FROIDEFOND, J. M., LAVENDER, S. & CASTAING, P. 2002. Spectral signature of highly turbid waters - Application with SPOT data to quantify suspended particulate matter concentrations. *Remote Sensing of Environment,* 81**,** 149-161.

DRAPER, F. C., ROUCOUX, K. H., LAWSON, I. T., MITCHARD, E. T. A., HONORIO CORONADO, E. N., LAHTEENOJA, O., TORRES MONTENEGRO, L., VALDERRAMA SANDOVAL, E., ZARATE, R. & BAKER, T. R. 2014. The distribution and amount of carbon in the largest peatland complex in Amazonia. *Environmental Research Letters,* 9.

DREXLER, J. Z., BEDROD, B. L., SCOGNAMIGLIO, R. & SIEGEL, D. I. 1999. Fine-scale characteristics of groundwater flow in a peatland. *Hydrological Processes,* 13**,** 1341-1359.

DUBOIS, G. & DUBOIS, C. 1939. Caractères micropaléobotaniques d'une tourbe du Togo. *Comptes Rendus Hebdomadaires Des Seances De L' Academie Des Sciences,* 208**,** 1421-1422.

DUESE, P. 1966. *Contribution à l'étude des tourbières du Rwanda et du Burundi,* Butare, Institut national de recherche scientifique.

DULLO, B. W., GROOTJANS, A. P., ROELOFS, J. G. M., SENBETA, A. F. & FRITZ, C. 2013. Fen mires with cushion plants in Bale Mountains, Ethiopia. *Mires and Peat,* 15**,** 1-10.

DUPRE, B., GAILLARDET, J., ROUSSEAU, D. & ALLEGRE, C. J. 1996. Major and trace elements of river-borne material: The Congo Basin. *Geochimica et Cosmochimica Acta,* 60**,** 1301-1321.

EFFIOM, E. O., NUNEZ-ITURRI, G., SMITH, H. G., OTTOSSON, U. & OLSSON, O. 2013. Bushmeat hunting changes regeneration of African rainforests. *Proceedings of the Royal Society B-Biological Sciences,* 280**,** 20130246.

ELENGA, H., SCHWARTZ, D. & VINCENS, A. 1994. Pollen evidence of late Quaternary vegetation and inferred climate changes in Congo. *Palaeogeography Palaeoclimatology Palaeoecology,* 109**,** 345-356.

ELENGA, H., SCHWARTZ, D., VINCENS, A., BERTAUX, J., DENAMUR, C., MARTIN, L., WIRRMANN, D. & SERVANT, M. 1996. Holocene pollen data from Kitina lake (Congo): Palaeoclimatic and palaeobotanical changes in the Mayombe forest area. *Comptes Rendus De L Academie Des Sciences Serie Ii Fascicule a-Sciences De La Terre Et Des Planetes,* 323**,** 403-410.

ELENGA, H., VINCENS, A. & SCHWARTZ, D. 1991. Presence d'elements forestiers montagnard sur les Plateaux Bateke (Congo) au Pleistocene superieur: Nouvellles donnees palynologiques. *Palaeoecology of Africa,* 22**,** 239-252.

ELENGA, H., VINCENS, A., SCHWARTZ, D., FABING, A., BERTAUX, J., WIRRMANN, D., MARTIN, L. & SERVANT, M. 2001. The Songolo estuarine swamp (South Congo) during the middle and late Holocene. *Bulletin De La Societe Geologique De France,* 172**,** 359-366.

ELLERY, W. N., ELLERY, K., MCCARTHY, T. S., CAIRNCROSS, B. & OELOFSE, R. 1989. A peat fire in the Okavango Delta, Botswana, and its importance as an ecosystem process. *African Journal of Ecology,* 27**,** 7-21.

ELLERY, W. N., ELLERY, K., ROGERS, K. H. & MCCARTHY, T. S. 1995. The role of Cyperus-papyrus in channel blockage and abandonment in the northeastern Okavango Delta, Botswana. *African Journal of Ecology,* 33**,** 25-49.

ELLERY, W. N., ELLERY, K., ROGERS, K. H., MCCARTHY, T. S. & WALKER, B. H. 1990. Vegetation of channels of the northeastern Okavango Delta, Botswana. *African Journal of Ecology,* 28**,** 276-290.

ELLERY, W. N., GRENFELL, S. E., GRENFELL, M. C., HUMPHRIES, M. S., BARNES, K., DAHLBERG, A. & KINDNESS, A. 2012. Peat formation in the context of the development of the Mkuze floodplain on the coastal plain of Maputaland, South Africa. *Geomorphology,* 141**,** 11-20.

EVRARD, C. 1968. *Recherches ecologiques sur le peuplement forestier des sols hydromorphes de la Cuvette centrale congolaise,* Bruxelles, INEAC.

FAO/UNESCO. 1971-1978. *Soil Map of the World*, 1:5000000.

FAY, J. M. & AGNAGNA, M. 1991. A population survey of forest elephants (*Loxodonta-africana-cyclotis*) in northern Congo. *African Journal of Ecology,* 29**,** 177-187.

FELDPAUSCH, T. R., LLOYD, J., LEWIS, S. L., BRIENEN, R. J. W., GLOOR, M., MONTEAGUDO MENDOZA, A., LOPEZ-GONZALEZ, G., BANIN, L., ABU SALIM, K., AFFUM-BAFFOE, K., ALEXIADES, M., ALMEIDA, S., AMARAL, I., ANDRADE, A., ARAGAO, L. E. O. C., ARAUJO MURAKAMI, A., ARETS, E. J. M. M., ARROYO, L., AYMARD, G. A., BAKER, T. R., BANKI, O. S., BERRY, N. J., CARDOZO, N., CHAVE, J., COMISKEY, J. A., ALVAREZ, E., DE OLIVEIRA, A., DI FIORE, A., DJAGBLETEY, G., DOMINGUES, T. F., ERWIN, T. L., FEARNSIDE, P. M., FRANCA, M. B., FREITAS, M. A., HIGUCHI, N., HONORIO, E., IIDA, Y., JIMENEZ, E., KASSIM, A. R., KILLEEN, T. J., LAURANCE, W. F., LOVETT, J. C., MALHI, Y., MARIMON, B. S., MARIMON-JUNIOR, B. H., LENZA, E., MARSHALL, A. R., MENDOZA, C., METCALFE, D. J., MITCHARD, E. T. A., NEILL, D. A., NELSON, B. W., NILUS, R., NOGUEIRA, E. M., PARADA, A., PEH, K. S. H., PENA CRUZ, A., PENUELA, M. C., PITMAN, N. C. A., PRIETO, A., QUESADA, C. A., RAMIREZ, F., RAMIREZ-ANGULO, H., REITSMA, J. M., RUDAS, A., SAIZ, G., SALOMAO, R. P., SCHWARZ, M., SILVA, N., SILVA-ESPEJO, J. E., SILVEIRA, M., SONKE, B., STROPP, J., TAEDOUMG, H. E., TAN, S., TER STEEGE, H., TERBORGH, J., TORELLO-RAVENTOS, M., VAN DER HEIJDEN, G. M. F., VASQUEZ, R., VILANOVA, E., VOS, V. A., WHITE, L., WILLCOCK, S., WOELL, H. & PHILLIPS, O. L. 2012. Tree height integrated into pantropical forest biomass estimates. *Biogeosciences,* 9**,** 3381-3403.

FENNER, N. & FREEMAN, C. 2011. Drought-induced carbon loss in peatlands. *Nature Geoscience,* 4**,** 895-900.

FENNER, N., WILLIAMS, R., TOBERMAN, H., HUGHES, S., REYNOLDS, B. & FREEMAN, C. 2011. Decomposition 'hotspots' in a rewetted peatland: implications for water quality and carbon cycling. *Hydrobiologia,* 674**,** 51-66.

FORTE, A. M., QUERE, S., MOUCHA, R., SIMMONS, N. A., GRAND, S. P., MITROVICA, J. X. & ROWLEY, D. B. 2010. Joint seismic-geodynamic-mineral physical modelling of African geodynamics: A reconciliation of deep-mantle convection with surface geophysical constraints. *Earth and Planetary Science Letters,* 295**,** 329-341.

FRITZ, C., CAMPBELL, D. I. & SCHIPPER, L. A. 2008. Oscillating peat surface levels in a restiad peatland, New Zealand - magnitude and spatiotemporal variability. *Hydrological Processes,* 22**,** 3264-3274.

FROIDEFOND, J. M., CASTAING, P., MIRMAND, M. & RUCH, P. 1991. Analysis of the turbid plume of the Gironde (France) based on spot radiometric data. *Remote Sensing of Environment,* 36**,** 149-163.

FROLKING, S. & ROULET, N. T. 2007. Holocene radiative forcing impact of northern peatland carbon accumulation and methane emissions. *Global Change Biology,* 13**,** 1079-1088.

FROLKING, S., ROULET, N. T., MOORE, T. R., RICHARD, P. J. H., LAVOIE, M. & MULLER, S. D. 2001. Modeling northern peatland decomposition and peat accumulation. *Ecosystems,* 4**,** 479-498.

FROLKING, S., ROULET, N. T., TUITTILA, E., BUBIER, J. L., QUILLET, A., TALBOT, J. & RICHARD, P. J. H. 2010. A new model of Holocene peatland net primary production, decomposition, water balance, and peat accumulation. *Earth System Dynamics,* 1**,** 1-21.

FRONTIER-TANZANIA 2005. luguru Component Biodiversity Survey 2005 (Volume I): Methods Manual. *In:* BRACEBRIDGE, C. N., FANNING, E., HOWELL, K. M. & ST. JOHN, F. A. V. (eds.) *Frontier Tanzania Environmental Research Report.* Society for Environmental Exploration and the University of Dar es Salaam; CARE-Tanzania, Conservation and Management of the Eastern Arc Mountain Forests (CMEAMF): Uluguru Component, Forestry and Beekeeping Division of the Ministry of Natural Resources and Tourism, GEF/UNDP:URT/01/G32.

GASSE, F. & VAN CAMPO, E. 2001. Late Quaternary environmental changes from a pollen and diatom record in the southern tropics (Lake Tritrivakely, Madagascar). *Palaeogeography Palaeoclimatology Palaeoecology,* 167**,** 287-308.

GHOLZ, H. L., WEDIN, D. A., SMITHERMAN, S. M., HARMON, M. E. & PARTON, W. J. 2000. Long-term dynamics of pine and hardwood litter in contrasting environments: toward a global model of decomposition. *Global Change Biology,* 6**,** 751-765.

GILLHAM, R. W. 1984. The capillary-fringe and its effect on water-table response. *Journal of Hydrology,* 67**,** 307-324.

GOND, V., FAYOLLE, A., PENNEC, A., CORNU, G., MAYAUX, P., CAMBERLIN, P., DOUMENGE, C., FAUVET, N. & GOURLET-FLEURY, S. 2013. Vegetation structure and greenness in Central Africa from MODIS multi-temporal data. *Philosophical Transactions of the Royal Society of London Series B-Biological Sciences,* 368**,** 20120309.

GOODMAN, R. C., PHILLIPS, O. L., DEL CASTILLO TORRES, D., FREITAS, L., TAPIA CORTESE, S., MONTEAGUDO, A. & BAKER, T. R. 2013. Amazon palm biomass and allometry. *Forest Ecology and Management,* 310**,** 994-1004.

GORHAM, E. 1961. Factors influencing supply of major ions to inland waters, with special reference to the atmosphere. *Geological Society of America Bulletin,* 72**,** 795-840.

GORHAM, E. 1991. Northern peatlands - role in the carbon-cycle and probable responses to climatic warming. *Ecological Applications,* 1**,** 182-195.

GORHAM, E., BAYLEY, S. E. & SCHINDLER, D. W. 1984. Ecological effects of acid deposition upon peatlands - a neglected field in acid-rain research. *Canadian Journal of Fisheries and Aquatic Sciences,* 41**,** 1256-1268.

GORHAM, E. & PEARSALL, W. H. 1956. Acidity, specific conductivity and calcium content of some bog and fen water in a Northern Britain. *Journal of Ecology,* 44**,** 129-141.

GOUDIE, A. S. 2005. The drainage of Africa since the cretaceous. *Geomorphology,* 67**,** 437-456.

GRACE, J., MITCHARD, E. & GLOOR, E. 2014. Perturbations in the carbon budget of the tropics. *Global Change Biology,* 20**,** 3238-3255.

GRAY, D. M. 2006. A comprehensive look at conductivity measurement in steam and power generation waters. *International Water Conference.* Pittsburgh, Pennsylvania, U.S.A.

GRENFELL, S. E., ELLERY, W. N., GRENFELL, M. C., RAMSAY, L. F. & FLUEGEL, T. J. 2010. Sedimentary facies and geomorphic evolution of a blocked-valley lake: Lake Futululu, northern Kwazulu-Natal, South Africa. *Sedimentology,* 57**,** 1159-1174.

GRUNDLING, P. 2004. The role of sea level rise in the formation of peatlands in Maputaland. *In:* MOMADE, F., ACHIMO, M. & HALDORSEN, S. (eds.) *The Impact of Sea-level Change: Past, Present, Future.*

GRUNDLING, P., GROOTJANS, A. P., PRICE, J. S. & ELLERY, W. N. 2013. Development and persistence of an African mire: How the oldest South African fen has survived in a marginal climate. *Catena,* 110**,** 176-183.

GUMBRICHT, T., MCCARTHY, T. S., MCCARTHY, J., ROY, D., FROST, P. E. & WESSELS, K. 2002. Remote sensing to detect sub-surface peat fires and peat fire scars in the Okavango Delta, Botswana. *South African Journal of Science,* 98**,** 351-358.

HABIB, E., HENSCHKE, A. & ADLER, R. F. 2009. Evaluation of TMPA satellite-based research and real-time rainfall estimates during six tropical-related heavy rainfall events over Louisiana, USA. *Atmospheric Research,* 94**,** 373-388.

HAENSLER, A., SAEED, F. & JACOB, D. 2013. Assessing the robustness of projected precipitation changes over central Africa on the basis of a multitude of global and regional climate projections. *Climatic Change,* 121**,** 349-363.

HAMILTON, A. C. 1982. *Environmental History of East Africa,* London, Academic Press Inc. Ltd.

HANSEN, M. C., POTAPOV, P. V., MOORE, R., HANCHER, M., TURUBANOVA, S. A., TYUKAVINA, A., THAU, D., STEHMAN, S. V., GOETZ, S. J., LOVELAND, T. R., KOMMAREDDY, A., EGOROV, A., CHINI, L., JUSTICE, C. O. & TOWNSHEND, J. R. G. 2013. High-Resolution Global Maps of 21st-Century Forest Cover Change. *Science,* 342**,** 850-853.

HARTLEY, R. W. & ALLEN, P. A. 1994. Interior cratonic basins of Africa: relation to continental break-up and role of mantle convection. *Basin Research,* 6**,** 95-113.

HEDBERG, O. 1964. Features of afroalpine plant ecology. *Acta Phytogeographica Suecica,* 49**,** 1-144.

HEIRI, O., LOTTER, A. F. & LEMCKE, G. 2001. Loss on ignition as a method for estimating organic and carbonate content in sediments: reproducibility and comparability of results. *Journal of Paleolimnology,* 25**,** 101-110.

HELIOTIS, F. D. & DEWITT, C. B. 1987. Rapid water-table responses to rainfall in a northern peatland ecosystem. *Water Resources Bulletin,* 23**,** 1011-1016.

HESS, L. L., MELACK, J. M., NOVO, E., BARBOSA, C. C. F. & GASTIL, M. 2003. Dual-season mapping of wetland inundation and vegetation for the central Amazon basin. *Remote Sensing of Environment,* 87**,** 404-428.

HESS, L. L., MELACK, J. M. & SIMONETT, D. S. 1990. Radar detection of flooding beneath the forest canopy - a review. *International Journal of Remote Sensing,* 11**,** 1313-1325.

HILL, M. J., DONALD, G. E. & VICKERY, P. J. 1999. Relating radar backscatter to biophysical properties of temperate perennial grassland. *Remote Sensing of Environment,* 67**,** 15-31.

HIRANO, T., KUSIN, K., LIMIN, S. & OSAKI, M. 2014. Carbon dioxide emissions through oxidative peat decomposition on a burnt tropical peatland. *Global Change Biology,* 20**,** 555-565.

HOFSTETTER, R. H. 1983. Wetlands in the United States. *In:* GORE, A. J. P. (ed.) *Ecosystems of the World 4B: Mires: Swamp, Bog, Fen and Moor.* Oxford, UK: Elsevier Scientific Publishing Company.

HOLM, G. O., SASSER, C. E., PETERSON, G. W. & SWENSON, E. M. 2000. Vertical movement and substrate characteristics of oligohaline marshes near a high-sediment, riverine system. *Journal of Coastal Research,* 16**,** 164-171.

HOOIJER, A., PAGE, S., CANADELL, J. G., SILVIUS, M., KWADIJK, J., WOSTEN, H. & JAUHIAINEN, J. 2010. Current and future CO_2 emissions from drained peatlands in Southeast Asia. *Biogeosciences,* 7**,** 1505-1514.

HOOIJER, A., PAGE, S., JAUHIAINEN, J., LEE, W. A., LU, X. X., IDRIS, A. & ANSHARI, G. 2012. Subsidence and carbon loss in drained tropical peatlands. *Biogeosciences,* 9**,** 1053-1071.

HORRITT, M. S., MASON, D. C., COBBY, D. M., DAVENPORT, I. J. & BATES, P. D. 2003. Waterline mapping in flooded vegetation from airborne SAR imagery. *Remote Sensing of Environment,* 85**,** 271-281.

HOUSEHOLDER, J. E., JANOVEC, J. P., TOBLER, M. W., PAGE, S. & LAHTEENOJA, O. 2012. Peatlands of the Madre de Dios River of Peru: Distribution, Geomorphology, and Habitat Diversity. *Wetlands,* 32**,** 359-368.

HOWA, H. L. & STANLEY, D. J. 1991. Plant-rich Holocene sequences in the northern Nile Delta plain, Egypt - petrology, distribution and depositional-environments. *Journal of Coastal Research,* 7**,** 1077-1096.

HUBAU, W., VAN DEN BULCKE, J., VAN ACKER, J. & BEECKMAN, H. 2015. Charcoal-inferred Holocene fire and vegetation history linked to drought periods in the Democratic Republic of Congo. *Global Change Biology,* 21**,** 2296-2308.

HUGHES, R. H. & HUGHES, J. S. 1992. *A Directory of African Wetlands,* Cambridge, IUCN.

IMCG. 2011. *Global Peatland Database- Africa* [Online]. International Mire Conservation Group. Available: http://www.imcg.net/pages/publications/imcg-materials/gpd-africa.php?lang=EN [Accessed 21 Dec 2011].

IMMIRZI, C. P., MALTBY, E. & CLYMO, R. S. 1992. The Global Status of Peatlands and their Role in Carbon Cycling. London: A report for Friends of the Earth produced by the Wetland Ecosystems Research Group, Department of Geography, University of Exeter.

INGRAM, H. A. P. 1978. Soil layers in mires - function and terminology. *Journal of Soil Science,* 29**,** 224-227.

INOGWABINI, B., NZALA, A. B. & BOKIKA, J. C. 2013. People and bonobos in the southern Lake Tumba landscape, Democratic Republic of Congo. *American Journal of Human Ecology,* 2**,** 44-53.

ISLAM, M. R., YAMAGUCHI, Y. & OGAWA, K. 2001. Suspended sediment in the Ganges and Brahmaputra Rivers in Bangladesh: observation from TM and AVHRR data. *Hydrological Processes,* 15**,** 493-509.

JABER, F. H., SHUKLA, S. & SRIVASTAVA, S. 2006. Recharge, upflux and water table response for shallow water table conditions in southwest Florida. *Hydrological Processes,* 20**,** 1895-1907.

JACOT-GUILLARMOD, A. 1962. The bogs and sponges of the Basutoland mountains. *South African Journal of Science,* 58**,** 179-182.

JAENICKE, J., RIELEY, J. O., MOTT, C., KIMMAN, P. & SIEGERT, F. 2008. Determination of the amount of carbon stored in Indonesian peatlands. *Geoderma,* 147**,** 151-158.

JAMES, R. & WASHINGTON, R. 2013. Changes in African temperature and precipitation associated with degrees of global warming. *Climatic Change,* 117**,** 859-872.

JAMES, R., WASHINGTON, R. & ROWELL, D. P. 2013. Implications of global warming for the climate of African rainforests. *Philosophical Transactions of the Royal Society B-Biological Sciences,* 368.

JANSEN, P. A., MULLER-LANDAU, H. C. & WRIGHT, S. J. 2010. Bushmeat Hunting and Climate: An Indirect Link. *Science,* 327**,** 30-30.

JAUHIAINEN, J., HOOIJER, A. & PAGE, S. E. 2012. Carbon dioxide emissions from an Acacia plantation on peatland in Sumatra, Indonesia. *Biogeosciences,* 9**,** 617-630.

JOHNSON, M. S., LEHMANN, J., COUTO, E. G., NOVAES FILHO, J. P. & RIHA, S. J. 2006. DOC and DIC in flowpaths of Amazonian headwater catchments with hydrologically contrasting soils. *Biogeochemistry,* 81**,** 45-57.

JONES, M. B. & MUTHURI, F. M. 1997. Standing biomass and carbon distribution in a papyrus (Cyperus papyrus L) swamp on Lake Naivasha, Kenya. *Journal of Tropical Ecology,* 13**,** 347-356.

JOOSTEN, H. 2009. The Global Peatland CO_2 Picture: Peatland Status and Emissions in All Countries of the World. Ede, Netherlands: Wetlands International.

JOOSTEN, H. & CLARKE, D. 2002. Wise Use of Mires and Peatlands- Background and Principles Including a Framework for Decision-Making. Saarijärven Offset Oy, Saarijärvi, Finland: International Mire Conservation Group and International Peat Society.

JOOSTEN, H., TAPIO-BISTRÖM, M. L. & TOL, S. 2012. Peatlands - guidance for climate change mitigation through conservation, rehabilitation and sustainable use. *Mitigation of Climate Change in Agriculture Series 5.* 2nd ed.: FAO and Wetlands International.

JUNG, H. C., HAMSKI, J., DURAND, M., ALSDORF, D., HOSSAIN, F., LEE, H., HOSSAIN, A. K. M. A., HASAN, K., KHAN, A. S. & HOQUE, A. K. M. Z. 2010a. Characterization of complex fluvial

systems using remote sensing of spatial and temporal water level variations in the Amazon, Congo, and Brahmaputra Rivers. *Earth Surface Processes and Landforms,* 35**,** 294-304.

JUNG, H. C., HAMSKI, J., DURAND, M., ALSDORF, D. E., HOSSAIN, F., LEE, H., AZAD HOSSAIN, A. K. M. A., HASAN, K., KHAN, A. S. & HOQUE, A. K. M. Z. 2010b. Characterization of complex fluvial systems using remote sensing of spatial and temporal water level variations in the Amazon, Congo, and Brahmaputra Rivers. *Earth Surface Processes and Landforms,* 35**,** 294-304.

JUNGINGER, A., ROLLER, S., OLAKA, L. A. & TRAUTH, M. H. 2014. The effects of solar irradiation changes on the migration of the Congo Air Boundary and water levels of paleo-Lake Suguta, Northern Kenya Rift, during the African Humid Period (15-5 ka BP). *Palaeogeography Palaeoclimatology Palaeoecology,* 396**,** 1-16.

JUNGINGER, A. & TRAUTH, M. H. 2013. Hydrological constraints of paleo-Lake Suguta in the Northern Kenya Rift during the African Humid Period (15-5 ka BP). *Global and Planetary Change,* 111**,** 174-188.

JUNK, W. J., FERNANDEZ PIEDADE, M. T., SCHOENGART, J., COHN-HAFT, M., ADENEY, J. M. & WITTMANN, F. 2011. A Classification of Major Naturally-Occurring Amazonian Lowland Wetlands. *Wetlands,* 31**,** 623-640.

JUSTICE, C., WILKIE, D., ZHANG, Q. F., BRUNNER, J. & DONOGHUE, C. 2001. Central African forests, carbon and climate change. *Climate Research,* 17**,** 229-246.

KADIMA, E., DELVAUX, D., SEBAGENZI, S. N., TACK, L. & KABEYA, S. M. 2011. Structure and geological history of the Congo Basin: an integrated interpretation of gravity, magnetic and reflection seismic data. *Basin Research,* 23**,** 499-527.

KADIMA KABONGO, E., SEBAGENZI MWENE NTABWOBA, S. & LUCAZEAU, F. 2011. A Proterozoic-rift origin for the structure and the evolution of the cratonic Congo basin. *Earth and Planetary Science Letters,* 304**,** 240-250.

KEDDY, P. A., FRASER, L. H., SOLOMESHCH, A. I., JUNK, W. J., CAMPBELL, D. R., ARROYO, M. T. K. & ALHO, C. J. R. 2009. Wet and wonderful: The world's largest wetlands are conservation priorities. *BioScience,* 59**,** 39-51.

KIAGE, L. M. & LIU, K.-B. 2006. Late Quaternary paleoenvironmental changes in East Africa: a review of multiproxy evidence from palynology, take sediments, and associated records. *Progress in Physical Geography,* 30**,** 633-658.

KIM, D.-H., SEXTON, J. O. & TOWNSHEND, J. R. 2015. Accelerated deforestation in the humid tropics from the 1990s to the 2000s. *Geophysical Research Letters,* 42**,** 3495-3501.

KNMI CLIMATE EXPLORER. 2015. *Yearly cycle and anomalies over 1981:2010: Impfondo GHCN v3 mean temperature.* [Online]. Available: http://climexp.knmi.nl/new_anomalies.cgi [Accessed 21 Dec. 2015.

KORHOLA, A., TOLONEN, K., TURUNEN, J. & JUNGNER, H. 1995. Estimating long-term carbon accumulation rates in boreal peatlands by radiocarbon dating. *Radiocarbon,* 37**,** 575-584.

KRISHNASWAMY, J., BONELL, M., VENKATESH, B., PURANDARA, B. K., LELE, S., KIRAN, M. C., REDDY, V., BADIGER, S. & RAKESH, K. N. 2012. The rain-runoff response of tropical humid forest ecosystems to use and reforestation in the Western Ghats of India. *Journal of Hydrology,* 472**,** 216-237.

KUHRY, P. & TURUNEN, J. 2006. The Postglacial Development of Boreal and Subarctic Peatlands. *In:* WIEDER, R. K. & VITT, D. H. (eds.) *Ecological Studies.* Verlag Berlin Heidelberg: Springer.

KUHRY, P. & VITT, D. H. 1996. Fossil carbon/nitrogen ratios as a measure of peat decomposition. *Ecology,* 77**,** 271-275.

KURNIANTO, S., WARREN, M., TALBOT, J., KAUFFMAN, J. B., MURDIYARSO, D. & FROLKING, S. 2015. Carbon accumulation of tropical peatlands over millennia: a modeling approach. *Global Change Biology,* 21**,** 431-444.

LÄHTEENOJA, H. & ROUCOUX, K. H. 2010. Inception, history and development of peatlands in the Amazon Basin. *PAGES news,* 18**,** 27-29.
LÄHTEENOJA, O., FLORES, B. & NELSON, B. 2013. Tropical Peat Accumulation in Central Amazonia. *Wetlands,* 33**,** 495-503.
LÄHTEENOJA, O. & PAGE, S. 2011. High diversity of tropical peatland ecosystem types in the Pastaza-Marañón basin, Peruvian Amazonia. *Journal of Geophysical Research-Biogeosciences,* 116.
LÄHTEENOJA, O., REATEGUI, Y. R., RASANEN, M., TORRES, D. D. C., OINONEN, M. & PAGE, S. 2012. The large Amazonian peatland carbon sink in the subsiding Pastaza-Maranon foreland basin, Peru. *Global Change Biology,* 18**,** 164-178.
LÄHTEENOJA, O., RUOKOLAINEN, K., SCHULMAN, L. & ALVAREZ, J. 2009a. Amazonian floodplains harbour minerotrophic and ombrotrophic peatlands. *Catena,* 79**,** 140-145.
LÄHTEENOJA, O., RUOKOLAINEN, K., SCHULMAN, L. & OINONEN, M. 2009b. Amazonian peatlands: an ignored C sink and potential source. *Global Change Biology,* 15**,** 2311-2320.
LALONDE, T., SHORTRIDGE, A. & MESSINA, J. 2010. The Influence of Land Cover on Shuttle Radar Topography Mission (SRTM) Elevations in Low-relief Areas. *Transactions in GIS,* 14**,** 461-479.
LAMB, H. F., BATES, C. R., COOMBES, P. V., MARSHALL, M. H., UMER, M., DAVIES, S. J. & DEJEN, E. 2007. Late Pleistocene desiccation of Lake Tana, source of the Blue Nile. *Quaternary Science Reviews,* 26**,** 287-299.
LAMPELA, M., JAUHIAINEN, J. & VASANDER, H. 2014. Surface peat structure and chemistry in a tropical peat swamp forest. *Plant and Soil,* 382**,** 329-347.
LANDING, W. M., PERRY, J. J., GUENTZEL, J. L., GILL, G. A. & POLLMAN, C. D. 1995. Relationships between the atmospheric deposition of trace-elements, major ions, and mercury in Florida - The Fams Project (1992-1993). *Water Air and Soil Pollution,* 80**,** 343-352.
LAPEN, D. R., PRICE, J. S. & GILBERT, R. 2005. Modelling two-dimensional steady-state groundwater flow and flow sensitivity to boundary conditions in blanket peat complexes. *Hydrological Processes,* 19**,** 371-386.
LAPPALAINEN, E. & ZUREK, S. 1996. Peat in Other African Countries. *In:* LAPPALAINEN, E. (ed.) *Global Peat Resources.* Jyskae, Finland: International Peat Society.
LARAQUE, A., BRICQUET, J. P., PANDI, A. & OLIVRY, J. C. 2009. A review of material transport by the Congo River and its tributaries. *Hydrological Processes,* 23**,** 3216-3224.
LARAQUE, A., MAHE, G., ORANGE, D. & MARIEU, B. 2001. Spatiotemporal variations in hydrological regimes within Central Africa during the XXth century. *Journal of Hydrology,* 245**,** 104-117.
LARAQUE, A., POUYAUD, B., ROCCHIA, R., ROBIN, E., CHAFFAUT, I., MOUTSAMBOTE, J. M., MAZIEZOULA, B., CENSIER, C., ALBOUY, Y., ELENGA, H., ETCHEBER, H., DELAUNE, M., SONDAG, F. & GASSE, F. 1998. Origin and function of a closed depression in equatorial humid zones: the Lake Télé in North Congo. *Journal of Hydrology,* 207**,** 236-253.
LAWSON, I. T., JONES, T. D., KELLY, T. J., CORONADO, E. N. H. & ROUCOUX, K. H. 2014. The Geochemistry of Amazonian Peats. *Wetlands,* 34**,** 905-915.
LAWSON, I. T., KELLY, T. J., APLIN, P., BOOM, A., DARGIE, G., DRAPER, F. C. H., HASSAN, P. N. Z. B. P., HOYOS-SANTILLAN, J., KADUK, J., LARGE, D., MURPHY, W., PAGE, S. E., ROUCOUX, K. H., SJOEGERSTEN, S., TANSEY, K., WALDRAM, M., WEDEUX, B. M. M. & WHEELER, J. 2015. Improving estimates of tropical peatland area, carbon storage, and greenhouse gas fluxes. *Wetlands Ecology and Management,* 23**,** 327-346.
LEBRUN, J. 1936a. *Bruxelles, Imprimerie industrielle et financière (Société anonyme),* Bruxelles, Imprimerie industrielle et financière (Société anonyme).
LEBRUN, J. 1936b. *Répartition de la forêt équatorial et des formations végétales limitrophes.,* Brussels.

LEBRUN, J. & GILBERT, G. 1954. *Une classification écologique des forêts du Congo,* Bruxelles, INEAC.

LEE, H., BEIGHLEY, R. E., ALSDORF, D., JUNG, H. C., SHUM, C. K., DUAN, J., GUO, J., YAMAZAKI, D. & ANDREADIS, K. 2011. Characterization of terrestrial water dynamics in the Congo Basin using GRACE and satellite radar altimetry. *Remote Sensing of Environment,* 115**,** 3530-3538.

LEWIS, S. L., SONKE, B., SUNDERLAND, T., BEGNE, S. K., LOPEZ-GONZALEZ, G., VAN DER HEIJDEN, G. M. F., PHILLIPS, O. L., AFFUM-BAFFOE, K., BAKER, T. R., BANIN, L., BASTIN, J.-F., BEECKMAN, H., BOECKX, P., BOGAERT, J., DE CANNIERE, C., CHEZEAUX, E., CLARK, C. J., COLLINS, M., DJAGBLETEY, G., DJUIKOUO, M. N. K., DROISSART, V., DOUCET, J.-L., EWANGO, C. E. N., FAUSET, S., FELDPAUSCH, T. R., FOLI, E. G., GILLET, J.-F., HAMILTON, A. C., HARRIS, D. J., HART, T. B., DE HAULLEVILLE, T., HLADIK, A., HUFKENS, K., HUYGENS, D., JEANMART, P., JEFFERY, K. J., KEARSLEY, E., LEAL, M. E., LLOYD, J., LOVETT, J. C., MAKANA, J.-R., MALHI, Y., MARSHALL, A. R., OJO, L., PEH, K. S. H., PICKAVANCE, G., POULSEN, J. R., REITSMA, J. M., SHEIL, D., SIMO, M., STEPPE, K., TAEDOUMG, H. E., TALBOT, J., TAPLIN, J. R. D., TAYLOR, D., THOMAS, S. C., TOIRAMBE, B., VERBEECK, H., VLEMINCKX, J., WHITE, L. J. T., WILLCOCK, S., WOELL, H. & ZEMAGHO, L. 2013. Above-ground biomass and structure of 260 African tropical forests. *Philosophical Transactions of the Royal Society B-Biological Sciences,* 368.

LIMPENS, J., BERENDSE, F., BLODAU, C., CANADELL, J. G., FREEMAN, C., HOLDEN, J., ROULET, N., RYDIN, H. & SCHAEPMAN-STRUB, G. 2008. Peatlands and the carbon cycle: from local processes to global implications - a synthesis. *Biogeosciences,* 5**,** 1475-1491.

LINDQUIST, E. J., HANSEN, M. C., ROY, D. P. & JUSTICE, C. O. 2008. The suitability of decadal image data sets for mapping tropical forest cover change in the Democratic Republic of Congo: implications for the global land survey. *International Journal of Remote Sensing,* 29**,** 7269-7275.

LINDSAY, R. 2010. Peatbogs and carbon: a critical synthesis to inform policy development in oceanic peat bog conservation and restoration in the context of climate change. University of East London, Environmental Research Group.

LOPES, A., TOUZI, R. & NEZRY, E. 1990. Adaptive speckle filters and scene heterogeneity. *IEEEE Transactions on Geoscience and Remote Sensing,* 28**,** 992-1000.

LOPEZ-BUENDIA, A. M., WHATELEY, M. K. G., BASTIDA, J. & URQUIOLA, M. M. 2007. Origins of mineral matter in peat marsh and peat bog deposits, Spain. *International Journal of Coal Geology,* 71**,** 246-262.

LOPEZ, O. R. & KURSAR, T. A. 2007. Interannual variation in rainfall, drought stress and seedling mortality may mediate monodominance in tropical flooded forests. *Oecologia,* 154**,** 35-43.

MA, R. H. & DAI, J. F. 2005. Investigation of chlorophyll-a and total suspended matter concentrations using Landsat ETM and field spectral measurement in Taihu Lake, China. *International Journal of Remote Sensing,* 26**,** 2779-2795.

MAISELS, F., STRINDBERG, S., BLAKE, S., WITTEMYER, G., HART, J., WILLIAMSON, E. A., ABA'A, R., ABITSI, G., AMBAHE, R. D., AMSINI, F., BAKABANA, P. C., HICKS, T. C., BAYOGO, R. E., BECHEM, M., BEYERS, R. L., BEZANGOYE, A. N., BOUNDJA, P., BOUT, N., AKOU, M. E., BENE, L. B., FOSSO, B., GREENGRASS, E., GROSSMANN, F., IKAMBA-NKULU, C., ILAMBU, O., INOGWABINI, B.-I., IYENGUET, F., KIMINOU, F., KOKANGOYE, M., KUJIRAKWINJA, D., LATOUR, S., LIENGOLA, I., MACKAYA, Q., MADIDI, J., MADZOKE, B., MAKOUMBOU, C., MALANDA, G.-A., MALONGA, R., MBANI, O., MBENDZO, V. A., AMBASSA, E., EKINDE, A., MIHINDOU, Y., MORGAN, B. J., MOTSABA, P., MOUKALA, G., MOUNGUENGUI, A., MOWAWA, B. S., NDZAI, C., NIXON, S., NKUMU, P., NZOLANI, F., PINTEA, L., PLUMPTRE, A., RAINEY, H., DE SEMBOLI, B. B., SERCKX, A., STOKES, E., TURKALO, A., VANLEEUWE, H., VOSPER, A. & WARREN, Y. 2013. Devastating Decline of Forest Elephants in Central Africa. *Plos One,* 8.

MAKILA, M. & MOISANEN, M. 2007. Holocene lateral expansion and carbon accumulation of Luovuoma, a northern fen in Finnish Lapland. *Boreas,* 36**,** 198-210.
MALEY, J. & BRENAC, P. 1998. Vegetation dynamics, palaeoenvironments and climatic changes in the forests of western Cameroon during the last 28,000 years BP. *Review of Palaeobotany and Palynology,* 99**,** 157-187.
MALMER, N. & HOLM, E. 1984. Variation in the C/N-quotient of peat in relation to decomposition rate and age-determination with Pb-210. *Oikos,* 43**,** 171-182.
MANLY, B. F. J. 1997. *Randomization, Bootstrap and Monte Carlo Methods in Biology,* London, UK, Chapman & Hall.
MANN, P. J., SPENCER, R. G. M., DINGA, B. J., POULSEN, J. R., HERNES, P. J., FISKE, G., SALTER, M. E., WANG, Z. A., HOERING, K. A., SIX, J. & HOLMES, R. M. 2014. The biogeochemistry of carbon across a gradient of streams and rivers within the Congo Basin. *Journal of Geophysical Research-Biogeosciences,* 119**,** 687-702.
MARENGO, J. A., TOMASELLA, J. & UVO, C. R. 1998. Trends in streamflow and rainfall in tropical South America: Amazonia, eastern Brazil, and northwestern Peru. *Journal of Geophysical Research-Atmospheres,* 103**,** 1775-1783.
MARKOV, V. D., OLUNIN, A. S., OSPENNIKOVA, L. A., SKOBEEVA, E. I. & KHOROSHEV, P. I. 1988. *World Peat Resources,* Moscow, Nedra.
MARTIN, A. R. & THOMAS, S. C. 2011. A Reassessment of Carbon Content in Tropical Trees. *Plos One,* 6.
MASON, D. C., HORRITT, M. S., DALL'AMICO, J. T., SCOTT, T. R. & BATES, P. D. 2007. Improving river flood extent delineation from synthetic aperture radar using airborne laser altimetry. *Ieee Transactions on Geoscience and Remote Sensing,* 45**,** 3932-3943.
MASTER, S. 2010. Lac Tele structure, Republic of Congo Geological setting of a cryptozoological and biodiversity hotspot, and evidence against an impact origin. *Journal of African Earth Sciences,* 58**,** 667-679.
MATSUYAMA, H., OKI, T., SHINODA, M. & MASUDA, K. 1994. THE SEASONAL CHANGE OF THE WATER BUDGE IN THE CONGO RIVER BASIN. *Journal of the Meteorological Society of Japan,* 72**,** 281-299.
MAYAUX, P., BARTHOLOME, E., FRITZ, S. & BELWARD, A. 2004. A new land-cover map of Africa for the year 2000. *Journal of Biogeography,* 31**,** 861-877.
MAYAUX, P., DE GRANDI, G. F., RAUSTE, Y., SIMARD, M. & SAATCHI, S. 2002. Large-scale vegetation maps derived from the combined L-band GRFM and C-band CAMP wide area radar mosaics of Central Africa. *International Journal of Remote Sensing,* 23**,** 1261-1282.
MAYAUX, P., PEKEL, J.-F., DESDEE, B., DONNAY, F., LUPI, A., ACHARD, F., CLERICI, M., BODART, C., BRINK, A., NASI, R. & BELWARD, A. 2013. State and evolution of the African rainforests between 1990 and 2010. *Philosophical Transactions of the Royal Society B-Biological Sciences,* 368.
MCCARTHY, T. S. & ELLERY, W. N. 1997. The fluvial dynamics of the Maunachira Channel system, northeastern Okavango Swamps, Botswana. *Water Sa,* 23**,** 115-125.
MCCARTHY, T. S., ELLERY, W. N., BACKWELL, L., MARREN, P., DE KLERK, B., TOOTH, S., BRANDT, D. & WOODBORNE, S. 2010. The character, origin and palaeoenvironmental significance of the Wonderkrater spring mound, South Africa. *Journal of African Earth Sciences,* 58**,** 115-126.
MCCARTHY, T. S., MCIVER, J. R., CAIRNCROSS, B., ELLERY, W. N. & ELLERY, K. 1989. The inorganic-chemistry of peat from the Maunachira channel-swamp system, Okavango Delta, Botswana. *Geochimica Et Cosmochimica Acta,* 53**,** 1077-1089.
MCCARTHY, T. S., STANISTREET, I. G. & CAIRNCROSS, B. 1991. The sedimentary dynamics of active fluvial channels on the Okavango Fan, Botswana. *Sedimentology,* 38**,** 471-487.
MEADOWS, M. E. 1984. Late Quaternary vegetation history of the Nyika Plateau, Malawi. *Journal of Biogeography,* 11**,** 209-222.

MEHRAN, A. & AGHAKOUCHAK, A. 2014. Capabilities of satellite precipitation datasets to estimate heavy precipitation rates at different temporal accumulations. *Hydrological Processes,* 28**,** 2262-2270.
MELLING, L., HATANO, R. & GOH, K. J. 2005. Soil CO2 flux from three ecosystems in tropical peatland of Sarawak, Malaysia. *Tellus Series B-Chemical and Physical Meteorology,* 57**,** 1-11.
MENGES, C. H., BARTOLO, R. E., BELL, D. & HILL, G. J. E. 2004. The effect of savanna fires on SAR backscatter in northern Australia. *International Journal of Remote Sensing,* 25**,** 4857-4871.
MERTES, L. A. K. 1997. Documentation and significance of the perirheic zone on inundated floodplains. *Water Resources Research,* 33**,** 1749-1762.
MIYAZAKI, T., IBRAHIMI, M. K. & NISHIMURA, T. 2012. Shallow Groundwater Dynamics Controlled by Lisse and Reverse Wieringermeer Effects. *Journal of Sustainable Watershed Science & Management,* 1**,** 36-45.
MOBBS, P. M. 2014. The Mineral Industry of Congo (Brazzaville). *2012 Minerals Yearbook: CONGO (BRAZZAVILLE).* USGS,.
MOHAMMED, M. U. & BONNEFILLE, R. 1998. A late Glacial late Holocene pollen record from a highland peat at Tamsaa, Bale Mountains, south Ethiopia. *Global and Planetary Change,* 17**,** 121-129.
MOONEY, C. 2015. Indonesian fires are pouring huge amounts of carbon into the atmosphere. *The Washington Post*, 20th October.
MOORE, P. D. 1987. Ecological and hydrological aspects of peat formation. *Geological Society, London, Special Publications.,* 32**,** 7-15.
MOORE, P. D. 1989. The ecology of peat-forming processes - a review. *International Journal of Coal Geology,* 12**,** 89-103.
MOORE, P. D. & BELLAMY, D. J. 1973. *Peatlands,* London, UK, Paul Elek (Scientific Books) Ltd.
MORLEY, R. J. 2000. *Origin and Evolution of Tropical Rain Forests.,* Chichester, UK, John Wiley & Sons Ltd.
MULLER, J., WUEST, R. A. J., WEISS, D. & HU, Y. 2006. Geochemical and stratigraphic evidence of environmental change at Lynch's Crater, Queensland, Australia. *Global and Planetary Change,* 53**,** 269-277.
MUMBI, C. T., MARCHANT, R. & LANE, P. 2014. Vegetation response to climate change and human impacts in the Usambara Mountains. *ISRN Forestry,* 2014**,** 1-12.
MURDIYARSO, D., KAUFFMAN, J. B. & VERCHOT, L. V. 2013. Climate change mitigation strategies should include tropical wetlands. *Carbon Management,* 4**,** 491-499.
NEGREL, P., ALLEGRE, C. J., DUPRE, B. & LEWIN, E. 1993. Erosion sources determined by inversion of major and trace-element ratios and strontium isotopic-ratios in river water - the Congo Basin case. *Earth and Planetary Science Letters,* 120**,** 59-76.
NGOMANDA, A., CHEPSTOW-LUSTY, A., MAKAYA, M., SCHEVIN, P., MALEY, J., FONTUGNE, M., OSLISLY, R., RABENKOGO, N. & JOLLY, D. 2005. Vegetation changes during the past 1300 years in western equatorial Africa: a high-resolution pollen record from Lake Kamalete, Lope Reserve, Central Gabon. *Holocene,* 15**,** 1021-1031.
NGOMANDA, A., NEUMANN, K., SCHWEIZER, A. & MALEY, J. 2009. Seasonality change and the third millennium BP rainforest crisis in southern Cameroon (Central Africa). *Quaternary Research,* 71**,** 307-318.
NOVAK, M., ZEMANOVA, L., VOLDRICHOVA, P., STEPANOVA, M., ADAMOVA, M., PACHEROVA, P., KOMAREK, A., KRACHLER, M. & PRECHOVA, E. 2011. Experimental Evidence for Mobility/Immobility of Metals in Peat. *Environmental Science & Technology,* 45**,** 7180-7187.
OJO, J. S. & OLUROTIMI, E. O. 2014. Tropical rainfall structure characterization over two stations in southwestern Nigeria for radiowave propagation purposes. *Journal of Engineering Trends in Engineering and Applied Sciences,* 5**,** 116-122.

OLOFSSON, P., FOODY, G. M., STEHMAN, S. V. & WOODCOCK, C. E. 2013. Making better use of accuracy data in land change studies: Estimating accuracy and area and quantifying uncertainty using stratified estimation. *Remote Sensing of Environment,* 129**,** 122-131.

OMEJA, P. A., JACOB, A. L., LAWES, M. J., LWANGA, J. S., ROTHMAN, J. M., TUMWESIGYE, C. & CHAPMAN, C. A. 2014. Changes in Elephant Abundance Affect Forest Composition or Regeneration? *Biotropica,* 46**,** 704-711.

ONO, K., HIRADATE, S., MORITA, S., HIRAIDE, M., HIRATA, Y., FUJIMOTO, K., TABUCHI, R. & LIHPAI, S. 2015. Assessing the carbon compositions and sources of mangrove peat in a tropical mangrove forest on Pohnpei Island, Federated States of Micronesia. *Geoderma,* 245**,** 11-20.

ORSTOM. 1968. *Congo. Phytogéographie. Atlas du Congo. Palnche X. 2000000.*

ORSTOM. 1969. *Congo. Géologie. Atlas du Congo. Planche VIII.*, 2000000.

OSFAC. 2014. *Forêts d'Afrique Centrale Evaluées par Télédétection* [Online]. Available: http://osfac.net/data-products/facet.

PAGE, S., WUST, R. A. J. & BANKS, C. J. 2010. Past and present carbon accumulation and loss in Southeast Asian peatlands. *PAGES news,* 18**,** 25-26.

PAGE, S., WUST, R. A. J., WEISS, D., RIELEY, J. O., SHOTYK, O. W. & LIMIN, S. H. 2004. A record of Late Pleistocene and Holocene carbon accumulation and climate change from an equatorial peat bog (Kalimantan, Indonesia): implications for past, present and future carbon dynamics. *Journal of Quaternary Science,* 19**,** 625-635.

PAGE, S. E., RIELEY, J. O. & BANKS, C. J. 2011. Global and regional importance of the tropical peatland carbon pool. *Global Change Biology,* 17**,** 798-818.

PAGE, S. E., RIELEY, J. O., SHOTYK, O. W. & WEISS, D. 1999. Interdependence of peat and vegetation in a tropical peat swamp forest. *Philosophical Transactions of the Royal Society of London Series B-Biological Sciences,* 354**,** 1885-1897.

PAGE, S. E., SIEGERT, F., RIELEY, J. O., BOEHM, H. D. V., JAYA, A. & LIMIN, S. 2002. The amount of carbon released from peat and forest fires in Indonesia during 1997. *Nature,* 420**,** 61-65.

PAJUNEN, H. 1996. Mires as late quaternary accumulation basins in Rwanda and Burundi, Central Africa. *Geological Survey of Finland,* Bulletin 384.

PARMENTIER, I., MALHI, Y., SENTERRE, B., WHITTAKER, R. J., ALONSO, A., BALINGA, M. P. B., BAKAYOKO, A., BONGERS, F., CHATELAIN, C., COMISKEY, J. A., CORTAY, R., KAMDEM, M.-N. D., DOUCET, J.-L., GAUTIER, L., HAWTHORNE, W. D., ISSEMBE, Y. A., KOUAME, F. N., KOUKA, L. A., LEAL, M. E., LEJOLY, J., LEWIS, S. L., NUSBAUMER, L., PARREN, M. P. E., PEH, K. S. H., PHILLIPS, O. L., SHEIL, D., SONKE, B., SOSEF, M. S. M., SUNDERLAND, T. C. H., STROPP, J., TER STEEGE, H., SWAINE, M. D., TCHOUTO, M. G. P., VAN GEMERDEN, B. S., VAN VALKENBURG, J. L. C. H., WOELL, H. & ATDN 2007. The odd man out? Might climate explain the lower tree alpha-diversity of African rain forests relative to Amazonian rain forests? *Journal of Ecology,* 95**,** 1058-1071.

PAROLIN, P., OLIVEIRA, A. C., PIEDADE, M. T. F., WITTMANN, F. & JUNK, W. J. 2002. Pioneer trees in Amazonian floodplains: Three key species form monospecific stands in different habitats. *Folia Geobotanica,* 37**,** 225-238.

PARRY, L. & CHARMAN, D. J. 2013. Modelling soil organic carbon distribution in blanket peatlands at a landscape scale. *Geoderma,* 211-212**,** 75-84.

PARRY, L. E., CHARMAN, D. J. & NOADES, J. P. W. 2012. A method for modelling peat depth in blanket peatlands. *Soil Use and Management,* 28**,** 614-624.

PEH, K. S. H., LEWIS, S. L. & LLOYD, J. 2011. Mechanisms of monodominance in diverse tropical tree-dominated systems. *Journal of Ecology,* 99**,** 891-898.

PETERS, C. R. & O'BRIEN, E. M. 2001. Palaeo-lake Congo: Implications for Africa's Late Cenozoic climate - some unanswered questions. *In:* HEINE, K. (ed.) *Palaeoecology of Africa and the Surrounding Islands, Vol 27.*

PFADENHAUER, J., SCHNEEKLOTH, H., SCHNEIDER, R. & SCHNEIDER, S. 1993. Mire Distribution. *In:* GOTTLICH, H. A. (ed.) *Mires: Process, Exploitation and Conservation.* Chichester, UK: John Wiley and Sons.

PHILLIPS, S., ROUSE, G. E. & BUSTIN, R. M. 1997. Vegetation zones and diagnostic pollen profiles of a coastal peat swamp, Bocas del Toro, Panama. *Palaeogeography Palaeoclimatology Palaeoecology,* 128**,** 301-338.

POSA, M. R. C. 2011. Peat swamp forest avifauna of Central Kalimantan, Indonesia: Effects of habitat loss and degradation. *Biological Conservation,* 144**,** 2548-2556.

POSA, M. R. C., WIJEDASA, L. S. & CORLETT, R. T. 2011. Biodiversity and Conservation of Tropical Peat Swamp Forests. *Bioscience,* 61**,** 49-57.

POSNER, S., MAERCKLEIN, D. & OVERTON, R. 2009. USDA Forest Service Mission to the Republic of Congo and the Democratic Republic of Congo: In Support for the Development of Community Fire Management and Restoration in the Congo Basin. USDA Forest Service.

PRICE, J. S. & SCHLOTZHAUER, S. M. 1999. Importance of shrinkage and compression in determining water storage changes in peat: the case of a mined peatland. *Hydrological Processes,* 13**,** 2591-2601.

PRIMACK, R. & CORLETT, R. 2005. *Tropical Rain Forests: An Ecological and Biogeographical Comparison.,* Oxford, Blackwell Publishing.

PROBST, J., NKOUNKOU, R., KREMPP, G., BRICQUET, J. P., THIEBAUX, J. & OLIVRY, J. C. 1992. Dissolved major elements exported by the Congo and the Ubangi rivers during the period 1987-1989. *Journal of HYdrology,* 135**,** 237-257.

R CORE TEAM 2014. R: A language and environment for statistical computing. Vienna, Austria: R Foundation for Statistical Computing.

RAINEY, H. J., IYENGUET, F. C., MALANDA, G.-A. F., MADZOKE, B., DOS SANTOS, D., STOKES, E. J., MAISELS, F. & STRINDBERG, S. 2010. Survey of Raphia swamp forest, Republic of Congo, indicates high densities of Critically Endangered western lowland gorillas *Gorilla gorilla gorilla*. *Oryx,* 44**,** 124-132.

REIMER, P. J., BARD, E., BAYLISS, A., BECK, J. W., BLACKWELL, P. G., BRONK RAMSEY, C., BUCK, C. E., EDWARDS, R. L., FRIEDRICH, M., GROOTES, P. M., GUILDERSON, T. P., HAFLIDASON, H., HAJDAS, I., HATTÉ, C., HEATON, T. J., HOFFMANN, D. L., HOGG, A. G., HUGHEN, K. A., KAISER, K. F., KROMER, B., MANNING, S. W., NIU, M., REIMER, R. W., RICHARDS, D. A., SCOTT, E. M., SOUTHON, J. R., TURNEY, C. S. M. & VAN DER PLICHT, J. 2013. IntCal13 and Marine13 radiocarbon age calibration curves, 0-50,000 years cal BP. *Radiocarbon,* 55**,** 1869-1887.

REYNOLDS, S. C., BAILEY, G. N. & KING, G. C. P. 2011. Landscapes and their relation to hominin habitats: Case studies from Australopithecus sites in eastern and southern Africa. *Journal of Human Evolution,* 60**,** 281-298.

RICHARDS, J. A., WOODGATE, P. W. & SKIDMORE, A. K. 1987. An explanation of enhanced radar backscattering from flooded forests. *International Journal of Remote Sensing,* 8**,** 1093-1100.

RICHARDS, P. W. 1952. *The Tropical Rainforest: An Ecological Study,* Cambridge, Cambridge University Press.

RICHARDS, P. W. 1996. *The Tropical Rainforest,* Cambridge, Cambridge University Press.

RILEY, J. & HUCHZERMEYER, F. W. 1999. African dwarf crocodiles in the Likouala swamp forests of the congo basin: Habitat, density, and nesting. *Copeia***,** 313-320.

RITCHIE, J. C., COOPER, C. M. & SCHIEBE, F. R. 1990. The relationship of MSS and TM digital data with suspended sediments, chlorophyll, and temperature in Moon Lake, Mississippi. *Remote Sensing of Environment,* 33**,** 137-148.

ROBERTS, G. C., ANDREAE, M. O., MAENHAUT, W. & FERNANDEZ-JIMENEZ, M. T. 2001. Composition and sources of aerosol in a central African rain forest during the dry season. *Journal of Geophysical Research-Atmospheres,* 106**,** 14423-14434.

RODELL, M., MCWILLIAMS, E. B., FAMIGLIETTI, J. S., BEAUDOING, H. K. & NIGRO, J. 2011. Estimating evapotranspiration using an observation based terrestrial water budget. *Hydrological Processes,* 25**,** 4082-4092.

ROOS-BARRACLOUGH, F., VAN DER KNAAP, W. O., VAN LEEUWEN, J. F. N. & SHOTYK, W. 2004. A Late-glacial and Holocene record of climatic change from a Swiss peat humification profile. *Holocene,* 14**,** 7-19.

ROUCOUX, K. H., LAWSON, I. T., JONES, T. D., BAKER, T. R., CORONADO, E. N. H., GOSLING, W. D. & LAHTEENOJA, O. 2013. Vegetation development in an Amazonian peatland. *Palaeogeography Palaeoclimatology Palaeoecology,* 374**,** 242-255.

ROWELL, D. L. 1994. *Soil Science: Methods and Applications,* Harlow, England, Addison Wesley Longman Limited.

RUDEL, T. K. 2013. The national determinants of deforestation in sub-Saharan Africa. *Philosophical Transactions of the Royal Society of London Series B-Biological Sciences,* 368**,** 20120405.

RUMPEL, C., GONZALEZ-PEREZ, J. A., BARDOUX, G., LARGEAU, C., GONZALEZ-VILA, F. J. & VALENTIN, C. 2007. Composition and reactivity of morphologically distinct charred materials left after slash-and-burn practices in agricultural tropical soils. *Organic Geochemistry,* 38**,** 911-920.

RUNGE, J. & NGUIMALET, C. R. 2005. Physiogeographic features of the Oubangui catchment and environmental trends reflected in discharge and floods at Bangui 1911-1999, Central African Republic. *Geomorphology,* 70**,** 311-324.

RUPPEL, M., VALIRANTA, M., VIRTANEN, T. & KORHOLA, A. 2013. Postglacial spatiotemporal peatland initiation and lateral expansion dynamics in North America and northern Europe. *Holocene,* 23**,** 1596-1606.

RUUHIJÄRVI, R. 1983. The Finnish Mire Types And Their Regional Distribution. *In:* GORE, A. J. P. (ed.) *Ecosystems of the World 4B: Mires: Swamp, Bog, Fen and Moor.* Oxford, UK: Elsevier Scientific Publishing Company.

RYDIN, H. & JEGLUM, J. K. 2006. *The Biology of Peatlands,* Oxford, UK, Oxford University Press.

SAHAGIAN, D. L. 1993. Structural evolution of African basins: stratigraphic synthesis. *Basin Research,* 5**,** 41-54.

SALAKO, F. K., GHUMAN, B. S. & LAL, R. 1995. Rainfall erosivity in south-central Nigeria. *Soil Technology,* 7**,** 279-290.

SAMBA, G. & NGANGA, D. 2012. Rainfall variability in Congo-Brazzaville: 1932-2007. *International Journal of Climatology,* 32**,** 854-873.

SAMBA, G., NGANGA, D. & MPOUNZA, M. 2008. Rainfall and temperature variations over Congo-Brazzaville between 1950 and 1998. *Theoretical and Applied Climatology,* 91**,** 85-97.

SANE, Y., BONAZZOLA, M., RIO, C., CHAMBON, P., FIOLLEAU, T., MUSAT, I., HOURDIN, F., ROCA, R., GRANDPEIX, J. Y. & DIEDHIOU, A. 2012. An analysis of the diurnal cycle of precipitation over Dakar using local rain-gauge data and a general circulation model. *Quarterly Journal of the Royal Meteorological Society,* 138**,** 2182-2195.

SAPKOTA, A., CHEBURKIN, A. K., BONANI, G. & SHOTYK, W. 2007. Six millennia of atmospheric dust deposition in southern South America (Isla Navarino, Chile). *Holocene,* 17**,** 561-572.

SCHILLING, K. E. 2007. Water table fluctuations under three riparian land covers, Iowa (USA). *Hydrological Processes,* 21**,** 2415-2424.

SCHNEIDER, S. 1958. Überseeische Moorvorkommen. *Vervielfaltiges Vortragsmanu skript.* Bonn: Tagung Arbeitskreis Torfwirtschaft Bundeswirtschaftsministerium.

SHAH, N. & ROSS, M. 2009. Variability in Specific Yield under Shallow Water Table Conditions. *Journal of Hydrologic Engineering,* 14**,** 1290-1298.

SHANAHAN, T. M., MCKAY, N. P., HUGHEN, K. A., OVERPECK, J. T., OTTO-BLIESNER, B., HEIL, C. W., KING, J., SCHOLZ, C. A. & PECK, J. 2015. The time-transgressive termination of the African Humid Period. *Nature Geoscience,* 8**,** 140-144.

SHENG, Y. W., SMITH, L. C., MACDONALD, G. M., KREMENETSKI, K. V., FREY, K. E., VELICHKO, A. A., LEE, M., BEILMAN, D. W. & DUBININ, P. 2004. A high-resolution GIS-based inventory of the west Siberian peat carbon pool. *Global Biogeochemical Cycles,* 18.

SHIER, C. Tropical peat resources- an overview. Proceedings of the Symposium on Tropical Peat Resources- Prospects and Potential, 1985 Kingston Jamaica. Helsinki: International Peat Society.

SHIMADA, S., TAKAHASHI, H., HARAGUCHI, A. & KANEKO, M. 2001. The carbon content characteristics of tropical peats in Central Kalimantan, Indonesia: Estimating their spatial variability in density. *Biogeochemistry,* 53**,** 249-267.

SHIMAMURA, T. & MOMOSE, K. 2005. Organic matter dynamics control plant species coexistence in a tropical peat swamp forest. *Proceedings of the Royal Society B-Biological Sciences,* 272**,** 1503-1510.

SHOTYK, W. 1988. Review of the inorganic geochemistry of peats and peatland waters. *Earth-Science Reviews,* 25**,** 95-176.

SILVA, T. S. F., COSTA, M. P. F., MELACK, J. M. & NOVO, E. M. L. M. 2008. Remote sensing of aquatic vegetation: theory and applications. *Environmental Monitoring and Assessment,* 140**,** 131-145.

SIMMONS, N. A., FORTE, A. M. & GRAND, S. P. 2007. Thermochemical structure and dynamics of the African superplume. *Geophysical Research Letters,* 34.

SJÖRS, H. 1983. Mires of Sweden. *In:* GORE, A. J. P. (ed.) *Ecosystems of the World 4B: Mires: Swamp, Bog, Fen and Moor.* Oxford, UK: Elsevier Scientific Publishing Company.

SORENSEN, K. W. 1993. Indonesian peat swamp forests and their role as a carbon sink. *Chemosphere,* 27**,** 1065-1082.

SPANNER, M., JOHNSON, L., MILLER, J., MCCREIGHT, R., FREEMANTLE, J., RUNYON, J. & GONG, P. 1994. Remote-sensing of seasonal leaf-area index across the Oregon transect. *Ecological Applications,* 4**,** 258-271.

SPANNER, M. A., PIERCE, L. L., PETERSON, D. L. & RUNNING, S. W. 1990. Remote-sensing of temperate coniferous forest leaf-area index - the influence of canopy closure, understory vegetation and background reflectance. *International Journal of Remote Sensing,* 11**,** 95-111.

STANISTREET, I. G., CAIRNCROSS, B. & MCCARTHY, T. S. 1993. Low sinuosity and meandering bedload rivers of the Okavango Fan - channel confinement by vegetated levees without fine sediment. *Sedimentary Geology,* 85**,** 135-156.

STANISTREET, I. G. & MCCARTHY, T. S. 1993. The Okavango Fan and the classification of subaerial fan systems. *Sedimentary Geology,* 85**,** 115-133.

SUKHDEV, P., PRABHU, R., KUMAR, P., BASSI, A., PATWA-SHAH, W., ENTERS, T., LABBATE, G. & GREENWALT, J. 2011. REDD+ and a Green Economy: Opportunities for a mutually supportive relationship. *UN-REDD Programme Policy Brief.*

SVENSEN, H., DYSTHE, D. K., BANDLIEN, E. H., SACKO, S., COULIBALY, H. & PLANKE, S. 2003. Subsurface combustion in Mali: Refutation of the active volcanism hypothesis in West Africa. *Geology,* 31**,** 581-584.

SYS, C. 1960. *Carte (1:5000000) des sols et de la végétation du Congo belge et du Ruanda-Urundi.*, 1:5000000. Brussells: INEAC.

TAYLOR, J. A. 1983. The Peatlands of Great Britain and Ireland. *In:* GORE, A. J. P. (ed.) *Ecosystems of the World 4B: Mires: Swamp, Bog, Fen and Moor.* Oxford, UK: Elsevier Scientific Publishing Company.

THAMM, A. G., GRUNDLING, P. & MAZUS, H. 1996. Holocene and Recent peat growth rates on the Zululand coastal plain. *Journal of African Earth Sciences,* 23**,** 119-124.

THEIMER, B. D., NOBES, D. C. & WARNER, B. G. 1994. A study of the geoelectrical properties of peatlands and their influence on ground-penetrating radar surveying. *Geophysical Prospecting,* 42**,** 179-209.

THOMPSON, K. & HAMILTON, A. C. 1983. Peatland and Swamps of the African Continent. *In:* GORE, A. J. P. (ed.) *Ecosystems of the World: 4B. Mires: Swamp, Bog, Fen and Moor.* Oxford, UK: Elsevier Scientific Publishing Company.

TIAN, G., KANG, B. T. & BRUSSAARD, L. 1992. Biological effects of plant residues with contrasting chemical compositions under humid tropical conditions- Decomposition and nutrient release. *Soil Biology & Biochemistry,* 24**,** 1051-1060.

TOMLINSON, R. W. 1974. Preliminary biogeographical studies on the Inyanga Mountains, Rhodesia. *South African Geographical Journal,* 56**,** 15-26.

TOOTH, S. & MCCARTHY, T. S. 2004. Controls on the transition from meandering to straight channels in the wetlands of the Okavango Delta, Botswana. *Earth Surface Processes and Landforms,* 29**,** 1627-1649.

UN-REDD PROGRAMME COLLABORATIVE ONLINE WORKSPACE. 2015. *UN-REDD Programme partner countries in Africa* [Online]. Available: http://www.unredd.net/index.php?option=com_unregions&view=unregion&id=2&Itemid=496 [Accessed 30th September 2015.

UNFCCC 2012. Report of the Conference of the Parties serving as the meeting of the Parties to the Kyoto Protocol on its seventh session, held in Durban from 28 November to 11 December 2011.

URQUHART, G. R. 1999. Long-term persistence of Raphia taedigera Mart. swamps in Nicaragua. *Biotropica,* 31**,** 565-569.

USGS 2006. Shuttle Radar Topography Mission, 1 Arc Second. *In:* GLOBAL LAND COVER FACILITY, U. O. M. (ed.). College Park, Maryland, USA.

USGS. 2014. *Frequently Asked Questions about the Landsat Missions* [Online]. Available: http://landsat.usgs.gov/band_designations_landsat_satellites.php [Accessed 5th October 2015].

VAN ASSELEN, S., KARSSENBERG, D. & STOUTHAMER, E. 2011. Contribution of peat compaction to relative sea-level rise within Holocene deltas. *Geophysical Research Letters,* 38.

VAN ENGELEN, V. & HUTING, J. 2002. *Peatlands of the World. An Interpretation of the World Soil Map.,* Unpublished. Wageningen, ISRIC. GPI Project 29 GPI 1.

VANCUTSEM, C., PEKEL, J. F., EVRARD, C., MALAISSE, F. & DEFOURNY, P. 2009. Mapping and characterizing the vegetation types of the Democratic Republic of Congo using SPOT VEGETATION time series. *International Journal of Applied Earth Observation and Geoinformation,* 11**,** 62-76.

VANTHOMME, H., BELLE, B. & FORGET, P.-M. 2010. Bushmeat Hunting Alters Recruitment of Large-seeded Plant Species in Central Africa. *Biotropica,* 42**,** 672-679.

VCS 2015. VCS Methodology: VM0007: REDD+ Methodology Framework (REDD-MF).

VERHOEVEN, J. T. A. 1986. Nutrient dynamics in minerotrophic peat mires. *Aquatic Botany,* 25**,** 117-137.

VINCENS, A., BUCHET, G., SERVANT, M. & COLLABORATORS, E. M. 2010. Vegetation response to the 'African Humid Period' termination in Central Cameroon (7 degrees N) - new pollen insight from Lake Mbalang. *Climate of the Past,* 6**,** 281-294.

VINCENS, A., SCHWARTZ, D., ELENGA, H., REYNAUD-FARRERA, I., ALEXANDRE, A., BERTAUX, J., MARIOTTI, A., MARTIN, L., MEUNIER, J. D., NGUETSOP, F., SERVANT, M., SERVANT-VILDARY, S. & WIRRMANN, D. 1999. Forest response to climate changes in Atlantic Equatorial Africa during the last 4000 years BP and inheritance on the modern landscapes. *Journal of Biogeography,* 26**,** 879-885.

WAHYUNTO, RITUNG, S. & SUBAGJO, H. 2003. Peta Luas Sebaran Lahan Gambut dan Kandungan Kargon di Pulau Sumatera/maps of area of peatland distribution and carbon content in Sumatera, 1990–2002. Bogor, Indonesia: Wetlands International—Indonesia Programme & Wildlife Habitat Canada.

WAHYUNTO, RITUNG, S. & SUBAGJO, H. 2004. Peta Sebaran Lahan Gambut, Luas dan Kandungan Karbon di Kalimantan/Map of Peatland Distribution Area and Carbon

Content in Kalimantan, 2000–2002. Bogor, Indonesia: Wetlands International—Indonesia Programme & Wildlife Habitat Canada.
WAHYUNTO & SURYADIPUTRA, I. N. N. 2008. Peatland Distribution in Sumatra and Kalimantan-explanation of its data sets including source of information, accuracy, data constraints and gaps. Bogor, Indonesia: Wetlands International – Indonesia Programme.
WALKER, M. J. C. 2005. Quaternary Dating Methods. Chichester, UK: J. Wiley.
WALKER, M. J. C., GIBBARD, P. L., BERKELHAMMER, M., BJORCK, S., CWYNAR, L. C., FISHER, D. A., LONG, A. J., LOWE, J. J., NEWNHAM, R. M., RASMUSSEN, S. O. & WEISS, H. 2014. Formal Subdivision of the Holocene Series/Epoch. *In:* ROCHA, R., PAIS, J., KULLBERG, J. C. & FINNEY, S. (eds.) *Strati 2013.*
WALTER, J., LUECK, E., BAURIEGEL, A., RICHTER, C. & ZEITZ, J. 2015. Multi-scale analysis of electrical conductivity of peatlands for the assessment of peat properties. *European Journal of Soil Science,* 66**,** 639-650.
WANG, J.-J., LU, X. X., LIEW, S. C. & ZHOU, Y. 2009. Retrieval of suspended sediment concentrations in large turbid rivers using Landsat ETM plus : an example from the Yangtze River, China. *Earth Surface Processes and Landforms,* 34**,** 1082-1092.
WANG, P., YU, J., POZDNIAKOV, S. P., GRINEVSKY, S. O. & LIU, C. 2014. Shallow groundwater dynamics and its driving forces in extremely arid areas: a case study of the lower Heihe River in northwestern China. *Hydrological Processes,* 28**,** 1539-1553.
WASHINGTON, R., JAMES, R., PEARCE, H., POKAM, W. M. & MOUFOUMA-OKIA, W. 2013. Congo Basin rainfall climatology: can we believe the climate models? *Philosophical Transactions of the Royal Society B-Biological Sciences,* 368.
WEAVER, J. N., BROWNFIELD, M. E. & BERGIN, M. J. 1990. COAL IN SUB-SAHARAN-AFRICAN COUNTRIES UNDERGOING DESERTIFICATION. *Journal of African Earth Sciences,* 11**,** 261-271.
WECKSTROM, J., SEPPA, H. & KORHOLA, A. 2010. Climatic influence on peatland formation and lateral expansion in sub-arctic Fennoscandia. *Boreas,* 39**,** 761-769.
WEEKS, E. P. 2002. The Lisse effect revisited. *Ground Water,* 40**,** 652-656.
WEISS, D., SHOTYK, W., RIELEY, J., PAGE, S., GLOOR, M., REESE, S. & MARTINEZ-CORTIZAS, A. 2002. The geochemistry of major and selected trace elements in a forested peat bog, Kalimantan, SE Asia, and its implications for past atmospheric dust deposition. *Geochimica et Cosmochimica Acta,* 66**,** 2307-2323.
WEYDAHL, D. J., SAGSTUEN, J., DICK, O. B. & RONNING, H. 2007. SRTM DEM accuracy assessment over vegetated areas in Norway. *International Journal of Remote Sensing,* 28**,** 3513-3527.
WHITE, W. N. 1932. Method of estimating groundwater supplies based on discharge by plants and evaporation from soil-results of investigation in Escalante, Utah. *US Geological Survey. Water Supply Paper 659-A.* Washington DC: United States Department of the Interior.
WHITTINGTON, P. N. & PRICE, J. S. 2006. The effects of water table draw-down (as a surrogate for climate change) on the hydrology of a fen peatland, Canada. *Hydrological Processes,* 20**,** 3589-3600.
WHITTINGTON, P. N., STRACK, M., VAN HAARLEM, R., KAUFMAN, S., STOESSER, P., MALTEZ, J., PRICE, J. S. & STONE, M. 2007. The influence of peat volume change and vegetation on the hydrology of a kettle-hole wetland in Southern Ontario, Canada. *Mires and Peat,* 2**,** 1-14.
WIRMVEM, M. J., OHBA, T., FANTONG, W. Y., AYONGHE, S. N., HOGARH, J. N., SUILA, J. Y., ASAAH, A. N. E., OOKI, S., TANYILEKE, G. & HELL, J. V. 2014. Origin of major ions in monthly rainfall events at the Bamenda Highlands, North West Cameroon. *Journal of Environmental Sciences-China,* 26**,** 801-809.
WU, J. & ROULET, N. T. 2014. Climate change reduces the capacity of northern peatlands to absorb the atmospheric carbon dioxide: The different responses of bogs and fens. *Global Biogeochemical Cycles,* 28**,** 1005-1024.

WUST, R. A. J. & BUSTIN, R. M. 2003. Opaline and Al-Si phytoliths from a tropical mire system of West Malaysia: abundance, habit, elemental composition, preservation and significance. *Chemical Geology,* 200**,** 267-292.

WUST, R. A. J., BUSTIN, R. M. & LAVKULICH, L. M. 2003. New classification systems for tropical organic-rich deposits based on studies of the Tasek Bera Basin, Malaysia. *Catena,* 53**,** 133-163.

WÜST, R. A. J., JACOBSEN, G. E., VAN DER GAAST, H. & SMITH, A. M. 2008. Comparison of radiocarbon ages from different organic fractions in tropical peat cores: Insights from Kalimantan, Indonesia. *Radiocarbon,* 50**,** 359-372.

WWF. 2015. *Species Directory* [Online]. Available: https://www.worldwildlife.org/species/directory?direction=desc&sort=extinction_status [Accessed 18th Dec. 2015.

YU, Z. C. 2012. Northern peatland carbon stocks and dynamics: a review. *Biogeosciences,* 9**,** 4071-4085.

YU, Z. C., CAMPBELL, I. D., VITT, D. H. & APPS, M. J. 2001. Modelling long-term peatland dynamics. I. Concepts, review, and proposed design. *Ecological Modelling,* 145**,** 197-210.

YUAN, T., LEE, H. & JUNG, H. C. 2015. Toward Estimating Wetland Water Level Changes Based on Hydrological Sensitivity Analysis of PALSAR Backscattering Coefficients over Different Vegetation Fields. *Remote Sensing,* 7**,** 3153-3183.

YULE, C. M. 2010. Loss of biodiversity and ecosystem functioning in Indo-Malayan peat swamp forests. *Biodiversity and Conservation,* 19**,** 393-409.

YULE, C. M. & GOMEZ, L. N. 2009. Leaf litter decomposition in a tropical peat swamp forest in Peninsular Malaysia. *Wetlands Ecology and Management,* 17**,** 231-241.

ZANNE, A. E., LOPEZ-GONZALEZ, G., COOMES, D. A., ILIC, J., JANSEN, S., LEWIS, S. L., MILLER, R. B., SWENSON, N. G., WIEMANN, M. C. & CHAVE, J. 2009. Global wood density database. *In:* DRYAD (ed.).

ZEILEIS, A. & GROTHENDIECK, G. 2005. zoo: S3 Infrastructure for Regular and Irregular Time Series. *Journal of Statistical Software,* 14**,** 1-27.

ZHOU, W., WANG, S., ZHOU, Y. & TROY, A. 2006. Mapping the concentrations of total suspended matter in Lake Tailm, China, using Landsat-5 TM data. *International Journal of Remote Sensing,* 27**,** 1177-1191.

ZOLTAI, S. C. & POLLETT, F. C. 1983. Wetlands in Canada: Their Classification, Distribution and Use. *In:* GORE, A. J. P. (ed.) *Ecosystems of the World 4B: Mires: Swamp, Bog, Fen and Moor.* Oxford, UK: Elsevier Scientific Publishing Company.

ZURBENKO, I. G. & POTRZEBA, A. L. 2013. Tides in the atmosphere. *Air Quality Atmosphere and Health,* 6**,** 39-46.

Appendix

Appendix 1. Description of variations in land cover characteristics along the Bondzale transect

Distance (m)	Vegetation Type	Vegetation Description	Flood Regime	Peat Present	Microtopography	Disturbance/ Anthropogenic Activity
0	TFF	Forest dominated by Marantaceae *Megaphrynium* or *Sarcophrynium* sp. understorey.	No flooding.	No	Slightly undulating. Undulations generally < 0.5 m.	Agricultural plantation, mainly for bananas, on transect surrounded by secondary species such as *Musanga cecropriodus*.
1000	SFF	Tree species such as *Guibourtia demeusei* and tree known locally as "Moumbaso" common. Trees frequently growing at unusual angles. Lianas and *Laccosperm secundiflorum* abundant. Understorey thicker and in places limited to mounds.	Seasonally flooded.	No	Undulating by 1-2 m.	Minor and major tree fall common. Secondary vegetation where lots of trees are down.
1500	HS	Tree species such as *Uapaca paludosa*, *Carapa procera*, *Cnestis iomalla*, *Xylopia aethiopica*, *Symponia globulifera* and *Manielkara* sp. common. Myrasticaceae sp. common mid-canopy. Initially *Macaranga* sp. quite common, but not seen further along transect. Likewise lianas are common initially but become less so further along transect. Although not flooded at the time shallow pools of water common along the transect. Aerial and stilt roots very characteristic of this forest and in places so numerous it is difficult to walk through. Understorey composed of ferns, although in places understorey sparse and limited to small mounds formed from aerial roots.	Seasonally flooded.	Yes	Generally flat, but some mounds up to 1 m where aerial roots are present.	Major and minor tree fall all along the transect.

TFF- *terra firme* forest, SFF-seasonally flooded forest, HS-hardwood swamp.

Appendix 2. Description of variations in land cover characteristics along the Centre transect

Distance (m)	Vegetation Type	Vegetation Description	Flood Regime	Peat Present	Microtopography	Disturbance/ Anthropogenic Activity
0	HS	Forest characterised by presence of lots of stilt and aerial roots. Tree species commonly present include *Entandrophragma candollei, Carapa procera, Uapaca paludosa, Xylopia rubescens, Xylopia aethiopica* and *Symphonia globulifera.* In understorey Myrasticaceae sp. very common and often dominant. *Pandanus candelabrum* also very common.	Seasonally flooded	Yes	Generally flat but tree mounds reaching up to ~1 m.	Some major and minor tree fall.
9000	HS and PS-RL mix.	Vegetation transitions to and from areas of hardwood swamp, palm dominated (*Raphia laurentii*) swamp and mix of the two classes over short distances. Tree species present often include *Entandrophragma candollei, Carapa procera, Uapaca paludosa, Xylopia rubescens, Xylopia aethiopica* and *Symphonia globulifera*.	Seasonally flooded	Yes	Generally flat but with occasional 0.5-1 m or more tree or root mounds.	Some major and minor tree fall.
19250	PS-RL	*Raphia laurentii* dominates, with few trees present. Canopy shorter and more open. Tree species present include *Carapa procera* and *Xylopia aethiopica*. In understorey ferns, *Afromunum* sp., Myrasticaceae sp., Melastomataceae sp. and *Pandanus candelabrum* are present.	Seasonally flooded	Yes	Undulations mostly up to 1 m, occasionally > 1 m where palms have been growing.	NA

HS-hardwood swamp, PS-RL-*Raphia laurentii* palm dominated swamp.

Appendix 3. Description of variations in land cover characteristics along the Ekolongouma transect

Distance (m)	Vegetation Type	Vegetation Description	Flood Regime	Peat Present	Microtopography	Disturbance/ Anthropogenic Activity
0	SFF	Channels present, with vegetation confined to higher ground. Upper canopy tree species include *Trichilia welwitschi*, *Cola* sp., *Stromboslopsis tetrandra*, *Guibourtia demeusei* and *Dialium pachyphilum*. Marantaceae *Megaphrynium* or *Sarcophrynium* sp. dominating understorey in places. Lianas common and sometimes dominate.	Seasonally flooded. Unclear if flooding ever breaches channels.	No	Undulating up to 3 m in places due to what look like channels.	Trails present. Clearing made for manioc plantation at very start of transect. Some major tree fall.
1500	HS	Swamp forest characterised by stilt and aerial roots. Upper canopy largely dominated by *Uapaca paludosa*, Myrasticaceae sp. common mid-canopy. *Pandanus candelabrum* and *Palisota* sp. common in understorey.	Seasonally flooded.	Yes	Generally flat, with some ca. 0.5 m undulations, occasionally 1 m.	Some signs if hunting.
3750	PS-RL	*Raphia laurentii* dominated. Some trees present. Most common tree species include *Uapaca paludosa*, *Carapa procera* and *Manielkara* sp. Understorey very sparse.	Seasonally flooded.	Yes	Generally flat. Some undulations < 0.5 m.	Some signs of hunting visible including a hunter's camp.
8250	PS-RL	*Raphia laurentii* monodominant swamp forest. Almost no trees visible. Ferns and *Pandanus candelabrum* in understorey.	Seasonally flooded	Yes	Flat. Occassionally undulating ca. 0.5 m.	NA

SFF-seasonally flooded forest, HS-hardwood swamp, PS-RL-*Raphia laurentii* palm dominated swamp.

Appendix 4. Description of variations in land cover characteristics along the Ekondzo transect

Distance (m)	Vegetation Type	Vegetation Description	Flood Regime	Peat Present	Microtopography	Disturbance/ Anthropogenic Activity
0	S	Burned savannah dominated by *Hyparrhenia diplondra*.	Seasonally flooded.	No	Flat, <15 cm undulations.	Anthropogenic burning.
250	SFF	Very open forest dominated by tree known locally as "Iyengue". *Pandanus candelabrum* in understorey.	Seasonally flooded.	No	Flat, < 30 cm undulations	NA
1000	PS-RL	*Raphia laurentii* dominated swamp forest, with some trees species present such as *Xylopia aethiopica* and *Mitragyna stipulosa*. Understorey very sparse.	Seasonally flooded.	Yes	Generally flat with <40 cm, occasionally > 1.5 m, undulations.	NA
1750	HS	Although *Raphia laurentii* still present, it is not dominant. Forest characterised by trees with stilt and aerial roots. Common tree species include *Mitragyna stipulosa*, *Cnestis iomalla*, *Carapa procera* and *Uapaca paludosa*. Myrasticaceae sp. is abundant mid-canopy. Ferns present in understorey.	Seasonally flooded.	Yes	Up to 1 m undulations.	NA
2750	PS-RL	*Raphia laurentii* dominant but still lots of trees present especially *Carapa procera*. Myrasticaceae sp. still present mid-canopy but less abundant. Ferns dominate understorey.	Seasonally flooded.	Yes	Up to 0.5 m undulations.	NA
3750	PS-RL	*Raphia laurentii* dominant with very few trees present. Trees present include *Mitragyna stipulosa*, *Alstonia boonei* and *Uapaca paludosa*. Myrasticaceae sp. common mid-canopy. Ferns dominate understorey and *Pandanus candelabrum* common.	Seasonally flooded.	Yes	Undulations mostly < 0.5 m.	NA

S-savannah, SFF-seasonally flooded forest, PS-RL-*Raphia laurentii* palm dominated swamp, HS-hardwood swamp.

Appendix 5. Description of variations in land cover characteristics along the Itanga transect

Distance (m)	Vegetation Type	Vegetation Description	Flood Regime	Peat Present	Microtopography	Disturbance/ Anthropogenic Activity
0	S	Seasonally flooded savannah dominated by Poaceae sp. Seems to be in channel that drains the forest.	Seasonally flooded.	Yes	Flat.	Seasonal anthropogenic burning.
250	S	Seasonally flooded savannah dominated by *Hyparenia diplondra*.	Seasonally flooded.	No	Flat but ca. 1 m higher than the savannah with peat.	Seasonal anthropogenic burning.
1000	Transition between S and SFF	Secondary vegetation as a result of a fire. Transition zone from savannah to forest. *Hyparrenia diplondra* dominates. *Raphia hookeri* most common species in upper canopy.	Seasonally flooded.	No	Flat	Surface and trees badly burned. Trees standing but dead. A result of out of control anthropogenic fire.
1250	SFF	Upper canopy tree species include *Lophira alata*, *Dialium pachyphilum*, *Strombosaia grandifolia*, *Guibourtia demeusei* and *Diopyros dendo*. Marantaceae *Megaphrynium* or *Sarcophrynium* sp. dominates understorey along with *Laccosperm secundiflorum* occassionally.	Seasonally flooded.	No	Up to 2 m undulations in places, but also flat in parts.	Some major and minor treefall.
2000	PS-RH	Channel dominated by *Raphia hookeri*. *Macaranga* sp. also common. Lots of lianas. *Crytosperma senegalense* also present.	Seasonally flooded.	Yes	At channel edges undulations can be up to 1-2 m due to root and liana mounds.	NA
2500	HS	Forest characterised by trees with stilt and aerial roots. Forest dominated by Myrasticaceae sp. mid-canopy. Trees species common in upper canopy include *Carapa procera*, *Aidia micrantha*, *Xylopia aethiopica* and *Uapaca paludosa*. *Pandanus candelabrum* common in understorey.	Seasonally flooded.	Yes	Ca. ½ m undulations caused by aerial roots.	Some major and minor tree fall.

S-savannah, SFF-seasonally flooded forest, PS-RH-*Raphia hookeri* palm dominated swamp, HS-hardwood swamp.

Appendix 6. Description of variations in land cover characteristics along the Makodi transect

Distance (m)	Vegetation Type	Vegetation Description	Flood Regime	Peat Present	Microtopography	Disturbance/ Anthropogenic Activity
0	S	Seasonally flooded savannah. Dominant grass species not identified at the time. Grasses reaching 1 to 3 m in height.	Seasonally flooded.	No	Undulating.	Seasonal anthropogenic burning.
600	PS-RH	*Raphia hookeri* dominates, sometimes forming monodominant stands. Vegetation very dense, particularly in understorey. *Laccosperm secundiflorum* also very common and occasionally codominant with *Raphia hookeri*. Occassionally some trees species are present such as *Uapaca paludosa*, *Xylopia rubescens* and *Macaranga* sp.	Seasonally flooded	Yes, but not consistently	Generally flat, but occasionally ½ to 1 m undulations.	NA
2000	HS	Although *Raphia hookeri* juveniles dominate understorey forming a canopy around 6 m, trees now much more abundant and form a canopy around 20 to 30 m. Dominant species include *Mitragyna stipulosa* and unidentified species known locally as "Bemba", "Moncako" and "Mombaka". *Gambeya perulchra* and *Blighia* sp. also common.	Seasonally flooded	Yes	Generally flat, but with some undulations up to 2 m.	NA
2600	PS-RH	*Raphia hookeri* dominates and in places *Raphia laurentii* is codominant. In the understorey *Afromonum* sp. and *Crytosperma senegalese* present in understorey. Canopy mostly around 8 to 10 m high, although some trees, such as *Blighia* sp. and *Mitragyna stipulosa* are present.	Seasonally flooded	Yes	Undulations <0.25 m	One trail spotted.
3000	HS	Trees with stilt roots. *Mitragyna stipulosa* dominates. *Blighia* sp. and a tree known locally as "Bemba" also very common, as is *Raphia laurentii*.	Seasonally flooded	No	Tree mounds up to 2 m.	Major tree fall

S-savannah, PS-RH-*Raphia hookeri* palm dominated swamp, HS-hardwood swamp.

Appendix 7. Description of variations in land cover characteristics along the Mbala transect

Distance (m)	Vegetation Type	Vegetation Description	Flood Regime	Peat Present	Microtopography	Disturbance/ Anthropogenic Activity
0	TFF	Quite open forest. Marantaceae *Megaphrynium* or *Sarcophrynium* sp. and *Palisota* sp. dominate understorey in parts. In upper canopy dominant tree species include *Guibourtia demeusei* and *Rhabdophyllum arnoldianum*.	No flooding	No	Generally flat, but some <1 m undulations.	Trails from Mbala village.
1250	PS-RL	*Raphia laurentii* dominated swamp on edge of channel. Marantaceae *Megaphrynium* or *Sarcophrynium* sp. and *Crytosperma senegalense* present in understorey. Myrasticaceae sp. common mid-canopy. Lianas common.	Seasonally flooded	Yes	Generally flat, but occasionally >1 m hummocks where there are plants.	NA
1500	HS	Although a hardwood swamp, young *Raphia laurentii* could be said to dominate, forming a lower canopy. Species common in upper canopy include *Manielkara* sp. and *Carapa procera*. Myrasticaceae sp. common mid-canopy. *Palisota* sp. often dominates understorey with Marantaceae *Megaphrynium* or *Sarcophrynium* sp. common in places.	Seasonally flooded	Yes	Undulating up to 1 m where there are tree roots.	NA
2500	PS-RL	*Raphia laurentii* dominated swamp. Quite a few trees present in upper canopy. Tree species include *Uapaca* sp. and *Manielkara* sp. Myrasticaceae sp. common mid-canopy. *Palisota* sp. often dominates understorey with *Crytosperma senegalense*. Ferns also common.	Seasonally flooded	Yes	Generally flat, but <0.5 m mounds where aerial roots are present.	NA
3250	PS-RL	*Raphia laurentii* monodominant swamp. Myrasticaceae sp. common mid-canopy. *Palisota* sp., *Crytosperma senegalense* and ferns common in understorey. Marantaceae *Megaphrynium* or *Sarcophrynium* sp. present in understorey in places.	Seasonally flooded	Yes	Generally flat, with gentle undulations up to 0.5 m.	NA

TFF- *terra firme* forest, PS-RL-*Raphia laurentii* palm dominated swamp, HS-hardwood swamp.

Appendix 8. Description of variations in land cover characteristics along the Moungouma transect

Distance (m)	Vegetation Type	Vegetation Description	Flood Regime	Peat Present	Microtopography	Disturbance/ Anthropogenic Activity
0	PS-RH	*Raphia hookeri* dominated swamp. Few trees present. *Diopyros dendo* most common tree species. *Laccosperm secundiflorum* abundant in understorey.	Seasonally flooded	No	Generally flat, with some 0.5 m undulations where trees present	Minor tree fall
380	TFF	Forest dominated by *Laccosperm secundiflorum* and Marantaceae *Megaphrynium* or *Sarcophrynium* sp. in understorey. Upper canopy tree species include *Diopyros dendo, Lecythidaceae brazzeia* and *Musanga cecropioides.*	No flooding	No	Undulating < 0.5 m	Major and minor tree fall
780	PS-RH	*Raphia hookeri* dominated swamp. Some trees present. *Guibourtia demeusei* quite common. Understorey very sparse.	Seasonally flooded	No	Undulating < 0.5 m	Major tree fall
1170	TFF	Very open secondary *terra firme*. Has been burned and possibly logged. *Laccosperm secundiflorum* dominates understorey.	No flooding	No	On gentle slope with a difference in elevation of ca. 1 m	Has been burned and possibly logged. Located between two plantations for bananas and manioc
1410	PS-RH	*Raphia hookeri* dominated swamp. Some trees present. *Guibourtia demeusei* quite common. Pools of water with lillipads and algae in them.	Seasonally (possibly permanently) flooded	No	Generally flat but undulations up to 0.5 m where there are trees	On edge of banana plantation. Forest partially burned from fire which has spread from plantation
1730	SFF	*Guibourtia demeusei* most common tree species followed by *Diopyros dendo*. *Laccosperm secundiflorum* dominates understorey.	Seasonally inundated	No	Undulating < 0.5 m	Minor tree fall
2180	PS-RH	*Raphia hookeri* dominant. Some trees present. *Xylopia aethiopica* common. Understorey sparse.	Seasonally inundated	No	Small undulations up to 0.5 m but generally ~30 cm	Minor tree fall
2480	HSS	Looks like initially it was forested, but now dominated by herbaceous secondary vegetation as a result of burning.	Seasonally (possibly permanently) flooded	No	Hummock-hollow system. Difference ~ 0.5 m	Severely burned from fire started in nearby plantation. Most trees standing dead. Soil severely eroded, except where protected by tree roots

PS-RH-*Raphia hookeri* palm dominated swamp, TFF- *terra firme* forest, SFF-seasonally flooded forest, HHS-herbaceous seasonally swamp.